Characterizing the Role of Palmitoylation in Cardiac Fibroblast Activation and Fibrosis

by

Robert S. Goldsmith

A dissertation submitted in partial fulfillment
of the requirements for the degree of
Doctor of Philosophy
(Pharmacology)
in the University of Michigan
2024

Doctoral Committee:

Assistant Professor Matthew J. Brody, Chair
Assistant Professor Adam S. Helms
Professor Lori Isom
Clinical Professor David B. Lombard
Professor Alan Smrcka

Robert S. Goldsmith

goldrob@umich.edu

ORCID iD: 0000-0001-8292-6330

Dedication

To my mother, whose boundless love gave me an unshakeable spirit

To my father, whose fearlessness taught me to explore the world without hesitation

To my brother, who imparted me with the understanding of equivalent exchange

To my partner, whose infectious positivity strengthens me every day

To Twig, whose presence lifts everyone around him

“But I'll tell you what hermits realize. If you go off into a far, far forest and get very quiet, you'll come to understand that you're connected with everything.” -Alan Watts

Acknowledgments

I would like to extend my biggest thanks to my mentor, Dr. Matthew Brody, for his continual support of my project and my development as a scientist throughout my degree. His bright scientific mind, rigorous approach to experimental problem-solving, and experienced academic mentorship have been instrumental in honing my abilities as a researcher and giving me the tools to overcome challenges in the lab. Further, I'm hugely grateful for his continual support of my career development pursuits outside of the lab, which has allowed me to simultaneously grow as a business professional and push myself to achieve and have an impact in all aspects of my career.

To my lab, you have my sincere gratitude for the innumerable ways in which you have supported me over the years. Special thank you's go out to Dr.'s Kobina Essandoh and Arasakumar Subramani for all of their help training me in the fundamentals of molecular biology, throughout the pandemic and onward. I am forever grateful for their guidance, expertise, and willingness to listen to my questions over the years. To the honorary Smrcka lab members, it has been a pleasure working alongside all of you and I appreciate all of the lab meeting feedback I've received throughout our time together.

To my committee members, Dr. Alan Smrcka, Dr. Lori Isom, Dr. Adam Helms, and Dr. David Lombard, thank you immensely for your attention, understanding, and efforts towards shaping my project and your help in troubleshooting different areas of my work. You have all

contributed in a big way to the successes I've had throughout this process, and I am sincerely grateful for the personal and experimental guidance each one of you has provided me with.

To my mentor and friend, Dr. Jon Sprague, thank you for inspiring me with your love of science, your faith in me as a researcher, and your continued support of me throughout my scientific career.

To the miLEAD community, thank you for all of the training, mentorship, opportunity, and fun that we shared together as part of our projects. To the 2022 Midwest Healthcare Case Competition Organizing Team, especially Dr.'s Ish Mawla and Sydney Smith, thank you for taking me under your wing and pushing me to help accomplish something so special, and I'm massively grateful for everything you taught me in the consulting world.

To the Fast Forward Medical Innovation Team, especially Dr. Jon Servoss and Ashley Schorck, thank you for the valuable training you gave me as part of my fellowship. I look forward to using the knowledge and skills that you have imparted to me as I move into the next stage of my career.

To my partner, Manna, the grace, patience, and laughter that you have brought into my life throughout the past few years have made an untold difference. I'm eternally grateful for your constant support, care, and friendship.

And finally, to my friends and family… Will, Karly, Alejandro, Amal, Max, and Luke, and most importantly to my Mom, Dad, and my brother Mike, thank you all for believing in me to achieve my dreams and the ways in which you have all supported me throughout my academic career. Your love, presence, and the smiles and experiences we have shared have been great comforts to me and the wind in my sails as I undertook this challenge.

Table of Contents

List of Figures

Abstract

Cardiac fibrosis is characterized by maladaptive accumulation of collagen and extracellular matrix (ECM) components in the heart, a condition that decreases cardiac function and accelerates heart failure. Cardiac fibroblasts, the principal cellular mediators of cardiac fibrosis, are normally quiescent, though injury-related signals trigger their activation and increases in their proliferation, migration, and synthesis and secretion of ECM materials. While a number of cardiac fibroblast activation pathways are established, much remains unknown about how these pathways are regulated, in part from the difficulty of their study in vitro posed by their spontaneous activation in non-physiologic stiffness conditions present in cell culture. The post-translational lipid modification known as palmitoylation, mediated by a family of enzymes called S-acyltransferases, has emerged as a critical regulator of disease signaling, though little is known of how palmitoylation influences pathways in the heart. Recently, pro-fibrotic signaling pathways have been shown to be regulated by palmitoylation in other cell types by the S-acyltransferases zDHHC3 and zDHHC7, including the GTPase Rac1, stressing the need to explore the possibility that palmitoylation is regulating adult cardiac fibroblast (ACF) signaling. We hypothesized that deletion of *Zdhhc3*, *Zdhhc7*, or their combined deletion in ACFs would result in blunted fibroblast activation and reduced fibrosis in vivo. Further, we hypothesized that ACFs with impaired Rac1 palmitoylation (Rac1 ConKI) would show reduced activation in vitro. To test these hypotheses, a physiologic-stiffness polydimethylsiloxane (PDMS) coverslip coating protocol was developed to maintain ACF quiescence in vitro. *Zdhhc*3 fl/fl mice and whole-body *Zdhhc7* knockout (KO) mice were used to test for changes in ACF activation in vitro and cardiac

fibrosis in vivo, and our newly developed Cre-inducible Rac1 palmitoylation-deficient mutant knock-in mouse model (Rac1 ConKI) was used to test for changes in ACF activation in vitro. *Zdhhc3* KO ACFs in vitro responded comparably to controls in migration and levels of TGFβ1-induced α-smooth muscle actin (αSMA, hallmark activated fibroblast marker) expression, and levels of the fibroblast marker genes *Postn* and *Tcf21*. Using an in vivo pressure overload model of cardiac injury, no significant differences were observed in cardiac function, hypertrophy, or fibrosis in myofibroblast *Zdhhc3* KO mice compared to controls. *Zdhhc7* KO and *Zdhhc3/7* KO ACFs in vitro exhibited reduced *Postn* expression in response to TGFβ1 compared to controls, though no significant differences were observed in collagen gene expression or nuclear factor of activated T cells (NFAT) transcription factor activity. A migratory defect was present in *Zdhhc7* KO ACFs, and a downward trend was seen in *Zdhhc3/7* KO ACFs compared to controls. In vivo, hypertrophy and contractility in response to chronic angiotensin II/phenylephrine (AngII/PE) infusion were unchanged in *Zdhhc7* KO and cardiac fibroblast-specific *Zdhhc3/7* KO mice compared to controls. *Zdhhc7* and *Zdhhc3/7* KO mice similarly exhibited comparable fibrotic gene mRNA levels in response to AngII/PE, and no significant differences were detected in ventricular fibrosis. Rac1 ConKI ACFs had increased levels of stress-inducible NFAT and SRF transcription factor activity, though showed no differences in αSMA expression or fibrotic gene mRNA levels compared to controls when treated with TGFβ1, nor were changes observed in migration. These data suggest that ACF zDHHC3 and zDHHC7 are not essential for the development of cardiac fibrosis and that TGFβ1-induced ACF activation is not dependent on Rac1 palmitoylation. Future experiments will focus on identifying key S-acyltransferases and palmitoylated substrates involved in the cardiac fibroblast activation process.

Chapter I: Palmitoylation-mediated Regulation of Cardiac Fibroblast Signaling Pathways

Cardiovascular Disease Health Burden

Cardiovascular disease (CVD), in its many forms, remains an immense public health issue both in the United States and globally (Martin et al., 2024). Per 2021 data, CVD represented the leading cause of mortality in the US and was directly implicated in more deaths than cancer, COVID-19, and stroke (Xu et al., 2022). CVD patients suffer from symptom profiles including pain, fatigue, reduced stamina, and shortness of breath, and as a result can experience a dramatically reduced quality of life (Jurgens et al., 2022). Necessary treatments for CVD can be extremely costly even when life-saving treatment is not required, and it is estimated that the combined direct and indirect costs of CVD in the United States between 2019 and 2020 in summation were over 423 billion USD (Martin et al., 2024). Individuals experiencing various types of CVD may also exhibit a reduced ability to maintain gainful employment, increasing the economic burden component of these diseases, with the cost of lost annual income as a result of CVD exceeding 200 billion USD (Weintraub, 2023). Furthermore, the advancement of CVD can eventually lead to the development of heart failure, where the heart is insufficiently able to pump enough blood to meet the metabolic demands of the body, leading to fatal outcomes (Schwinger, 2021). Collectively, it is estimated that CVD results in a death occurring every 34 seconds in the United States, according to the American Heart Association (Martin et al., 2024). As such, significant efforts have been undertaken to understand the pathophysiology of many different types of CVD to determine novel treatment strategies and reduce loss of life (Frąk et al., 2022; Schwinger, 2021; Severino et al., 2020).

One major area of advancement in our understanding of heart biology involves insights into how the heart compensates and adapts in response to stressors incurred in patients with CVD (López et al., 2021; Nakamura & Sadoshima, 2018; Schirone et al., 2017). Throughout the progression of many CVDs, changes in cardiac workload can lead to remodeling in the form of structural alterations to heart composition (Azevedo et al., 2016; Wu et al., 2017). In addition to hypertrophic remodeling, where ventricular size increases to meet increased cardiac workload (Bazgir et al., 2023; Nakamura & Sadoshima, 2018), one key area of remodeling that accompanies many types of CVD involves changes to the extracellular matrix (ECM) (Frangogiannis, 2017; Silva et al., 2020). The ECM is a structural network of proteins and proteoglycans assembled throughout tissues to provide support and stability for cellular activities, movement, and communication (Frangogiannis, 2017; Muncie & Weaver, 2018; Silva et al., 2020). Efficient contraction of the heart relies upon the sturdy yet flexible cellular support structure provided by the ECM, which ensures cardiomyocytes can mechanically and electrically couple with each other to coordinate the heartbeat (Silva et al., 2020). Thus, homeostatic maintenance of the ECM in the heart is crucial for healthy heart function (Frangogiannis, 2019). However, a variety of CVDs can contribute to dysregulations in ECM structure, leading to the overaccumulation of ECM and resultant deleterious effects on cardiac function (Kim et al., 2000; Silva et al., 2020). Maladaptive dysregulation of cardiac ECM that leads to reduced cardiac function is collectively known as cardiac fibrosis, and there are varying types and degrees of severity depending on the precipitating conditions (Frangogiannis, 2021; López et al., 2021).

In the past few decades, cardiac biologists have dramatically increased their attention on the role of scar formation in the heart and cardiac fibrosis, as well as its contributing role in CVD (Frangogiannis, 2021; López et al., 2021; Ravassa et al., 2023). Cardiac fibrosis is a condition

characterized by the excess accumulation of scar tissue in the heart and often exists comorbidly with common diseases such as hypertension (Díez, 2007; Kuwahara et al., 2004; Narayanan et al., 2023), diabetic cardiomyopathy (Cheng et al., 2023; Russo & Frangogiannis, 2016; Tuleta & Frangogiannis, 2021; van den Borne et al., 2010), and is perhaps most well-known for its involvement in myocardial infarction (MI) (Hinderer & Schenke-Layland, 2019; Liang et al., 2019). Cardiac scar formation can be essential for maintaining the structural integrity of the heart, and in the context of MI, when a large population of cardiomyocytes dies, it is often a life-saving response to the consequences of cardiomyocyte death after a heart attack (Shinde & Frangogiannis, 2014; van den Borne et al., 2010). “Replacement” fibrosis, or scarring of the infarct zone, prevents deadly rupture events when pressurized ventricular tissue is weakened, even if that scarring cannot provide the functional capacities of the cardiomyocytes that preceded it (Talman & Ruskoaho, 2016; Travers et al., 2016). From this vantage point, the formation of these scars can be a valuable and necessary response to cardiac injury. However, increased accumulation of cardiac scarring can impact cardiac function by impairing both contraction and relaxation of the heart (Ma et al., 2018). The development of these scars in response to MI, as well as additional fibrotic responses observed in the heart, such as in response to pressure overload, contribute to the reduction in heart function and acceleration towards heart failure (Hara et al., 2017; Schimmel et al., 2022).

In other non-MI diseases, maladaptive accumulation of ECM can additionally occur (Hara et al., 2017; Schimmel et al., 2022; Travers et al., 2016). Often referred to as “reactive” fibrosis, cardiac scarring can be present throughout the cardiac interstitium, commonly within the left ventricle (Hara et al., 2017; Schimmel et al., 2022). In less developed cases, minor scarring is relatively inconsequential and may not result in any functional consequences to the heart.

Though as it increases in severity, interstitial fibrosis can begin to interfere with cardiomyocyte communication, and the mechanical and electrical coupling of cardiomyocytes can be impaired to an extent that prohibits efficient contraction and relaxation of the heart (H. Liu et al., 2022; Pellman et al., 2016; Reed et al., 2011). Severe changes to the ECM through excessive scar formation and alterations in fibroblast/cardiomyocyte communication have additionally been shown to be responsible for potentiating arrhythmia (Kazbanov et al., 2016; Nguyen et al., 2014; Pellman et al., 2016; Schiau et al., 2021). The resultant loss of function from decreased contractile ability, as well as arrhythmogenesis, can contribute to a patient developing heart failure (Hinderer & Schenke-Layland, 2019). Further, at present cardiac fibrosis is generally considered to be irreversible in most cases (Nagaraju et al., 2019). As cardiac fibrosis worsens, the potential for adverse events becomes elevated, contributing to the acceleration of fatal outcomes (Ravassa et al., 2023; Webber et al., 2020).

In response to the major economic consequences and loss-of-life associated with CVD, cardiac fibrosis, and heart failure, significant work has been performed towards research that aims to generate effective therapeutic modalities, which over the years have included small molecules, biologics, and even Car-T strategies (Morfino et al., 2023; Raziyeva et al., 2022; Ren et al., 2023; Travers et al., 2022). Unfortunately, efforts towards the treatment of cardiac fibrosis have largely been non-viable clinically, and at present, there are no known clinically approved primarily anti-fibrotic therapies indicated for this condition (Morfino et al., 2023). As such, future examination is critically needed to determine novel targets and develop therapies for the prevention, treatment, and reversal of cardiac fibrosis.

Cardiac Fibroblasts and Pro-Fibrotic Signaling

Cardiac Fibroblast Activation and ECM Remodeling

In order to understand the cellular basis for the development of cardiac fibrosis, increasing attention has been shifted to elucidating the biology of its principal mediator, the cardiac fibroblast (CF) (Ivey & Tallquist, 2016; Souders et al., 2009; Tallquist & Molkentin, 2017). CFs are one of the most abundant non-myocyte cell types in the heart (Camelliti et al., 2005), and while estimations vary, recent reports indicate that they represent upwards of ~30% of observed cells in the healthy heart (Tucker et al., 2020). Exploring the many ways in which CFs contribute to the regulation of the heart has become an exciting frontier in cardiac biology, in the hopes that increasing our understanding of these cells may allow us to modulate their activity in the future to prevent, treat or even reverse fibrosis in the heart.

As part of these investigations, significant advances have been made in recent years toward characterizing the many roles of CFs in the heart (Fu et al., 2020; Kanisicak et al., 2016; Tallquist & Molkentin, 2017). CFs predominantly arise from both the epicardium and endocardium and at present, it is generally understood that the collective responses of these cells are consistent both at baseline and during injury despite differences in embryonic origin (Tallquist, 2020). Amongst their most important roles in the heart is the generation and maintenance of the cardiac ECM (Humeres & Frangogiannis, 2019). This function is primarily accomplished through the production of both structural and functional proteins that compose the ECM, including collagen types I and III, fibronectin, proteoglycans, and glycoproteins (Fan et al., 2012; Humeres & Frangogiannis, 2019; Sarohi et al., 2022). These structural proteins are secreted and arranged into their matrix composition to provide a stable environment for cardiac cells to arrange into tissue and additionally serve as a functional substrate for the transmission of

mechanical signals throughout the heart (Fan et al., 2012; Song & Zhang, 2020). Critically, continuously maintaining the ECM to achieve a balance between secretion and degradation is required to provide the proper homeostatic environment for cardiomyocyte communication and contraction (Fan et al., 2012). This maintenance process is achieved in part through CF-mediated secretion of metalloproteinases (MMPs) (Creemers et al., 2001; Fan et al., 2012; Ridwan et al., 2023). MMPs are responsible for the degradation of the ECM, and the sensing of the cardiac microenvironment by CFs enables them to regulate ECM homeostasis through the release of MMPs or, alternatively, through the release of tissue inhibitors of metalloproteinases (TIMPs) to either up- or down-regulate changes in ECM formation (Creemers et al., 2001; Fan et al., 2012). In doing so, the ECM is maintained in such a way that it provides an optimal environment for cardiac function and contraction.

In the event of injury-related signaling processes associated with many CVDs, major changes in CF activity can occur, and as a result, dramatic alterations to the structure of the ECM in the heart (Fan et al., 2012; Frangogiannis, 2021; Humeres & Frangogiannis, 2019). In the case of myocardial infarction, for example, chemical signals in the cardiac microenvironment can trigger changes in CF activity that allow for an adequate response to injury (Humeres & Frangogiannis, 2019; Shinde & Frangogiannis, 2014). Cardiac injury can trigger the release of damage-associated molecular patterns (DAMPs) and cytokines to the cardiac microenvironment (Chen & Frangogiannis, 2013; Turner, 2016), and when sensed by CFs, induce multi-phasic morphological and phenotypic changes in these cells (Gibb et al., 2020; Humeres & Frangogiannis, 2019; Kanisicak et al., 2016).

In the immediate response to these signals, CFs undergo an upregulation in their own inflammatory signaling molecule secretion, including tumor necrosis factor α (TNFα),

interleukin 1β (IL-1β), MMPs, and chemokine monocyte chemoattractant protein-1 (MCP1), and in turn promote the recruitment of immune cells critical for the injury response and the facilitation of dead cell clearance (Humeres & Frangogiannis, 2019; Souders et al., 2009). To begin scar formation, pro-fibrotic signaling molecules present in the injured heart, such as transforming growth factor β 1 (TGFβ1), angiotensin II (AngII), and cytokines such as interleukin-6 (IL6), stimulate CFs to transition into an "activated" state (Figure 1.1). This activation process primarily involves increased cellular proliferation, cytokine production and release, and synthesis and deposition of collagen and other ECM proteins that will be used in the formation of scar tissue (Bertaud et al., 2023; Jiang et al., 2021; Umbarkar et al., 2021). This transition into the canonical "myofibroblast" is characterized by increased expression of activated fibroblast marker genes *Postn*, *Col1a1*, *Col3a1*, *Nox4*, and *Thbs4*, as well as the expression and cytoskeletal incorporation of the hallmark activated fibroblast protein α-smooth muscle actin (αSMA) (Chaffin et al., 2022; Kanisicak et al., 2016; Shinde et al., 2017; Tallquist & Molkentin, 2017). Myofibroblast activation is key to the wound healing process and the development of protective scar tissue (Chen & Frangogiannis, 2013; Fu et al., 2018; Tallquist, 2020; Tallquist & Molkentin, 2017). Chronic myofibroblast activation is also observed in the heart in other types of CVD outside of the context of myocardial infarction. In the pressure-overloaded heart, similar pro-fibrotic chemical signaling patterns can be recognized by these cells, resulting in myofibroblast activation and, ultimately, reactive interstitial fibrosis that can contribute to the worsening of heart function and contribute to heart failure (Nagalingam et al., 2022; Tallquist, 2020). In addition to chemical stimuli, CFs possess mechanosensitive signaling systems that allow them to sense changes in the stiffness and mechanical strain of the heart (Pesce et al., 2023; Tian & Ren, 2023). Collectively, the combinatorial influences of these

chemical and mechanical pro-fibrotic signals and their effectors elicit the ECM dysregulation and cardiac fibrosis observed accompanying many types of CVD.

CFs serve a variety of important functions in the heart, from maintaining the ECM, modulating cardiac immune responses, and responding to injury (Pesce et al., 2023; Tallquist, 2020). While CF activation in response to injury plays an essential role in survival, chronic myofibroblast activity in the absence of cardiomyocyte death represents a significant contribution to the development of heart failure (Fan et al., 2012; Nagalingam et al., 2022). The complex mechanisms involved in the facilitation of CF responses in the heart are not fully understood, but a variety of major ligand/receptor systems and their downstream signaling axes have begun to be elucidated (Bertaud et al., 2023; Jiang et al., 2021; Umbarkar et al., 2021). Continual investigations into myofibroblast signaling mechanisms seek to characterize the nuances of CF activation pathways and establish a solid understanding of how they elicit the dynamic responses of this critical cardiac cell type.

Notable Cardiac Fibroblast Activation Signaling Pathways

In order to establish a deeper understanding of myofibroblasts and the signaling pathways that underlie their activation, many groups have sought to elucidate the mechanisms responsible for the dynamic regulation of these cells at baseline and in response to injury (Bertaud et al., 2023; Umbarkar et al., 2021). In doing so, a number of key signaling axes have been demonstrated to underlie the myofibroblast transition and contribute to increases in the development of fibrosis.

TGFβ1/SMAD2/3 Signaling

One of the most important pathways that has been established in the fibroblast to myofibroblast transition is the TGFβ1/SMAD2/3 signaling axis (Hanna et al., 2021; Khalil et al.,

2017). TGFβ isoforms 1,2 and 3 are a family of cytokine signaling proteins that bind to TGFβ receptors (I, II), and upon ligand binding, these receptors canonically signal through a family of effector proteins/transcription factors known as mothers against decapentaplegic (SMADs) (Heldin & Moustakas, 2016). In the context of pro-fibrotic signaling, the binding of TGFβ1 to transforming growth factor β receptor II (TGFβRII) at the plasma membrane of CFs promotes recruitment of their main effectors SMAD2/3 (Hu et al., 2018). SMAD2/3 phosphorylation by receptor kinase activity drives disassociation from the receptor and binding with cytosolic SMAD4, and upon complex formation, nuclear localization of the complex results in changes in gene expression related to proliferation, myofibroblast activation, and collagen synthesis (Hu et al., 2018).

Due to the importance of TGFβ1 in inducing the myofibroblast transition, its influence on cardiac remodeling has been extensively characterized (Dobaczewski et al., 2011; Frangogiannis, 2020; Frangogiannis, 2022). TGFβ1 has become an essential agonist for experiments analyzing in vitro CF activation, as treatment of quiescent CFs with TGFβ1 results in a dramatic increase in αSMA expression and myofibroblast induction (Luo et al., 2017; Mia et al., 2014; Ranjan et al., 2021). A variety of groups have investigated the consequences of interrupting TGFβ1/SMAD2/3 signaling in order to determine the downstream effects on CF activation and fibrosis. Removal of TGFβ receptors through fibroblast-specific deletion of *Tgfbr1/2* resulted in a significant reduction in the development of cardiac fibrosis in mice subject to 12-weeks of transverse aortic constriction (TAC)-induced pressure overload (Khalil et al., 2017). Further, mice with fibroblast-specific deletion of *Smad2* and *Smad3* exhibited significantly reduced levels of activated CFs in response to 7-day TAC, as well as reductions in myocardial fibrosis in *Tgfb1*-overexpressed transgenic mice (Khalil et al., 2017). Selective deletion of *Smad3* alone resulted in an equal

reduction in fibrosis compared to *Smad2/3* deletion, suggesting that the pro-fibrotic effects of TGFβ1 are more dependent on SMAD3 than SMAD2 (Khalil et al., 2017). Other studies have provided additional evidence for this effect, as in vivo cardiac fibroblast-specific deletion of *Smad3* in fibroblasts via an inducible *Col1a2*-promotor significantly reduced histological measures of myocardial collagen content at baseline, as well as reductions in mRNA levels of *Col1a1*, *Col2a1*, *Col4a1*, and *Thbs1*, whereas cardiac fibroblast-specific *Smad2* knockout mice exhibited comparable responses to controls in these measures (Huang et al., 2020). Through explorations into signaling upstream of TGFβ1 activity at its receptors, it was recently determined that high-temperature requirement A serine peptidase 3 (Htra3) regulates the development of fibrosis in the injured heart through degradation of TGFβ1, thus maintaining the quiescent state of fibroblasts (Ko et al., 2022). Whole-body *Htra3* knockout mice yielded significant upregulation of phosphorylated SMAD2/3 in both sham and TAC groups, as well as a significant increase in fibrosis in the heart in response to TAC compared to controls (Ko et al., 2022). Thus, the interruption of TGFβ1/SMAD2/3 signaling can result in major changes to the CF activation in vitro and in vivo.

In addition to canonical SMAD signaling, non-canonical pathways induced by TGFβRII activation have also been characterized. In particular, effectors in the mitogen-activated protein kinases (MAPK) family with known roles in proliferation, differentiation, and inflammation (Cargnello & Roux, 2011) have been demonstrated to play crucial roles in fibroblast activity and the development of fibrosis in vivo (Frangogiannis, 2020; Molkentin et al., 2017; Turner & Blythe, 2019). p38 MAPK is known to be activated by mitogen-activated protein kinase kinase 3/6 (MKK3/6) downstream of TGFβRs, independent of SMAD, and then activate downstream signaling effectors including the transcription factor nuclear factor kappa-light-chain-enhancer of

activated B cells (NFκB) and the transcription coactivator yes-associated protein (YAP) which upregulate cytokine release and collagen synthesis from their activity in mediating transcriptional changes in the nucleus (Francisco et al., 2020; Lu et al., 2021; Umbarkar et al., 2021). Deletion of p38 in fibroblasts in vivo was shown to reduce cardiac myofibroblast transition as well as result in a significant reduction in fibrosis induced through an ischemia/reperfusion injury model (Molkentin et al., 2017). Further, phosphorylation of extracellular signal-regulated kinase 1/2 (ERK1/2) is significantly upregulated in response to TGFβ1 in CFs (Luo et al., 2017; Peng et al., 2010), and in vitro administration of PD98059, an ERK inhibitor, has been shown to abrogate TGFβ1-induced pro-fibrotic effector activity, including reducing myocardin related transcription factor A (MRTF-A) nuclear localization.

Recent discoveries of TGFβ1 signaling in CFs have provided insights into how Wnt/β-catenin regulates myofibroblast proliferation and fibrosis. The Wnt/β-catenin pathway has become increasingly recognized for its role in regulating cell homeostasis, proliferation, and migration, with known roles in the disease signaling of cancer, pulmonary disorders, CVD, and Alzheimer's disease (J. Liu et al., 2022). Mechanistically, binding of Wnt to the extracellular portion of the transmembrane Frizzled receptor activates downstream de-phosphorylation of β-catenin, facilitating its nuclear localization and binding to T-cell factor/lymphoid enhancer factor (TCF/LEF) to initiate transcriptional changes (Cadigan & Waterman, 2012; J. Liu et al., 2022). In vitro administration of secreted Frizzled-related protein 2 (sFRP2), an endogenous inhibitor of Wnt, completely abrogated TGFβ1-induced increases to CF αSMA expression and mRNA levels of pro-fibrotic genes, including *Col1a1*, *Fn1*, and *Tnc* (Blyszczuk et al., 2017). Further, in vivo deletion of β-catenin in CFs significantly reduced levels of fibrosis and hypertrophy following an 8-week TAC exposure (Xiang et al., 2017). β-catenin deletion additionally yielded a protective

effect on cardiac function, with *Ctnnb1* KO animals exhibiting significant improvements in contractility as measured by ejection fraction and fractional shortening (Xiang et al., 2017). Together, these data highlight the major importance of TGFβ1 and its associated signaling axes in CF activation and the development of cardiac fibrosis in vivo.

Angiotensin II/Ga_q Signaling

Another critical regulator of fibroblast activation is the renin-angiotensin-aldosterone-system (RAAS) peptide angiotensin II (AngII) (Forrester et al., 2018). AngII is well known as a major contributor to cardiac remodeling in terms of both hypertrophy and fibrosis, and circulating levels of AngII are increased in response to myocardial infarction and other CVDs inducing pressure or volume overload (De Mello & Danser, 2000). Signaling of this peptide is mediated through binding to the plasma membrane-localized angiotensin II receptor type I (AT1R), a G-protein coupled receptor (GPCR) that primarily couples to G-alpha q (Ga_q) (Forrester et al., 2018). Upon binding of AngII to AT1R, Ga_q dissociates from the receptor and initiates its signaling primarily through the activation of phospholipase C (PLC) (Kamato et al., 2015). PLC activation mediates the conversion of membrane-bound phosphatidylinositol 4,5-bisphosphate (PIP2) into the second messenger's inositol trisphosphate (IP3) and diacylglycerol (DAG) (Bill & Vines, 2020; Putney & Tomita, 2012). IP3 can then localize to the endoplasmic reticulum, bind to IP3 receptors, and initiate Ca^{2+} release that initiates a host of effects, notably calmodulin-calcineurin-mediated increases in activity of the pro-fibrotic transcription factor nuclear factor of activated T cells (NFAT) (Bill & Vines, 2020; Lighthouse & Small, 2016; Park et al., 2020). DAG can also lead to downstream intracellular Ca^{2+} increases, as well as activate protein kinase C (PKC) (Black & Black, 2012). PKC contributes to the activation of a wide spectrum of downstream effectors implicated in fibroblast signaling including MAPKs, Rho

GTPases, MMPs, and the transcription factors NFAT and NFκB (Lim et al., 2015; Trappanese et al., 2016). Activation of AT1R by AngII can also increase pro-fibrotic intracellular oxidative stress and reactive oxygen species (ROS) through activation of nicotinamide adenine dinucleotide phosphate (NADPH) oxidases like Nox4, and mRNA levels of this enzyme serve as a marker for activated CFs (Chaffin et al., 2022; Cucoranu et al., 2005; Hecker et al., 2009; Wen et al., 2012).

The effects of AngII on CFs are well characterized both in vitro and in vivo, and stimulation of these cells with AngII induces an upregulation in proliferation, migration, adhesion, ECM synthesis, and cytokine release (Chen et al., 2004; Kawano et al., 2000; Schnee & Hsueh, 2000). CFs treated with AngII exhibited a dose-dependent increase in collagen type I protein levels, a marked increase in intracellular ROS, and mRNA level increases of *Col1a1*, *Col3a1*, and *Acta2* (Chen et al., 2004; Francisco et al., 2020). In other works, treatment of CFs with AngII in vitro resulted in a significantly heightened expression of αSMA and the incorporation of αSMA into the cytoskeleton (Bai et al., 2013; Cao et al., 2018; Wu et al., 2021). In vivo, infusion of AngII is one of the most common models of cardiac injury due to its effectiveness in inducing ROS generation, inflammation, elevated pro-fibrotic gene mRNA levels, and cardiac fibrosis in mice (Cao et al., 2018; García-Martín et al., 2021; Lyu et al., 2021; Z.-G. Ma et al., 2023; Matsumoto et al., 2013; Pan et al., 2012). As such, AngII plays an essential role in regulating CF activation, and its upregulation is a major contributor to the progression of myocardial fibrosis (Murphy et al., 2015).

Mechanical Stress/YAP/TAZ Signaling

Unlike other organs, the unique functions of the heart lead to the generation of physical forces that are constantly changing at baseline and throughout the process of cardiac remodeling

(Garoffolo & Pesce, 2019). The mechanical properties of the heart, such as stiffness, mechanical tension, stretch, and pressure, are subject to substantial changes as a result of injury, and CFs continuously sense the cardiac microenvironment in order to respond appropriately in their regulation of ECM deposition and turnover (X. Li et al., 2022; Pesce et al., 2023; Tian & Ren, 2023).

While ligand/receptor interactions play a major role in these responses, the heart possesses specialized mechanisms to specifically sense changes to these forces and modify their cellular responses accordingly (Pesce et al., 2023; Tian & Ren, 2023). CFs utilize mechanosensitive machinery, including integrins, cadherins, and focal adhesions, to convert mechanical stimuli outside of the cell into changes in intracellular signaling cascades that regulate their responses (Pesce et al., 2023; Tian & Ren, 2023). Further, certain receptor subtypes, including AT1R as previously described, have also been shown to be activated by mechanical stretch and contribute to these signaling pathways (Yatabe et al., 2009). Using these mechanisms, CFs possess the ability to sense changes in mechanical parameters that can occur as a result of CVD in order to modify their responses and regulate the ECM (Pesce et al., 2023; Tian & Ren, 2023).

One of the most important signaling pathways that orchestrates the intracellular transduction of mechanosensitive signaling processes involved in CF activation is the Hippo/YAP/TAZ pathway (Del Re, 2022; Landry & Dixon, 2020; Mia et al., 2022; Mia & Singh, 2022). Yes associated protein (YAP) and transcriptional coactivator with PDZ-binding motif (TAZ) are transcriptional coactivators who primarily signal through their activation of TEA domain transcription factors (TEADs) in the nucleus (Guo & Zhao, 2013; Lin et al., 2017). The role of TEADs in other cell types is well characterized, and these proteins are known to

coordinate the transcription of target genes associated with tumorigenesis, invasion, adhesion, proliferation, and migration (Wang et al., 2022; Zhou et al., 2016). The YAP/TAZ interaction with TEADs is actively downregulated through the activation of kinases composing the Hippo signaling pathway (Rausch & Hansen, 2020; Werneburg et al., 2020). In the "Hippo-on" state, the cytosolic kinases large tumor suppressor kinase 1 and 2 (LATS1/2) maintain the phosphorylation of YAP/TAZ, a post-translational modification that prevents its nuclear localization (Rausch & Hansen, 2020; Werneburg et al., 2020). However, extracellular changes, including those involving ECM stiffness and stretch detected by integrins and focal adhesions, can inactivate this inhibition of YAP/TAZ nuclear localization in what is known as the "Hippo-off" state (Rausch & Hansen, 2020; Werneburg et al., 2020)., In the Hippo-off state, decreases in kinase activity upstream of LATS1/2 result in its de-phosphorylation, and as the phosphorylation state of LATS1/2 gives rise to its enzymatic ability, this process results in increased dephosphorylation of YAP/TAZ thus increasing YAP/TAZ nuclear localization and transcriptional changes (Rausch & Hansen, 2020; Werneburg et al., 2020).

The consequences of interrupting LATS1/2 and YAP/TAZ signaling on CF activation are well established, and this pathway has now been demonstrated as a crucial regulator of fibroblast responses at baseline and in response to injury (Del Re, 2022; Mia & Singh, 2022). In vitro, overexpression of YAP in neonatal rat CFs significantly increased αSMA expression and mRNA levels of *Col1a1*, *Col3a1*, and *Tgfb1*, as well as induced a significantly increased contraction of collagen gels (Francisco et al., 2020). Adeno-associated virus-mediated overexpression of YAP in CFs in vivo has been shown to significantly upregulate fibrosis and mRNA levels of *Col1a1*, *Col3a1*, and *Tgfb1*(Francisco et al., 2021). In a fibroblast-specific *Lats1/2* KO mouse model, *Lats1/2* KO mice developed a spontaneous fibrotic phenotype in the heart and reduced cardiac

output in the absence of injury (Xiao et al., 2019). Further, *Lats1/2* KO mice subject to MI exhibited extremely high levels of fibrosis compared to controls, an effect that was partially rescued by the concurrent knockdown of YAP/TAZ (Xiao et al., 2019). Investigations into the consequences of YAP deletion in fibroblasts discovered that fibroblast-specific *Yap* KO mice subject to MI exhibited a significantly lower population of activated fibroblasts, which corresponded with less pro-fibrotic gene expression, fibrosis, and improved contractility (Francisco et al., 2020). Overall, these data highlight that YAP/TAZ signaling contributes significantly to the development of CF activation and cardiac fibrosis.

Another intriguing facet of CF mechanosensation is its involvement in CF activation in cell culture, as commonly occurs with in vitro experimentation. The sensitivity of CFs to mechanical stiffness has contributed to challenges in their study in vitro, as the physical properties of traditional cell culture vary greatly from that of their endogenous environment (Felisbino et al., 2024; Gałdyszyńska et al., 2021; Hall et al., 2023; Landry et al., 2019). Stiffness is measured through a rating system known as Young's modulus in units of Pascals, and the Young's modulus of the adult heart is estimated to be between 5-40 kPa (Emig et al., 2021; Wells, 2013). Traditional two-dimensional (2D) cell culture plastic and glass, however, yield ratings of ~1 GPa to 70 GPa, respectively, which are orders of magnitude greater than the endogenous environment in the heart (Acevedo-Acevedo & Crone, 2015). Consequently, spontaneous activation of isolated quiescent fibroblast in culture occurs almost immediately, which can pose difficulties in experimental procedures that rely on baseline inactivation (Landry et al., 2019). To navigate this, a number of groups have pioneered the use of modified substrates with Young's moduli approximating that of the endogenous environment in attempts to increase the physiological relevance of in vitro studies with these cells (Childers et al., 2021; Felisbino et

al., 2024; Landry et al., 2019, 2021). CFs plated on substrates from 4-8 kPa exhibit a marked reduction in spontaneous activation, allowing for prolonged quiescence in culture and increased ability to induce meaningful activation with agonists/treatments as part of experimentation (Childers et al., 2021; Felisbino et al., 2024; Landry et al., 2019, 2021). These models provide a useful tool for future work related to in vitro analyses of cardiac fibroblast activation.

IL6/JAK/STAT Signaling

In addition to TGFβ1, the pro-inflammatory cytokine IL6 has also been shown to regulate CF activation and fibrosis in part through its activation and involvement with the Janus kinase/signal transducer and activator of transcription (JAK/STAT) signaling pathway (Y. Li et al., 2022). IL6 commonly serves as a regulator of inflammation and is secreted from a wide variety of cells in the heart, including monocytes, macrophages, and cardiomyocytes, and recent work provides evidence that fibroblasts themselves are the major contributor of IL6 production and secretion in response to myocardial infarction (Alter et al., 2023; Y. Li et al., 2022). Release of IL6 triggers cellular transformation, wound repair, autophagy, and apoptosis (Y. Li et al., 2022). IL6-mediated signaling is predominantly through the JAK/STAT pathway, which has been implicated in a variety of diseases related to inflammation, including fibrosis, irritable bowel disease, and many types of cancers (Hu et al., 2018; Hu et al., 2023). Initiation of this signaling pathway involves IL6 binding to the interleukin-6 receptor (IL6R), a membrane-bound cytokine receptor (Wolf et al., 2014). IL6R at the plasma membrane associates with non-receptor tyrosine kinases such as Janus kinase 1 (JAK1) and Janus kinase 2 (JAK2), and phosphorylation mediated by JAK1 and JAK2 induce the activation of the main IL6R effector, STAT3, in its monomeric form (Harrison, 2012). Upon phosphorylation, phosphorylated-STAT3 homodimers are formed

in the cytosol and then translocate to the nucleus to mediate transcriptional changes in the inflammatory response (Harrison, 2012; Hu et al., 2023).

As part of works to investigate the influence of IL6 on CF activation, it was found that the treatment of cultured murine CFs with IL6 induced significant increases in pro-fibrotic marker gene expression (Zhang et al., 2016). Mice experiencing diabetic cardiomyopathy exhibited consistent upregulation of protein levels of collagen I and III in the heart, and notably, these effects were significantly abrogated in whole-body *Il6* KO mice, suggesting a role for IL6 in their expression in vivo (Zhang et al., 2016). At the tissue level, a reduction in collagen in histological sections of the heart was also observed in *Il6* KO mice (Zhang et al., 2016). Further, IL6 treatment of rat CFs resulted in a significant increase in αSMA expression, as well as stimulated increased collagen gel contraction relative to controls (Meléndez et al., 2010). In fibroblast-like hepatic stellate cells, IL6 treatment elicited a dose-dependent increase in *Acta2* mRNA levels and significant increases in both phosphorylated STAT3 and p38 (Kagan et al., 2017). Finally, chronic infusion of IL-6 in adult rats induced a 3-fold increase in interstitial fibrosis, as well as a significant increase in ventricular concentric hypertrophy (Meléndez et al., 2010). Thus, it is clear that IL6 is notably involved in the regulation of CF activation, and its signaling significantly contributes to the development of myocardial fibrosis.

The signaling pathways that underlie CF activation and scar formation are complicated, and their responses are determined by the influence of a wide variety of inflammatory molecules, signaling ligands, and mechanical stimuli (Bertaud et al., 2023; Umbarkar et al., 2021). There is significant evidence detailing major intra- and intercellular crosstalk in these signaling pathways, including between fibroblasts and other cell types in the heart, where one pathway further contributes to activation of additional pathways in a feed-forward mechanism (Alter et al., 2023;

Kapur, 2011; J. C. Li et al., 2023; Ma et al., 2012; Nicin et al., 2022; Uscategui Calderon et al., 2023; Van Linthout et al., 2014). The complex interplay of these activation mechanisms ultimately regulates the dynamic responses observed in CFs in the heart (Zeigler et al., 2016). As such, further work is required to characterize the relative contributions of these signaling pathways towards the homeostatic maintenance of the ECM and scar formation in response to injury (Kong et al., 2014; Zeigler et al., 2016). One area of future investigation into the regulation of these pathways is the contribution of the post-translational modifications in fine-tuning these cellular responses at the protein level.

The Role of Palmitoylation in Signaling and Disease

Palmitoylation, a Reversible Lipid Modification

While great strides have been made in uncovering major signaling axes involved in CF activation, there is still much to be done toward elucidating how the relevant signaling molecules in these pathways are fine-tuned to produce the dynamic and context-dependent responses of these cells. One area of continual investigation seeks to determine how post-translational modifications (PTMs) direct signaling pathways, influence downstream receptor responses, orchestrate gene expression changes, and ultimately alter cellular responses in the context of disease (Kitamura & Galligan, 2023; Zhong et al., 2023). Of the many currently under investigation, one PTM of particular interest is palmitoylation, which describes a type of reversible lipid modification that can exert key changes in protein signaling and trafficking (Chamberlain & Shipston, 2015; Jiang et al., 2018; Linder & Deschenes, 2007; Tabaczar et al., 2017). Estimates of the size of the palmitoyl-proteome reveal that approximately 10% of all proteins undergo this PTM (Blanc et al., 2019), suggesting that there is still much to discover about how palmitoylation plays a role in protein biology.

To elaborate, palmitoylation is a type of reversible lipid PTM that involves the attachment of a fatty acid chain to a substrate protein (Jiang et al., 2018; Linder & Deschenes, 2007; Tabaczar et al., 2017). This PTM is mediated by a family of enzymes known as S-acyltransferases that are canonically referred to as "zDHHCs" in reference to their conserved aspartic acid-histidine-histidine-cysteine catalytic domain (Anwar & van der Goot, 2023; Stix et al., 2020). There are 23 known S-acyltransferases expressed in mammals, and these membrane-bound enzymes are typically localized to the Golgi apparatus, endoplasmic reticulum, and plasma membrane (Anwar & van der Goot, 2023; Chamberlain & Shipston, 2015). To mediate this PTM, S-acyltransferases must first "auto-palmitoylate" by acquiring a palmitate group from palmitoyl-CoA and attaching it to the cysteine residue of its catalytic domain via a thioester bond (Dietrich & Ungermann, 2004; Guan & Fierke, 2011). Following this auto-palmitoylation process, an S-acyltransferase can then catalytically transfer the palmitate group to the cysteine residue of an interacting substrate protein that has localized to its respective cellular domain (Chen et al., 2021; Main & Fuller, 2022; Tabaczar et al., 2017). Once the palmitate group has been transferred, the S-acyltransferase must then undergo an additional interaction with palmitoyl-CoA prior to mediating further enzymatic activity.

In recent past, the consequences of protein palmitoylation on intracellular signaling have become increasingly characterized and have been shown to crucially regulate a wide variety of downstream signaling processes (Chamberlain & Shipston, 2015; Guan & Fierke, 2011). Primarily, palmitoylation is the attachment of a highly lipophilic side chain, and thus, this PTM increases the substrate's affinity for membrane domains in the cell (Tabaczar et al., 2017). Palmitoylation commonly drives the association of substrate proteins to different membranes, such as the plasma and Golgi membranes, resulting in influencing further signaling that can

proceed from this domain of the cell (Aicart-Ramos et al., 2011; Dennis & Heather, 2023; Guan & Fierke, 2011). Interestingly, not only does palmitoylation drive membrane association in general, but it can also drive association with specific types of membrane domains, such as lipid rafts, increasing the specificity of their interactor profiles and downstream signaling (Chamberlain & Shipston, 2015; Guan & Fierke, 2011; Levental et al., 2010; Navarro-Lérida et al., 2012; Sun et al., 2020). Aside from localization, there is additional evidence that S-acyltransferase-mediated palmitoylation can critically regulate substrate stability (Chamberlain & Shipston, 2015; Linder & Deschenes, 2007; Maeda et al., 2010), protein-protein interactions (Charollais & Van Der Goot, 2009), and protein trafficking (Aicart-Ramos et al., 2011; Chamberlain et al., 2013). Thus, protein palmitoylation plays a variety of essential roles in directing intracellular signaling.

Notably, unlike other lipid modifications, palmitoylation is reversible, yielding unique ways of modifying protein signaling and localization (Linder & Deschenes, 2003). Another family of enzymes, the acyl-protein thioesterases (APTs), are capable of hydrolyzing the thioester bond between palmitate and protein substrates, rendering them “de-palmitoylated” (Chen et al., 2021; Zeidman et al., 2009). Upon removing the lipophilic group, plasma membrane-docked proteins are often then released from the membrane and either continue to signal or are otherwise de-activated from their contributions to interactors at the membrane (Chamberlain & Shipston, 2015; M. Zhang et al., 2020). This palmitoylation/depalmitoylation “cycling” can be critical in advancing proteins through their signaling pathways (Baekkeskov & Kanaani, 2009; M. Zhang et al., 2020). Given that the reversible nature of this PTM can lead to unique signaling outcomes through both activating and inhibiting substrate activity, its role in the

protein regulation underlying disease has become of particular interest, and many groups have since discovered key roles for palmitoylation in a host of pathologies.

Recent Contributions to Disease Regulation through Palmitoylation

In the past decade, a variety of novel investigations into the contributions of palmitoylation in disease signaling have established this PTM as having an emerging role in human health conditions such as cancer, immunity, neurological disorders, and CVD (Cai et al., 2023; Essandoh et al., 2020; M. Li et al., 2023; Liao et al., 2023). Here, a number of recent advances highlighting the key roles of palmitoylation signaling in disease, as well as their clinical value for therapeutic targeting, are presented.

Cancer/Immune Disorders

One of the major disease areas being uncovered in relation to palmitoylation-driven signaling pathways is the involvement of this lipid modification in the mechanisms and treatment of cancer and tumorigenesis (Kong et al., 2023; M. Li et al., 2023; Zhou et al., 2023). A number of recent works have elucidated novel roles for S-acyltransferases in the pathophysiology and treatment of hepatocellular carcinoma (HCC), such as zDHHC16 contributing to resistance to sorafenib, an FDA-approved tyrosine kinase inhibitor that serves as the first line treatment for HCC (Sun et al., 2022). Mechanistically, palmitoylation of cysteine 600 of proprotein convertase subtilisin/kexin type 9 (PCSK9) by zDHHC16 increases its affinity with tumor-suppressing protein phosphatase and tensin homolog (PTEN). PTEN plays a critical role in reducing Akt signaling, which has previously been demonstrated to majorly contribute to the resistance of sorafenib (Zhai et al., 2014). As the binding of PSCK9 to PTEN drives its lysosomal degradation, the cell experiences a reduction of PTEN signaling and, correspondingly, an increase in Akt signaling that inhibits the effectiveness of sorafenib. To disrupt this, targeted

peptides were used to inhibit PCSK9 palmitoylation, successfully reducing Akt activation and contributing to the restoration of sorafenib's anti-tumor effects. There are additional examples of palmitoylation inducing tumorigenic signaling in HCC, such as the palmitoylation of plant homeodomain finger protein 2 (PHF2) by zDHHC23. PHF2 is a nodal regulator of cell cycle progression, with previously described roles in migration and tumor suppression (Fu et al., 2019; Lee et al., 2015). As a new facet of PHF2 regulation, it was recently discovered that palmitoylation of PHF2 at cysteine 23 promotes its ubiquitin-mediated degradation (Jeong et al., 2023) and resultingly reduces its anti-tumor effects in HCC. In both of these pathways, S-acyltransferase-mediated palmitoylation was found to contribute to the pathogenesis of HCC through the downregulation of tumor-suppressing signaling proteins.

Another S-acyltransferase, zDHHC9, has been shown to play an important role in cancer progression. It was recently found that the localization of glucose transporter 1 (GLUT1) to the plasma membrane is dependent on palmitoylation by zDHHC9 in glioblastoma cells (Z. Zhang et al., 2021). Given the dependence of all cells on the uptake of glucose as a source of cellular energy, glucose transporters such as GLUT1 are critical for cellular survival and proper function (Pragallapati & Manyam, 2019). To this end, cancer cells have been shown to upregulate GLUT1 expression to upregulate glucose intake, increasing their survival (Zambrano et al., 2019). Additionally, highlighting how palmitoylation inhibition can be effective in reducing cancer cell survival, the authors showed that both *Zdhhc9* KO and palmitoylation-deficient GLUT1-mutant cells exhibited reduced GLUT1 at the plasma membrane, reducing glucose intake and inhibiting glioblastoma tumorigenesis (Z. Zhang et al., 2021). Additional involvement of this enzyme in cancer is demonstrated through works showing zDHHC9 activity can modulate cyclic GMP-AMP synthase (cGAS)-stimulator of interferon genes (STING) pathway, a pro-inflammatory

cascade that can elicit anti-tumor effects (Decout et al., 2021; Fan et al., 2023). It was shown that cGAS dimer formation, a process crucial for its downstream immune response signaling, was dependent on palmitoylation at cysteines 405/405 by zDHHC9 (Fan et al., 2023). Further, it was found that dimer formation of cGAS was majorly decreased through the activity of the depalmitoylating enzyme lysophospholipase-like 1 (LYPLA1). In trials with *Lyplal1* KO mice, it was determined that the resultant reduction in depalmitoylation of cGAS promoted its plasma membrane localization and thus its anti-tumor activity, with *Lyplal1* KO mice exhibiting significantly increased survival and elevated immune responses in a herpes simplex virus 1 (HSV-1) injury model. This mechanism provides evidence that in certain signaling pathways, maintaining palmitoylation levels of endogenous anti-tumor proteins can sustain their activity and contribute to improved outcomes in vivo. Alternatively, pro-inflammatory cGAS-STING signaling can lead to the development of auto-immune conditions such as systemic lupus erythematosus (SLE) (Kato et al., 2018), rheumatoid arthritis (Wang et al., 2019), Aicardi-Goutières syndrome (AGS) (Giordano et al., 2022), and STING-associated vasculopathy with onset in infancy (SAVI) (Frémond & Crow, 2021; Liu & Pu, 2023). To this end, small molecule cGAS inhibitors have been developed (Hall et al., 2017; Vincent et al., 2017), and the cGAS inhibitor compound RU.521 has been shown to improve inflammatory phenotypes in a mouse model of Aicardi-Goutières syndrome (Vincent et al., 2017) In the context of palmitoylation, it was found that palmitoylation of STING directly regulates its activation and contribution to interferon release (Mukai et al., 2016). To this end, others have inhibited this pathway by directly targeting the STING palmitoylation sites (cysteines 88 and 91) with cysteine alkylation using nitro-fatty acids, preventing STING signaling and reducing type I interferon release in mouse and human immune cells (Hansen et al., 2018; Hansen et al., 2019). The STING cysteine

alkylation lead compound CXA-10 progressed to Stage II clinical trials towards the treatment of both segmental glomerulosclerosis and pulmonary arterial hypertension, providing evidence that strategies for inhibiting substrate cysteine palmitoylation can be effective clinically (Hansen et al., 2019).

zDHHC9 has also been demonstrated to play a role in leukemogenesis by regulating the oncogenic signaling protein N-Ras. N-Ras serves as a major contributor to cancer progression through its activation of oncogenic signaling pathways from the plasma membrane (Kwong et al., 2012; Prior & Hancock, 2001), a process now known to be promoted through N-Ras palmitoylation at cysteine 181 (C181) (Cuiffo & Ren, 2010). N-Ras palmitoylation mutant NIH3T3 cells exhibit reduced proliferation, as well as reduced phosphorylation levels of Akt and Erk1/2 (Cuiffo & Ren, 2010). The dependence of N-Ras signaling on palmitoylation has been further investigated in vivo using an oncogenic *Nras* G12D mutation mouse model (Zambetti et al., 2020). *Nras* G12D mice develop the fatal condition myeloproliferative neoplasm, though mice with an additional C181S N-Ras palmitoylation mutation in hematopoietic stem cells exhibited a complete rescue in survival compared to wildtype palmitoylation animals (Zambetti et al., 2020). Further, they found that N-Ras C181S were protected from *Nras* G12D-induced changes to myeloid transformation and that this was due in part mechanistically through increased cytosolic localization of N-Ras C181S (Zambetti et al., 2020). The S-acyltransferase responsible for this regulation of N-Ras was previously determined to be zDHHC9 (Swarthout et al., 2005). Notably, *Nras* G12D mice with whole-body Zdhhc9 knockout exhibited decreased N-Ras palmitoylation, reduced oncogenic cellular transformation, and increased survival (Liu et al., 2016).

Glioblastoma risk has also been linked with activity of the S-acyltransferase zDHHC17 and an interaction with octamer-binding transcription factor A (Oct4A) (Chen et al., 2023). Oct4A is an oncogenic protein implicated in glioblastoma pluripotency and tumorigenesis (G. Wang et al., 2018; Wang et al., 2013; Q. Zhang et al., 2020). Oct4A levels are controlled through lysosomal degradation, and it has now been determined that palmitoylation of Oct4A by zDHHC17 stabilizes the protein and reduces its proteolysis (Chen et al., 2023). Further experiments demonstrated that a newly developed Oct4A palmitoylation inhibitor was effective in reducing tumorigenicity in mouse models of cancer, a result that highlights the translational value of targeting these pathways (Chen et al., 2023). The S-acyltransferase zDHHC15 was also recently implicated in the signaling of glioblastoma and was found to be significantly upregulated in glioma tissues (Z. Y. Liu et al., 2023). Characterization of this enzyme in vitro showed that siRNA-mediated knockdown of zDHHC15 reduced human glioma cell proliferation and migration, suggesting an important role for this enzyme in the activity of these cells (Z. Y. Liu et al., 2023). This effect was complemented by additional results showing that in vitro overexpression of zDHHC15 in these cells yielded increased migration compared to controls (Z. Y. Liu et al., 2023). While the full mechanism for this effect is still being uncovered, preliminary probes revealed that zDHHC15 knockdown significantly reduced STAT3 phosphorylation, suggesting that the regulation of STAT3, a protein with established roles in cancer signaling (Tolomeo & Cascio, 2021; Zou et al., 2020), may be influenced by palmitoylation in glioma cells.

In addition to its role in cancer, palmitoylation has concurrently been implicated in a number of immune-related signaling pathways, exhibiting regulatory roles in inflammation, auto-immunity, and irritable bowel syndrome (IBS) (Cai et al., 2023; Lin, 2021; Y. Zhang et al.,

2021). Notably, palmitoylation cycling has been shown to critically regulate the signaling of the previously described STAT3 protein, with major consequences on the development of IBS (M. Zhang et al., 2020). It was discovered that the Golgi-localized S-acyltransferase zDHHC7 palmitoylates STAT3 at cysteine 108, driving its localization to the plasma membrane (M. Zhang et al., 2020). Palmitoylated STAT3 then becomes phosphorylated by JAK2 at the PM, an additional PTM that is essential for its activity in the nucleus (Hu et al., 2023). Interestingly, prior to nuclear localization following STAT3 phosphorylation, STAT3 must first be depalmitoylated by APT2 to release it from the membrane and allow for STAT3 dimer formation and downstream changes to transcription (M. Zhang et al., 2020). Consequently, interfering with STAT3 palmitoylation either by *Zdhhc7* KO or APT2-inhibition can interrupt STAT3 signaling either by prohibiting its phosphorylation or preventing its dissociation from the plasma membrane, respectively (M. Zhang et al., 2020). Using a dextran-sulfate-sodium injury model of colitis in mice, administering the APT2-inhibitor ML349 significantly improved weight loss, reduced colon shortening, and increased overall survival along the experimental time course (M. Zhang et al., 2020). Thus, palmitoylation plays an assortment of roles in regulating cancer and tumorigenic signaling, and attempts to disrupt these pathways have been successful through targeting APTs, cysteine alkylation, and enzyme/substrate interactions.

Neurological disorders

Palmitoylation has additionally been implicated in a wide variety of signaling mechanisms in the brain, as well as the transduction pathways underlying common neurological disorders (Buszka et al., 2023; Ramzan et al., 2023). Recently, an exome sequencing study of familial Alzheimer's disease patients revealed a rare gain-of-function heterozygous genetic mutation (*p.T209S)* in *ZDHHC21* (W. Li et al., 2023). Further work to characterize the

consequences of this mutation determined that as a result of increased enzymatic activity, zDHHC21-mediated palmitoylation increased plasma membrane localization of the proteins proto-oncogene tyrosine-protein kinase Fyn (FYN) and amyloid beta precursor protein (APP), the cellular location from which they exert pathogenic signaling that induces excitotoxicity and amyloid-β plaque formation (W. Li et al., 2023). Using a homozygous knock-in mouse model of the *ZDHHC21 p.T209S* gene variant, researchers found that mice with this mutation exhibited reduced cognitive function as measured by Morris water maze performance (W. Li et al., 2023). Thus, these works provide evidence that genetic mutations inducing changes to S-acyltransferase activity can contribute to the development of neurological disorders such as Alzheimer's disease through increased pathogenic plaque formation.

Palmitoylation has also been shown to regulate pathogenic signaling underlying Parkinson's disease (PD) (Calabresi et al., 2023). While the mechanistic basis for Parkinson's is not entirely understood, it has been determined that monomeric α-synuclein (αS) aggregation within dopaminergic neurons can disturb neurotransmitter release and contribute to symptom development (Calabresi et al., 2023). It was recently found that an interaction of αS at the plasma membrane with synaptotagmin-11 (Syt11), a vesicular trafficking protein also linked with Parkinsons pathogenesis (C. Wang et al., 2018), dysregulates physiologic αS and promotes pathogenic monomer formation (Ho et al., 2023). Critically, Syt11 palmitoylation at cysteine 39/40 promoted localization to the membrane domains from which this interaction occurs, significantly decreasing physiologic αS tetramer formation in patient-derived iPSC neurons (Ho et al., 2023). Thus, palmitoylation can contribute to the dysregulation of αS by inhibiting its physiologic state through a promoted interaction with Syt11. Related in vivo experiments showed that chronic administration of the small molecule APT1 inhibitor ML348 in male and

female mice overexpressing αS resulted in improved cognitive performance and reduced the monomer form of αS in the hippocampus and cortex (Moors et al., 2023).

Analyzing the contribution of palmitoylation in regulating neuron activity has yielded additional roles for zDHHC7 in its interaction with the neuronal regulatory protein family known as septins (H. Liu et al., 2023). Septins are a family of GTP-binding proteins with high expression in the brain, of which many have been linked with synaptic function and neurodegenerative disease (Marttinen et al., 2015). Sept8-204 is a recently discovered brain-specific variant of Sept8, whose contribution to regulating filopodia outgrowth and neurite arborization was determined to be dependent on palmitoylation of cysteines 470/472 by zDHHC7 (H. Liu et al., 2023). Analyses of hippocampal neurons from *Sept8* KO mice demonstrated that loss of Sept8 resulted in neurite outgrowth inhibition. Critically, re-expression of a Sept8-204 with functional palmitoylation sites partially rescued neurite outgrowth, an effect that was not observed in cells where Sept8 was re-expressed with critical cysteine to alanine mutations (C469A/C470A/C472A) that prevent palmitoylation (H. Liu et al., 2023). This result highlights that palmitoylation can contribute to the signaling underlying homeostatic regulation of neural systems.

Collectively, the results from these studies illustrate essential roles of palmitoylation in the pathophysiology of human diseases. Contributing both to disease pathogenesis and suppression, palmitoylation can contextually regulate protein signaling by influencing stability, inducing degradation, modifying localization, and controlling complex formation (Calabresi et al., 2023; W. Li et al., 2023; Wang et al., 2013; M. Zhang et al., 2020). Further, these data critically highlight the growing translational importance of this PTM, in the sense that manipulating palmitoylation cycling with APT inhibitors can yield improvements to in vivo

symptom profiles associated with a variety of disease models (Moors et al., 2023; M. Zhang et al., 2020).

Palmitoylation in Cardiac Signaling and Disease

There is a clear case that palmitoylation can prove to be an essential regulator of protein signaling and that manipulating palmitoylation machinery can result in major changes to the development of disease. As such, the elucidation of how palmitoylation may additionally regulate signaling in the heart is of great interest. Though at present, little is known about the role of palmitoylation in the heart, prompting further work to establish how this critical signaling regulator may be modifying cardiac remodeling pathways. In recent years, the first works have emerged that provide evidence for palmitoylation playing key roles in cardiac signaling and disease.

Of the many areas in cardiac signaling, there is a growing body of evidence illuminating the role of palmitoylation in the context of ion channel physiology (Essandoh et al., 2020). Precise ion channel electrophysiological mechanisms underlie the coordinated beating of cardiomyocytes, and the dynamic flow of Na^+, Ca^{2+}, and K^+ ions is regulated by corresponding ion channels and pumps that maintain concentration gradients and facilitate myofilament contraction (Essandoh et al., 2020; Huang & Lei, 2023; Varró et al., 2021). Alterations in the homeostatic function of these ion channels can contribute to fatal arrhythmogenesis and other CVDs, necessitating tight regulation (Kingma et al., 2023; Schwartz et al., 2020). Amongst the initial insights into the role of palmitoylation in cardiac electrophysiology, it was determined that the primary inward sodium channel ($Na_v1.5$) that predominantly controls cardiac action potential is palmitoylated (Pei et al., 2016). Further, it was found that a $Na_v1.5$ palmitoylation mutant reduced $Na_v1.5$ channel availability and excitability, yielding potential implications in the

context of arrhythmogenesis (Pei et al., 2016). Another major area of investigation is how palmitoylation regulates the sodium-calcium exchanger (NCX1) in the heart (Gök et al., 2022; Reilly et al., 2015). NCX1 is the major mediator of calcium efflux in the heart and thus holds an important role in cardiac contractility (Ottolia et al., 2013). Increased NCX1 activity can lead to delayed arrhythmogenic afterdepolarizations (Reilly et al., 2015; Venetucci et al., 2007). Here, it was found that NCX1 is palmitoylated at cysteine 179 (Reilly et al., 2015). Surprisingly, NCX1 membrane localization was not found to be altered by palmitoylation, but rather, it was discovered that palmitoylation-deficient NCX1 exhibits the inability to inactivate due to changes in the interaction of its large intracellular loop with membrane proteins (Reilly et al., 2015). In recent works further exploring the regulation of NCX1, it was found that zDHHC5 is the critical S-acyltransferase for NCX1 palmitoylation and that zDHHC5 activity is driven by insulin circulation-induced increases in free fatty acids (Gök et al., 2022). These works provide evidence that insulin-induced changes to S-acyltransferase activity can impart downstream effects on cardiac ion channel structure and function (Gök et al., 2022).

Other studies provide evidence that the cardiac ion channel hyperpolarization-activated cyclic nucleotide-gated potassium channel 4 (HCN4) is palmitoylated (Congreve et al., 2023). Interestingly, it was found that depalmitoylated HCN4 in cardiomyocytes displayed reductions in the magnitude of its current, an effect that was hypothesized to be due to conformational changes to the protein's amino terminus influenced by the PTM (Congreve et al., 2023). Other investigations on the role of palmitoylation in cardiomyocyte electrophysiology are centered around Ca(v)1.2, where it was determined that palmitoylation of the alpha-1 subunit of this voltage-dependent calcium channel influences voltage sensitivity (Kuo et al., 2023). From a translational perspective, this is of interest given the contribution of Ca(v)1.2 activity with

induction of early-after depolarizations, a process that can subsequently trigger arrhythmias such as ventricular fibrillation and ventricular tachycardia (Kuo et al., 2023). This finding raises the possibility of inhibiting Ca(v)1.2 palmitoylation to reduce the likelihood of such fatal events.

Outside of ion channel function, recent works additionally highlight the importance of S-acyltransferases in other areas of cardiac biology. Of note, work from our lab has uncovered a novel role for zDHHC9 in the regulation of the GTPase Rab3a (Essandoh et al., 2023). The activity of Rab3a has been explored previously in other cell types, notably its importance in mediating neuronal exocytosis (Huang et al., 2011), but how Rab3a functions in the heart has not been extensively explored (Essandoh et al., 2023). Like other GTPases, Rab3a activation is regulated through interactions with guanine nucleotide exchange factors (GEFs) and GTPase-activating proteins (GAPs) that cycle the GDP/GTP-loading of the enzyme (Stenmark, 2009). Here, it was shown that the Golgi-localized S-acyltransferase zDHHC9 palmitoylates Rab3gap1, a GAP responsible for the hydrolysis of GTP-bound Rab3a (Essandoh et al., 2023). Interestingly, although this PTM commonly drives plasma membrane association (Chamberlain & Shipston, 2015), palmitoylation of Rab3gap1 was found to retain its localization to the Golgi and increase the amount of GTP-loaded Rab3a (Essandoh et al., 2023). Critically, the exocytotic mechanism underlying final membrane fusion and release of vesicular cargo is preceded by Rab3a dissociation from the membrane, achieved through GAP action to catalyze the GTP to GDP transfer of Rab3a (Huang et al., 2011). As this palmitoylation-mediated increase in GTP-bound Rab3a would likely have consequences on cardiomyocyte secretion, further characterization of this effect uncovered that zDHHC9 over-expression in cardiomyocytes inhibited secretion of atrial natriuretic peptide (ANP), a cardioprotective peptide released by these cells in response to injury in the heart (Essandoh et al., 2023; Song et al., 2015). Consistent with these results,

siRNA-mediated zDHHC9 knockdown resulted in an increase in phenylephrine-induced ANP secretion in cardiomyocytes compared to controls (Essandoh et al., 2023). These data provide the first evidence for S-acyltransferase-mediated regulation of Rab3Gap1, Rab3a, and ANP secretion in the heart and represent a promising future avenue of exploration into how palmitoylation influences the secretory activity of cardiomyocytes.

In another CVD area, the S-acyltransferases zDHHC3 and zDHHC7 have recently been demonstrated as having key roles in hypertrophic cardiac remodeling (Baldwin et al., 2023). Overexpression of *Zdhhc3* and *Zdhhc7* in mouse cardiomyocytes was shown to dramatically increase ventricular hypertrophy and induce a significant decrease in contractility as measured by fractional shortening (Baldwin et al., 2023). Subsequent unbiased palmitoyl-proteomic screens to determine critical substrates potentially responsible for these observed effects yielded Rac1 as a top hit for substrates of zDHHC3 (Baldwin et al., 2023). Rac1, a small Rho-family GTPase, is a nodal regulator of cytoskeletal organization and pro-hypertrophic signaling (Bosco et al., 2009; Higuchi et al., 2003). Further, cardiomyocyte-specific deletion of *Rac1* has been shown to decrease AngII-induced cardiac hypertrophy, NADPH oxidase activity, and NFκB signaling (Satoh et al., 2006). Follow-up studies exploring this interaction showed that the overexpression of *Zdhhc3* in the heart increased Rac1 palmitoylation, as well as increased activation of not only Rac1 but also RhoA, Cdc42, and RhoGDI, suggesting the zDHHC3-mediated palmitoylation plays a role in the activation of all Rho-family GTPases in cardiomyocytes in vivo (Baldwin et al., 2023). Notably, cardiomyocyte-specific deletion of *Zdhhc3* and *Zdhhc7* resulted in a reduced initial phase of hypertrophic remodeling in response to TAC, although this deletion was not sufficient to ameliorate cardiac remodeling at later time points, possibly due to compensation by other Golgi-localized S-acyltransferases (Baldwin et al., 2023).

Together, these studies suggest that palmitoylation mechanistically contributes to cardiac signaling involved in the development of arrhythmias (Reilly et al., 2015), exocytosis (Essandoh et al., 2020), and hypertrophy (Baldwin et al., 2023). Considering the appearance of strategies to target disease signaling regulated by palmitoylation through APT inhibition, substrate cysteine alkylation, and preventing enzyme/substrate interactions (Chen et al., 2023; Hansen et al., 2019; Moors et al., 2023; M. Zhang et al., 2020), the continual advancement of our understanding of palmitoylation in the context of cardiac biology is critical in establishing targets for novel treatments to CVD.

Emerging Role of Palmitoylation in Fibrotic Signaling

Notably, a number of proteins previously described as regulating pro-fibrotic signaling in CFs have been linked with palmitoylation-mediated regulation in non-cardiac cell types (Figure 1.2). As previously mentioned, zDHHC7-mediated palmitoylation has been established as crucially regulating the signaling of STAT3 in a manner that was shown to majorly contribute to the development of IBS (M. Zhang et al., 2020). In the context of fibroblast biology, STAT3 is known to play a key role in activating pro-fibrotic transcriptional pathways in response to the pro-fibrotic ligands TGFβ1, IL6, AngII, and platelet-derived growth factors (PDGFs) (J. Liu et al., 2023; Tang et al., 2017; Xu et al., 2019). Notably, knockdown of STAT3 in dermal fibroblasts has been shown to inhibit TGFβ1-induced transition from quiescent fibroblasts into their activated state (Chakraborty et al., 2017). Further, in vivo inhibition of STAT3 results in significant reductions in the development of cardiac fibrosis in βIV-spectrin deficient mouse models (Patel et al., 2019). Small molecule STAT3 inhibitors preventing STAT3 phosphorylation or dimerization have also proven to be effective in reducing stress-induced fibrosis in the heart (Chen et al., 2017; Dong et al., 2019). From previous works highlighting major deficits in STAT3

signaling due to targeted manipulations into palmitoylation machinery (M. Zhang et al., 2020), it remains a possibility that similar mechanisms of STAT3 palmitoylation deficiency could reduce pro-fibrotic activation if STAT3 activity was similarly regulated by this PTM in fibroblasts.

Another major area of interest for establishing the role of palmitoylation-mediated signaling in disease is how G-proteins are regulated by this PTM. Activation of G-protein coupled receptors (GPCRs) and the signaling associated with downstream G-proteins has been extensively characterized as being pivotal for a host of pathophysiologies throughout nearly every major organ system in the body (Kaur et al., 2023; Weis & Kobilka, 2018; Wong et al., 2023). At present, GPCRs have become one of the most successful classes of drug targets of all time as a result of their major contribution to the transduction of extracellular signals into intracellular signaling responses (Alhosaini et al., 2021; Yang et al., 2021). Previous investigations into how GPCR signaling is regulated by palmitoylation found that $G\alpha_q$ is palmitoylated by zDHHC3 and zDHHC7, which drives its plasma membrane localization (Tsutsumi et al., 2009). $G\alpha_q$ is well documented in directing signaling relevant to cardiac remodeling such as AngII-mediated fibrosis (Schnee & Hsueh, 2000) and has recently been shown to be essential for myofibroblast differentiation in response to AngII in CFs in vitro (Parichatikanond et al., 2023). Further, recent works have also demonstrated that IL6 production in the heart is predominantly mediated by CFs through activation of adenosine A2B receptor (A2BR) expressed on their plasma membrane in a Gaq-dependent manner (Alter et al., 2023). Despite the growing body of literature implicating the role of $G\alpha_q$ in fibroblast activation, at present, little is known about how palmitoylation regulates G-protein signaling in CFs, necessitating future work in this area.

zDHHC3 activity has also been linked with the pathogenic signaling of non-alcoholic

steatohepatitis (NASH) (Xu et al., 2023), a condition characterized by fat accumulation in the liver that, upon disease progression, can result in the development of hepatic fibrosis (Schwabe et al., 2020). Mechanistically, inactive rhomboid protein 2 (IRHOM2) promotes mitogen-activated protein kinase kinase kinase 7 (MAP3K7)-mediated inflammatory signaling from the plasma membrane (Xu et al., 2023). Palmitoylation of IRHOM2 by zDHHC3 was found to promote its plasma membrane localization, and hepatocyte-specific deletion of *Zdhhc3* in mice resulted in significantly reduced hepatic inflammation and pro-fibrotic gene expression in mouse models of NASH (Xu et al., 2023).

Another interesting candidate for establishing key roles for palmitoylation in CF biology is the previously described Rho-family GTPase Rac1 (Bosco et al., 2009). In addition to its involvement with hypertrophic signaling, Rac1 displays regulatory roles in a variety of fibroblast processes, including activation and migration in vitro and the development of remodeling and wound closure in vivo (Kunschmann et al., 2019; Lavall et al., 2017; Liu et al., 2009; Lyu et al., 2021; N. Ma et al., 2023). Critically, previous work on Rac1 signaling provides evidence that Rac1 is palmitoylated at cysteine 178 (C178) and that the consequences of this PTM influence its intracellular localization and GTP-loading in COS7 cells (Navarro-Lérida et al., 2012). Further, COS7 cells with over-expressed palmitoylation-deficient Rac1 exhibited migrational deficits, suggesting a potential role for palmitoylation in the regulation of Rac1 in migration (Navarro-Lérida et al., 2012). While these experiments did not provide insights into which S-acyltransferase is responsible for Rac1 palmitoylation at C178, as previously described, our lab recently established that Rac1 is palmitoylated at this site by zDHHC3 by performing an unbiased palmitoyl-proteomic screen in a fibroblast cell line (Baldwin et al., 2023). Due to the combination of both the critical role of Rac1 in fibroblast activation and migration (Kunschmann

et al., 2019; Lavall et al., 2017; Lyu et al., 2021; N. Ma et al., 2023), as well as its regulation of signaling activity by palmitoylation in other cell types (Navarro-Lérida et al., 2012), there is substantial need for future investigations probing for the regulation of Rac1 by palmitoylation in CFs.

In recent work, other groups have begun to investigate the role of S-acyltransferases in fibrosis occurring in other major organ systems, providing additional insights into how palmitoylation regulates fibrotic activity. Interestingly, preliminary works exploring palmitoylation-mediated signaling in the kidneys suggest novel protective roles for zDHHC9 in renal fibrosis through its influence on Wnt/β-catenin (Gu et al., 2023). Wnt/β-catenin signaling has established roles in renal fibrosis and is known to promote both the expression of pro-fibrotic genes such as *Snail1*, *MMP-7*, and the activation of effectors through RAAS (Tan et al., 2014). In terms of its regulation by zDHHC9, palmitoylation of β-catenin leads to an increase in its ubiquitination and subsequent degradation in murine kidney cells, reducing its ability to induce fibrotic responses (Gu et al., 2023). Further highlighting the importance of the reversible nature of palmitoylation and the activity of APT1, inhibition of the depalmitoylating enzyme APT1 in kidney cells promoted β-catenin degradation and resulted in significant reductions in kidney fibrosis in an ischemia/reperfusion injury (IRI) model (Gu et al., 2023). These data provide additional insight into how palmitoylation can result in anti-fibrotic signaling outcomes, stressing the need to determine if comparable mechanisms are at play in CF signaling.

Thus, we sought to contribute to this area through preliminary investigations into the role of palmitoylation in CF activation and cardiac fibrosis with the intention of identifying novel targets for more effective and clinically relevant therapies.

Aims in Exploring the Role of Palmitoylation in Cardiac Fibroblast Biology

Toward determining future therapeutic avenues that can be explored in relation to modulating CF activity, we considered that the unique regulation of signaling pathways by S-acyltransferase activity could play a crucial role in the protein pathways beginning to be characterized in CFs. Here, we sought to explore the role of palmitoylation in CF biology to establish a relationship between the dynamic signaling that underlies CF activation and the fine-tuning of substrate regulation by S-acyltransferase enzymes (Figure 1.2). To this end, we aimed to measure changes in CF activation in response to pro-fibrotic stimuli in wild-type CFs to compare responses to those from cells with knockouts of key S-acyltransferase enzymes. Given the role of zDHHC3 and zDHHC7 in regulating STAT3 signaling (M. Zhang et al., 2020), Ga_q signaling (Tsutsumi et al., 2009), Rac1 activation (Baldwin et al., 2023), and the development of cardiac hypertrophy (Baldwin et al., 2023), we hypothesized that these enzymes may play critical roles in regulating CF activation. Primarily, we hypothesized that the deletion of the S-acyltransferases zDHHC3 and zDHHC7 in CFs would elicit dysregulation in pro-fibrotic signaling pathways. As a result, we anticipated that gene-targeted cell and mouse models lacking these enzymes in CFs would exhibit a blunted activation response and a reduced development of remodeling and fibrosis in the heart, respectively.

Our initial investigations into the role of zDHHCs in the heart centered around in vitro activation assays, where fibroblast activation was assessed in response to the pro-fibrotic agonist TGFβ1 to compare effects in the absence of *Zdhhc3* and *Zdhhc7*. However, this type of assay requires a quiescent population of fibroblasts so as to be reactive to exogenous stimuli like TGFβ1. However, given the aforementioned sensitivity of CFs to traditional cell culture conditions, isolated quiescent primary adult CFs to be used for these experiments quickly

became activated. As a result, baseline activation was too high to effectively see changes when TGFβ1 was introduced. To overcome this problem, others have explored the use of commercially-available modified substrates that provide a more physiologically-relevant stiffness made from synthetic hydrogels and the biologically compatible polymer polydimethylsiloxane (PDMS) (Herum et al., 2017; Landry et al., 2019; Wang et al., 2021). To eliminate this baseline activation, we performed an extensive optimization process to determine assay conditions that would reduce baseline activation utilizing in-house generated 8kPa PDMS substrates that allow for successful induction of the myofibroblast transition with TGFβ1. Chapter II provides a detailed description of the development of the assay conditions required to reliably measure changes to CF activation in vitro.

In Chapter III, I performed the first investigations into the role of S-acyltransferases in CF biology. We hypothesized that the deletion of *Zdhhc3* in CFs would lead to reductions in activation as measured by αSMA positivity and fibrotic gene expression in vitro and the development of fibrosis in vivo. I first examined the expression of the S-acyltransferase zDHHC3 in CFs, as well as examined its cellular localization. Proceeding from the confirmation that zDHHC3 is expressed in CFs, I utilized LoxP-targeted *Zdhhc3* fl/fl mice to investigate changes to CF activation and migration in the absence of zDHHC3 in vitro. I performed in vitro assessments of CF activation, including fibrotic gene expression and αSMA staining experiments to compare responses between control and *Zdhhc3* KO cells. Migration ability was also tested in cells with *Zdhhc3* KO using the scratch assay. Further, I generated a tamoxifen-inducible mouse model that allows for the deletion of *Zdhhc3* in activated CFs by crossing *Zdhhc3* fl/fl mice with the *Postn-MCM +/-* line. To test the requirement of *Zdhhc3* towards the development of fibrosis in vivo, control and activated CF-specific *Zdhhc3* KO mice were subject to an 8-week pressure-

overload injury model using TAC. Common metrics of cardiac remodeling, including hypertrophy, fibrosis, and mRNA levels of pro-fibrotic genes, were compared between control and *Zdhhc3* KO mice. Echocardiographic parameters were also measured to evaluate changes to cardiac contractile function.

In Chapter IV, I continue with additional explorations into the role of palmitoylation in CF activation and fibrosis. Preceding these experiments and in relation to results from the previous chapter, I hypothesized that changes to CF pro-fibrotic signaling may not be fully elicited when a single S-acyltransferase is knocked out, potentially as a result of compensation from other zDHHCs. Considering that zDHHC7 is known to share common substrates with zDHHC3, I thought it might be possible that a dual deletion of both *Zdhhc3* and *Zdhhc7* may be required to observe the hypothesized reductions in CF activation (Tsutsumi et al., 2009; M. Zhang et al., 2020). I performed in vitro analyses to assess how the deletion of *Zdhhc7* alone, as well as a combined deletion of *Zdhhc3* and *Zdhhc7*, may elicit reductions in CF activation. I tested for changes in fibrotic gene expression, migration, and pro-fibrotic transcription factor activity in vitro in the absence of these enzymes. Additionally, I explored the requirement of zDHHC3 and zDHHC7 for the development of fibrosis and other previously described measures of cardiac remodeling in vivo. Combining both enzyme level and substrate level analyses, I also characterized the role of Rac1 palmitoylation in CF activation and migration in vitro using our newly generated Cre-inducible conditional Rac1 palmitoylation-mutant mouse model (Rac1 ConKI). I compared activation responses to TGFβ1 in control and Rac1 ConKI cells in measures of αSMA positivity, pro-fibrotic gene expression, and pro-fibrotic transcription factor activity assays. Finally, given Rac1's established role in cellular movement, scratch assays were also

performed to determine whether Rac1 palmitoylation was essential for the migratory ability of cardiac fibroblasts.

Here, I present in the following chapters a collection of data describing our probes into the hypotheses that palmitoylation modulates CF activation. Chapter II provides a comprehensive protocol for the in-house generation of 8kPa PDMS and the corresponding cell culture conditions to assess CF activation at physiological stiffness. The data presented in Chapter 3 provides insights into the consequences of *Zdhhc3* knockout in TGFβ1-induced CF activation, in vitro migration, and pressure overload-induced remodeling in vivo. Chapter IV details a continuation of these investigations detailing the results of testing where *Zdhhc7 and Zdhhc3/7* were knocked out in CFs to determine how these enzymes contribute to cardiac remodeling in terms of fibroblast fibrotic gene expression, migration, transcription factor activity, and the development of hypertrophy and fibrosis in vivo in response to pro-fibrotic drugs. Further, the in vitro analyses performed here utilizing our Rac1 ConKI CFs represent the foremost examinations into how the palmitoylation status of Rac1 influences its role in fibroblast activation in response to TGFβ1, as well as the requirement for Rac1 palmitoylation in migration. Together, these studies represent the first probes into the role of palmitoylation and S-acyltransferases in CF biology and serve as a basis for future investigations into how these enzymes modulate signaling pathways involved in the activation processes of fibroblasts in the heart.

Chapter I Figures

Figure 1.1. Cardiac Fibroblast Activation in the Injured Heart Leads to Cardiac Fibrosis and Worsened Heart Function

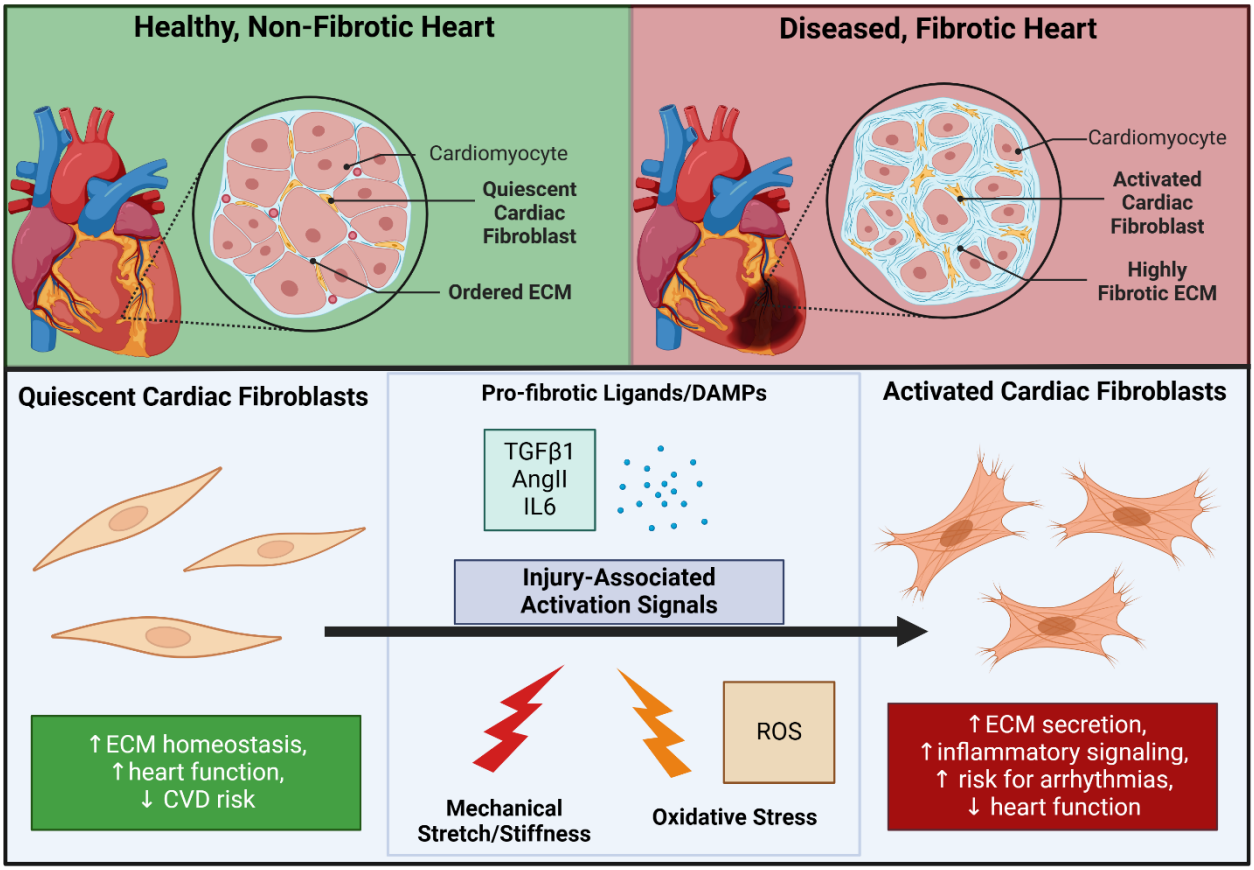

Figure 1.1: Cardiac Fibroblast Activation in the Injured Heart Leads to Cardiac Fibrosis and Worsened Heart Function. *Diagram depicting the injury-induced ECM remodeling within the heart tissue as part of CVD. Quiescent cardiac fibroblasts are stimulated by both chemical and mechanical signals to transition into their activated state, increasing the ECM component synthesis and secretion that leads to scar formation. Continued activation of these cells can lead to cardiac fibrosis, a maladaptive state that can reduce heart function and precipitate heart failure. Created with Biorender.com.*

Figure 1.2. Diagram of Fibrotic Signaling Regulated by zDHHC3 in Non-CF Cell Types

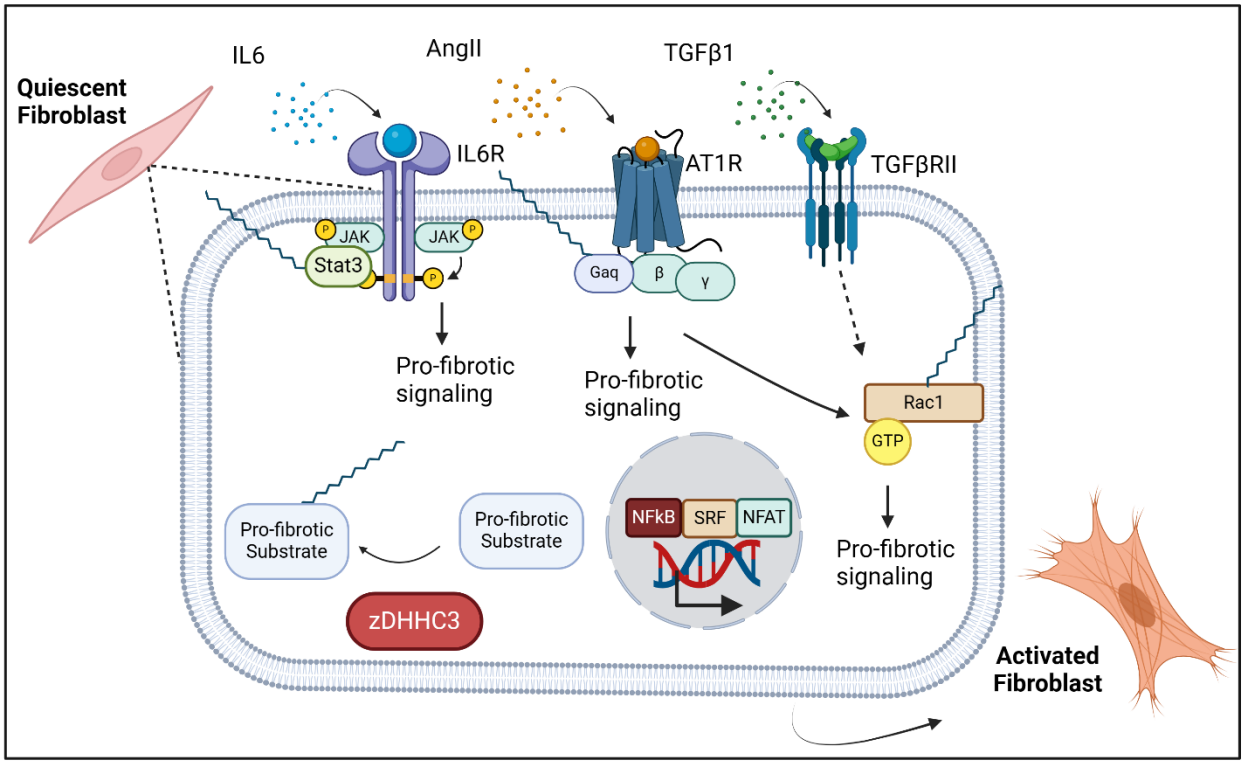

Figure 1.2: Diagram of Fibrotic Signaling Regulated by zDHHC3 in Non-CF cell types. *Hypothesized role of zDHHC3 in regulating the signaling underlying the transition of quiescent to activated fibroblast. A number of proteins involved in pro-fibrotic responses have been shown to be regulated by palmitoylation in other cell types. Signal transducer and activator of transcription 3 (Stat3), a transcription factor whose nuclear activity leads to fibroblast activation, is activated downstream of the cytokines interleukin-6's (IL6) agonism of the interleukin 6 receptor (IL6R) as part of the hearts inflammatory signaling. zDHHC3-mediated palmitoylation of Stat3 directs its plasma membrane localization where it can be phosphorylated by Janus kinase, a process required for its ability to mediate transcriptional changes in the nucleus. The pro-fibrotic ligand angiotensin II (AngII) mediates its remodeling influence on the heart through binding to angiotensin II receptor type 1 (AT1R), a G-protein coupled receptor that signals through Gaq. The Gaq subunit is palmitoylated by zDHHC3, directing its plasma membrane localization, though the role of how this PTM regulates its signaling ability in CFs remains unknown. The small Rho-family GTPase Ras-related C3 botulinum toxin substrate 1 or Rac1 is a known regulator of cardiac fibroblast activation, and is activated directly downstream of Gaq signaling and indirectly downstream of the major pro-fibrotic cytokine transforming growth factor beta 1 (TGFβ1) binding to transforming growth factor beta receptor II (TGFβRII). Rac1 is palmitoylated by zDHHC3 at cysteine 178, and this PTM influences its plasma membrane localization and GTP loaded state. Despite the evidence that palmitoylation critically regulates pro-fibrotic signaling molecules like Stat3, Gaq, and Rac1, it has not been directly tested how this influences the activity of pro-fibrotic transcription factors such as nuclear factor kappa-light-chain-enhancer of activated B cells (NFκB), serum response factor (SRF), and nuclear factor of activated T cells (NFAT) and cardiac fibroblast activation. Created with Biorender.com.*

References

Acevedo-Acevedo, S., & Crone, W. C. (2015, Dec 18). Substrate stiffness effect and chromosome missegregation in hIPS cells. J Negat Results Biomed, 14, 22. https://doi.org/10.1186/s12952-015-0042-8

Aicart-Ramos, C., Valero, R. A., & Rodriguez-Crespo, I. (2011, 2011/12/01/). Protein palmitoylation and subcellular trafficking. Biochimica et Biophysica Acta (BBA) - Biomembranes, 1808(12), 2981-2994. https://doi.org/https://doi.org/10.1016/j.bbamem.2011.07.009

Alhosaini, K., Azhar, A., Alonazi, A., & Al-Zoghaibi, F. (2021, 2021/06/01/). GPCRs: The most promiscuous druggable receptor of the mankind. Saudi Pharmaceutical Journal, 29(6), 539-551. https://doi.org/https://doi.org/10.1016/j.jsps.2021.04.015

Alter, C., Henseler, A. S., Owenier, C., Hesse, J., Ding, Z., Lautwein, T., Bahr, J., Hayat, S., Kramann, R., Kostenis, E., Scheller, J., & Schrader, J. (2023, Jun 1). IL-6 in the infarcted heart is preferentially formed by fibroblasts and modulated by purinergic signaling. J Clin Invest, 133(11). https://doi.org/10.1172/jci163799

Anwar, M. U., & van der Goot, F. G. (2023, Nov 6). Refining S-acylation: Structure, regulation, dynamics, and therapeutic implications. J Cell Biol, 222(11). https://doi.org/10.1083/jcb.202307103

Azevedo, P. S., Polegato, B. F., Minicucci, M. F., Paiva, S. A., & Zornoff, L. A. (2016, Jan). Cardiac Remodeling: Concepts, Clinical Impact, Pathophysiological Mechanisms and Pharmacologic Treatment. Arq Bras Cardiol, 106(1), 62-69. https://doi.org/10.5935/abc.20160005

Baekkeskov, S., & Kanaani, J. (2009, Jan). Palmitoylation cycles and regulation of protein function (Review). Mol Membr Biol, 26(1), 42-54. https://doi.org/10.1080/09687680802680108

Bai, J., Zhang, N., Hua, Y., Wang, B., Ling, L., Ferro, A., & Xu, B. (2013). Metformin inhibits angiotensin II-induced differentiation of cardiac fibroblasts into myofibroblasts. PLoS One, 8(9), e72120. https://doi.org/10.1371/journal.pone.0072120

Baldwin, T. A., Teuber, J. P., Kuwabara, Y., Subramani, A., Lin, S. J., Kanisicak, O., Vagnozzi, R. J., Zhang, W., Brody, M. J., & Molkentin, J. D. (2023, Nov 3). Palmitoylation-Dependent Regulation of Cardiomyocyte Rac1 Signaling Activity and Minor Effects on Cardiac Hypertrophy. J Biol Chem, 105426. https://doi.org/10.1016/j.jbc.2023.105426

Bazgir, F., Nau, J., Nakhaei-Rad, S., Amin, E., Wolf, M. J., Saucerman, J. J., Lorenz, K., & Ahmadian, M. R. (2023, Jul 4). The Microenvironment of the Pathogenesis of Cardiac Hypertrophy. Cells, 12(13). https://doi.org/10.3390/cells12131780

Bertaud, A., Joshkon, A., Heim, X., Bachelier, R., Bardin, N., Leroyer, A. S., & Blot-Chabaud, M. (2023, Jan 16). Signaling Pathways and Potential Therapeutic Strategies in Cardiac Fibrosis. Int J Mol Sci, 24(2). https://doi.org/10.3390/ijms24021756

Bill, C. A., & Vines, C. M. (2020). Phospholipase C. Adv Exp Med Biol, 1131, 215-242. https://doi.org/10.1007/978-3-030-12457-1_9

Black, A. R., & Black, J. D. (2012). Protein kinase C signaling and cell cycle regulation. Front Immunol, 3, 423. https://doi.org/10.3389/fimmu.2012.00423

Blanc, M., David, F. P. A., & van der Goot, F. G. (2019). SwissPalm 2: Protein S-Palmitoylation Database. Methods Mol Biol, 2009, 203-214. https://doi.org/10.1007/978-1-4939-9532-5_16

Blyszczuk, P., Müller-Edenborn, B., Valenta, T., Osto, E., Stellato, M., Behnke, S., Glatz, K., Basler, K., Lüscher, T. F., Distler, O., Eriksson, U., & Kania, G. (2017, May 7). Transforming growth factor-β-dependent Wnt secretion controls myofibroblast formation and myocardial fibrosis progression in experimental autoimmune myocarditis. Eur Heart J, 38(18), 1413-1425. https://doi.org/10.1093/eurheartj/ehw116

Bosco, E. E., Mulloy, J. C., & Zheng, Y. (2009, Feb). Rac1 GTPase: a "Rac" of all trades. Cell Mol Life Sci, 66(3), 370-374. https://doi.org/10.1007/s00018-008-8552-x

Buszka, A., Pytyś, A., Colvin, D., Włodarczyk, J., & Wójtowicz, T. (2023, Jan 21). S-Palmitoylation of Synaptic Proteins in Neuronal Plasticity in Normal and Pathological Brains. Cells, 12(3). https://doi.org/10.3390/cells12030387

Cadigan, K. M., & Waterman, M. L. (2012, Nov 1). TCF/LEFs and Wnt signaling in the nucleus. Cold Spring Harb Perspect Biol, 4(11). https://doi.org/10.1101/cshperspect.a007906

Cai, J., Cui, J., & Wang, L. (2023, Oct). S-palmitoylation regulates innate immune signaling pathways: molecular mechanisms and targeted therapies. Eur J Immunol, 53(10), e2350476. https://doi.org/10.1002/eji.202350476

Calabresi, P., Mechelli, A., Natale, G., Volpicelli-Daley, L., Di Lazzaro, G., & Ghiglieri, V. (2023, 2023/03/01). Alpha-synuclein in Parkinson's disease and other synucleinopathies: from overt neurodegeneration back to early synaptic dysfunction. Cell Death & Disease, 14(3), 176. https://doi.org/10.1038/s41419-023-05672-9

Camelliti, P., Borg, T. K., & Kohl, P. (2005, Jan 1). Structural and functional characterisation of cardiac fibroblasts. Cardiovasc Res, 65(1), 40-51. https://doi.org/10.1016/j.cardiores.2004.08.020

Cao, L., Chen, Y., Lu, L., Liu, Y., Wang, Y., Fan, J., & Yin, Y. (2018, Sep 1). Angiotensin II upregulates fibroblast-myofibroblast transition through Cx43-dependent CaMKII and TGF-β1 signaling in neonatal rat cardiac fibroblasts. Acta Biochim Biophys Sin (Shanghai), 50(9), 843-852. https://doi.org/10.1093/abbs/gmy090

Cargnello, M., & Roux, P. P. (2011, Mar). Activation and function of the MAPKs and their substrates, the MAPK-activated protein kinases. Microbiol Mol Biol Rev, 75(1), 50-83. https://doi.org/10.1128/mmbr.00031-10

Chaffin, M., Papangeli, I., Simonson, B., Akkad, A.-D., Hill, M. C., Arduini, A., Fleming, S. J., Melanson, M., Hayat, S., Kost-Alimova, M., Atwa, O., Ye, J., Bedi, K. C., Nahrendorf, M., Kaushik, V. K., Stegmann, C. M., Margulies, K. B., Tucker, N. R., & Ellinor, P. T. (2022, 2022/08/01). Single-nucleus profiling of human dilated and hypertrophic cardiomyopathy. Nature, 608(7921), 174-180. https://doi.org/10.1038/s41586-022-04817-8

Chakraborty, D., Šumová, B., Mallano, T., Chen, C. W., Distler, A., Bergmann, C., Ludolph, I., Horch, R. E., Gelse, K., Ramming, A., Distler, O., Schett, G., Šenolt, L., & Distler, J. H. W. (2017, Oct 24). Activation of STAT3 integrates common profibrotic pathways to promote fibroblast activation and tissue fibrosis. Nat Commun, 8(1), 1130. https://doi.org/10.1038/s41467-017-01236-6

Chamberlain, L. H., Lemonidis, K., Sanchez-Perez, M., Werno, M. W., Gorleku, O. A., & Greaves, J. (2013, Feb 1). Palmitoylation and the trafficking of peripheral membrane proteins. Biochem Soc Trans, 41(1), 62-66. https://doi.org/10.1042/bst20120243

Chamberlain, L. H., & Shipston, M. J. (2015, Apr). The physiology of protein S-acylation. Physiol Rev, 95(2), 341-376. https://doi.org/10.1152/physrev.00032.2014

Charollais, J., & Van Der Goot, F. G. (2009, Jan). Palmitoylation of membrane proteins (Review). Mol Membr Biol, 26(1), 55-66. https://doi.org/10.1080/09687680802620369

Chen, J. J., Fan, Y., & Boehning, D. (2021). Regulation of Dynamic Protein S-Acylation. Front Mol Biosci, 8, 656440. https://doi.org/10.3389/fmolb.2021.656440

Chen, K., Chen, J., Li, D., Zhang, X., & Mehta, J. L. (2004, Nov). Angiotensin II regulation of collagen type I expression in cardiac fibroblasts: modulation by PPAR-gamma ligand pioglitazone. Hypertension, 44(5), 655-661. https://doi.org/10.1161/01.HYP.0000144400.49062.6b

Chen, W., & Frangogiannis, N. G. (2013, 2013/04/01/). Fibroblasts in post-infarction inflammation and cardiac repair. Biochimica et Biophysica Acta (BBA) - Molecular Cell Research, 1833(4), 945-953. https://doi.org/https://doi.org/10.1016/j.bbamcr.2012.08.023

Chen, X., Niu, W., Fan, X., Yang, H., Zhao, C., Fan, J., Yao, X., & Fang, Z. (2023, Jan 5). Oct4A palmitoylation modulates tumorigenicity and stemness in human glioblastoma cells. Neuro Oncol, 25(1), 82-96. https://doi.org/10.1093/neuonc/noac157

Chen, Y., Surinkaew, S., Naud, P., Qi, X. Y., Gillis, M. A., Shi, Y. F., Tardif, J. C., Dobrev, D., & Nattel, S. (2017, Mar 1). JAK-STAT signalling and the atrial fibrillation promoting fibrotic substrate. Cardiovasc Res, 113(3), 310-320. https://doi.org/10.1093/cvr/cvx004

Cheng, Y., Wang, Y., Yin, R., Xu, Y., Zhang, L., Zhang, Y., Yang, L., & Zhao, D. (2023). Central role of cardiac fibroblasts in myocardial fibrosis of diabetic cardiomyopathy. Front Endocrinol (Lausanne), 14, 1162754. https://doi.org/10.3389/fendo.2023.1162754

Childers, R. C., Lucchesi, P. A., & Gooch, K. J. (2021, Jun 9). Decreased Substrate Stiffness Promotes a Hypofibrotic Phenotype in Cardiac Fibroblasts. Int J Mol Sci, 22(12). https://doi.org/10.3390/ijms22126231

Congreve, S. D., Main, A., Butler, A. S., Gao, X., Brown, E., Du, C., Choisy, S. C., Cheng, H., Hancox, J. C., & Fuller, W. (2023). Palmitoylation regulates the magnitude of HCN4-mediated currents in mammalian cells. Front Physiol, 14, 1163339. https://doi.org/10.3389/fphys.2023.1163339

Creemers, E. E., Cleutjens, J. P., Smits, J. F., & Daemen, M. J. (2001, Aug 3). Matrix metalloproteinase inhibition after myocardial infarction: a new approach to prevent heart failure? Circ Res, 89(3), 201-210. https://doi.org/10.1161/hh1501.094396

Cucoranu, I., Clempus, R., Dikalova, A., Phelan, P. J., Ariyan, S., Dikalov, S., & Sorescu, D. (2005, Oct 28). NAD(P)H oxidase 4 mediates transforming growth factor-beta1-induced differentiation of cardiac fibroblasts into myofibroblasts. Circ Res, 97(9), 900-907. https://doi.org/10.1161/01.Res.0000187457.24338.3d

Cuiffo, B., & Ren, R. (2010, Apr 29). Palmitoylation of oncogenic NRAS is essential for leukemogenesis. Blood, 115(17), 3598-3605. https://doi.org/10.1182/blood-2009-03-213876

De Mello, W. C., & Danser, A. H. (2000, Jun). Angiotensin II and the heart : on the intracrine renin-angiotensin system. Hypertension, 35(6), 1183-1188. https://doi.org/10.1161/01.hyp.35.6.1183

Decout, A., Katz, J. D., Venkatraman, S., & Ablasser, A. (2021, 2021/09/01). The cGAS–STING pathway as a therapeutic target in inflammatory diseases. Nature Reviews Immunology, 21(9), 548-569. https://doi.org/10.1038/s41577-021-00524-z

Del Re, D. P. (2022, Apr). Hippo-Yap signaling in cardiac and fibrotic remodeling. Curr Opin Physiol, 26. https://doi.org/10.1016/j.cophys.2022.100492

Dennis, K., & Heather, L. C. (2023). Post-translational palmitoylation of metabolic proteins. Front Physiol, 14, 1122895. https://doi.org/10.3389/fphys.2023.1122895

Dietrich, L. E., & Ungermann, C. (2004, Nov). On the mechanism of protein palmitoylation. EMBO Rep, 5(11), 1053-1057. https://doi.org/10.1038/sj.embor.7400277

Díez, J. (2007, Jul). Mechanisms of cardiac fibrosis in hypertension. J Clin Hypertens (Greenwich), 9(7), 546-550. https://doi.org/10.1111/j.1524-6175.2007.06626.x

Dobaczewski, M., Chen, W., & Frangogiannis, N. G. (2011, Oct). Transforming growth factor (TGF)-β signaling in cardiac remodeling. J Mol Cell Cardiol, 51(4), 600-606. https://doi.org/10.1016/j.yjmcc.2010.10.033

Dong, Q., Li, S., Wang, W., Han, L., Xia, Z., Wu, Y., Tang, Y., Li, J., & Cheng, X. (2019, Nov). FGF23 regulates atrial fibrosis in atrial fibrillation by mediating the STAT3 and SMAD3 pathways. J Cell Physiol, 234(11), 19502-19510. https://doi.org/10.1002/jcp.28548

Emig, R., Zgierski-Johnston, C. M., Timmermann, V., Taberner, A. J., Nash, M. P., Kohl, P., & Peyronnet, R. (2021, Oct). Passive myocardial mechanical properties: meaning, measurement, models. Biophys Rev, 13(5), 587-610. https://doi.org/10.1007/s12551-021-00838-1

Essandoh, K., Philippe, J. M., Jenkins, P. M., & Brody, M. J. (2020). Palmitoylation: A Fatty Regulator of Myocardial Electrophysiology. Front Physiol, 11, 108. https://doi.org/10.3389/fphys.2020.00108

Essandoh, K., Subramani, A., Ferro, O. A., Teuber, J. P., Koripella, S., & Brody, M. J. (2023, May). zDHHC9 Regulates Cardiomyocyte Rab3a Activity and Atrial Natriuretic Peptide Secretion Through Palmitoylation of Rab3gap1. JACC Basic Transl Sci, 8(5), 518-542. https://doi.org/10.1016/j.jacbts.2022.11.003

Fan, D., Takawale, A., Lee, J., & Kassiri, Z. (2012, Sep 3). Cardiac fibroblasts, fibrosis and extracellular matrix remodeling in heart disease. Fibrogenesis Tissue Repair, 5(1), 15. https://doi.org/10.1186/1755-1536-5-15

Fan, Y., Gao, Y., Nie, L., Hou, T., Dan, W., Wang, Z., Liu, T., Wei, Y., Wang, Y., Liu, B., Que, T., Lei, Y., Zeng, J., Ma, J., Wei, W., & Li, L. (2023, Oct 5). Targeting LYPLAL1-mediated cGAS depalmitoylation enhances the response to anti-tumor immunotherapy. Mol Cell, 83(19), 3520-3532.e3527. https://doi.org/10.1016/j.molcel.2023.09.007

Felisbino, M. B., Rubino, M., Travers, J. G., Schuetze, K. B., Lemieux, M. E., Anseth, K. S., Aguado, B. A., & McKinsey, T. A. (2024, Jan 1). Substrate stiffness modulates cardiac fibroblast activation, senescence, and proinflammatory secretory phenotype. Am J Physiol Heart Circ Physiol, 326(1), H61-h73. https://doi.org/10.1152/ajpheart.00483.2023

Forrester, S. J., Booz, G. W., Sigmund, C. D., Coffman, T. M., Kawai, T., Rizzo, V., Scalia, R., & Eguchi, S. (2018, Jul 1). Angiotensin II Signal Transduction: An Update on Mechanisms of Physiology and Pathophysiology. Physiol Rev, 98(3), 1627-1738. https://doi.org/10.1152/physrev.00038.2017

Frąk, W., Wojtasińska, A., Lisińska, W., Młynarska, E., Franczyk, B., & Rysz, J. (2022, Aug 10). Pathophysiology of Cardiovascular Diseases: New Insights into Molecular Mechanisms of Atherosclerosis, Arterial Hypertension, and Coronary Artery Disease. Biomedicines, 10(8). https://doi.org/10.3390/biomedicines10081938

Francisco, J., Zhang, Y., Jeong, J. I., Mizushima, W., Ikeda, S., Ivessa, A., Oka, S., Zhai, P., Tallquist, M. D., & Del Re, D. P. (2020, Sep). Blockade of Fibroblast YAP Attenuates Cardiac Fibrosis and Dysfunction Through MRTF-A Inhibition. JACC Basic Transl Sci, 5(9), 931-945. https://doi.org/10.1016/j.jacbts.2020.07.009

Francisco, J., Zhang, Y., Nakada, Y., Jeong, J. I., Huang, C. Y., Ivessa, A., Oka, S., Babu, G. J., & Del Re, D. P. (2021, May 18). AAV-mediated YAP expression in cardiac fibroblasts promotes inflammation and increases fibrosis. Sci Rep, 11(1), 10553. https://doi.org/10.1038/s41598-021-89989-5

Frangogiannis, N. (2020, Mar 2). Transforming growth factor-β in tissue fibrosis. J Exp Med, 217(3), e20190103. https://doi.org/10.1084/jem.20190103

Frangogiannis, N. G. (2017, May 1). The extracellular matrix in myocardial injury, repair, and remodeling. J Clin Invest, 127(5), 1600-1612. https://doi.org/10.1172/jci87491

Frangogiannis, N. G. (2019, Jun 21). The Extracellular Matrix in Ischemic and Nonischemic Heart Failure. Circ Res, 125(1), 117-146. https://doi.org/10.1161/circresaha.119.311148

Frangogiannis, N. G. (2021, May 25). Cardiac fibrosis. Cardiovasc Res, 117(6), 1450-1488. https://doi.org/10.1093/cvr/cvaa324

Frangogiannis, N. G. (2022, Jul). Transforming growth factor-β in myocardial disease. Nat Rev Cardiol, 19(7), 435-455. https://doi.org/10.1038/s41569-021-00646-w

Frémond, M. L., & Crow, Y. J. (2021, Apr). STING-Mediated Lung Inflammation and Beyond. J Clin Immunol, 41(3), 501-514. https://doi.org/10.1007/s10875-021-00974-z

Fu, X., Khalil, H., Kanisicak, O., Boyer, J. G., Vagnozzi, R. J., Maliken, B. D., Sargent, M. A., Prasad, V., Valiente-Alandi, I., Blaxall, B. C., & Molkentin, J. D. (2018, May 1). Specialized fibroblast differentiated states underlie scar formation in the infarcted mouse heart. J Clin Invest, 128(5), 2127-2143. https://doi.org/10.1172/jci98215

Fu, X., Liu, Q., Li, C., Li, Y., & Wang, L. (2020). Cardiac Fibrosis and Cardiac Fibroblast Lineage-Tracing: Recent Advances. Front Physiol, 11, 416. https://doi.org/10.3389/fphys.2020.00416

Fu, Y., Liu, M., Li, F., Qian, L., Zhang, P., Lv, F., Cheng, W., & Hou, R. (2019). MiR-221 Promotes Hepatocellular Carcinoma Cells Migration via Targeting PHF2. Biomed Res Int, 2019, 4371405. https://doi.org/10.1155/2019/4371405

Gałdyszyńska, M., Radwańska, P., Szymański, J., & Drobnik, J. (2021, Dec 11). The Stiffness of Cardiac Fibroblast Substrates Exerts a Regulatory Influence on Collagen Metabolism via α2β1 Integrin, FAK and Src Kinases. Cells, 10(12). https://doi.org/10.3390/cells10123506

García-Martín, A., Navarrete, C., Garrido-Rodríguez, M., Prados, M. E., Caprioglio, D., Appendino, G., & Muñoz, E. (2021, 2021/10/01/). EHP-101 alleviates angiotensin II-induced fibrosis and inflammation in mice. Biomedicine & Pharmacotherapy, 142, 112007. https://doi.org/https://doi.org/10.1016/j.biopha.2021.112007

Garoffolo, G., & Pesce, M. (2019, Dec 11). Mechanotransduction in the Cardiovascular System: From Developmental Origins to Homeostasis and Pathology. Cells, 8(12). https://doi.org/10.3390/cells8121607

Gibb, A. A., Lazaropoulos, M. P., & Elrod, J. W. (2020, Jul 17). Myofibroblasts and Fibrosis: Mitochondrial and Metabolic Control of Cellular Differentiation. Circ Res, 127(3), 427-447. https://doi.org/10.1161/circresaha.120.316958

Giordano, A. M. S., Luciani, M., Gatto, F., Abou Alezz, M., Beghè, C., Della Volpe, L., Migliara, A., Valsoni, S., Genua, M., Dzieciatkowska, M., Frati, G., Tahraoui-Bories, J., Giliani, S. C., Orcesi, S., Fazzi, E., Ostuni, R., D'Alessandro, A., Di Micco, R., Merelli, I., Lombardo, A., Reijns, M. A. M., Gromak, N., Gritti, A., & Kajaste-Rudnitski, A. (2022, Apr 4). DNA damage contributes to neurotoxic inflammation in Aicardi-Goutières syndrome astrocytes. J Exp Med, 219(4). https://doi.org/10.1084/jem.20211121

Gök, C., Robertson, A. D., & Fuller, W. (2022, 2022/06/01/). Insulin-induced palmitoylation regulates the Cardiac Na+/Ca2+ exchanger NCX1. Cell Calcium, 104, 102567. https://doi.org/https://doi.org/10.1016/j.ceca.2022.102567

Gu, M., Jiang, H., Tan, M., Yu, L., Xu, N., Li, Y., Wu, H., Hou, Q., & Dai, C. (2023, 2023/10/21). Palmitoyltransferase DHHC9 and acyl protein thioesterase APT1 modulate renal fibrosis through regulating β-catenin palmitoylation. Nature Communications, 14(1), 6682. https://doi.org/10.1038/s41467-023-42476-z

Guan, X., & Fierke, C. A. (2011, Dec). Understanding Protein Palmitoylation: Biological Significance and Enzymology. Sci China Chem, 54(12), 1888-1897. https://doi.org/10.1007/s11426-011-4428-2

Guo, X., & Zhao, B. (2013, 2013/08/28). Integration of mechanical and chemical signals by YAP and TAZ transcription coactivators. Cell & Bioscience, 3(1), 33. https://doi.org/10.1186/2045-3701-3-33

Hall, C., Law, J. P., Reyat, J. S., Cumberland, M. J., Hang, S., Vo, N. T. N., Raniga, K., Weston, C. J., O'Shea, C., Townend, J. N., Gehmlich, K., Ferro, C. J., Denning, C., & Pavlovic, D. (2023, 2023/07/26). Chronic activation of human cardiac fibroblasts in vitro attenuates the reversibility of the myofibroblast phenotype. Scientific Reports, 13(1), 12137. https://doi.org/10.1038/s41598-023-39369-y

Hall, J., Brault, A., Vincent, F., Weng, S., Wang, H., Dumlao, D., Aulabaugh, A., Aivazian, D., Castro, D., Chen, M., Culp, J., Dower, K., Gardner, J., Hawrylik, S., Golenbock, D., Hepworth, D., Horn, M., Jones, L., Jones, P., Latz, E., Li, J., Lin, L. L., Lin, W., Lin, D., Lovering, F., Niljanskul, N., Nistler, R., Pierce, B., Plotnikova, O., Schmitt, D., Shanker, S., Smith, J., Snyder, W., Subashi, T., Trujillo, J., Tyminski, E., Wang, G., Wong, J., Lefker, B., Dakin, L., & Leach, K. (2017). Discovery of PF-06928215 as a high affinity inhibitor of cGAS enabled by a novel fluorescence polarization assay. PLoS One, 12(9), e0184843. https://doi.org/10.1371/journal.pone.0184843

Hanna, A., Humeres, C., & Frangogiannis, N. G. (2021, Jan). The role of Smad signaling cascades in cardiac fibrosis. Cell Signal, 77, 109826. https://doi.org/10.1016/j.cellsig.2020.109826

Hansen, A. L., Buchan, G. J., Rühl, M., Mukai, K., Salvatore, S. R., Ogawa, E., Andersen, S. D., Iversen, M. B., Thielke, A. L., Gunderstofte, C., Motwani, M., Møller, C. T., Jakobsen, A. S., Fitzgerald, K. A., Roos, J., Lin, R., Maier, T. J., Goldbach-Mansky, R., Miner, C. A., Qian, W., Miner, J. J., Rigby, R. E., Rehwinkel, J., Jakobsen, M. R., Arai, H., Taguchi, T., Schopfer, F. J., Olagnier, D., & Holm, C. K. (2018, Aug 14). Nitro-fatty acids are formed in response to virus infection and are potent inhibitors of STING palmitoylation and signaling. Proc Natl Acad Sci U S A, 115(33), E7768-e7775. https://doi.org/10.1073/pnas.1806239115

Hansen, A. L., Mukai, K., Schopfer, F. J., Taguchi, T., & Holm, C. K. (2019, 2019/03/01). STING palmitoylation as a therapeutic target. Cellular & Molecular Immunology, 16(3), 236-241. https://doi.org/10.1038/s41423-019-0205-5

Hara, H., Takeda, N., & Komuro, I. (2017, 2017/07/17). Pathophysiology and therapeutic potential of cardiac fibrosis. Inflammation and Regeneration, 37(1), 13. https://doi.org/10.1186/s41232-017-0046-5

Harrison, D. A. (2012, Mar 1). The Jak/STAT pathway. Cold Spring Harb Perspect Biol, 4(3). https://doi.org/10.1101/cshperspect.a011205

Hecker, L., Vittal, R., Jones, T., Jagirdar, R., Luckhardt, T. R., Horowitz, J. C., Pennathur, S., Martinez, F. J., & Thannickal, V. J. (2009, Sep). NADPH oxidase-4 mediates myofibroblast activation and fibrogenic responses to lung injury. Nat Med, 15(9), 1077-1081. https://doi.org/10.1038/nm.2005

Heldin, C. H., & Moustakas, A. (2016, Aug 1). Signaling Receptors for TGF-β Family Members. Cold Spring Harb Perspect Biol, 8(8). https://doi.org/10.1101/cshperspect.a022053

Herum, K. M., Choppe, J., Kumar, A., Engler, A. J., & McCulloch, A. D. (2017, Jul 7). Mechanical regulation of cardiac fibroblast profibrotic phenotypes. Mol Biol Cell, 28(14), 1871-1882. https://doi.org/10.1091/mbc.E17-01-0014

Higuchi, Y., Otsu, K., Nishida, K., Hirotani, S., Nakayama, H., Yamaguchi, O., Hikoso, S., Kashiwase, K., Takeda, T., Watanabe, T., Mano, T., Matsumura, Y., Ueno, H., & Hori, M. (2003, Jun 6). The small GTP-binding protein Rac1 induces cardiac myocyte hypertrophy through the activation of apoptosis signal-regulating kinase 1 and nuclear factor-kappa B. J Biol Chem, 278(23), 20770-20777. https://doi.org/10.1074/jbc.M213203200

Hinderer, S., & Schenke-Layland, K. (2019, 2019/06/01/). Cardiac fibrosis – A short review of causes and therapeutic strategies. Advanced Drug Delivery Reviews, 146, 77-82. https://doi.org/https://doi.org/10.1016/j.addr.2019.05.011

Ho, G. P. H., Wilkie, E. C., White, A. J., & Selkoe, D. J. (2023, Feb 14). Palmitoylation of the Parkinson's disease-associated protein synaptotagmin-11 links its turnover to α-synuclein homeostasis. Sci Signal, 16(772), eadd7220. https://doi.org/10.1126/scisignal.add7220

Hu, H.-H., Chen, D.-Q., Wang, Y.-N., Feng, Y.-L., Cao, G., Vaziri, N. D., & Zhao, Y.-Y. (2018, 2018/08/25/). New insights into TGF-β/Smad signaling in tissue fibrosis. Chemico-Biological Interactions, 292, 76-83. https://doi.org/https://doi.org/10.1016/j.cbi.2018.07.008

Hu, Q., Bian, Q., Rong, D., Wang, L., Song, J., Huang, H. S., Zeng, J., Mei, J., & Wang, P. Y. (2023). JAK/STAT pathway: Extracellular signals, diseases, immunity, and therapeutic regimens. Front Bioeng Biotechnol, 11, 1110765. https://doi.org/10.3389/fbioe.2023.1110765

Huang, C. C., Yang, D. M., Lin, C. C., & Kao, L. S. (2011, Oct). Involvement of Rab3A in vesicle priming during exocytosis: interaction with Munc13-1 and Munc18-1. Traffic, 12(10), 1356-1370. https://doi.org/10.1111/j.1600-0854.2011.01237.x

Huang, C. L., & Lei, M. (2023, Jun 19). Cardiomyocyte electrophysiology and its modulation: current views and future prospects. Philos Trans R Soc Lond B Biol Sci, 378(1879), 20220160. https://doi.org/10.1098/rstb.2022.0160

Huang, S., Chen, B., Humeres, C., Alex, L., Hanna, A., & Frangogiannis, N. G. (2020, 2020/07/01/). The role of Smad2 and Smad3 in regulating homeostatic functions of fibroblasts in vitro and in adult mice. Biochimica et Biophysica Acta (BBA) - Molecular Cell Research, 1867(7), 118703. https://doi.org/https://doi.org/10.1016/j.bbamcr.2020.118703

Humeres, C., & Frangogiannis, N. G. (2019, Jun). Fibroblasts in the Infarcted, Remodeling, and Failing Heart. JACC Basic Transl Sci, 4(3), 449-467. https://doi.org/10.1016/j.jacbts.2019.02.006

Ivey, M. J., & Tallquist, M. D. (2016, Oct 25). Defining the Cardiac Fibroblast. Circ J, 80(11), 2269-2276. https://doi.org/10.1253/circj.CJ-16-1003

Jeong, D.-W., Park, J.-W., Kim, K. S., Kim, J., Huh, J., Seo, J., Kim, Y. L., Cho, J.-Y., Lee, K.-W., Fukuda, J., & Chun, Y.-S. (2023, 2023/10/12). Palmitoylation-driven PHF2 ubiquitination remodels lipid metabolism through the SREBP1c axis in hepatocellular carcinoma. Nature Communications, 14(1), 6370. https://doi.org/10.1038/s41467-023-42170-0

Jiang, H., Zhang, X., Chen, X., Aramsangtienchai, P., Tong, Z., & Lin, H. (2018, Feb 14). Protein Lipidation: Occurrence, Mechanisms, Biological Functions, and Enabling Technologies. Chem Rev, 118(3), 919-988. https://doi.org/10.1021/acs.chemrev.6b00750

Jiang, W., Xiong, Y., Li, X., & Yang, Y. (2021). Cardiac Fibrosis: Cellular Effectors, Molecular Pathways, and Exosomal Roles. Front Cardiovasc Med, 8, 715258. https://doi.org/10.3389/fcvm.2021.715258

Jurgens, C. Y., Lee, C. S., Aycock, D. M., Masterson Creber, R., Denfeld, Q. E., DeVon, H. A., Evers, L. R., Jung, M., Pucciarelli, G., Streur, M. M., & Konstam, M. A. (2022, Sep 20). State of the Science: The Relevance of Symptoms in Cardiovascular Disease and Research: A Scientific Statement From the American Heart Association. Circulation, 146(12), e173-e184. https://doi.org/10.1161/cir.0000000000001089

Kagan, P., Sultan, M., Tachlytski, I., Safran, M., & Ben-Ari, Z. (2017). Both MAPK and STAT3 signal transduction pathways are necessary for IL-6-dependent hepatic stellate cells activation. PLoS One, 12(5), e0176173. https://doi.org/10.1371/journal.pone.0176173

Kamato, D., Thach, L., Bernard, R., Chan, V., Zheng, W., Kaur, H., Brimble, M., Osman, N., & Little, P. J. (2015). Structure, Function, Pharmacology, and Therapeutic Potential of the G Protein, Gα/q,11. Front Cardiovasc Med, 2, 14. https://doi.org/10.3389/fcvm.2015.00014

Kanisicak, O., Khalil, H., Ivey, M. J., Karch, J., Maliken, B. D., Correll, R. N., Brody, M. J., SC, J. L., Aronow, B. J., Tallquist, M. D., & Molkentin, J. D. (2016, Jul 22). Genetic lineage tracing defines myofibroblast origin and function in the injured heart. Nat Commun, 7, 12260. https://doi.org/10.1038/ncomms12260

Kapur, N. K. (2011). Transforming Growth Factor-β. Circulation: Heart Failure, 4(1), 5-7. https://doi.org/doi:10.1161/CIRCHEARTFAILURE.110.960054

Kato, Y., Park, J., Takamatsu, H., Konaka, H., Aoki, W., Aburaya, S., Ueda, M., Nishide, M., Koyama, S., Hayama, Y., Kinehara, Y., Hirano, T., Shima, Y., Narazaki, M., & Kumanogoh, A. (2018, Oct). Apoptosis-derived membrane vesicles drive the cGAS-STING pathway and enhance type I IFN production in systemic lupus erythematosus. Ann Rheum Dis, 77(10), 1507-1515. https://doi.org/10.1136/annrheumdis-2018-212988

Kaur, G., Verma, S. K., Singh, D., & Singh, N. K. (2023, Jan 6). Role of G-Proteins and GPCRs in Cardiovascular Pathologies. Bioengineering (Basel), 10(1). https://doi.org/10.3390/bioengineering10010076

Kawano, H., Do, Y. S., Kawano, Y., Starnes, V., Barr, M., Law, R. E., & Hsueh, W. A. (2000, Mar 14). Angiotensin II has multiple profibrotic effects in human cardiac fibroblasts. Circulation, 101(10), 1130-1137. https://doi.org/10.1161/01.cir.101.10.1130

Kazbanov, I. V., ten Tusscher, K. H. W. J., & Panfilov, A. V. (2016, 2016/02/10). Effects of Heterogeneous Diffuse Fibrosis on Arrhythmia Dynamics and Mechanism. Scientific Reports, 6(1), 20835. https://doi.org/10.1038/srep20835

Khalil, H., Kanisicak, O., Prasad, V., Correll, R. N., Fu, X., Schips, T., Vagnozzi, R. J., Liu, R., Huynh, T., Lee, S. J., Karch, J., & Molkentin, J. D. (2017, Oct 2). Fibroblast-specific TGF-β-Smad2/3 signaling underlies cardiac fibrosis. J Clin Invest, 127(10), 3770-3783. https://doi.org/10.1172/jci94753

Kim, H. E., Dalal, S. S., Young, E., Legato, M. J., Weisfeldt, M. L., & D'Armiento, J. (2000, Oct). Disruption of the myocardial extracellular matrix leads to cardiac dysfunction. J Clin Invest, 106(7), 857-866. https://doi.org/10.1172/jci8040

Kingma, J., Simard, C., & Drolet, B. (2023, Jun 6). Overview of Cardiac Arrhythmias and Treatment Strategies. Pharmaceuticals (Basel), 16(6). https://doi.org/10.3390/ph16060844

Kitamura, N., & Galligan, J. J. (2023, Aug 30). A global view of the human post-translational modification landscape. Biochem J, 480(16), 1241-1265. https://doi.org/10.1042/bcj20220251

Ko, T., Nomura, S., Yamada, S., Fujita, K., Fujita, T., Satoh, M., Oka, C., Katoh, M., Ito, M., Katagiri, M., Sassa, T., Zhang, B., Hatsuse, S., Yamada, T., Harada, M., Toko, H., Amiya, E., Hatano, M., Kinoshita, O., Nawata, K., Abe, H., Ushiku, T., Ono, M., Ikeuchi, M., Morita, H., Aburatani, H., & Komuro, I. (2022, 2022/06/07). Cardiac fibroblasts regulate the development of heart failure via Htra3-TGF-β-IGFBP7 axis. Nature Communications, 13(1), 3275. https://doi.org/10.1038/s41467-022-30630-y

Kong, P., Christia, P., & Frangogiannis, N. G. (2014, Feb). The pathogenesis of cardiac fibrosis. Cell Mol Life Sci, 71(4), 549-574. https://doi.org/10.1007/s00018-013-1349-6

Kong, Y., Liu, Y., Li, X., Rao, M., Li, D., Ruan, X., Li, S., Jiang, Z., & Zhang, Q. (2023, 2023/11/17). Palmitoylation landscapes across human cancers reveal a role of palmitoylation in tumorigenesis. Journal of Translational Medicine, 21(1), 826. https://doi.org/10.1186/s12967-023-04611-8

Kunschmann, T., Puder, S., Fischer, T., Steffen, A., Rottner, K., & Mierke, C. T. (2019, May 22). The Small GTPase Rac1 Increases Cell Surface Stiffness and Enhances 3D Migration Into Extracellular Matrices. Sci Rep, 9(1), 7675. https://doi.org/10.1038/s41598-019-43975-0

Kuo, C. S., Dobi, S., Gök, C., Da Silva Costa, A., Main, A., Robertson-Gray, O., Baptista-Hon, D., Wypijewski, K. J., Costello, H., Hales, T. G., MacQuaide, N., Smith, G. L., & Fuller, W. (2023, Feb 14). Palmitoylation of the pore-forming subunit of Ca(v)1.2 controls channel voltage sensitivity and calcium transients in cardiac myocytes. Proc Natl Acad Sci U S A, 120(7), e2207887120. https://doi.org/10.1073/pnas.2207887120

Kuwahara, F., Kai, H., Tokuda, K., Takeya, M., Takeshita, A., Egashira, K., & Imaizumi, T. (2004, Apr). Hypertensive myocardial fibrosis and diastolic dysfunction: another model of inflammation? Hypertension, 43(4), 739-745. https://doi.org/10.1161/01.HYP.0000118584.33350.7d

Kwong, L. N., Costello, J. C., Liu, H., Jiang, S., Helms, T. L., Langsdorf, A. E., Jakubosky, D., Genovese, G., Muller, F. L., Jeong, J. H., Bender, R. P., Chu, G. C., Flaherty, K. T., Wargo, J. A., Collins, J. J., & Chin, L. (2012, Oct). Oncogenic NRAS signaling differentially regulates survival and proliferation in melanoma. Nat Med, 18(10), 1503-1510. https://doi.org/10.1038/nm.2941

Landry, N. M., & Dixon, I. M. C. (2020, Dec). Fibroblast mechanosensing, SKI and Hippo signaling and the cardiac fibroblast phenotype: Looking beyond TGF-β. Cell Signal, 76, 109802. https://doi.org/10.1016/j.cellsig.2020.109802

Landry, N. M., Rattan, S. G., & Dixon, I. M. C. (2019, Sep 9). An Improved Method of Maintaining Primary Murine Cardiac Fibroblasts in Two-Dimensional Cell Culture. Sci Rep, 9(1), 12889. https://doi.org/10.1038/s41598-019-49285-9

Landry, N. M., Rattan, S. G., & Dixon, I. M. C. (2021). Soft Substrate Culture to Mechanically Control Cardiac Myofibroblast Activation. Methods Mol Biol, 2299, 171-179. https://doi.org/10.1007/978-1-0716-1382-5_13

Lavall, D., Schuster, P., Jacobs, N., Kazakov, A., Böhm, M., & Laufs, U. (2017, May 5). Rac1 GTPase regulates 11β hydroxysteroid dehydrogenase type 2 and fibrotic remodeling. J Biol Chem, 292(18), 7542-7553. https://doi.org/10.1074/jbc.M116.764449

Lee, K. H., Park, J. W., Sung, H. S., Choi, Y. J., Kim, W. H., Lee, H. S., Chung, H. J., Shin, H. W., Cho, C. H., Kim, T. Y., Li, S. H., Youn, H. D., Kim, S. J., & Chun, Y. S. (2015, May 28). PHF2 histone demethylase acts as a tumor suppressor in association with p53 in cancer. Oncogene, 34(22), 2897-2909. https://doi.org/10.1038/onc.2014.219

Levental, I., Lingwood, D., Grzybek, M., Coskun, U., & Simons, K. (2010, Dec 21). Palmitoylation regulates raft affinity for the majority of integral raft proteins. Proc Natl Acad Sci U S A, 107(51), 22050-22054. https://doi.org/10.1073/pnas.1016184107

Li, J. C., Jia, J., Dong, L., Hu, Z. J., Huang, X. R., Wang, H. L., Wang, L., Yang, S. J., & Lan, H. Y. (2023, Sep 12). Angiotensin II mediates hypertensive cardiac fibrosis via an Erbb4-IR-dependent mechanism. Mol Ther Nucleic Acids, 33, 180-190. https://doi.org/10.1016/j.omtn.2023.06.017

Li, M., Zhang, L., & Chen, C. W. (2023, Sep 5). Diverse Roles of Protein Palmitoylation in Cancer Progression, Immunity, Stemness, and Beyond. Cells, 12(18). https://doi.org/10.3390/cells12182209

Li, W., Pang, Y., Wang, Y., Mei, F., Guo, M., Wei, Y., Li, X., Qin, W., Wang, W., Jia, L., & Jia, J. (2023, 2023/06/26). Aberrant palmitoylation caused by a ZDHHC21 mutation contributes to pathophysiology of Alzheimer's disease. BMC Medicine, 21(1), 223. https://doi.org/10.1186/s12916-023-02930-7

Li, X., Garcia-Elias, A., Benito, B., & Nattel, S. (2022, Jan 29). The effects of cardiac stretch on atrial fibroblasts: analysis of the evidence and potential role in atrial fibrillation. Cardiovasc Res, 118(2), 440-460. https://doi.org/10.1093/cvr/cvab035

Li, Y., Zhao, J., Yin, Y., Li, K., Zhang, C., & Zheng, Y. (2022). The Role of IL-6 in Fibrotic Diseases: Molecular and Cellular Mechanisms. International journal of biological sciences, 18(14), 5405-5414. https://doi.org/10.7150/ijbs.75876

Liang, C., Wang, K., Li, Q., Bai, J., & Zhang, H. (2019, Oct 2). Influence of the distribution of fibrosis within an area of myocardial infarction on wave propagation in ventricular tissue. Sci Rep, 9(1), 14151. https://doi.org/10.1038/s41598-019-50478-5

Liao, D., Huang, Y., Liu, D., Zhang, H., Shi, X., Li, X., & Luo, P. (2023). The role of s-palmitoylation in neurological diseases: implication for zDHHC family. Front Pharmacol, 14, 1342830. https://doi.org/10.3389/fphar.2023.1342830

Lighthouse, J. K., & Small, E. M. (2016, Feb). Transcriptional control of cardiac fibroblast plasticity. J Mol Cell Cardiol, 91, 52-60. https://doi.org/10.1016/j.yjmcc.2015.12.016

Lim, P. S., Sutton, C. R., & Rao, S. (2015, Dec). Protein kinase C in the immune system: from signalling to chromatin regulation. Immunology, 146(4), 508-522. https://doi.org/10.1111/imm.12510

Lin, H. (2021, Dec). Protein cysteine palmitoylation in immunity and inflammation. Febs j, 288(24), 7043-7059. https://doi.org/10.1111/febs.15728

Lin, K. C., Park, H. W., & Guan, K. L. (2017, Nov). Regulation of the Hippo Pathway Transcription Factor TEAD. Trends Biochem Sci, 42(11), 862-872. https://doi.org/10.1016/j.tibs.2017.09.003

Linder, M. E., & Deschenes, R. J. (2003, Apr 22). New insights into the mechanisms of protein palmitoylation. Biochemistry, 42(15), 4311-4320. https://doi.org/10.1021/bi034159a

Linder, M. E., & Deschenes, R. J. (2007, 2007/01/01). Palmitoylation: policing protein stability and traffic. Nature Reviews Molecular Cell Biology, 8(1), 74-84. https://doi.org/10.1038/nrm2084

Liu, H., Fan, P., Jin, F., Huang, G., Guo, X., & Xu, F. (2022). Dynamic and static biomechanical traits of cardiac fibrosis. Front Bioeng Biotechnol, 10, 1042030. https://doi.org/10.3389/fbioe.2022.1042030

Liu, H., Yan, P., Wu, C., Rao, M., Zhu, J., Lv, L., Li, W., Liang, Y., Qi, S., Lu, K., & Kong, E. (2023, Dec 5). Palmitoylated Sept8-204 modulates learning and anxiety by regulating filopodia arborization and actin dynamics. Sci Signal, 16(814), eadi8645. https://doi.org/10.1126/scisignal.adi8645

Liu, J., Wang, F., & Luo, F. (2023, Jan 6). The Role of JAK/STAT Pathway in Fibrotic Diseases: Molecular and Cellular Mechanisms. Biomolecules, 13(1). https://doi.org/10.3390/biom13010119

Liu, J., Xiao, Q., Xiao, J., Niu, C., Li, Y., Zhang, X., Zhou, Z., Shu, G., & Yin, G. (2022, 2022/01/03). Wnt/β-catenin signalling: function, biological mechanisms, and therapeutic opportunities. Signal Transduction and Targeted Therapy, 7(1), 3. https://doi.org/10.1038/s41392-021-00762-6

Liu, P., Jiao, B., Zhang, R., Zhao, H., Zhang, C., Wu, M., Li, D., Zhao, X., Qiu, Q., Li, J., & Ren, R. (2016, 2016/05/01). Palmitoylacyltransferase Zdhhc9 inactivation mitigates leukemogenic potential of oncogenic Nras. Leukemia, 30(5), 1225-1228. https://doi.org/10.1038/leu.2015.293

Liu, S., Kapoor, M., & Leask, A. (2009, May). Rac1 expression by fibroblasts is required for tissue repair in vivo. Am J Pathol, 174(5), 1847-1856. https://doi.org/10.2353/ajpath.2009.080779

Liu, Y., & Pu, F. (2023). Updated roles of cGAS-STING signaling in autoimmune diseases. Front Immunol, 14, 1254915. https://doi.org/10.3389/fimmu.2023.1254915

Liu, Z. Y., Lan, T., Tang, F., He, Y. Z., Liu, J. S., Yang, J. Z., Chen, X., Wang, Z. F., & Li, Z. Q. (2023, May 9). ZDHHC15 promotes glioma malignancy and acts as a novel prognostic biomarker for patients with glioma. BMC Cancer, 23(1), 420. https://doi.org/10.1186/s12885-023-10883-6

López, B., Ravassa, S., Moreno, M. U., José, G. S., Beaumont, J., González, A., & Díez, J. (2021, 2021/07/01). Diffuse myocardial fibrosis: mechanisms, diagnosis and therapeutic approaches. Nature Reviews Cardiology, 18(7), 479-498. https://doi.org/10.1038/s41569-020-00504-1

Lu, W., Meng, Z., Hernandez, R., & Zhou, C. (2021, Sep 22). Fibroblast-specific IKK-β deficiency ameliorates angiotensin II-induced adverse cardiac remodeling in mice. JCI Insight, 6(18). https://doi.org/10.1172/jci.insight.150161

Luo, S., Hieu, T. B., Ma, F., Yu, Y., Cao, Z., Wang, M., Wu, W., Mao, Y., Rose, P., Law, B. Y.-K., & Zhu, Y. Z. (2017, 2017/03/07). ZYZ-168 alleviates cardiac fibrosis after myocardial infarction through inhibition of ERK1/2-dependent ROCK1 activation. Scientific Reports, 7(1), 43242. https://doi.org/10.1038/srep43242

Lyu, L., Chen, J., Wang, W., Yan, T., Lin, J., Gao, H., Li, H., Lv, R., Xu, F., Fang, L., & Chen, Y. (2021, Mar). Scoparone alleviates Ang II-induced pathological myocardial hypertrophy in mice by inhibiting oxidative stress. J Cell Mol Med, 25(6), 3136-3148. https://doi.org/10.1111/jcmm.16304

Ma, F., Li, Y., Jia, L., Han, Y., Cheng, J., Li, H., Qi, Y., & Du, J. (2012). Macrophage-stimulated cardiac fibroblast production of IL-6 is essential for TGF β/Smad activation and cardiac fibrosis induced by angiotensin II. PLoS One, 7(5), e35144. https://doi.org/10.1371/journal.pone.0035144

Ma, N., Xu, E., Luo, Q., & Song, G. (2023, Mar 27). Rac1: A Regulator of Cell Migration and a Potential Target for Cancer Therapy. Molecules, 28(7). https://doi.org/10.3390/molecules28072976

Ma, Z.-G., Yuan, Y.-P., Fan, D., Zhang, X., Teng, T., Song, P., Kong, C.-Y., Hu, C., Wei, W.-Y., & Tang, Q.-Z. (2023, 2023/08/16). IRX2 regulates angiotensin II-induced cardiac fibrosis by transcriptionally activating EGR1 in male mice. Nature Communications, 14(1), 4967. https://doi.org/10.1038/s41467-023-40639-6

Ma, Z. G., Yuan, Y. P., Wu, H. M., Zhang, X., & Tang, Q. Z. (2018). Cardiac fibrosis: new insights into the pathogenesis. International journal of biological sciences, 14(12), 1645-1657. https://doi.org/10.7150/ijbs.28103

Maeda, A., Okano, K., Park, P. S., Lem, J., Crouch, R. K., Maeda, T., & Palczewski, K. (2010, May 4). Palmitoylation stabilizes unliganded rod opsin. Proc Natl Acad Sci U S A, 107(18), 8428-8433. https://doi.org/10.1073/pnas.1000640107

Main, A., & Fuller, W. (2022, Feb). Protein S-Palmitoylation: advances and challenges in studying a therapeutically important lipid modification. Febs j, 289(4), 861-882. https://doi.org/10.1111/febs.15781

Martin, S. S., Aday, A. W., Almarzooq, Z. I., Anderson, C. A. M., Arora, P., Avery, C. L., Baker-Smith, C. M., Barone Gibbs, B., Beaton, A. Z., Boehme, A. K., Commodore-Mensah, Y., Currie, M. E., Elkind, M. S. V., Evenson, K. R., Generoso, G., Heard, D. G., Hiremath, S., Johansen, M. C., Kalani, R., Kazi, D. S., Ko, D., Liu, J., Magnani, J. W., Michos, E. D., Mussolino, M. E., Navaneethan, S. D., Parikh, N. I., Perman, S. M., Poudel, R., Rezk-Hanna, M., Roth, G. A., Shah, N. S., St-Onge, M. P., Thacker, E. L., Tsao, C. W., Urbut, S. M., Van Spall, H. G. C., Voeks, J. H., Wang, N. Y., Wong, N. D., Wong, S. S., Yaffe, K., & Palaniappan, L. P. (2024, Jan 24). 2024 Heart Disease and Stroke Statistics: A Report of US and Global Data From the American Heart Association. Circulation. https://doi.org/10.1161/cir.0000000000001209

Marttinen, M., Kurkinen, K. M., Soininen, H., Haapasalo, A., & Hiltunen, M. (2015, Apr 3). Synaptic dysfunction and septin protein family members in neurodegenerative diseases. Mol Neurodegener, 10, 16. https://doi.org/10.1186/s13024-015-0013-z

Matsumoto, E., Sasaki, S., Kinoshita, H., Kito, T., Ohta, H., Konishi, M., Kuwahara, K., Nakao, K., & Itoh, N. (2013, Jul). Angiotensin II-induced cardiac hypertrophy and fibrosis are promoted in mice lacking Fgf16. Genes Cells, 18(7), 544-553. https://doi.org/10.1111/gtc.12055

Meléndez, G. C., McLarty, J. L., Levick, S. P., Du, Y., Janicki, J. S., & Brower, G. L. (2010, Aug). Interleukin 6 mediates myocardial fibrosis, concentric hypertrophy, and diastolic dysfunction in rats. Hypertension, 56(2), 225-231. https://doi.org/10.1161/hypertensionaha.109.148635

Mia, M. M., Boersema, M., & Bank, R. A. (2014). Interleukin-1β attenuates myofibroblast formation and extracellular matrix production in dermal and lung fibroblasts exposed to transforming growth factor-β1. PLoS One, 9(3), e91559. https://doi.org/10.1371/journal.pone.0091559

Mia, M. M., Cibi, D. M., Ghani, S., Singh, A., Tee, N., Sivakumar, V., Bogireddi, H., Cook, S. A., Mao, J., & Singh, M. K. (2022, Jun 22). Loss of Yap/Taz in cardiac fibroblasts attenuates adverse remodelling and improves cardiac function. Cardiovasc Res, 118(7), 1785-1804. https://doi.org/10.1093/cvr/cvab205

Mia, M. M., & Singh, M. K. (2022, Jun 29). New Insights into Hippo/YAP Signaling in Fibrotic Diseases. Cells, 11(13). https://doi.org/10.3390/cells11132065

Molkentin, J. D., Bugg, D., Ghearing, N., Dorn, L. E., Kim, P., Sargent, M. A., Gunaje, J., Otsu, K., & Davis, J. (2017, Aug 8). Fibroblast-Specific Genetic Manipulation of p38 Mitogen-Activated Protein Kinase In Vivo Reveals Its Central Regulatory Role in Fibrosis. Circulation, 136(6), 549-561. https://doi.org/10.1161/circulationaha.116.026238

Moors, T. E., Li, S., McCaffery, T. D., Ho, G. P. H., Bechade, P. A., Pham, L. N., Ericsson, M., & Nuber, S. (2023, Nov 15). Increased palmitoylation improves estrogen receptor alpha-dependent hippocampal synaptic deficits in a mouse model of synucleinopathy. Sci Adv, 9(46), eadj1454. https://doi.org/10.1126/sciadv.adj1454

Morfino, P., Aimo, A., Castiglione, V., Gálvez-Montón, C., Emdin, M., & Bayes-Genis, A. (2023, Mar). Treatment of cardiac fibrosis: from neuro-hormonal inhibitors to CAR-T cell therapy. Heart Fail Rev, 28(2), 555-569. https://doi.org/10.1007/s10741-022-10279-x

Mukai, K., Konno, H., Akiba, T., Uemura, T., Waguri, S., Kobayashi, T., Barber, G. N., Arai, H., & Taguchi, T. (2016, 2016/06/21). Activation of STING requires palmitoylation at the Golgi. Nature Communications, 7(1), 11932. https://doi.org/10.1038/ncomms11932

Muncie, J. M., & Weaver, V. M. (2018). The Physical and Biochemical Properties of the Extracellular Matrix Regulate Cell Fate. Curr Top Dev Biol, 130, 1-37. https://doi.org/10.1016/bs.ctdb.2018.02.002

Murphy, A. M., Wong, A. L., & Bezuhly, M. (2015). Modulation of angiotensin II signaling in the prevention of fibrosis. Fibrogenesis Tissue Repair, 8, 7. https://doi.org/10.1186/s13069-015-0023-z

Nagalingam, R. S., Chattopadhyaya, S., Al-Hattab, D. S., Cheung, D. Y. C., Schwartz, L. Y., Jana, S., Aroutiounova, N., Ledingham, D. A., Moffatt, T. L., Landry, N. M., Bagchi, R. A., Dixon, I. M. C., Wigle, J. T., Oudit, G. Y., Kassiri, Z., Jassal, D. S., & Czubryt, M. P. (2022). Scleraxis and fibrosis in the pressure-overloaded heart. European Heart Journal, 43(45), 4739-4750. https://doi.org/10.1093/eurheartj/ehac362

Nakamura, M., & Sadoshima, J. (2018, Jul). Mechanisms of physiological and pathological cardiac hypertrophy. Nat Rev Cardiol, 15(7), 387-407. https://doi.org/10.1038/s41569-018-0007-y

Narayanan, G., Halim, A., Hu, A., Avin, K. G., Lu, T., Zehnder, D., Hato, T., Chen, N. X., Moe, S. M., & Lim, K. (2023, Nov 1). Molecular Phenotyping and Mechanisms of Myocardial Fibrosis in Advanced Chronic Kidney Disease. Kidney360, 4(11), 1562-1579. https://doi.org/10.34067/kid.0000000000000276

Navarro-Lérida, I., Sánchez-Perales, S., Calvo, M., Rentero, C., Zheng, Y., Enrich, C., & Del Pozo, M. A. (2012, Feb 1). A palmitoylation switch mechanism regulates Rac1 function and membrane organization. Embo j, 31(3), 534-551. https://doi.org/10.1038/emboj.2011.446

Nguyen, T. P., Qu, Z., & Weiss, J. N. (2014, May). Cardiac fibrosis and arrhythmogenesis: the road to repair is paved with perils. J Mol Cell Cardiol, 70, 83-91. https://doi.org/10.1016/j.yjmcc.2013.10.018

Nicin, L., Wagner, J. U. G., Luxán, G., & Dimmeler, S. (2022, Mar). Fibroblast-mediated intercellular crosstalk in the healthy and diseased heart. FEBS Lett, 596(5), 638-654. https://doi.org/10.1002/1873-3468.14234

Ottolia, M., Torres, N., Bridge, J. H., Philipson, K. D., & Goldhaber, J. I. (2013, Aug). Na/Ca exchange and contraction of the heart. J Mol Cell Cardiol, 61, 28-33. https://doi.org/10.1016/j.yjmcc.2013.06.001

Pan, L., Li, Y., Jia, L., Qin, Y., Qi, G., Cheng, J., Qi, Y., Li, H., & Du, J. (2012). Cathepsin S deficiency results in abnormal accumulation of autophagosomes in macrophages and enhances Ang II-induced cardiac inflammation. PLoS One, 7(4), e35315. https://doi.org/10.1371/journal.pone.0035315

Parichatikanond, W., Duangrat, R., & Mangmool, S. (2023, Jul 15). G(αq) protein-biased ligand of angiotensin II type 1 receptor mediates myofibroblast differentiation through TGF-β1/ERK axis in human cardiac fibroblasts. Eur J Pharmacol, 951, 175780. https://doi.org/10.1016/j.ejphar.2023.175780

Park, Y. J., Yoo, S. A., Kim, M., & Kim, W. U. (2020). The Role of Calcium-Calcineurin-NFAT Signaling Pathway in Health and Autoimmune Diseases. Front Immunol, 11, 195. https://doi.org/10.3389/fimmu.2020.00195

Patel, N. J., Nassal, D. M., Greer-Short, A. D., Unudurthi, S. D., Scandling, B. W., Gratz, D., Xu, X., Kalyanasundaram, A., Fedorov, V. V., Accornero, F., Mohler, P. J., Gooch, K. J., & Hund, T. J. (2019, Oct 17). βIV-Spectrin/STAT3 complex regulates fibroblast phenotype, fibrosis, and cardiac function. JCI Insight, 4(20). https://doi.org/10.1172/jci.insight.131046

Pei, Z., Xiao, Y., Meng, J., Hudmon, A., & Cummins, T. R. (2016, Jun 23). Cardiac sodium channel palmitoylation regulates channel availability and myocyte excitability with implications for arrhythmia generation. Nat Commun, 7, 12035. https://doi.org/10.1038/ncomms12035

Pellman, J., Zhang, J., & Sheikh, F. (2016, May). Myocyte-fibroblast communication in cardiac fibrosis and arrhythmias: Mechanisms and model systems. J Mol Cell Cardiol, 94, 22-31. https://doi.org/10.1016/j.yjmcc.2016.03.005

Peng, H., Carretero, O. A., Peterson, E. L., & Rhaleb, N. E. (2010, May). Ac-SDKP inhibits transforming growth factor-beta1-induced differentiation of human cardiac fibroblasts into myofibroblasts. Am J Physiol Heart Circ Physiol, 298(5), H1357-1364. https://doi.org/10.1152/ajpheart.00464.2009

Pesce, M., Duda, G. N., Forte, G., Girao, H., Raya, A., Roca-Cusachs, P., Sluijter, J. P. G., Tschöpe, C., & Van Linthout, S. (2023, May). Cardiac fibroblasts and mechanosensation in heart development, health and disease. Nat Rev Cardiol, 20(5), 309-324. https://doi.org/10.1038/s41569-022-00799-2

Pragallapati, S., & Manyam, R. (2019, Sep-Dec). Glucose transporter 1 in health and disease. J Oral Maxillofac Pathol, 23(3), 443-449. https://doi.org/10.4103/jomfp.JOMFP_22_18

Prior, I. A., & Hancock, J. F. (2001, May). Compartmentalization of Ras proteins. J Cell Sci, 114(Pt 9), 1603-1608. https://doi.org/10.1242/jcs.114.9.1603

Putney, J. W., & Tomita, T. (2012, Jan). Phospholipase C signaling and calcium influx. Adv Biol Regul, 52(1), 152-164. https://doi.org/10.1016/j.advenzreg.2011.09.005

Ramzan, F., Abrar, F., Mishra, G. G., Liao, L. M. Q., & Martin, D. D. O. (2023). Lost in traffic: consequences of altered palmitoylation in neurodegeneration. Front Physiol, 14, 1166125. https://doi.org/10.3389/fphys.2023.1166125

Ranjan, P., Kumari, R., Goswami, S. K., Li, J., Pal, H., Suleiman, Z., Cheng, Z., Krishnamurthy, P., Kishore, R., & Verma, S. K. (2021). Myofibroblast-Derived Exosome Induce Cardiac Endothelial Cell Dysfunction. Front Cardiovasc Med, 8, 676267. https://doi.org/10.3389/fcvm.2021.676267

Rausch, V., & Hansen, C. G. (2020, Jan). The Hippo Pathway, YAP/TAZ, and the Plasma Membrane. Trends Cell Biol, 30(1), 32-48. https://doi.org/10.1016/j.tcb.2019.10.005

Ravassa, S., López, B., Treibel, T. A., San José, G., Losada-Fuentenebro, B., Tapia, L., Bayés-Genís, A., Díez, J., & González, A. (2023, 2023/10/01/). Cardiac Fibrosis in heart failure: Focus on non-invasive diagnosis and emerging therapeutic strategies. Molecular Aspects of Medicine, 93, 101194. https://doi.org/https://doi.org/10.1016/j.mam.2023.101194

Raziyeva, K., Kim, Y., Zharkinbekov, Z., Temirkhanova, K., & Saparov, A. (2022, Sep 2). Novel Therapies for the Treatment of Cardiac Fibrosis Following Myocardial Infarction. Biomedicines, 10(9). https://doi.org/10.3390/biomedicines10092178

Reed, A. L., Tanaka, A., Sorescu, D., Liu, H., Jeong, E. M., Sturdy, M., Walp, E. R., Dudley, S. C., Jr., & Sutliff, R. L. (2011, Sep). Diastolic dysfunction is associated with cardiac fibrosis in the senescence-accelerated mouse. Am J Physiol Heart Circ Physiol, 301(3), H824-831. https://doi.org/10.1152/ajpheart.00407.2010

Reilly, L., Howie, J., Wypijewski, K., Ashford, M. L., Hilgemann, D. W., & Fuller, W. (2015, Nov). Palmitoylation of the Na/Ca exchanger cytoplasmic loop controls its inactivation and internalization during stress signaling. Faseb j, 29(11), 4532-4543. https://doi.org/10.1096/fj.15-276493

Ren, Z., Zhang, Z., Ling, L., Liu, X., & Wang, X. (2023). Drugs for treating myocardial fibrosis. Front Pharmacol, 14, 1221881. https://doi.org/10.3389/fphar.2023.1221881

Ridwan, M., Dimiati, H., Syukri, M., & Lesmana, R. (2023, Jun 12). Potential molecular mechanism underlying cardiac fibrosis in diabetes mellitus: a narrative review. Egypt Heart J, 75(1), 46. https://doi.org/10.1186/s43044-023-00376-z

Russo, I., & Frangogiannis, N. G. (2016, Jan). Diabetes-associated cardiac fibrosis: Cellular effectors, molecular mechanisms and therapeutic opportunities. J Mol Cell Cardiol, 90, 84-93. https://doi.org/10.1016/j.yjmcc.2015.12.011

Sarohi, V., Chakraborty, S., & Basak, T. (2022). Exploring the cardiac ECM during fibrosis: A new era with next-gen proteomics. Front Mol Biosci, 9, 1030226. https://doi.org/10.3389/fmolb.2022.1030226

Satoh, M., Ogita, H., Takeshita, K., Mukai, Y., Kwiatkowski, D. J., & Liao, J. K. (2006, May 9). Requirement of Rac1 in the development of cardiac hypertrophy. Proc Natl Acad Sci U S A, 103(19), 7432-7437. https://doi.org/10.1073/pnas.0510444103

Schiau, C., Leucuța, D. C., Dudea, S. M., & Manole, S. (2021, May-Jun). Myocardial Fibrosis as a Predictor of Ventricular Arrhythmias in Patients With Non-ischemic Cardiomyopathy. In Vivo, 35(3), 1677-1685. https://doi.org/10.21873/invivo.12427

Schimmel, K., Ichimura, K., Reddy, S., Haddad, F., & Spiekerkoetter, E. (2022). Cardiac Fibrosis in the Pressure Overloaded Left and Right Ventricle as a Therapeutic Target. Front Cardiovasc Med, 9, 886553. https://doi.org/10.3389/fcvm.2022.886553

Schirone, L., Forte, M., Palmerio, S., Yee, D., Nocella, C., Angelini, F., Pagano, F., Schiavon, S., Bordin, A., Carrizzo, A., Vecchione, C., Valenti, V., Chimenti, I., De Falco, E., Sciarretta, S., & Frati, G. (2017). A Review of the Molecular Mechanisms Underlying the Development and Progression of Cardiac Remodeling. Oxid Med Cell Longev, 2017, 3920195. https://doi.org/10.1155/2017/3920195

Schnee, J. M., & Hsueh, W. A. (2000). Angiotensin II, adhesion, and cardiac fibrosis. Cardiovascular Research, 46(2), 264-268. https://doi.org/10.1016/S0008-6363(00)00044-4

Schwabe, R. F., Tabas, I., & Pajvani, U. B. (2020, May). Mechanisms of Fibrosis Development in Nonalcoholic Steatohepatitis. Gastroenterology, 158(7), 1913-1928. https://doi.org/10.1053/j.gastro.2019.11.311

Schwartz, P. J., Ackerman, M. J., Antzelevitch, C., Bezzina, C. R., Borggrefe, M., Cuneo, B. F., & Wilde, A. A. M. (2020, 2020/07/16). Inherited cardiac arrhythmias. Nature Reviews Disease Primers, 6(1), 58. https://doi.org/10.1038/s41572-020-0188-7

Schwinger, R. H. G. (2021, Feb). Pathophysiology of heart failure. Cardiovasc Diagn Ther, 11(1), 263-276. https://doi.org/10.21037/cdt-20-302

Severino, P., D'Amato, A., Pucci, M., Infusino, F., Adamo, F., Birtolo, L. I., Netti, L., Montefusco, G., Chimenti, C., Lavalle, C., Maestrini, V., Mancone, M., Chilian, W. M., & Fedele, F. (2020, Oct 30). Ischemic Heart Disease Pathophysiology Paradigms Overview: From Plaque Activation to Microvascular Dysfunction. Int J Mol Sci, 21(21). https://doi.org/10.3390/ijms21218118

Shinde, A. V., & Frangogiannis, N. G. (2014, May). Fibroblasts in myocardial infarction: a role in inflammation and repair. J Mol Cell Cardiol, 70, 74-82. https://doi.org/10.1016/j.yjmcc.2013.11.015

Shinde, A. V., Humeres, C., & Frangogiannis, N. G. (2017, Jan). The role of α-smooth muscle actin in fibroblast-mediated matrix contraction and remodeling. Biochim Biophys Acta Mol Basis Dis, 1863(1), 298-309. https://doi.org/10.1016/j.bbadis.2016.11.006

Silva, A. C., Pereira, C., Fonseca, A., Pinto-do-Ó, P., & Nascimento, D. S. (2020). Bearing My Heart: The Role of Extracellular Matrix on Cardiac Development, Homeostasis, and

Injury Response. Front Cell Dev Biol, 8, 621644. https://doi.org/10.3389/fcell.2020.621644

Song, R., & Zhang, L. (2020, Nov 15). Cardiac ECM: Its Epigenetic Regulation and Role in Heart Development and Repair. Int J Mol Sci, 21(22). https://doi.org/10.3390/ijms21228610

Song, W., Wang, H., & Wu, Q. (2015, Sep 10). Atrial natriuretic peptide in cardiovascular biology and disease (NPPA). Gene, 569(1), 1-6. https://doi.org/10.1016/j.gene.2015.06.029

Souders, C. A., Bowers, S. L., & Baudino, T. A. (2009, Dec 4). Cardiac fibroblast: the renaissance cell. Circ Res, 105(12), 1164-1176. https://doi.org/10.1161/circresaha.109.209809

Stenmark, H. (2009, 2009/08/01). Rab GTPases as coordinators of vesicle traffic. Nature Reviews Molecular Cell Biology, 10(8), 513-525. https://doi.org/10.1038/nrm2728

Stix, R., Lee, C.-J., Faraldo-Gómez, J. D., & Banerjee, A. (2020, 2020/08/21/). Structure and Mechanism of DHHC Protein Acyltransferases. Journal of Molecular Biology, 432(18), 4983-4998. https://doi.org/https://doi.org/10.1016/j.jmb.2020.05.023

Sun, F., Schroer, C. F. E., Palacios, C. R., Xu, L., Luo, S. Z., & Marrink, S. J. (2020, Apr). Molecular mechanism for bidirectional regulation of CD44 for lipid raft affiliation by palmitoylations and PIP2. PLoS Comput Biol, 16(4), e1007777. https://doi.org/10.1371/journal.pcbi.1007777

Sun, Y., Zhang, H., Meng, J., Guo, F., Ren, D., Wu, H., & Jin, X. (2022, Aug 16). S-palmitoylation of PCSK9 induces sorafenib resistance in liver cancer by activating the PI3K/AKT pathway. Cell Rep, 40(7), 111194. https://doi.org/10.1016/j.celrep.2022.111194

Swarthout, J. T., Lobo, S., Farh, L., Croke, M. R., Greentree, W. K., Deschenes, R. J., & Linder, M. E. (2005, Sep 2). DHHC9 and GCP16 constitute a human protein fatty acyltransferase with specificity for H- and N-Ras. J Biol Chem, 280(35), 31141-31148. https://doi.org/10.1074/jbc.M504113200

Tabaczar, S., Czogalla, A., Podkalicka, J., Biernatowska, A., & Sikorski, A. F. (2017, Jun). Protein palmitoylation: Palmitoyltransferases and their specificity. Exp Biol Med (Maywood), 242(11), 1150-1157. https://doi.org/10.1177/1535370217707732

Tallquist, M. D. (2020, Feb 10). Cardiac Fibroblast Diversity. Annu Rev Physiol, 82, 63-78. https://doi.org/10.1146/annurev-physiol-021119-034527

Tallquist, M. D., & Molkentin, J. D. (2017, Aug). Redefining the identity of cardiac fibroblasts. Nat Rev Cardiol, 14(8), 484-491. https://doi.org/10.1038/nrcardio.2017.57

Talman, V., & Ruskoaho, H. (2016, Sep). Cardiac fibrosis in myocardial infarction-from repair and remodeling to regeneration. Cell Tissue Res, 365(3), 563-581. https://doi.org/10.1007/s00441-016-2431-9

Tan, R. J., Zhou, D., Zhou, L., & Liu, Y. (2014, Nov). Wnt/β-catenin signaling and kidney fibrosis. Kidney Int Suppl (2011), 4(1), 84-90. https://doi.org/10.1038/kisup.2014.16

Tang, L. Y., Heller, M., Meng, Z., Yu, L. R., Tang, Y., Zhou, M., & Zhang, Y. E. (2017, Mar 10). Transforming Growth Factor-β (TGF-β) Directly Activates the JAK1-STAT3 Axis to Induce Hepatic Fibrosis in Coordination with the SMAD Pathway. J Biol Chem, 292(10), 4302-4312. https://doi.org/10.1074/jbc.M116.773085

Tian, G., & Ren, T. (2023, Jun). Mechanical stress regulates the mechanotransduction and metabolism of cardiac fibroblasts in fibrotic cardiac diseases. Eur J Cell Biol, 102(2), 151288. https://doi.org/10.1016/j.ejcb.2023.151288

Tolomeo, M., & Cascio, A. (2021, Jan 9). The Multifaced Role of STAT3 in Cancer and Its Implication for Anticancer Therapy. Int J Mol Sci, 22(2). https://doi.org/10.3390/ijms22020603

Trappanese, D. M., Sivilich, S., Ets, H. K., Kako, F., Autieri, M. V., & Moreland, R. S. (2016, Jun 1). Regulation of mitogen-activated protein kinase by protein kinase C and mitogen-activated protein kinase phosphatase-1 in vascular smooth muscle. Am J Physiol Cell Physiol, 310(11), C921-930. https://doi.org/10.1152/ajpcell.00311.2015

Travers, J. G., Kamal, F. A., Robbins, J., Yutzey, K. E., & Blaxall, B. C. (2016, Mar 18). Cardiac Fibrosis: The Fibroblast Awakens. Circ Res, 118(6), 1021-1040. https://doi.org/10.1161/circresaha.115.306565

Travers, J. G., Tharp, C. A., Rubino, M., & McKinsey, T. A. (2022, Mar 1). Therapeutic targets for cardiac fibrosis: from old school to next-gen. J Clin Invest, 132(5). https://doi.org/10.1172/jci148554

Tsutsumi, R., Fukata, Y., Noritake, J., Iwanaga, T., Perez, F., & Fukata, M. (2009, Jan). Identification of G protein alpha subunit-palmitoylating enzyme. Mol Cell Biol, 29(2), 435-447. https://doi.org/10.1128/mcb.01144-08

Tucker, N. R., Chaffin, M., Fleming, S. J., Hall, A. W., Parsons, V. A., Bedi, K. C., Jr., Akkad, A. D., Herndon, C. N., Arduini, A., Papangeli, I., Roselli, C., Aguet, F., Choi, S. H., Ardlie, K. G., Babadi, M., Margulies, K. B., Stegmann, C. M., & Ellinor, P. T. (2020, Aug 4). Transcriptional and Cellular Diversity of the Human Heart. Circulation, 142(5), 466-482. https://doi.org/10.1161/circulationaha.119.045401

Tuleta, I., & Frangogiannis, N. G. (2021, Sep). Fibrosis of the diabetic heart: Clinical significance, molecular mechanisms, and therapeutic opportunities. Adv Drug Deliv Rev, 176, 113904. https://doi.org/10.1016/j.addr.2021.113904

Turner, N. A. (2016, May). Inflammatory and fibrotic responses of cardiac fibroblasts to myocardial damage associated molecular patterns (DAMPs). J Mol Cell Cardiol, 94, 189-200. https://doi.org/10.1016/j.yjmcc.2015.11.002

Turner, N. A., & Blythe, N. M. (2019, Aug 7). Cardiac Fibroblast p38 MAPK: A Critical Regulator of Myocardial Remodeling. J Cardiovasc Dev Dis, 6(3). https://doi.org/10.3390/jcdd6030027

Umbarkar, P., Ejantkar, S., Tousif, S., & Lal, H. (2021, Sep 14). Mechanisms of Fibroblast Activation and Myocardial Fibrosis: Lessons Learned from FB-Specific Conditional Mouse Models. Cells, 10(9). https://doi.org/10.3390/cells10092412

Uscategui Calderon, M., Gonzalez, B. A., & Yutzey, K. E. (2023). Cardiomyocyte-fibroblast crosstalk in the postnatal heart. Front Cell Dev Biol, 11, 1163331. https://doi.org/10.3389/fcell.2023.1163331

van den Borne, S. W., Diez, J., Blankesteijn, W. M., Verjans, J., Hofstra, L., & Narula, J. (2010, Jan). Myocardial remodeling after infarction: the role of myofibroblasts. Nat Rev Cardiol, 7(1), 30-37. https://doi.org/10.1038/nrcardio.2009.199

Van Linthout, S., Miteva, K., & Tschöpe, C. (2014, May 1). Crosstalk between fibroblasts and inflammatory cells. Cardiovasc Res, 102(2), 258-269. https://doi.org/10.1093/cvr/cvu062

Varró, A., Tomek, J., Nagy, N., Virág, L., Passini, E., Rodriguez, B., & Baczkó, I. (2021, Jul 1). Cardiac transmembrane ion channels and action potentials: cellular physiology and arrhythmogenic behavior. Physiol Rev, 101(3), 1083-1176. https://doi.org/10.1152/physrev.00024.2019

Venetucci, L. A., Trafford, A. W., O'Neill, S. C., & Eisner, D. A. (2007, Mar). Na/Ca exchange: regulator of intracellular calcium and source of arrhythmias in the heart. Ann N Y Acad Sci, 1099, 315-325. https://doi.org/10.1196/annals.1387.033

Vincent, J., Adura, C., Gao, P., Luz, A., Lama, L., Asano, Y., Okamoto, R., Imaeda, T., Aida, J., Rothamel, K., Gogakos, T., Steinberg, J., Reasoner, S., Aso, K., Tuschl, T., Patel, D. J., Glickman, J. F., & Ascano, M. (2017, 2017/09/29). Small molecule inhibition of cGAS reduces interferon expression in primary macrophages from autoimmune mice. Nature Communications, 8(1), 750. https://doi.org/10.1038/s41467-017-00833-9

Wang, A., Cao, S., Stowe, J. C., & Valdez-Jasso, D. (2021, Apr 23). Substrate Stiffness and Stretch Regulate Profibrotic Mechanosignaling in Pulmonary Arterial Adventitial Fibroblasts. Cells, 10(5). https://doi.org/10.3390/cells10051000

Wang, C., Kang, X., Zhou, L., Chai, Z., Wu, Q., Huang, R., Xu, H., Hu, M., Sun, X., Sun, S., Li, J., Jiao, R., Zuo, P., Zheng, L., Yue, Z., & Zhou, Z. (2018, Jan 8). Synaptotagmin-11 is a critical mediator of parkin-linked neurotoxicity and Parkinson's disease-like pathology. Nat Commun, 9(1), 81. https://doi.org/10.1038/s41467-017-02593-y

Wang, G., Zhou, H., Gu, Z., Gao, Q., & Shen, G. (2018, Aug). Oct4 promotes cancer cell proliferation and migration and leads to poor prognosis associated with the survivin/STAT3 pathway in hepatocellular carcinoma. Oncol Rep, 40(2), 979-987. https://doi.org/10.3892/or.2018.6491

Wang, J., Li, R., Lin, H., Qiu, Q., Lao, M., Zeng, S., Wang, C., Xu, S., Zou, Y., Shi, M., Liang, L., Xu, H., & Xiao, Y. (2019, Nov). Accumulation of cytosolic dsDNA contributes to fibroblast-like synoviocytes-mediated rheumatoid arthritis synovial inflammation. Int Immunopharmacol, 76, 105791. https://doi.org/10.1016/j.intimp.2019.105791

Wang, M. H., Li, B. Z., Chen, Y., & Wang, J. (2022, Jun 24). TEADs serve as potential prognostic biomarkers and targets for human gastric cancer. BMC Gastroenterol, 22(1), 308. https://doi.org/10.1186/s12876-022-02386-8

Wang, Y. D., Cai, N., Wu, X. L., Cao, H. Z., Xie, L. L., & Zheng, P. S. (2013, 2013/08/01). OCT4 promotes tumorigenesis and inhibits apoptosis of cervical cancer cells by miR-125b/BAK1 pathway. Cell Death & Disease, 4(8), e760-e760. https://doi.org/10.1038/cddis.2013.272

Webber, M., Jackson, S. P., Moon, J. C., & Captur, G. (2020, Dec). Myocardial Fibrosis in Heart Failure: Anti-Fibrotic Therapies and the Role of Cardiovascular Magnetic Resonance in Drug Trials. Cardiol Ther, 9(2), 363-376. https://doi.org/10.1007/s40119-020-00199-y

Weintraub, W. S. (2023). The Economic Burden of Illness. JAMA Network Open, 6(3), e232663-e232663. https://doi.org/10.1001/jamanetworkopen.2023.2663

Weis, W. I., & Kobilka, B. K. (2018, Jun 20). The Molecular Basis of G Protein-Coupled Receptor Activation. Annu Rev Biochem, 87, 897-919. https://doi.org/10.1146/annurev-biochem-060614-033910

Wells, R. G. (2013, Jul). Tissue mechanics and fibrosis. Biochim Biophys Acta, 1832(7), 884-890. https://doi.org/10.1016/j.bbadis.2013.02.007

Wen, H., Gwathmey, J. K., & Xie, L. H. (2012, Aug 23). Oxidative stress-mediated effects of angiotensin II in the cardiovascular system. World J Hypertens, 2(4), 34-44. https://doi.org/10.5494/wjh.v2.i4.34

Werneburg, N., Gores, G. J., & Smoot, R. L. (2020, Jun 12). The Hippo Pathway and YAP Signaling: Emerging Concepts in Regulation, Signaling, and Experimental Targeting Strategies With Implications for Hepatobiliary Malignancies. Gene Expr, 20(1), 67-74. https://doi.org/10.3727/105221619x15617324583639

Wolf, J., Rose-John, S., & Garbers, C. (2014, Nov). Interleukin-6 and its receptors: a highly regulated and dynamic system. Cytokine, 70(1), 11-20. https://doi.org/10.1016/j.cyto.2014.05.024

Wong, T.-S., Li, G., Li, S., Gao, W., Chen, G., Gan, S., Zhang, M., Li, H., Wu, S., & Du, Y. (2023, 2023/05/03). G protein-coupled receptors in neurodegenerative diseases and psychiatric disorders. Signal Transduction and Targeted Therapy, 8(1), 177. https://doi.org/10.1038/s41392-023-01427-2

Wu, H.-h., Meng, T.-t., Chen, J.-m., Meng, F.-l., Wang, S.-y., Liu, R.-h., Chen, J.-n., Ning, B., Li, Y., & Su, G.-h. (2021, 2021/05/14/). Asenapine maleate inhibits angiotensin II-induced proliferation and activation of cardiac fibroblasts via the ROS/TGFβ1/MAPK signaling pathway. Biochemical and Biophysical Research Communications, 553, 172-179. https://doi.org/https://doi.org/10.1016/j.bbrc.2021.03.042

Wu, Q.-Q., Xiao, Y., Yuan, Y., Ma, Z.-G., Liao, H.-H., Liu, C., Zhu, J.-X., Yang, Z., Deng, W., & Tang, Q.-z. (2017). Mechanisms contributing to cardiac remodelling. Clinical Science, 131(18), 2319-2345. https://doi.org/10.1042/cs20171167

Xiang, F. L., Fang, M., & Yutzey, K. E. (2017, Sep 28). Loss of β-catenin in resident cardiac fibroblasts attenuates fibrosis induced by pressure overload in mice. Nat Commun, 8(1), 712. https://doi.org/10.1038/s41467-017-00840-w

Xiao, Y., Hill, M. C., Li, L., Deshmukh, V., Martin, T. J., Wang, J., & Martin, J. F. (2019, Nov 1). Hippo pathway deletion in adult resting cardiac fibroblasts initiates a cell state transition with spontaneous and self-sustaining fibrosis. Genes Dev, 33(21-22), 1491-1505. https://doi.org/10.1101/gad.329763.119

Xu, J., Murphy, S. L., Kochanek, K. D., & Arias, E. (2022, Dec). Mortality in the United States, 2021. NCHS Data Brief(456), 1-8.

Xu, M., Tan, J., Zhu, L., Ge, C., Zhang, Y., Gao, F., Dai, X., Kuang, Q., Chai, J., Zou, B., & Wang, B. (2023, Oct). Palmitoyltransferase ZDHHC3 Aggravates Nonalcoholic Steatohepatitis by Targeting S-Palmitoylated IRHOM2. Adv Sci (Weinh), 10(28), e2302130. https://doi.org/10.1002/advs.202302130

Xu, Z., Zou, C., Yu, W., Xu, S., Huang, L., Khan, Z., Wang, J., Liang, G., & Wang, Y. (2019, Jul). Inhibition of STAT3 activation mediated by toll-like receptor 4 attenuates angiotensin II-induced renal fibrosis and dysfunction. Br J Pharmacol, 176(14), 2627-2641. https://doi.org/10.1111/bph.14686

Yang, D., Zhou, Q., Labroska, V., Qin, S., Darbalaei, S., Wu, Y., Yuliantie, E., Xie, L., Tao, H., Cheng, J., Liu, Q., Zhao, S., Shui, W., Jiang, Y., & Wang, M.-W. (2021, 2021/01/08). G protein-coupled receptors: structure- and function-based drug discovery. Signal Transduction and Targeted Therapy, 6(1), 7. https://doi.org/10.1038/s41392-020-00435-w

Yatabe, J., Sanada, H., Yatabe, M. S., Hashimoto, S., Yoneda, M., Felder, R. A., Jose, P. A., & Watanabe, T. (2009, May). Angiotensin II type 1 receptor blocker attenuates the activation of ERK and NADPH oxidase by mechanical strain in mesangial cells in the absence of angiotensin II. Am J Physiol Renal Physiol, 296(5), F1052-1060. https://doi.org/10.1152/ajprenal.00580.2007

Zambetti, N. A., Firestone, A. J., Remsberg, J. R., Huang, B. J., Wong, J. C., Long, A. M., Predovic, M., Suciu, R. M., Inguva, A., Kogan, S. C., Haigis, K. M., Cravatt, B. F., & Shannon, K. (2020, May 14). Genetic disruption of N-RasG12D palmitoylation perturbs hematopoiesis and prevents myeloid transformation in mice. Blood, 135(20), 1772-1782. https://doi.org/10.1182/blood.2019003530

Zambrano, A., Molt, M., Uribe, E., & Salas, M. (2019, Jul 9). Glut 1 in Cancer Cells and the Inhibitory Action of Resveratrol as A Potential Therapeutic Strategy. Int J Mol Sci, 20(13). https://doi.org/10.3390/ijms20133374

Zeidman, R., Jackson, C. S., & Magee, A. I. (2009, 2009/01/01). Protein acyl thioesterases (Review). Molecular Membrane Biology, 26(1-2), 32-41. https://doi.org/10.1080/09687680802629329

Zeigler, A. C., Richardson, W. J., Holmes, J. W., & Saucerman, J. J. (2016, May). A computational model of cardiac fibroblast signaling predicts context-dependent drivers of myofibroblast differentiation. J Mol Cell Cardiol, 94, 72-81. https://doi.org/10.1016/j.yjmcc.2016.03.008

Zhai, B., Hu, F., Jiang, X., Xu, J., Zhao, D., Liu, B., Pan, S., Dong, X., Tan, G., Wei, Z., Qiao, H., Jiang, H., & Sun, X. (2014, Jun). Inhibition of Akt reverses the acquired resistance to

sorafenib by switching protective autophagy to autophagic cell death in hepatocellular carcinoma. Mol Cancer Ther, 13(6), 1589-1598. https://doi.org/10.1158/1535-7163.Mct-13-1043

Zhang, M., Zhou, L., Xu, Y., Yang, M., Xu, Y., Komaniecki, G. P., Kosciuk, T., Chen, X., Lu, X., Zou, X., Linder, M. E., & Lin, H. (2020, Oct). A STAT3 palmitoylation cycle promotes T(H)17 differentiation and colitis. Nature, 586(7829), 434-439. https://doi.org/10.1038/s41586-020-2799-2

Zhang, Q., Han, Z., Zhu, Y., Chen, J., & Li, W. (2020, Nov 30). The Role and Specific Mechanism of OCT4 in Cancer Stem Cells: A Review. Int J Stem Cells, 13(3), 312-325. https://doi.org/10.15283/ijsc20097

Zhang, Y., Qin, Z., Sun, W., Chu, F., & Zhou, F. (2021). Function of Protein S-Palmitoylation in Immunity and Immune-Related Diseases. Front Immunol, 12, 661202. https://doi.org/10.3389/fimmu.2021.661202

Zhang, Y., Wang, J. H., Zhang, Y. Y., Wang, Y. Z., Wang, J., Zhao, Y., Jin, X. X., Xue, G. L., Li, P. H., Sun, Y. L., Huang, Q. H., Song, X. T., Zhang, Z. R., Gao, X., Yang, B. F., Du, Z. M., & Pan, Z. W. (2016, Mar 14). Deletion of interleukin-6 alleviated interstitial fibrosis in streptozotocin-induced diabetic cardiomyopathy of mice through affecting TGFβ1 and miR-29 pathways. Sci Rep, 6, 23010. https://doi.org/10.1038/srep23010

Zhang, Z., Li, X., Yang, F., Chen, C., Liu, P., Ren, Y., Sun, P., Wang, Z., You, Y., Zeng, Y.-X., & Li, X. (2021, 2021/10/07). DHHC9-mediated GLUT1 S-palmitoylation promotes glioblastoma glycolysis and tumorigenesis. Nature Communications, 12(1), 5872. https://doi.org/10.1038/s41467-021-26180-4

Zhong, Q., Xiao, X., Qiu, Y., Xu, Z., Chen, C., Chong, B., Zhao, X., Hai, S., Li, S., An, Z., & Dai, L. (2023, Jun). Protein posttranslational modifications in health and diseases: Functions, regulatory mechanisms, and therapeutic implications. MedComm (2020), 4(3), e261. https://doi.org/10.1002/mco2.261

Zhou, B., Hao, Q., Liang, Y., & Kong, E. (2023, Jan). Protein palmitoylation in cancer: molecular functions and therapeutic potential. Mol Oncol, 17(1), 3-26. https://doi.org/10.1002/1878-0261.13308

Zhou, Y., Huang, T., Cheng, A. S., Yu, J., Kang, W., & To, K. F. (2016, Jan 21). The TEAD Family and Its Oncogenic Role in Promoting Tumorigenesis. Int J Mol Sci, 17(1). https://doi.org/10.3390/ijms17010138

Zou, S., Tong, Q., Liu, B., Huang, W., Tian, Y., & Fu, X. (2020, 2020/09/24). Targeting STAT3 in Cancer Immunotherapy. Molecular Cancer, 19(1), 145. https://doi.org/10.1186/s12943-020-01258-7

Chapter II: In Vitro Assessment of Cardiac Fibroblast Activation at Physiologic Stiffness

Abstract

Cardiac fibroblasts (CF) are an essential cell type in cardiac physiology, playing a diverse role in maintaining structural integrity, extracellular matrix (ECM) synthesis, and tissue repair. Under normal conditions, these cells reside in the interstitium in a quiescent state poised to sense and respond to injury by synthesizing and secreting collagen, vimentin, hyaluronan, and other ECM components. In response to mechanical and chemical stimuli, these "resident" fibroblasts can undergo a transformation through a continuum of activation states into the commonly known "myofibroblast", a process critical for injury response. Despite progress in understanding the contribution of fibroblasts to cardiac health and disease, much remains unknown about the signaling mediating this activation, in part owed to technical challenges in evaluating CF function and activation status in vitro. Given their role in monitoring the ECM, CFs are acutely sensitive to stiffness/pressure. High basal activation of isolated CFs is common due to the super-physiologic stiffness of traditional cell culture substrates, making assays dependent on quiescent cells challenging. To overcome this, cell culture parameters must be tightly controlled, and utilization of dishes coated with biocompatible reduced-stiffness substrates, such as 8 kPa polydimethylsiloxane (PDMS), have shown promise in reducing basal activation of fibroblasts. Here, we describe a cell culture protocol to maintain CF quiescence in vitro to enable a dynamic range for assessment of activation status in response to fibrogenic stimuli using PDMS-coated coverslips. Our protocol provides a cost-effective tool to study fibroblast signaling and activity,

allowing researchers to better understand the underlying mechanisms involved in cardiac fibrosis.

Introduction

Cardiac fibroblasts have gained recognition as crucial cellular regulators that contribute to both normal cardiac function and disease progression (Fu et al., 2018; Ivey & Tallquist, 2016; Kanisicak et al., 2016; Tallquist & Molkentin, 2017). Traditionally considered support cells involved in the maintenance of the extracellular matrix (ECM), it is now well-established that cardiac fibroblasts play multifaceted roles in the heart (Tallquist, 2020). From regulating ECM homeostasis and providing structural integrity, CFs also actively participate in tissue repair, remodeling, and the inflammatory response (Tallquist, 2020). However, the complex interactions and signaling cascades responsible for modulating these cellular responses remain incompletely understood.

Recently, significant efforts have been made to elucidate the molecular mechanisms that underlie the different phenotypic states of cardiac fibroblasts (Fu et al., 2020; Kanisicak et al., 2016; Umbarkar et al., 2021). While normally in a quiescent state, CFs undergo a transformation known as activation during pathological conditions, such as in response to myocardial injury or chronic pressure overload (Bretherton et al., 2020). Cardiac fibroblast activation is a complex process that involves the transition from a quiescent state to the canonical “myofibroblast” phenotype, characterized by increased proliferation, migration, release of inflammatory cytokines, and synthesis of ECM proteins such as collagens (Alter et al., 2023; Gibb et al., 2020; Khalil et al., 2019). This phenotypic and morphological transformation is triggered by a variety of stimuli, including pro-inflammatory cytokines and peptide hormones released from surrounding cells, as well as physical stimuli such as mechanical stress (Bertaud et al., 2023;

Herum, Lunde, et al., 2017). The dysregulated activation of myofibroblasts underlies the development and progression of maladaptive scar formation in the heart called cardiac fibrosis, a hallmark feature of ischemic heart disease as well as many inherited and acquired cardiomyopathies, and heart failure (Kanisicak et al., 2016; Teuber et al., 2022). Elucidating the intricate signaling networks involved in cardiac fibroblast activation could potentially reveal novel therapeutic targets for preventing or reversing cardiac fibrosis. Therefore, there is an urgent need for comprehensive investigations aimed at unraveling mechanisms that drive cardiac fibroblast activation.

In vitro assays are indispensable tools for studying cardiac fibroblast activation under controlled conditions, however, cardiac fibroblast researchers have encountered a number of technical challenges associated with traditional cell culture. Due to their role in sensing and modifying the properties of the cardiac microenvironment, cardiac fibroblasts are highly responsive to the stiffness of surrounding tissue (Childers et al., 2021; Meagher et al., 2021). The use of common 2-D cell culture methods utilizing glass or plastic substrates thus poses limitations arising from their non-physiologic stiffness that can trigger a spontaneous increase in fibroblast activation (Herum, Choppe, et al., 2017). As a result, the relative magnitude of induction of fibroblast activation observed when using pro-fibrotic agonists like transforming growth factor β1 (TGFβ1) becomes less significant, as the activation relative to the "unstimulated" control condition is blunted. This confounding factor compromises the ability to study the specific mechanisms underlying the transition from quiescent to activated cardiac fibroblasts, as well as their responsiveness to external stimuli.

To overcome these challenges, researchers have begun to optimize 2-D cell culture conditions for maintaining quiescent populations of cardiac fibroblasts. Previous work in the

field has established highly variable fibroblast responses as a result of differences in the composition of media and serum, time in culture, and plate stiffness (Landry et al., 2019; Santiago et al., 2010). However, even with consistent cell density and culture conditions, high plate stiffness will still likely result in a highly activated fibroblast population in vitro, even when all other variables are tightly controlled. Efforts to address this have focused on generating substrates with physiologic stiffness ratings to be used as an alternative to traditional cell culture plastic. Polydimethylsiloxane (PDMS) substrates have become widely utilized for cell culture due to their tunable mechanical properties and compatibility with a wide range of assays (Palchesko et al., 2012; Yeh et al., 2017). By adjusting the formulation and curing process of PDMS, researchers can tailor the substrate stiffness to better mimic the mechanical properties of native tissue, including more appropriately mimicking the physiologic stiffness of the myocardium. This enables the creation of a more physiologically relevant microenvironment for studying cardiac fibroblast activation.

The use of soft substrates has become increasingly common in fibroblast in vitro experimentation due to attenuation of the mechanosensitive activation observed with traditional cell culture, allowing for a better representation of the physiological responses of these cells (Cheng et al., 2021; Landry et al., 2019; Morningstar et al., 2021; Shiraishi et al., 2023; Wang et al., 2021). Further, the utilization of “soft” substrates has been demonstrated to reduce cardiac fibroblast activation and promote a more quiescent phenotype (Landry et al., 2019). Consequently, the use of soft substrates at physiological stiffness provides researchers with a valuable tool for studying the underlying mechanisms of cardiac fibroblast activation and their responses to various stimuli. However, commercially available options for cell culture plates

with physiological stiffness ratings can be prohibitively expensive, stressing the need for a more cost-effective alternative.

Here, we developed a cost-effective protocol for culturing cardiac fibroblasts at physiologic stiffness on PDMS-coated coverslips to address the limitations associated with traditional cardiac fibroblast activation assays. These PDMS-coated coverslips generated in-house provide an affordable and accessible alternative that yield a comparable level of baseline cardiac fibroblast quiescence compared to commercially available cell culture soft substrates (Landry et al., 2019). Additionally, we present a comprehensive cell culture experimental timeline for assessing cardiac fibroblast activation from quiescent cells cultured on PDMS-coated coverslips. This protocol will enable investigation of the cellular and molecular mechanisms governing cardiac fibroblast activation using an in vitro system that more accurately models the physiologic stiffness of the myocardium.

Basic Protocol 1: Generation of 8 kPa Polydimethylsiloxane (PDMS)/ Gelatin-coated Coverslips for Cardiac Fibroblast Cell Culture

This protocol describes a detailed procedure for the generation of 8 kPa PDMS (Palchesko et al., 2012), and the steps for coating this PDMS solution on cell culture coverslips for use in in vitro fibroblast assays. First, commercially available PDMS solutions of various stiffness ratings are mixed to generate an 8 kPa polymer that more closely replicates the endogenous pressure of the cardiac fibroblast environment. A thin layer of this polymer is then applied to coverslips and cured. After sterilizing, the PDMS coated coverslips can then be additionally coated with gelatin to increase cell adherence prior to use in downstream applications.

Materials

24-well plates (Fisherbrand, FB012929)

12 mm glass coverslips (Electron Microscopy Sciences, #72230-01)

Plastic Dixie cups (Krayden Dow, #NC9285739)

Sylgard 184 and curing agent (Krayden Dow, #NC9285739)

Disposable Plastic Cell Scrapers (Santa Cruz, #sc-395251)

Sylgard 527 A and B (Krayden Dow, #NC1208196)

5 mL serological pipettes (Falcon, #357543)

10 mL serological pipettes (Falcon, 357551)

50 mL conical tubes (Fisherbrand, #05-539-7) and tube holder

P10 pipette tips (TipOne, #1110-3700)

P200 pipette tips (TipOne, #1111-1706)

P20 filter pipette tips (SureOne, #02-707-432)

1 mL syringe (Becton Dickinson, #309659)

PrecisionGlide 1.5 in, 21 gauge needle (Becton Dickinson, #305167)

Porcine skin gelatin aliquots (See Reagents and Solutions)

Phosphate buffered saline (Corning, #21-040-CV)

1 mL serological pipettes (Falcon, #357506)

Equipment

Fine tip straight forceps (WPI, #14099) or equivalent

Precision balance

Serological pipette controller

Vacuum desiccator

P10, P20 & P200 pipettes

Vortex mixer

Tabletop centrifuge

50°C oven

Class II biological safety cabinet

Vacuum aspirator

37°C water bath

37°C 5% CO_2 incubator

Note: PDMS is difficult to remove from surfaces with normal solvents. Cover any workspaces during the creation of the PDMS mixture to ensure ease of clean-up in the event of a spill.

PDMS Creation/Coverslip Coating

For this protocol, 10 g of 8 kPa PDMS solution will be made by mixing two different Sylgard solutions together at the appropriate ratio.

1. Carefully place one 12 mm coverslip into each well of a 24-well plate with forceps. *This protocol generates between 6-8 full 24-well plates of coverslips but can be scaled up or down accordingly.*
2. Separately, form two different Sylgard mixtures.
    a. Sylgard 184: Place an empty disposable plastic cup onto a precision balance. To it, add exactly 10 g of Sylgard 184 base with a 10 mL serological pipette (tip can be cut off to improve pipetting efficiency), followed by exactly 1 g of Sylgard 184 curing agent with a 5 mL serological pipette. Remove the cup from the balance, and using a plastic cell scraper, mix vigorously for 5 minutes. Place the cup with mixed components into the vacuum desiccator to remove bubbles.

    Due to the fact that PDMS is highly viscous and does not readily dissolve in

common solvents, disposable containers such as the cups described in this protocol are recommended for ease of handling/cleaning.

b. Sylgard 527: Again, place an empty disposable plastic cup onto a precision balance. With a 10 mL serological pipette, add exactly 6 g Sylgard 527 Part A to the disposable cup. Then, with a new 10 mL serological pipette, add exactly 6 g Sylgard 527 Part B to the cup for a total mass of 12 g. Mix vigorously in the cup with a plastic cell scraper for 5 minutes. Bubbles will likely not be present in this solution (does not require vacuum desiccation).

3. Combine the Sylgard 184 and 527 at the precise ratio (0.102:9.90) to obtain an 8 kPa PDMS solution.

   a. Place an empty 50 mL conical tube into a small tube holder that fits on the precision balance. Place tube/holder onto the balance and tare the balance. Using a P10 pipette tip, without depressing the pipette, dip the P10 tip into the Sylgard 184 mixture. Once the solution has adhered to the tip, move the tip over to the 50 mL conical tube on the balance and allow it to drip off without depressing the pipette. Repeat until *exactly* 102 mg has been added to the conical tube. Be careful to achieve this mass as closely as possible. When 102 mg is reached, tare the balance.

   b. Using a 5 mL serological pipette, add 9.90 g of Sylgard 527 to the tube containing the 102 mg of Sylgard 184. It is recommended to use the serological pipette for the majority of the mass being added, and then use a P200 tip to add the Sylgard 527 drop wise in a similar fashion to Step 3a at the end to reach exactly 9.90 g.

4. Mix the two PDMS solutions very thoroughly.
    a. Secure the lid on the conical tube and vortex the tube on high for ~10 seconds, before orbitally tilting the tube and rolling the Sylgard mixture around the interior surface for another ~10 seconds. Repeat vortexing/mixing 5 times to ensure an extremely well-mixed, homogenous solution.
    b. Centrifuge the mixture at room temperature at 3,200 x g for 3 min to get the PDMS to the bottom of the conical tube.
    c. Vortex again for several seconds, while tilting the tube in different directions.
5. Pipette the PDMS solution onto coverslips.
    a. Load a P20 pipette with a 20 µL filter tip, then cut off the tip of the pipette (approximately 2-3 mm). Set the volume on the pipette to 14 µL and pipette the thoroughly mixed PDMS solution up and down into the tip slowly 3 times to coat the inside of the pipette and reduce the formation of bubbles.
    The repeated pipetting is only necessary upon first introduction of the solution to the tip, prior to first coverslip loading.
    b. Eject all of the 14 µL of mixed PDMS onto the direct center of each coverslip within each well of the 24-well plate. To achieve consistent volumes, after pulling the PDMS into the pipette, drag the tip along the inside of the tube to 'brush off' extra PDMS that coats the outside of the pipette tip (it is highly viscous) before pipetting onto the coverslip.

    Once the PDMS has been applied, it will slowly begin to spread out to the edges of the coverslip. It is normal for the PDMS to not be completely spread

out prior to curing in the oven, and will likely be uniformly distributed following the overnight incubation in the 50°C oven.

Any unused PDMS solution remaining following coverslip coating should be discarded, as it will solidify. A fresh PDMS solution should be prepared for each subsequent batch of coverslips at later dates.

6. Place the lids on the 24-well plates and place plates with coated coverslips into the vacuum desiccator for 30-45 min.
7. Transfer the plates to the 50°C oven and cure PDMS overnight.
8. Remove plastic plates containing the cured coverslips from the oven. Coverslips can be stored at room temperature indefinitely in the plastic plates that they were cured in until ready for experiments. Only proceed to gelatin coating (Step 9-13) when ready to perform experiments, as once gelatin coated is performed, it is recommended that the coverslips be used immediately.

   The PDMS in most cases will diffuse across the coverslip evenly. Some coverslips may have small sections at the periphery that are not covered, these coverslips are still usable for most applications as long as the majority of the surface area is covered. Some coverslips (<10%) may become attached to the 24-well dish used in coverslip preparation due to the PDMS leaking over the side of the coverslip and bonding with the plastic. When ready for experimentation, only the unattached coverslips should be moved to a new 24-well plate to be used.

Preparation, Sterilization and Gelatin Coating of Coverslips

9. Load new 24-well experimental plates with unattached PDMS-coated coverslips from the plastic plates in which they were cured.
    a. Using the forceps and bent needle/syringe lifting tool (see Figure 2.1), lift the unattached, freely moving PDMS-coated coverslips from the preparation plate, and transfer the desired number to a new experimental 24-well plate. *When transferring coverslips, use the forceps pointed down towards the bottom of the well to push each coverslip sideways gently against the plastic well with one hand and gingerly lift up, just enough to break the surface tension between the coverslip and the plastic. Simultaneously with the other hand, using the bent needle lifting tool, position the needle under the coverslip that is being barely lifted with the forceps. Once the needle is under the coverslip, the forceps can be released. While elevating the coverslip with the bent needle lifting tool, grip the edge of the coverslip with the forceps as minimally as possible so as not to disturb the PDMS coating, and lift, then transfer the coverslip to the desired location. When releasing the coverslip from the forceps, the PDMS-coated side may stick to the forceps. When this happens, the bent needle tool can be used to gently scrape the attachment point of the forceps to the PDMS to release it.*

For the remainder of the protocol, steps will take place in a Class II biological safety cabinet (BSC). Coverslip PDMS coating takes place in a non-sterile environment, whereas experimental plates must be properly sterilized to prevent contamination. It

is assumed that all steps in the BSC and the transfer of materials into and out of the BSC will be done with the proper aseptic techniques.

Preparation, Sterilization and Gelatin Coating of Coverslips steps 10-13 adapted from (Landry et al., 2021).

The process to coat the PDMS coverslips with gelatin requires an overnight incubation. While PDMS coated coverslips can be stored indefinitely, it is recommended that once the gelatin coating is performed that the coverslips be used for experimentation immediately. Thus, Steps 10 through 12 should be performed the day prior to planned cardiac fibroblast isolation to ensure that they are ready for plating.

10. Place the plate in the BSC, remove the lid and flip it so that the outer surface of the lid rests on the cabinet surface. Liberally spray the PDMS-coated coverslips and rest of the plastic plate, including the overturned lid, with 70% ethanol, effectively soaking them. Ethanol should cover the coverslip entirely. Close the cabinet sash, turn on the UV light and allow coverslips to sit in ethanol/UV for 20-30 minutes. Place a bottle of sterile PBS and an aliquot of porcine skin gelatin stock (See Reagents and Solutions) in a 37°C water bath in the meantime.
11. Thoroughly aspirate the ethanol covering each coverslip by pointing the 1 mL serological pipette towards the sides of the well to avoid direct contact with the coverslips. Additionally, aspirate the lid of the plastic dish. Once the majority of the

ethanol has been removed, allow the remainder to air dry in the cabinet for ~20-30 min until dry. Coverslips are now ready for downstream applications.

Do not try to directly aspirate small droplets of ethanol from the coverslips, as this may damage the coating. Any remaining ethanol of the coverslips after aspiration will be removed from the air-drying process.

12. Dilute porcine skin gelatin stock in sterile, warm PBS to make a sufficient volume of porcine skin gelatin working solution (10-100 µg/mL, concentration can be adjusted depending on cell adherence) (Landry et al., 2021). Each coverslip requires 500 µL of working solution. To make enough 100 µg/mL solution to coat one 24-well dish (12 mL), use a serological pipette to add 15 mL pre-warmed PBS into a 50 mL conical tube. Then add 150 µL porcine skin gelatin stock solution from the pre-warmed aliquot to the PBS. Mix by pipetting up and down with the serological pipette. Pipette 500 µL of the porcine skin gelatin working solution onto each PDMS-coated coverslip, ensuring that each coverslip is completely submerged in the solution. Cover the plate with the lid and place the plate in the 37°C 5% CO2 incubator overnight.
13. The next day when ready for cell plating, move the plates from the 37°C 5% CO2 incubator back into the BSC. Remove plate lids as before, aspirate using a 1 mL serological pipette to remove the gelatin solution from each well and allow the coverslips to air dry in the BSC for ~10 min. Coverslips are now ready for cell plating (see Step 35).

Basic Protocol 2: Adult Cardiac Fibroblast Isolation and Plating onto PDMS-Coated Coverslips

This protocol describes the isolation of primary murine adult cardiac fibroblasts for use in in vitro fibroblast assays adapted from (Kanisicak et al., 2016), in addition to their direct plating onto PDMS-coated coverslips. First, mouse hearts are enzymatically digested to separate myocardial tissue into its cellular components. The cell suspension is then plated onto PDMS/gelatin-coated coverslips to allow for preferential adherence of fibroblasts. This process maintains the fibroblasts on a physiologically relevant substrate for the duration of the experiment and removes any alterations to the fibroblasts associated with passaging primary cardiac fibroblasts prior to experimental assays.

Note: All experiments involving animals should abide by institutional protocols governing animal use and care (IACUC) and governmental agency guidelines, and protocols should be reviewed and approved prior to conducting any experimental procedures.

Note: ACFs are most commonly isolated and cultured from 8-12 weeks old mice of the C57/Bl6 strain but can be isolated from adult mice of any strain or genetic background.

Materials

Dulbecco's Modified Eagle's Medium (DMEM, Corning, #10-013-CV)

FBS aliquot (See Reagents and Solutions)

Pen/Strep (P/S, Corning, #30-002-CV)

Dispase buffer (See Reagents and Solutions)

Enzymatic digestion buffer (See Reagents and Solutions)

15 mL conical tubes (Basix, #14-955-237)

50 mL conical tubes (Fisherbrand, #05-539-12)

10 cm culture dishes (Fisherbrand, #FB012924)

10 mL serological pipettes (Falcon, 357551)

C57BL/6 mice, aged 8-12 weeks

Razor blades

40 µm mesh strainer (Fisherbrand, #22-363-547)

P1000 pipette tips (TipOne, #1112-1720)

10% FBS 1% P/S DMEM (See Reagents and Solutions)

1 mL serological pipettes (Falcon, #357506)

PDMS/gelatin coated coverslips (See Basic Protocol 1)

Equipment

37°C water bath

Ice bucket

Gyromini Nutator (Labnet, #S0500) or equivalent

Class II Biosafety Cabinet

37°C 5% CO_2 incubator

Serological pipette controller

Fine tip straight forceps (WPI, #14099) or equivalent (2)

Surgical scissors

P1000 pipette

Tabletop centrifuge

Vacuum aspirator

Inverted bright-field tissue culture microscope

Cardiac Fibroblast Isolation

Note: This section of the protocol explains the procedure for isolating primary adult mouse cardiac fibroblasts. For an alternative isolation protocol, see Isolation of Adult Mouse Cardiac Fibroblasts (Almazloum & Khalil, 2023).

14. Before beginning, place DMEM, and one (or more depending on number of hearts being isolated) FBS aliquot (refer to Reagents and Solutions) into the 37°C water bath. Warm P/S and Dispase buffer (See Reagents and Solutions) to room temperature, prepare an ice bucket, and place nutator in the 37°C 5% CO2 incubator.
15. Determine the number of hearts to be isolated and prepare enzymatic digestion buffer (See Reagents and Solutions) accordingly. Store in water bath at 37°C until ready to use.

    As one mouse heart will be digested with 6 mL enzymatic digestion buffer, the protocol details the proportional volumes of each buffer component to generate 6 mL total. If additional hearts are to be isolated, the total volume of enzymatic digestion buffer needed will increase accordingly to achieve 6 mL per heart. In this protocol, there are 3 rounds of digestion/sedimentation. Each round, 2 mL of enzymatic digestion buffer is used, for a total of 6 mL used to digest each heart.
16. Pre-label three conical tubes per sample.

    For each sample condition (i.e. different genotypes/biological replicates, etc.), there will be 3 tubes: 1. A 15 mL conical tube with 5-10 mL serum-free DMEM that will receive whole hearts upon isolation for transfer back to the biosafety cabinet, 2. an empty 15 mL or 50 mL conical tube (depending on how many hearts are being digested) to receive the minced heart tissue to be digested, and 3. an empty 50 mL conical tube to collect digested cell suspension supernatant and placed on ice. For

tube no.2, use a 15 mL conical tube when isolating up to 5 pooled hearts, and a 50 mL conical tube when digesting from 6 to 20 pooled hearts.

17. When DMEM is warm and enzymatic digestion buffer is ready, pipette 5-10 mL of serum-free DMEM into 1st set of pre-labeled 15 mL conical tubes with a 10 mL serological pipette. Then, pipette 10 mL of serum-free DMEM into 1 or multiple 10 cm culture dishes with a 10 mL serological pipette, one for each sample condition. Bring the 10 cm dish(es) and 15 mL conical(s) with media to location of animal sacrifice/heart isolation. Prepare the benchtop ahead of time to contain relevant euthanasia and sterile surgical tools (forceps, scissors) necessary to remove and dissect the heart after sacrifice.
18. Isolate heart(s). Following sacrifice of animal in accordance with respective approved animal protocols, use surgical scissors to open the thoracic cavity and expose the heart. Using two sets of forceps, with one grip the aorta and extracardiac tissue superior to the ventricles and with the other forceps gently grip and pull the ventricles away from chest cavity to isolate the heart.
19. Place the isolated heart into the 10 cm dish containing pre-warmed DMEM and squeeze the heart repeatedly with forceps in pre-warmed DMEM to remove remaining blood cells. Move each heart with the forceps to the respective pre-labeled 15 mL conical tube containing 5-10 mL serum-free DMEM and bring the tubes containing the heart(s) to the BSC.

    For the remainder of the protocol, steps will take place in a Class II BSC and a 37°C 5% CO2 incubator.

20. Using the P1000 pipette with filter tips, pipette 2 mL *per heart* of fresh enzymatic digestion buffer into a pre-labeled empty 15 or 50 mL conical tube (See Step 16 note). *Return 50 mL conical containing enzymatic digestion buffer to the 37°C water bath during each incubation period to ensure it stays warm through the three stages of the isolation.*
21. Remove the lid from a sterile 10 cm dish, then place the internal side of the lid facing up. Pour out the 15 mL conical containing the media/isolated hearts into the 10 cm dish base, then transfer (using forceps or lifting up with razor blades) each heart from the media in the 10 cm dish to the dry lid that was set facing up. Pinch the heart with the forceps, and use a razor blade to make a transverse cut of roughly the "top" 1mm of the heart to remove atria/vasculature above the ventricles, while maintaining as much of the ventricles as possible (see Figure 2.2). Then, mince ventricles using a razor blade and or surgical scissors, forming approximately 1-2 mm^3 pieces (~8-10 pieces per heart) and transfer minced ventricular tissue from one or more pooled heart(s) into the 15 or 50 mL conical tube containing the enzymatic digestion buffer for that sample.
22. When all samples are in their corresponding tubes, cap tubes and then transfer and secure the tubes in a nutator inside the 37°C 5% CO2 incubator to provide gentle agitation. Incubate tissues in a 37°C 5% CO_2 incubator for 20 min.
23. Remove the tubes from the nutator, transfer the tubes back to the BSC and for each tube perform manual trituration 12-15 times with a 5 mL serological pipette until all tissue pieces are able to travel through the pipette without resistance.

24. Settle the tissue by sedimentation (~30 sec-1 min), and carefully collect the supernatant using a P1000 filter pipette tip without disturbing the tissue at the bottom of the tube.
25. Using the P1000 pipette, pass the supernatant through a 40 μm mesh strainer into its corresponding pre-labeled 50 mL conical and store immediately on ice.

    Following the filter step, filters can be placed in a separate 50 mL conical to be reused for the following two filter steps, however, this only applies during smaller preps (1-3 hearts). In larger preps, due to the volume of enzymatic digestion buffer flowing through the filter from multiple hearts, the filters may become clogged and will not filter properly during the 2nd and 3rd filter steps. If running bulk preps with 5-10 pooled hearts per condition, a new filter can be used at each filtration step. Ensure that re-used filters are always placed in the proper collection 50 mL conical so that samples are not inadvertently contaminated.
26. Using the P1000, add 2 mL fresh enzymatic digestion buffer *per heart* to the previously sedimented ventricular tissue (not the digested supernatant on ice) in its existing tube and place back on the nutator in the 37°C 5% CO_2 incubator for 20 min.
27. Remove the tubes from the nutator, transfer the tubes back to the BSC and for each tube perform manual trituration 12-15 times with a P1000 pipette tip until there is not resistance.
28. Settle the tissue by sedimentation (~30 sec-1 min), and carefully collect the supernatant using a P1000 without disturbing the tissue at the bottom of the tube.
29. Using the P1000, pipette the supernatant through a 40 μm mesh strainer (either reused from the same sample or a new filter if doing bulk preps and the previous filter is

clogged) into the same corresponding 50 mL collection tube that was on ice and return the tube(s) to the ice bucket.

30. Using the P1000, add the final 2 mL fresh enzymatic digestion buffer *per heart* to the previously sedimented tissue in its existing tube and place on the nutator in the 37°C 5% CO_2 incubator for the final 20 min digestion. Add pre-made 10% FBS 1% P/S DMEM (See Reagents and Solutions) to the 37°C water bath, and pre-cool the tabletop centrifuge to 4°C.
31. Remove the tubes from the 37°C 5% CO2 incubator, transfer to the BSC and perform manual trituration 12-15 times through a P1000 pipette tip.
32. Settle the tissue by sedimentation (~30 sec-1 min), and carefully collect the supernatant using a P1000 pipette tip without disturbing the tissue at the bottom of the tube.
33. Using the P1000, pipette the supernatant through a 40 μm mesh strainer (either reused from the same sample or a new filter if doing bulk preps and the previous filter is clogged) into the corresponding 50 mL collection tube.
34. Centrifuge the pooled sample supernatant from the 3 digestions (6 mL total per heart per tube) in the 50 mL collection tube(s) at 350 x g for 20 min at 4°C using a fixed angle rotor.

    Swinging bucket rotors may result in lower yield as the cell pellet will be more dispersed along the side of the conical tube and more likely to be disturbed when removing supernatant.
35. During the spin, remove PDMS/gelatin-coated coverslips from the 37°C 5% CO2 incubator, and aspirate gelatin solution to prepare for cell plating (See Step 13).

36. Carefully remove tube(s) from centrifuge to not disturb the pelleted cells. Gently pour off supernatant from each tube and discard, with the pellet facing "up" in such a way that the supernatant is not flowing over the cell pellet as it leaves the tube.
37. Resuspend the cell pellet in 6.5 mL per heart of fresh pre-warmed 10% FBS 1% P/S DMEM (See Reagents and Solutions) using a 10 mL serological pipette.

    For this protocol, one mouse heart should generate enough fibroblasts to optimally grow on ~12 PDMS-coated coverslips. This is considering the growth rate of adult cardiac fibroblasts over the course of a 5-day experimental time course that ideally should not become over-confluent at the end of the experimental assay, while still achieving sufficient density for healthy cells at the time of plating. Dilution ratio can be modified as needed to account for differences in isolation efficiency of viable fibroblasts and achieve the desired plating density for the experimental conditions.
38. Pipette 500 µL of the cell suspension/media onto each PDMS/gelatin coated-coverslip, so that the coverslip is submerged in the solution. Place lid on 24-well plate. Transfer the plates to the 37°C 5% CO_2 incubator to allow the fibroblasts to adhere to the coverslips for 2 hours (See Figure 2.3).

    Given the hydrophobic properties of PDMS, the solution may not completely cover the coverslip upon initially dispensing into the well. The plate can be gently manually rocked back and forth to allow cells and media to completely cover the surface of the coverslip, or the cell suspension can be re-pipetted directly onto the coverslip until the coverslip is uniformly submerged in cell suspension media for plating.
39. Warm an FBS aliquot and P/S to room temp, and warm SF DMEM in the 37°C water bath. Following 2 hr incubation, transfer the plates to the BSC and gently wash the

cell solution (read non-fibroblast cells, fibroblasts have attached to coverslips) from the coverslips. Aspirate media/cell suspension from the plate ~4 wells at a time using a 1 mL serological pipette. Then, using the P1000, immediately cover each coverslip again in fresh media by gently pipetting 500 µL warm serum free (SF) DMEM onto the side of each well to avoid disturbing attached cells. Repeat until all wells in the dish have been washed once, and then repeat the washing process until the majority of the free floating/dead cells have been removed (~3 washes per coverslip total).

If aspiration with the serological pipette is resulting in loss of cells, wash steps can also be performed using P1000 for introduction and removal of media.

Attached fibroblasts will initially appear as small dark circles under the inverted bright-field tissue culture microscope, and should be able to be seen after about two washes. Canonical spindle morphology will appear ~2 days following plating.

40. Following the final wash, the incubation medium composition/volume will depend on downstream assay requirements. If no transduction is required, use a P1000 to replace wash media with 500 µL of freshly made 1% FBS 1% P/S DMEM using the pre-warmed components from Step 39. Incubate for 48-hours before proceeding to Basic Protocol 3, Step 43. If transduction is required, immediately following the isolation washing step, use the P1000 to pipette 250 µL 1% FBS DMEM (no P/S) into each well and proceed to Basic Protocol 3, Step 41.

    Given the hydrophobic properties of PDMS, the DMEM may not completely cover the coverslip upon initial administration, especially at such a low volume (250 µL) if performing a transduction. The plate can be gently manually rocked back and forth to allow cells and media to completely cover the surface of the coverslip, or the cell

suspension can be re-pipetted directly onto the coverslip until the coverslip is uniformly submerged in cell suspension media for plating. Note that these steps should be performed with caution as excess force can free attached fibroblasts from the PDMS substrate.

Basic Protocol 3: Assessment of Cardiac Fibroblast Activation by αSMA (alpha Smooth Muscle Actin) Immunocytochemistry

This protocol describes the process of performing an immunocytochemical assay using primary adult cardiac fibroblasts to assess their transformation into activated myofibroblasts. Parameters have been optimized for reduced background activation, efficient transduction in vitro (if applicable), and successful induction of activation using a profibrotic agonist. Following cell culture, fibroblasts on PDMS-coated coverslips are then fixed and prepared for downstream immunocytochemistry for α-smooth muscle actin (αSMA).

Materials

Adenovirus (if applicable)

P10 filter tips (SureOne, #02-707-001)

P20 filter pipette tips (SureOne, #02-707-432)

P1000 filter tips (VWR, #76322-156)

Dulbecco's Modified Eagle's Medium (Corning, #10-013-CV)

Fetal Bovine Serum (FBS, Corning, #35-010-CV)

Pen/Strep (P/S, Corning, #30-002-CV)

TGF-β1 Aliquots (See Reagents and Solutions)

Phosphate buffered saline (PBS, Corning, #21-040-CV)

Methanol (Sigma, #179337)

Parafilm (Fisher Scientific, #S37440)

15 cm plastic dishes (Fisherbrand, #FB012925)

Blocking solution (See Reagents and Solutions)

anti-αSMA primary antibody (Sigma, #A5228)

P200 pipette tips (TipOne, #1111-1706)

Paper towels (Scott, #01510)

Goat Anti-mouse AlexaFlour 488 secondary antibody (Invitrogen, #A-11029)

Prolong Gold with DAPI Mounting Solution (Cell Signaling, #8961)

35 mm Glass-bottom dishes (Cellvis, D35-28-1.5-N)

Equipment

Class II biosafety cabinet (BSC)

P10, P20, P200, P1000 pipettes

37°C water bath

37°C 5% CO_2 incubator

Gyromini Nutator (Labnet, #S0500) or equivalent

Fine tip straight forceps (WPI, #14099) or equivalent

Bent needle lifting tool (See Figure 2.1)

Vacuum aspirator

4°C refrigerator

Confocal or epifluorescence microscope compatible with imaging of 35 mm dishes

41. If the assay requires a transduction step, thaw adenovirus and using a P10 with filter tips, pipette respective volume of virus into each experimental well of the 24-well plate in a BSC (See Figure 2.3). Incubate overnight.

Cardiac fibroblasts can be highly resistant to transduction. The amount of virus necessary for transduction can vary, and volume to load will depend on individual viral titers. An excess of 100+ multiplicity of infection (MOI) may be required for efficient transduction of murine adult cardiac fibroblasts.

42. Following overnight incubation, gently aspirate virus-containing media from the coverslips. Remove media from the plate ~4 wells at a time using a P1000 with filter tips, and immediately cover each coverslip again in fresh media using the P1000 to gently pipette 500 µL warm SF DMEM into each well. Repeat until all the wells have been washed once, and then repeat twice more, adding warm 500 µL freshly made 1% FBS 1% P/S DMEM following the final wash. Incubate for 24 hours.
Pipetting gently on the side of the well is recommended for all media changes/wash steps to prevent displacing cells from the coverslip.
43. Following the post-isolation 48 hour incubation with or without virus, prepare treatment solutions (See Figure 2.3). Calculate for 500 µL per well to determine appropriate volumes of media and saline/TGFβ1 treatments. Briefly thaw frozen TGFβ1 (transforming growth factor β1) aliquot(s) (see Reagents and Solutions) at room temperature. Prepare pre-warmed 1% FBS 1% P/S DMEM media, and in separate 15 mL conical tubes, pipette 1 µL of TGFβ1 or saline per mL of media for a 1:1000 dilution (to achieve a final concentration of 10 ng/mL TGFβ1). Mix the solutions by placing them on the nutator inside the 37°C 5% CO_2 incubator for 5 minutes.
44. To begin treatments, remove media from the wells ~4 wells at a time using P1000 with filter tips, then immediately cover each coverslip again in fresh media by gently

pipetting 500 µL of treatment solutions of 1% FBS 1% P/S DMEM with saline or 10 ng/mL TGFβ1. Incubate inside the 37°C 5% CO_2 incubator for 72 hours.

45. Remove media from the wells ~4 wells at a time using P1000 with filter tips, then using the P1000 gently pipette 500 µL PBS onto each coverslip. Repeat so that all coverslips have been PBS-washed twice.

    Continue to perform all washes gently to reduce loss of cells.

46. Following the second wash, remove PBS with P1000 filter tips. Then, with the P1000 pipette, add 500 µL ice cold methanol onto each coverslip. Incubate for 15 min at 4ºC.

47. Remove methanol from each coverslip with P1000 filter tips, and gently wash twice with PBS with P1000 filter tips.

    For the remainder of the protocol, a sterile environment is not necessary and can be performed at a conventional lab bench.

48. Immunocytochemistry is performed as described (Brody et al., 2012; Essandoh et al., 2023) and adapted for detection and imaging of αSMA stress fibers in adult cardiac fibroblasts cultured on PDMS-coated coverslips. Coat a 15 cm non-sterile petri dish with one layer of parafilm to create an incubation chamber for immunostaining. Using the forceps and bent needle lifting tool (see Figure 2.1), remove each coverslip from its well and place onto the parafilm layer with the cells facing up. Immediately cover each coverslip with ~70 µL PBS using the P200. PBS should form a meniscus on the coverslip.

    Additional PBS volume is okay for the washing steps if 70 µL is not sufficient to fully cover the surface the coverslip.

49. When all coverslips have been placed on the parafilm, aspirate PBS with 1 mL serological pipette, and use a P200 pipette to add ~70 µL blocking solution (see Reagents and Solutions) to each coverslip, enough to sufficiently cover the whole surface. Incubate for 1 hr at room temp.

    Due to the hydrophobicity of the PDMS, solutions will not as easily spread across the surface of the coverslips. If there are sections where the coverslip is not covered by solution, the bent needle tool (Figure 2.1) or a pipette tip can be used to gently drag the solution across the surface of the coverslip without directly touching the coverslip/adhered fibroblasts to ensure all cells on the coverslip are covered and incubated in blocking solution.

50. Following blocking, incubate the coverslips with anti-αSMA primary antibody diluted 1:1000 in blocking buffer. Prepare primary antibody dilution (e.g. 1 µL of primary antibody in 1 mL blocking buffer). Aspirate the blocking buffer from each coverslip using a 1 mL serological pipette, and using P200 pipette, add ~70 µL of the primary antibody diluted in blocking buffer onto each coverslip.

    αSMA protein expression and incorporation into stress fibers is a hallmark of fibroblast activation.

51. Wet small pieces of paper towels, fold, and place on the sides of the 15 cm dish away from the coverslips to create a humidity chamber, then place the lid on to prevent coverslips from drying out. Move to a cold room or refrigerator to incubate overnight at 4°C.

52. The following day, wash each coverslip three times with PBS. Following the washes, incubate at room temperature for 1 hr in blocking buffer containing goat anti-mouse AlexaFlour 488 secondary antibody diluted 1:1000 in PBS.
53. Wash each coverslip three times with PBS in a similar fashion as previous washing steps. Coverslips are now ready for mounting.
54. Mount coverslips onto 35 mm glass-bottom dishes for imaging. 3 coverslips can be mounted on each 35 mm dish. Label 35 mm dishes to appropriately identify coverslips before mounting. Using a P20 filter tip, apply three small drops of Prolong Gold with DAPI mounting solution to each glass-bottom dish in a triangular pattern (See Figure 2.4).

    Conventional mounting procedures are not recommended as the PDMS coating increases the distance between the bottom edge of the coverslip and the focal plane of the cells. This can make resolving the cells difficult with normal mounting procedures. To overcome this, the coverslips should instead be mounted on an image compatible surface (35 mm glass bottom dishes), allowing for images to be taken without the PDMS distorting the light or decreasing the resolution. Each glass bottom dish will fit three coverslips in a triangular arrangement.
55. Lift each coverslip from the parafilm and flip it with the forceps so that the cell-side makes contact with the drop of mounting solution and gently lay it over the drop of mounting solution on the 35 mm glass bottom dish (See Figure 2.4). Coverslips can be left to dry at room temperature and are ready for imaging.

    The mounting solution will not cover the PDMS coated coverslips as quickly as an uncoated glass coverslip. If it appears to be mounting slowly, do NOT manually push

the coverslip down onto the glass bottom dish to even out the seal, as this will potentially damage the cells.

56. Coverslips can now be imaged using fluorescence microscopy (see Figure 2.5). Images can be taken with lower magnification (10X) to achieve fields-of-view (FOV) with an ample number of cells (50+ ACFs per FOV) to be representative during quantification steps.

57. Differences in αSMA response can be quantified using ImageJ.

Differences in αSMA signal in response to pro-fibrotic agonists are most commonly reported as the percent of cells positive for αSMA divided by the total number of cells (Davis et al., 2015). In some situations, αSMA signal can also be reported as differences in whole FOV signal intensity between treatment groups. Immunofluorescence data can be complemented by western blotting for αSMA protein levels. Due to the high baseline αSMA protein levels often seen in fibroblast culture, the % αSMA positivity method of quantification is often more sensitive.

Reagents and Solutions

Dispase Buffer

For 300 mL Stock Solution:

1. On a precision balance, weigh:
    a. 3.57 g HEPES (Fisher BioReagents, #BP310)
    b. 2.63 g NaCl (Fisher BioReagents, #BP358)

   Add weighed solids into a 500 mL glass beaker with approximately 280 mL ddH20.
2. Calibrate pH meter. Stir solution. Add KOH dropwise until the solution reaches pH 7.4.

3. Transfer solution to a graduated cylinder and bring solution to final volume of 300 mL with ddH_2O. Sterilize solution with 0.2 µm filter flasks (Fisherbrand, #FB12566500) and create six 50 mL conical aliquots to store at 4°C until use. Aliquots should be used within 6 months.

Porcine Skin Gelatin Aliquots

1% w/v porcine skin gelatin aliquots for coating the coverslips can be made as previously described (Landry et al., 2021).

1. In a glass autoclave bottle, add 100 mL ddH20, cap the bottle, and incubate in 37°C water bath.
2. When warm, add 1 g Porcine Gelatin Type A (Sigma-Aldrich, #G1980). Allow solution to dissolve.
3. Following dissolution, autoclave the solution at 121 °C, 15 psi, for 30 min to ensure sterility.
4. Carefully remove the solution from the autoclave, and aliquot in the BSC while the solution is still warm (~50 °C). Aliquots can then be stored indefinitely at 4 °C.

FBS Aliquots

1. Thaw frozen FBS (Corning, #35-010-CV), pipette up and down with serological pipette until solution is mixed.
2. Aliquot small volumes of FBS into 1.5 mL microfuge tubes, in amounts sufficient for isolating cells from a few hearts with some extra. Example: For an aliquot for a 5-heart isolation, 5 x 120 µL FBS per heart is 600 µL, plus 20 µL extra for a total of 620 µL per aliquot.

3. Store at -20°C until ready for use. Always use a fresh aliquot for each isolation, do not use FBS that has been freeze/thawed.

Enzymatic Digestion Buffer

The steps listed here will yield 6 mL enzymatic digestion buffer, enough for one heart.

All listed amounts need only be multiplied by the number of hearts being isolated to generate larger amounts of enzymatic digestion buffer.

1. Pre-warm serum-free DMEM in the 37°C water bath. Incubate dispase buffer (see Reagents and Solutions), an FBS aliquot (See Reagents and Solutions), and P/S at room temperature.
2. Using the precision balance weigh out 14 mg of Dispase II (Sigma, #D4693) and 11 mg of Collagenase IV (Worthington, #LS004188). Bring weighed solids to the biosafety cabinet.
3. Using a serological pipette, add 1.5 mL room temperature Dispase Buffer to a 50 mL conical tube. Carefully pour in the 14 mg Dispase II. Invert the tube manually and gently swirl to dissolve the solid.
4. Using a serological pipette, add 4.1 mL of serum-free warm DMEM to the 50 mL conical tube.
5. Using a pipette, add 300 µL P/S and 120 µL FBS to the tube.
6. Carefully pour in the 11 mg collagenase IV to the tube, cap and again manually invert the tube to ensure a mixed solution. Place the tube in the 37°C water bath until ready to use.

10% FBS 1% P/S DMEM

1. Open a fresh 500 mL bottle of DMEM. Using a serological pipette, remove 55 mL of media and discard.
2. Using a new serological pipette, add 50 mL FBS (Corning, #35-010-CV).
3. Using a new serological pipette, add 5 mL P/S (Corning, #30-002-CV).
4. Cap bottle and store at 4°C. Use within ~2 months.

TGFβ1 Aliquots

1. Reconstitute lyophilized TGFβ1 (Peprotech, #100-21) according to manufacturer's instructions. For Peprotech recombinant Human TGFβ1, reconstitute in sterile filtered 10 mM citric acid (Sigma, #251275) (in ddH_2O), pH 3.0, at a concentration of 20 µg/mL. Incubate at 4ºC for 10 minutes.
2. Further dilute 1:1 by adding an equal volume of 0.2% bovine serum albumin (BSA, Sigma Aldrich, #A9647) (in PBS) solution to the TGFβ1/citric acid solution to achieve a final stock concentration of 10 µg/mL TGFβ1, 0.1% BSA.
3. Aliquot the final TGFβ1 solution into 0.2 mL PCR tubes (VWR, #93001-118) by pipetting 10 µL into each tube. Aliquots can be stored at -20ºC for up to 1 year.

Blocking Solution

1. Generate 1 L of 10X phosphate buffered saline solution

NaCl	80g	(Fisher BioReagents, #BP358)
KCl	2g	(Sigma, #P9541)
Na_2HPO_4	14.4g	(Sigma, #S9763)

KH_2PO_4 2.4g (Sigma, #P5655)

pH to 7.4

2. Dilute 10X PBS 1:10 in ddH20 to generate 1X PBS.
3. Generate blocking solution with 1X PBS.

   1X Phosphate Buffered Saline

   5% Goat serum (Sigma Aldrich, #G6767)

   1% BSA (Sigma Aldrich, #A9647)

   1% Glycine (Thermo Scientific, #AAA138160E)

   0.2% Triton X-100 (Fisher BioReagents, #BP151-500)

Commentary

Background Information

Recent exploration into the mechanisms underlying cardiac fibroblast activity and phenotypic transformation to elicit ECM remodeling and cardiac fibrosis in many forms of heart disease is an exciting frontier for cardiac biology. Given the sensitivity of cardiac fibroblasts to their environment, 2D cell culture experimentation can represent a significant technical challenge. Towards solving this problem, researchers have adopted new strategies including the use of substrates like polydimethylsiloxane (PDMS), a silicon-based organic polymer that is widely used in the fields of cell biology and bioengineering for this application due to its unique biocompatibility, transparency, and tunable elasticity (Palchesko et al., 2012). Coverslips coated with PDMS provide a simple yet robust method to model a variety of in vivo environments in vitro with a range of practical applications spanning cell and tissue culture, biomechanical studies, and high-resolution imaging applications. In the context of fibroblast research, it has been demonstrated that fibroblasts plated and maintained on 8 kPa soft substrate-coated plates

exhibit reduced baseline activation compared to standard plastic plates used for in vitro studies (Landry et al., 2019). Here we provide a straightforward and cost-effective protocol for assessment of cardiac fibroblast activation.

Critical Parameters

Cardiac fibroblasts are particularly sensitive to a variety of cell culture conditions that can influence experimental results, and attention to small details throughout the course of preparation, from coverslip generation to the activation treatments, is necessary for these assays. Carefully mixing the PDMS reagents at the proper ratios when generating batches of coverslips is critical for consistent results between experiments. Coverslips must be cured at the same temperature and length of time in order to achieve the proper stiffness rating; curing for too long or too short may result in variation in the performance of the substrate. The gelatin coating step is additionally important to ensure that the fibroblasts properly attach to the PDMS substrate during the cell plating step. Ensure that the filtered supernatants are kept on ice for the duration of the isolation process, including pre-cooling the centrifuge. After spinning the cells down, the cell pellet should appear red at the center of the pellet (red blood cells), with the larger white/pale portion of the cell pellet containing the fibroblasts. When pouring off the media to resuspend the pellet, hold the tube in such a way that the media does not travel over the pellet as it is being poured to reduce loss of fibroblasts in this step. During plating, achieving the proper confluency of fibroblasts is critical for the success of the 5-day activation experiment and may need to be adjusted to accommodate different experimental time courses. Overly confluent (>~40-50%) cells on the coverslips in the beginning of the experiment will lead to high baseline activation, as after 5 days of growth the monolayer will be overly confluent. Conversely, fibroblast populations that are under confluent (<~15%) at the beginning of the experiment will not grow properly and

there will not be enough cells to analyze at the conclusion of the assay. Ideally, the confluency should be kept between 20-80% confluent throughout the 5-day time course. In all washing steps following plating, the amount of time that the cells are not covered in media should be reduced as much as possible. The hydrophobicity of the PDMS can lead to the cells drying out much faster than on standard coverslips, and thus it is critical to swiftly re-introduce fresh media. When pipetting media into the dishes, it should be pipetted gently into the side of the well in order to reduce cells being washed away. Fibroblasts generally attach well to their plates, however, on the PDMS they are more easily dislodged. If using a virus in the experiment, the transduction process will need to take place as early as possible so as to reduce the total amount of time in culture for the experimental time course. Generally, 48 hours after transduction provides sufficient time for robust expression of the desired constructs before beginning the activation assay. Additionally, the amount of virus needed to successfully transduce cardiac fibroblasts will likely be far greater than that needed for other cell types. Since fibroblasts exhibit increased activation with higher concentrations of FBS (10-20%), the TGFβ induction of activation will be less effective at these FBS concentrations. Thus, 1% FBS DMEM should be used for all culture steps aside from the initial isolation and plating steps. For additional troubleshooting, see Table 1.

Understanding Results

Carrying out this protocol will allow for the maintenance of a quiescent population of primary murine cardiac fibroblasts for a 5-day time-course. One of the most common ways in which cardiac fibroblasts are classified as activated is through their expression of αSMA. Successful completion of this protocol is simply interpreted through evaluation of immunocytochemical detection of αSMA expression in the cytoskeleton of the fibroblasts. Quiescent cells will

predominantly be absent of this activated fibroblast marker (~20% positive for αSMA), as seen in Figure 2.5 in the left panel. Induction of activation with TGFβ1 treatment leads to a significant upregulation of αSMA expression, seen in the right panel of Figure 2.5 (~50-60% positive for αSMA). Due to the extreme sensitivity of these cells to substrate stiffness, false negatives of αSMA expression are not to be expected, thus a population of cells that is predominantly absent of αSMA for 3-5 days in culture would be considered quiescent.

Time Considerations

Coverslip Preparation: PDMS-coating

Making the PDMS-coated coverslips will take ~ 2 hours of work followed by an overnight incubation. This step can produce between 150-200 coverslips at a time which can be used discretionarily over the course of many experiments. PDMS-coated coverslips (without gelatin coating) can be stored at room temperature indefinitely.

Coverslip Preparation: Gelatin-coating

Coating the coverslips with gelatin (beginning the day prior to fibroblast isolation) takes about 15 min of work followed by an overnight incubation. Once the gelatin coating is performed on the PDMS-coated coverslips, it is recommended that they be used immediately.

Cardiac Fibroblast Isolation

The cardiac fibroblast isolation takes about 2 hours of work, followed by a 2-hour incubation period while the fibroblasts attach to the coverslip, then a ~15 min washing process. The process in its entirety will span ~4.5 hours, though there is only about 2.5 hours of this process that involve active work.

Cell Culture/Activation Assay

The activation assay takes 5 full days, beginning at the washing step following fibroblast isolation and plating. The first 24-48 hours are used for desired experimental genetic manipulations (viral transduction and expression of engineered constructs). 72-hours is needed for TGFβ1 treatment to induce sufficient activation in the fibroblasts.

Chapter II Figures

Figure 2.1. Depiction of Bent-needle Tool

Figure 2.1: Depiction of Bent-needle Tool. *Coverslip lifting tool for coverslip transfer. Image of coverslip lifting tool generated by bending the tip (~ 3 mm) of a 1.5 inch, 21-gauge needle. Forceps are used in tandem with the bent-needle tool to transfer coverslips between dishes.*

Figure 2.2. Cardiac Fibroblast Isolation Atria Removal Diagram

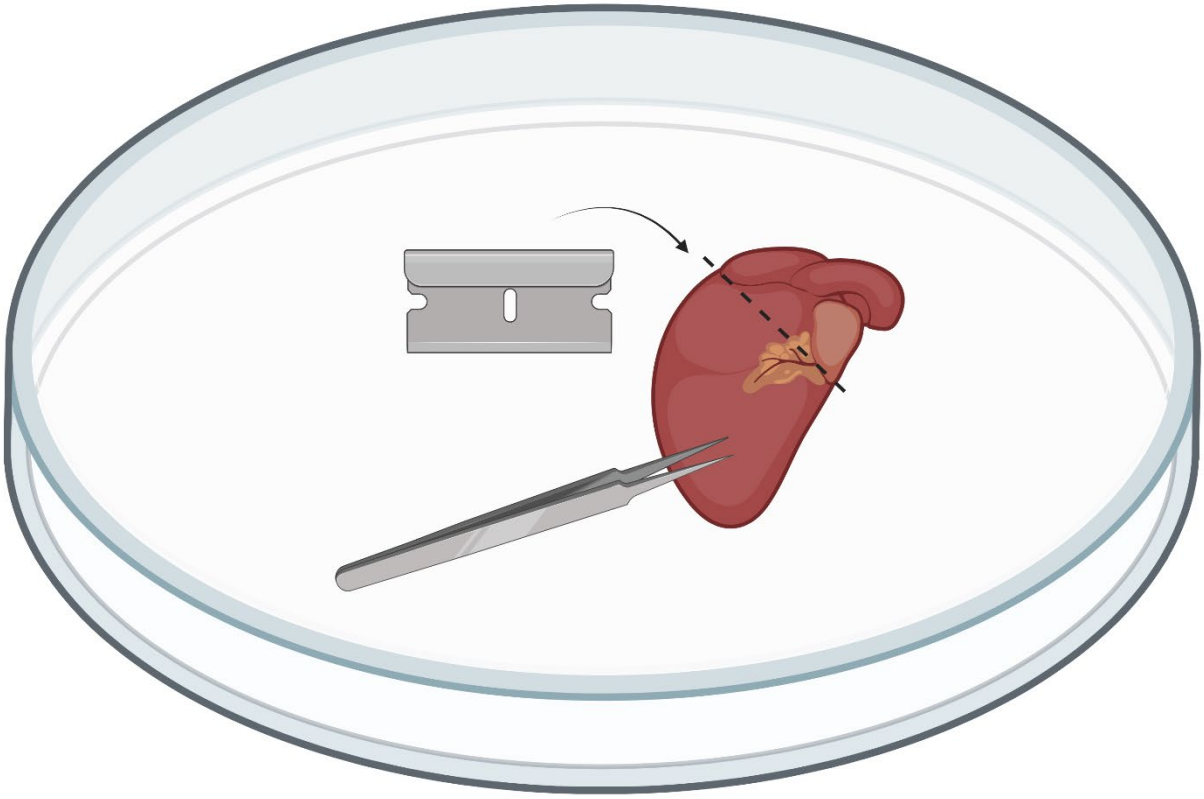

Figure 2.2. Cardiac Fibroblast Isolation Atria Removal Diagram. *Schematic of murine heart dissection for fibroblast isolation. Diagram illustrating use of razor blade to remove atria/vessels from dissected heart, allowing for digestion of ventricular tissue for fibroblast isolation. Created with BioRender.com*

Figure 2.3. Cardiac Fibroblast αSMA Assay Steps and Mounting

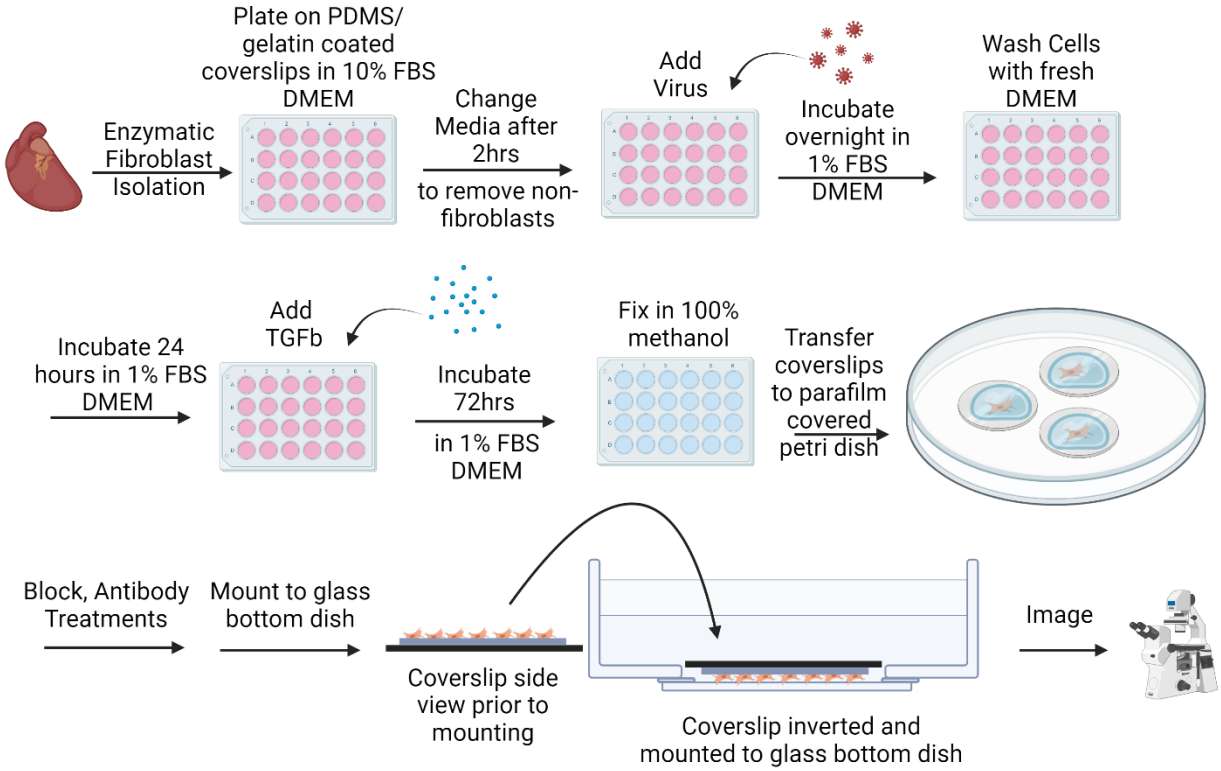

Figure 2.3: Cardiac Fibroblast αSMA Assay Steps and Mounting. *Adult cardiac fibroblast (ACF) activation assay protocol experimental workflow. Following fibroblast isolation, plating, and washing steps, fibroblasts can be immediately transduced for genetic manipulation if desired. ACFs can then be treated with a pro-fibrotic agonist (TGFβ1) to induce αSMA stress fiber formation. 72-hours later, cells are methanol-fixed and immunocytochemistry steps are performed prior to mounting and imaging. Created with BioRender.com.*

Figure 2.4. PDMS-coverslip Mounting Arrangement Diagram

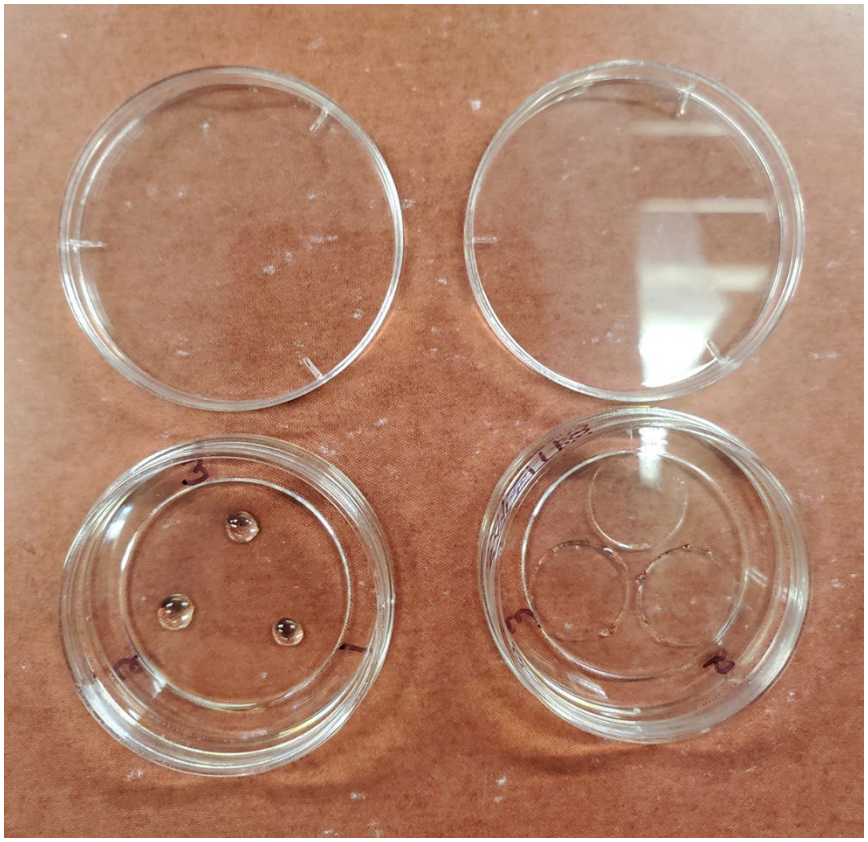

Figure 2.4: PDMS-coverslip Mounting Arrangement Diagram. *Mounting configuration of PDMS-coated coverslips onto 35-mm glass bottom dishes. Three dots of mounting solution can be applied to each 35-mm glass bottom dish (bottom left) and PDMS-coated coverslips mounted face down onto the 35-mm dish such that the cells are mounted against the glass bottom dish (bottom right), allowing for imaging of the cells on an inverted microscope without negative effects associated with imaging through the PDMS layer.*

Figure 2.5. αSMA Immunocytochemical Detection, Quiescence and Successful Induction with TGFβ1

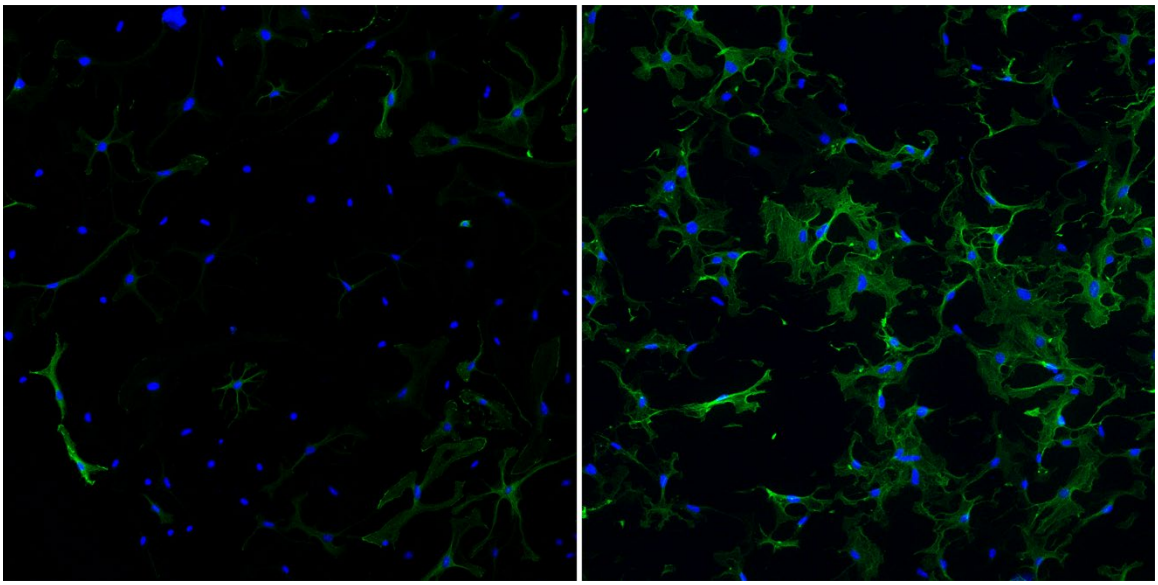

Figure 2.5: αSMA Immunocytochemical Detection, Quiescence and Successful Induction with TGFβ1*. Adult cardiac fibroblast (ACF) activation assay on PDMS-coated coverslips. Immunocytochemistry for α-smooth muscle actin (αSMA, green) in ACFs cultured on PDMS-coated coverslips treated with saline or TGFβ1 (10 ng/mL) for three days as outlined in Fig 3. Under these conditions, a quiescent population of fibroblasts can be achieved (left), allowing for greater relative induction of myofibroblast transformation in response to profibrotic stimuli such as TGFβ1 (right). Nuclei were stained blue with DAPI.*

Chapter II Tables

Table 2.1. Troubleshooting Guidelines for PDMS-coating, Fibroblast Isolation and Culture

Problem	Possible Cause	Solution
PDMS-coated coverslips consistently stuck to bottom of loading plate	Overloading coverslips with PDMS, pipetting not centered	Reduce loading volume, optimal range is between 12-14 µL per coverslip
Low Fibroblast Isolation Yield	Not completing overnight gelatin coating	Make sure to coat wells overnight in gelatin solution
	Losing cells in washing step	Add media very gently during washing steps, and make sure the amount of time without media is reduced as much as possible during each wash (only aspirate ~4 wells at a time).
Non-fibroblasts present in plates	Extended plating duration	Reduce plating time before wash
Fibroblasts are overly confluent	Insufficient dilution when plating	Increase dilution prior to plating
Cells exhibit high baseline activation without stimulation	Errors during PDMS generation	Remake solution/coverslips
	Cells become over confluent by time of fixing	Increase dilution to reduce endpoint confluency (ideally <80% at day 5)
Low transduction efficiency	Insufficient viral load	Increase viral load (300-500 MOI)
	Insufficient transduction time	Transduce with viruses overnight
Cells appear damaged when imaging	Pushing down on coverslips during mounting	Allow the mounting solution to fully seal the coverslip without disturbing it manually
Cells are contaminated	Insufficient ethanol coverage/UV treatment in sterilization step	Make sure ethanol covers coverslip, and time course in ethanol/UV is carried out
	Media/aliquot sterility not carefully maintained	Maintain strict adherence to sterile technique, use sterile filter flasks when applicable

Table 2.1: Troubleshooting Guidelines for PDMS-coating, Fibroblast Isolation and Culture. *Problems, possible causes, and solutions for an assortment of trouble areas in the generation of 8kPa PDMS coated coverslips, cardiac fibroblast isolation, and maintaining a quiescent population of cells over a 5-day time course.*

References

Almazloum, A., & Khalil, H. (2023, Jul). Isolation of Adult Mouse Cardiac Fibroblasts. Curr Protoc, 3(7), e840. https://doi.org/10.1002/cpz1.840

Alter, C., Henseler, A. S., Owenier, C., Hesse, J., Ding, Z., Lautwein, T., Bahr, J., Hayat, S., Kramann, R., Kostenis, E., Scheller, J., & Schrader, J. (2023, Jun 1). IL-6 in the infarcted heart is preferentially formed by fibroblasts and modulated by purinergic signaling. J Clin Invest, 133(11). https://doi.org/10.1172/JCI163799

Bertaud, A., Joshkon, A., Heim, X., Bachelier, R., Bardin, N., Leroyer, A. S., & Blot-Chabaud, M. (2023, Jan 16). Signaling Pathways and Potential Therapeutic Strategies in Cardiac Fibrosis. Int J Mol Sci, 24(2). https://doi.org/10.3390/ijms24021756

Bretherton, R., Bugg, D., Olszewski, E., & Davis, J. (2020, Sep). Regulators of cardiac fibroblast cell state. Matrix Biol, 91-92, 117-135. https://doi.org/10.1016/j.matbio.2020.04.002

Brody, M. J., Hacker, T. A., Patel, J. R., Feng, L., Sadoshima, J., Tevosian, S. G., Balijepalli, R. C., Moss, R. L., & Lee, Y. (2012). Ablation of the cardiac-specific gene leucine-rich repeat containing 10 (Lrrc10) results in dilated cardiomyopathy. PLoS One, 7(12), e51621. https://doi.org/10.1371/journal.pone.0051621

Cheng, X., Wang, L., Wen, X., Gao, L., Li, G., Chang, G., Qin, S., & Zhang, D. (2021, May). TNAP is a novel regulator of cardiac fibrosis after myocardial infarction by mediating TGF-β/Smads and ERK1/2 signaling pathways. EBioMedicine, 67, 103370. https://doi.org/10.1016/j.ebiom.2021.103370

Childers, R. C., Lucchesi, P. A., & Gooch, K. J. (2021, Jun 9). Decreased Substrate Stiffness Promotes a Hypofibrotic Phenotype in Cardiac Fibroblasts. Int J Mol Sci, 22(12). https://doi.org/10.3390/ijms22126231

Davis, J., Salomonis, N., Ghearing, N., Lin, S. C., Kwong, J. Q., Mohan, A., Swanson, M. S., & Molkentin, J. D. (2015, Dec 16). MBNL1-mediated regulation of differentiation RNAs promotes myofibroblast transformation and the fibrotic response. Nat Commun, 6, 10084. https://doi.org/10.1038/ncomms10084

Essandoh, K., Subramani, A., Ferro, O. A., Teuber, J. P., Koripella, S., & Brody, M. J. (2023, May). zDHHC9 Regulates Cardiomyocyte Rab3a Activity and Atrial Natriuretic Peptide Secretion Through Palmitoylation of Rab3gap1. JACC Basic Transl Sci, 8(5), 518-542. https://doi.org/10.1016/j.jacbts.2022.11.003

Fu, X., Khalil, H., Kanisicak, O., Boyer, J. G., Vagnozzi, R. J., Maliken, B. D., Sargent, M. A., Prasad, V., Valiente-Alandi, I., Blaxall, B. C., & Molkentin, J. D. (2018, May 1). Specialized fibroblast differentiated states underlie scar formation in the infarcted mouse heart. J Clin Invest, 128(5), 2127-2143. https://doi.org/10.1172/jci98215

Fu, X., Liu, Q., Li, C., Li, Y., & Wang, L. (2020). Cardiac Fibrosis and Cardiac Fibroblast Lineage-Tracing: Recent Advances. Front Physiol, 11, 416. https://doi.org/10.3389/fphys.2020.00416

Gibb, A. A., Lazaropoulos, M. P., & Elrod, J. W. (2020, Jul 17). Myofibroblasts and Fibrosis: Mitochondrial and Metabolic Control of Cellular Differentiation. Circ Res, 127(3), 427-447. https://doi.org/10.1161/circresaha.120.316958

Herum, K. M., Choppe, J., Kumar, A., Engler, A. J., & McCulloch, A. D. (2017, Jul 7). Mechanical regulation of cardiac fibroblast profibrotic phenotypes. Mol Biol Cell, 28(14), 1871-1882. https://doi.org/10.1091/mbc.E17-01-0014

Herum, K. M., Lunde, I. G., McCulloch, A. D., & Christensen, G. (2017, May 19). The Soft- and Hard-Heartedness of Cardiac Fibroblasts: Mechanotransduction Signaling Pathways in Fibrosis of the Heart. J Clin Med, 6(5). https://doi.org/10.3390/jcm6050053

Ivey, M. J., & Tallquist, M. D. (2016, Oct 25). Defining the Cardiac Fibroblast. Circ J, 80(11), 2269-2276. https://doi.org/10.1253/circj.CJ-16-1003

Kanisicak, O., Khalil, H., Ivey, M. J., Karch, J., Maliken, B. D., Correll, R. N., Brody, M. J., SC, J. L., Aronow, B. J., Tallquist, M. D., & Molkentin, J. D. (2016, Jul 22). Genetic lineage tracing defines myofibroblast origin and function in the injured heart. Nat Commun, 7, 12260. https://doi.org/10.1038/ncomms12260

Khalil, H., Kanisicak, O., Vagnozzi, R. J., Johansen, A. K., Maliken, B. D., Prasad, V., Boyer, J. G., Brody, M. J., Schips, T., Kilian, K. K., Correll, R. N., Kawasaki, K., Nagata, K., & Molkentin, J. D. (2019, Aug 8). Cell-specific ablation of Hsp47 defines the collagen-

producing cells in the injured heart. JCI Insight, 4(15), e128722. https://doi.org/10.1172/jci.insight.128722

Landry, N. M., Rattan, S. G., & Dixon, I. M. C. (2019, Sep 9). An Improved Method of Maintaining Primary Murine Cardiac Fibroblasts in Two-Dimensional Cell Culture. Sci Rep, 9(1), 12889. https://doi.org/10.1038/s41598-019-49285-9

Landry, N. M., Rattan, S. G., & Dixon, I. M. C. (2021). Soft Substrate Culture to Mechanically Control Cardiac Myofibroblast Activation. Methods Mol Biol, 2299, 171-179. https://doi.org/10.1007/978-1-0716-1382-5_13

Meagher, P. B., Lee, X. A., Lee, J., Visram, A., Friedberg, M. K., & Connelly, K. A. (2021, Mar 31). Cardiac Fibrosis: Key Role of Integrins in Cardiac Homeostasis and Remodeling. Cells, 10(4). https://doi.org/10.3390/cells10040770

Morningstar, J. E., Gensemer, C., Moore, R., Fulmer, D., Beck, T. C., Wang, C., Moore, K., Guo, L., Sieg, F., Nagata, Y., Bertrand, P., Spampinato, R. A., Glover, J., Poelzing, S., Gourdie, R. G., Watts, K., Richardson, W. J., Levine, R. A., Borger, M. A., & Norris, R. A. (2021, Dec 21). Mitral Valve Prolapse Induces Regionalized Myocardial Fibrosis. J Am Heart Assoc, 10(24), e022332. https://doi.org/10.1161/jaha.121.022332

Palchesko, R. N., Zhang, L., Sun, Y., & Feinberg, A. W. (2012). Development of polydimethylsiloxane substrates with tunable elastic modulus to study cell mechanobiology in muscle and nerve. PLoS One, 7(12), e51499. https://doi.org/10.1371/journal.pone.0051499

Santiago, J. J., Dangerfield, A. L., Rattan, S. G., Bathe, K. L., Cunnington, R. H., Raizman, J. E., Bedosky, K. M., Freed, D. H., Kardami, E., & Dixon, I. M. (2010, Jun). Cardiac fibroblast to myofibroblast differentiation in vivo and in vitro: expression of focal adhesion components in neonatal and adult rat ventricular myofibroblasts. Dev Dyn, 239(6), 1573-1584. https://doi.org/10.1002/dvdy.22280

Shiraishi, M., Suzuki, K., & Yamaguchi, A. (2023, Apr). Effect of mechanical tension on fibroblast transcriptome profile and regulatory mechanisms of myocardial collagen turnover. Faseb j, 37(4), e22841. https://doi.org/10.1096/fj.202201899R

Tallquist, M. D. (2020, Feb 10). Cardiac Fibroblast Diversity. Annu Rev Physiol, 82, 63-78. https://doi.org/10.1146/annurev-physiol-021119-034527

Tallquist, M. D., & Molkentin, J. D. (2017, Aug). Redefining the identity of cardiac fibroblasts. Nat Rev Cardiol, 14(8), 484-491. https://doi.org/10.1038/nrcardio.2017.57

Teuber, J. P., Essandoh, K., Hummel, S. L., Madamanchi, N. R., & Brody, M. J. (2022, Sep 16). NADPH Oxidases in Diastolic Dysfunction and Heart Failure with Preserved Ejection Fraction. Antioxidants (Basel), 11(9). https://doi.org/10.3390/antiox11091822

Umbarkar, P., Ejantkar, S., Tousif, S., & Lal, H. (2021, Sep 14). Mechanisms of Fibroblast Activation and Myocardial Fibrosis: Lessons Learned from FB-Specific Conditional Mouse Models. Cells, 10(9). https://doi.org/10.3390/cells10092412

Wang, A., Cao, S., Stowe, J. C., & Valdez-Jasso, D. (2021, Apr 23). Substrate Stiffness and Stretch Regulate Profibrotic Mechanosignaling in Pulmonary Arterial Adventitial Fibroblasts. Cells, 10(5). https://doi.org/10.3390/cells10051000

Yeh, Y. C., Corbin, E. A., Caliari, S. R., Ouyang, L., Vega, S. L., Truitt, R., Han, L., Margulies, K. B., & Burdick, J. A. (2017, Nov). Mechanically dynamic PDMS substrates to investigate changing cell environments. Biomaterials, 145, 23-32. https://doi.org/10.1016/j.biomaterials.2017.08.033

Chapter III: zDHHC3-mediated Palmitoylation is Dispensable for Cardiac Fibroblast Activation

Abstract

Cardiac fibroblasts (CFs) have become an increasingly recognized cell type in the heart due to their role in sensing the cardiac microenvironment and maintaining the extracellular matrix (ECM). Initiated both by chemical and mechanical signaling, CFs undergo a transition from their usual quiescence into their canonical "myofibroblast" phenotype to regulate collagen production and secretion, release cytokines, and respond to injury. The signaling pathways that underlie this activation have begun to be explored, but there is still a great deal unknown surrounding the regulation of CF activation in both physiologic and pathologic processes. Palmitoylation, a reversible fatty acid post-translational modification mediated by the S-acyltransferase family of enzymes, has been implicated in dynamically regulating signaling protein substrates in terms of localization, trafficking, and stability. One of these enzymes, zDHHC3, has been shown to regulate a variety of signaling molecules by palmitoylation in other cell types, including many canonically involved in pro-fibrotic signaling, though the role that zDHHC3 plays in CFs remains unexplored. Given the importance of protein palmitoylation in signal transduction, we aimed to elucidate the role of zDHHC3 in CF activation and fibrosis in vitro and in vivo. Here, we show that zDHHC3-mediated palmitoylation is not required for transforming growth factor β 1 (TGFβ1)-induced myofibroblast differentiation in vitro, and myofibroblast-specific *Zdhhc3* knockout (KO) mice exhibit similar cardiac remodeling, hypertrophy, and cardiac dysfunction in response to pressure overload in vivo compared to

controls. These studies provide evidence that despite the known regulation of key fibrotic signaling proteins by this enzyme in other cell types, zDHHC3 activity does not appear to play an indispensable role in CF biology, though further work is required to determine whether compensatory effects of additional S-acyltransferases are present.

Introduction

Cardiac fibroblasts (CFs) play a number of crucial roles in the heart, primarily maintaining the extracellular matrix (ECM), releasing cytokines to communicate with other cardiac cell types, and remodeling the heart in the event of injury (Fu et al., 2018; Ivey & Tallquist, 2016; Kanisicak et al., 2016; Tallquist & Molkentin, 2017). While normally in a quiescent state, resident CFs are sensitive to both chemical and mechanical stimuli that direct their transition from inactive cells into canonical "myofibroblasts" (Bretherton et al., 2020; Umbarkar et al., 2021). In their activated state, myofibroblasts exhibit increased proliferative capacity, elevated paracrine signaling, and upregulation in the synthesis, trafficking, and secretion of collagen and other ECM proteins as a response to cardiac injury (Bretherton et al., 2020; Reichardt et al., 2021). As such, significant attention has been placed on understanding the signaling that facilitates this activation process due to their role in the maladaptive phenotypes associated with the development of cardiac fibrosis (Fu et al., 2020; Kanisicak et al., 2016; Umbarkar et al., 2021).

Progress has been made in identifying a number of major ligands, cell surface receptors and their associated downstream signaling cascades from efforts to understand the transition from quiescence to activated fibroblast (Frangogiannis, 2021; Landry & Dixon, 2020; Umbarkar et al., 2021). Notable pathways that have been demonstrated to be involved in CF activation include transforming growth factor β 1 (TGFβ1) activating SMAD2/3 through transforming growth

factor β receptor II (TGFβRII), angiotensin II (AngII) activating G-alpha q ($G\alpha_q$) signaling through angiotensin II receptor type I (AT1R), and interleukin-6 (IL6) initiating Janus kinase/signal transducer and activator of transcription JAK/STAT signaling through binding to the interleukin-6 receptor (IL6R) (Bertaud et al., 2023; Landry & Dixon, 2020; Umbarkar et al., 2021). Despite significant headway in understanding the major proteins involved in these pathways, there is still much unknown about how the protein signals downstream of these receptors are fine-tuned to produce the dynamic responses seen in CF biology.

While it is currently understood that the activation of CFs and their ability to respond to injury is regulated by a complex interplay of these signaling pathways, one area of continued investigation is the importance of protein post-translational modifications (PTMs) as key modulators of these cellular responses. Palmitoylation, a reversible PTM involving the addition of a saturated fatty acid to cysteine residues of protein substrates, is one such critical modulator (Chamberlain & Shipston, 2015; De & Sadhukhan, 2018; Jiang et al., 2018; Tabaczar et al., 2017). Palmitoylation is mediated by a family of enzymes called S-acyltransferases that play a crucial role in the intracellular fate of a variety of signaling proteins and can influence stability, protein-protein association, and, most predominantly, localization to a variety of lipophilic cellular compartments from which additional signaling can occur (Chamberlain & Shipston, 2015; De & Sadhukhan, 2018; Jiang et al., 2018; Tabaczar et al., 2017). Notably, S-acyltransferase enzymes have been established to play key roles in cardiomyocytes, from the regulation of a variety of ion channels (Essandoh et al., 2020), GTPase activation and hypertrophy (Baldwin et al., 2023), and cardiomyocyte exocytosis (Essandoh et al., 2023). However, at present, the role of palmitoylation in fine-tuning the signal transduction processes of CFs remains unexplored.

Recent work has demonstrated that these enzymes, or "zDHHCs" in reference to their conserved aspartic acid-histidine-histidine cysteine catalytic domain, play a significant role in signaling underlying a variety of diseases, including cancer, irritable bowel disease (IBS), and neurological disorders (Cho & Park, 2016; Main & Fuller, 2022; Zhang et al., 2021). Interestingly, exploration into these enzymes in a variety of cell types has shown that a number of pathways associated with CF signaling are modified by palmitoylation, in particular by one of the Golgi-localized enzymes, zDHHC3. One nodal regulator of CF activation, STAT3, has been shown to be palmitoylated by zDHHC3 in the Golgi, driving its phosphorylation at the plasma membrane, an additional PTM critical for its activity in the nucleus (Zhang et al., 2020). $G\alpha_q$, a major signaling protein for the pro-fibrotic agonist AngII, has also been shown to be palmitoylated by zDHHC3 (Tsutsumi et al., 2009), though the consequences of the PTM in this context are unknown. Rac1, a small Rho-GTPase known to be important for fibroblast activation/wound healing (Kunschmann et al., 2019; Liu et al., 2009; Martínez-López et al., 2021; Xu et al., 2009), has been shown to be regulated by palmitoylation, influencing the cellular localization and its GTP-loaded status of Rac1 (Navarro-Lérida et al., 2012). Notably, Rac1 was recently shown to be palmitoylated by zDHHC3 in the heart, and further, Rac1 expression levels and GTP-loading were upregulated in cardiomyocytes upon overexpression of zDHHC3 (Baldwin et al., 2023). While all of these signaling pathways are known to play a role in fibroblast activation, how zDHHC3 activity influences CF signaling and activation remains entirely unexplored, necessitating future work in this area.

Given the established importance of the aforementioned signaling pathways in CF activation, in addition to the established role of palmitoylation in regulating these pathways in other cell types, we sought to establish whether zDHHC3 is similarly expressed in CFs, and how zDHHC3

activity may be influencing CF activation. The present study was conducted to explore the hypothesis that S-acyltransferase-mediated palmitoylation is critical to the activation and migration of CFs. We hypothesized that the deletion of *Zdhhc3* would result in a blunted fibroblast activation in response to the pro-fibrotic agonist TGFβ1 in vitro, as well as a reduced fibrotic response to pressure overload in vivo.

Methods

Animal models

Zdhhc3 fl/fl mice (Baldwin et al., 2023) were acquired as previously described (Cincinnati Children's Hospital). *Zdhhc3* fl/fl mice were crossed with *Postn-MCM +/-* mice (Kanisicak et al., 2016) (Strain #:029645) to generate myofibroblast-specific *Zdhhc3* knockout (*Zdhhc3* fKO) animals for in vivo assays. All animal procedures were approved by the Institutional Animal Care and Use Committee at the University of Michigan (IACUC protocol #PRO00009098) and were in accordance with the Guide for the Care and Use of Laboratory Animals (National Institutes of Health).

Cardiac fibroblast isolation

Neonatal rat cardiomyocytes (NRCMs) were isolated according to the manufacturer's protocol (Worthington, CAS: 9035-81-1). Neonatal rat CF (NRCF) isolation was adapted from the Neonatal Cardiomyocyte Isolation System (Worthington, CAS: 9035-81-1). Hearts were digested according to the manufacturer's instructions, and digested cell suspension was plated on uncoated 10 cm dishes for 90-120 min for fibroblasts to attach to the dish. Following attachment, dishes were washed twice with warm serum-free Dulbecco's Modified Eagle Medium (DMEM) media and incubated in 10% fetal bovine serum (FBS) and 1% penicillin/streptomycin (P/S) DMEM media. Adult cardiac fibroblast (ACF) isolation protocol was adapted from (Kanisicak et

al., 2016). In brief, hearts were removed and minced into 8-10 pieces before being placed in a microfuge tube containing enzymatic digestion buffer made with 1.2 U/mL Dispase II (Sigma, #D4693) and 2 mg/mL Collagenase IV (Worthington, #LS004188) in DMEM media (Corning, #10-013-CV), with 2% FBS (Corning, #35-010-CV) and 5% P/S (Corning, #30-002-CV). The tissue was then nutated in an incubator at 37°C for 20 min. Cells were then triturated with a serological pipette, allowed to settle by sedimentation, and the supernatant was passed through a 40 μm filter into a fresh sterile collection tube. The collection tube was placed on ice, and fresh digestion buffer was added to the heart pieces to repeat the process for two additional digestions. Following the third digestion, cooled samples were centrifuged at 4°C for 20 min at 350 x g to pellet cells. The supernatant was poured off from the tubes, and fibroblasts were resuspended in 37°C 10% FBS 1% P/S DMEM media. Cells were then plated and stored in a 37°C 5% CO2 incubator for 2 hours while fibroblasts became attached to the dish. Media was then carefully aspirated and washed with warm serum-free DMEM media twice. Following the final wash step, cells were incubated in 1% FBS 1% P/S DMEM media in the 37°C 5% CO_2 incubator.

PDMS coverslip creation

PDMS-coated coverslip generation was performed as previously described (Goldsmith et al., 2024). In brief, 10 g Sylgard 184 (Krayden Dow, #NC9285739) base was mixed with 1 g Sylgard 184 curing agent in a plastic cup, stirring vigorously for 5 minutes with a plastic scraper. The mixture was then placed in a vacuum desiccator for 10 minutes. Meanwhile, 6 g each of Sylgard 527 (Krayden Dow, #NC1208196) A and B were mixed in a separate plastic cup, again stirring vigorously for 5 min with a plastic scraper. Sylgard 184 and 527 solutions were then mixed by adding 102 mg Sylgard 184 to a 50 mL conical, then adding 9.9 g Sylgard 527. The 50 mL conical containing both solutions was then thoroughly mixed by 5 sets of 10 sec vortexing

followed by orbitally tilting the tube and rolling the Sylgard mixture around the interior of the tube for 10 sec. The solution was centrifuged for 3 min at 3200 x g and vortexed again briefly, tilting the tube in different directions. 14 µL of the solution was then pipetted onto 12 mm glass coverslips (Electron Microscopy Sciences, #72230-01), degassed in a vacuum desiccator for 30 min, then cured at 50°C overnight.

Cell culture/transductions

Wild type and *Zdhhc3* KO mouse embryonic fibroblasts (MEFs) immortalized with SV40 lentivirus were obtained as gifts from Jeff Molkentin (Cincinnati Childrens Hospital). MEFs were plated in 10% FBS 1% P/S DMEM media and incubated in the 37°C 5% CO_2 incubator until ~80% confluency was achieved, and then harvested or split into new dishes. Primary *Zdhhc3* fl/fl ACFs were plated at ~30% confluency in 1% FBS DMEM media, and immediately transduced overnight with either pLpA empty vector control adenovirus (Ad-pLpA) (University of Michigan Vector Core) for control (Ctrl) conditions or with Cre adenovirus (Ad-Cre) (University of Michigan Vector Core) to achieve *Zdhhc3* KO. Following transductions, P0 ACFs were washed three times with warm serum-free DMEM and were cultured in 1% FBS DMEM media with 1% P/S for all other treatment conditions. For fibrotic gene expression and αSMA expression experiments, cells were incubated for an additional 24 hours following the Ad-Cre wash before beginning a 72-hour treatment time course of either saline or 10 ng/mL TGFβ1 (Peprotech, #100-21).

mRNA isolation and real-time PCR

For gene expression experiments, whole RNA samples were extracted from cardiac samples using the corresponding RNeasy kit (Qiagen), depending on the sample type. ACF samples intended for RNA extraction were aspirated to remove media, then washed twice with

room temperature nuclease-free water. RNeasy Micro Kit (Qiagen, #74004) lysis buffer was added directly to experimental wells, and RNA was extracted according to the manufacturer's protocol. For cardiac ventricle samples, heart tissue was placed in a nuclease-free tube before adding the appropriate volume of RNeasy Mini Kit (Qiagen, #74104) lysis buffer to the tube. Metal beads of equal volume to the sample were added to the tube, and samples were run at full power in a bead homogenizer for 5 min. RNA was then extracted from homogenized samples according to the manufacturer's protocol. Samples were then quantified and assessed for quality with a Nanodrop. Prior to cDNA synthesis, samples were treated with DNase (Promega, #M6101) for 30 min to remove any remaining genomic DNA present in the sample. cDNA synthesis was performed using the High-Capacity cDNA Reverse Transcription Kit (Applied Biosystems, #4368814). mRNA levels were then quantified via RTqPCR using Power SYBR Green (Applied Biosystems, #4367659) reagent and gene-specific primers (total reaction volume 15 µl). RTqPCR was performed using a QuantStudio 7 Flex (Applied Biosystems). Primer sequences for all genes used in these experiments: *Zdhhc3* For 5'-TGCCCAAAGGAAATGCCAC-3', Rev 5'-CGAATGCACCGCTTACAAAC-3'; *Postn* For 5'-CTGCTTCAGGGAGACACACC-3', Rev 5'-TCTGGCCTCTGGGTTTTCAC*TCF21; Col1a1* For 5'- CGATGGATTCCCGTTCGAGT-3', Rev 5'- GAGGCCTCGGTGGACATTAG-3'; *Nox4* For 5'- CCAAATGTTGGGCGATTGTGT-3', Rev 5'- CAGGACTGTCCGGCACATAG-3'; *Thbs4* For 5'- TGTGCGCTGTGTGAATTTGG-3', Rev 5'-CAACATCAGTGCACACCTGC-3'; *Tcf21* For 5'- CCAACTGTACTTACCGATTCT-3', Rev 5'-ACACATTGATAGGCTCTTCTTAT-3'.

Scratch assay

Primary ACFs plated in 24-well dishes were transduced as described previously and cultured in 1% FBS 1% P/S DMEM media until confluent, changing media every 2 days. Upon confluency, a P20 pipette tip was used to manually scratch across the center of each well. Images of the scratch were taken on a Celigo Image Cytometer (Model 200-BFFL-5C) immediately after the scratch, then 24-hours post-scratch. Surface area of the scratch was quantified via ImageJ (NIH).

Immunocytochemistry and immunohistochemistry

Following experimental treatments, samples to be immunostained were washed twice with PBS and fixed for 20 min with 100% ice-cold methanol in a 4°C ambient environment. Following fixation, samples were blocked with ICC buffer (phosphate buffered saline (PBS), 5% goat serum, 1% bovine serum albumin (BSA), 1% glycine, 0.2% triton X-100) for 1 hour at room temperature. Blocking solution was removed, and respective primary antibody solutions diluted in blocking solution were applied to the samples to incubate at 4°C overnight. Following primary incubation, samples were washed with PBS three times for 5 min. Alexa Flour Secondary antibody solutions (Invitrogen) diluted in ICC buffer (1:1000) were then applied to the samples to incubate at room temperature for 1 hour. Samples were then washed again with PBS three times for 5 minutes. Stained coverslips were then mounted with ProLong Gold with DAPI (Invitrogen, #P36931). Images were taken using a Zeiss LSM 880 confocal microscope with 10x, 20x, and 40X objectives. Quantification was performed with ImageJ (NIH). Primary antibodies used in these experiments: anti-zDHHC3 (Abcam, # ab31837) (1:500), anti-GM130 (BD Transduction, #610822) (1:1000), anti-αSMA (Sigma-Aldrich, #A5228) (1:1000).

Picrosirius Red staining of histological sections was performed by personnel at the University of Michigan School of Dentistry Histology Core. Fibrotic area was quantified via ImageJ (NIH). Polarized light images were taken with Nikon Ti2 Widefield microscope with a linearly polarized light filter at the University of Michigan Microscopy Core. Fibrotic area was quantified using Nikon Elements software.

Western blotting

To assess zDHHC3 protein levels, cell pellets were lysed on ice in a urea lysis buffer (50 mM Tris•HCl pH 7.6, 10 mM $Na_4PO_2O_7•10H_2O$, 6 M urea, 10% glycerol, and 2% SDS) master mix containing protease inhibitors and nuclease. Chemically lysed samples were then sonicated and spun down for 8 minutes at 10,000 x g at 4°C, and supernatants were transferred to a new tube. Bradford assay was performed to quantify protein concentrations (BIORAD, #5000116). 80 µg of each sample was then loaded onto SDS-PAGE and subjected to electrophoresis at 90 mV for ~three hours until sufficiently run through the gel. Gels were then transferred to PVDF membranes for 4 hours at 70 mV at 4°C. Following transfer, membranes were blocked at room temperature for 1 hour in 5% dry milk dissolved in TBST (blocking solution). Once finished blocking, primary antibody solutions diluted in blocking solution were added to membranes housed in plastic sleeves and incubated 18-24 hours at 4°C. Membranes were then washed 3 times with TBST for 5 minutes on an orbital shaker, prior to adding secondary antibody (IRDye, LI-COR Biosciences) solutions diluted in blocking solution (1:5,000) for 1 hour at room temperature. At the conclusion of the secondary treatment, membranes were washed three times with TBST, and imaged on an Odyssey CLx imager (LI-COR Biosciences). Primary antibodies used in these experiments: anti-zDHHC3 (Abcam, # ab31837) (1:500), anti-GAPDH (Fitzgerald, #10R-G109A) (1:15,000).

In vivo cardiac injury model

Adult male and female *Postn-MCM +/-* and *Postn-MCM +/-; Zdhhc3* fl/fl mice aged 2-4 months were subjected to transverse aortic constriction (TAC) surgeries to induce cardiac pressure overload (Baldwin et al., 2023). Control mice received sham surgeries. All mice received 75 mg/kg tamoxifen injection (IP) the night prior to surgery, and were fed tamoxifen chow (Envigo, #TD.130860) for the duration of the experimental timeline. Animals were sacrificed after a total of 8-weeks TAC. All surgeries and echocardiography were performed by personnel at the University of Michigan Physiology Phenotyping Core.

Statistical analysis

All statistical analyses were performed using the statistical software package GraphPad Prism (Version 10.0.3). Independent samples t-tests were conducted to compare the means of two groups. A two-way ANOVA was conducted to explore the combinatorial effects of multiple groups, and Tukey's multiple comparisons test was conducted to further investigate significant main effects or interactions. Results were considered statistically significant if $p < 0.05$.

Results

zDHHC3 is expressed in cardiac fibroblasts and localized to the Golgi

In order to measure zDHHC3 expression in CFs, we first performed western blotting on protein lysates generated from NRCMs and NRCFs. Protein levels were comparable between both cell types (Figure 3.1A). Using an immortalized *Zdhhc3* KO MEF cell line (Baldwin et al., 2023), we were able to validate that we were indeed detecting zDHHC3 (Figure 3.1A). Immunocytochemical detection of zDHHC3 was then performed to confirm the expression of zDHHC3 in ACFs (Figure 3.1B). Having established the expression of zDHHC3 in CFs, we confirmed that Cre-induced recombination was occurring in our Ad-Cre treated *Zdhhc3* fl/fl

ACFs by measuring mRNA levels of *Zdhhc3*. ACFs were isolated from *Zdhhc3* fl/fl mice and transduced with either Ad-pLpA or Ad-Cre, and mRNA levels were quantified using RTqPCR (Figure 3.1C). Adenovirally-mediated Cre expression in *Zdhhc3* fl/fl ACFs successfully reduced *Zdhhc3* mRNA levels. We further confirmed *Zdhhc3* KO at the protein level. Westerns were performed using ACF samples from *Zdhhc3* fl/fl mice transduced with either Ad-pLpA or Ad-Cre. *Zdhhc3* KO was successful, as determined by the absence of a band immunoreactive for anti-zDHHC3 (Figure 3.1D).

Having established that *Zdhhc3* is expressed in both NRCFs and ACFs, we wanted to determine where in the cells it was localized. As zDHHC3 is canonically localized to the Golgi (Lu et al., 2012), we tested zDHHC3 localization in NRCFs by co-immunostaining for zDHHC3 and the Golgi-marker GM130 (Figure 3.1E). Signals for zDHHC3 and GM130 were superimposable, confirming that zDHHC3 is localized to the Golgi in NRCFs, as demonstrated by previous literature (Solis et al., 2022).

zDHHC3 is not required for ACF migration or TGFβ1-induced activation

To determine the necessity of zDHHC3 in fibroblast activation, we tested measures of activation at both the protein and transcript levels in Ctrl ACFs and those with *Zdhhc3* KO, treated with either saline or the pro-fibrotic agonist TGFβ1. We hypothesized that deletion of *Zdhhc3* would lead to a reduction in CF activation elicited by TGFβ1 compared to controls. Following the transduction period, Ctrl and *Zdhhc3* KO ACFs were subject to 72 hours of 10 ng/mL TGFβ1 treatment to induce myofibroblast transition. To assess activation, ACFs were fixed and immunostained for α-smooth muscle actin (αSMA), a commonly used marker of activated fibroblasts. Activation was quantified as the percentage of cells positive for αSMA (Figure 3.2A/B). TGFβ1 treatment successfully induced an increase in myofibroblasts at 72

hours in Ctrl ACFs, and *Zdhhc3* KO ACFs displayed comparable levels of activation both under saline and TGFβ1 conditions after the 72-hour treatment time course (Figure 3.2A/B).

To investigate CF activation at the transcript level, we performed the same TGFβ1 treatment time-course as described in the αSMA experiments in both Ctrl and *Zdhhc3* KO groups, and here isolated RNA to perform RT-qPCR and analyze the expression levels of genes associated with myofibroblast differentiation (Figure 3.2C-F). Consistent with αSMA data, TGFβ1 induced an increase in mRNA levels of *Postn*, *Col1a1*, and *Nox4* in Ctrl ACFs, as well as a significant decrease in the quiescent fibroblast marker *Tcf21* (Figure 3.2C-F). At baseline, *Zdhhc3* KO ACFs exhibited comparable levels of *Postn*, *Col1a1*, *Nox4,* and *Tcf21* mRNA levels compared to Ctrls. In response to TGFβ1, *Zdhhc3* KO ACFs responded comparably to Ctrls in terms of activation, with *Postn* levels significantly upregulated (Figure 3.2C). *Tcf21* was also observed to decrease upon TGFβ1 treatment in both Ctrl and *Zdhhc3* KO ACFs (Figure 3.2D). *Zdhhc3* KO ACFs did not exhibit statistically significant increases in *Col1a1* or *Nox4* levels, though no statistically significant differences were observed between genotypes in response to TGFβ1 (Figure 3.2E-F). Given that the migratory ability of fibroblasts is an important component in ACFs response to injury (Souders et al., 2009; Tschumperlin, 2013), we sought to determine the consequences of *Zdhhc3* KO on this metric. To assess this, scratch assays were performed on monolayers of Ctrl and *Zdhhc3* KO ACFs (Figure 3.2G-H). Under control conditions, ACFs without stimulation closed ~50% of the scratch by 24 hours. No differences were seen in the *Zdhhc3* KO ACFs in migratory ability, as at the same time point, the scratch had closed at comparable levels (Figure 3.2G-H).

Zdhhc3 fKO mice exhibit normal responses to TAC-induced cardiac hypertrophy and fibrosis

To characterize the role of zDHHC3 more fully in CF biology, further studies were conducted to assess the consequences of the loss of zDHHC3 in a more physiologic context aside from in vitro systems that do not fully recapitulate the endogenous environment of the heart. To this end, we generated an in vivo system to delete *Zdhhc3* in activated CFs by crossing *Zdhhc3* fl/fl mice with *Postn MCM* +/- mice (Figure 3.3A, top). Using this tamoxifen-inducible model, *Zdhhc3* KO can be achieved specifically in activated CFs (*Zdhhc3* fKO), allowing us to test how the absence of zDHHC3 in these cells influences cardiac fibrosis in a pressure overload injury model (Figure 3.3A, bottom). *Postn-MCM* +/- (Ctrl) and *Zdhhc3* fKO mice were subjected to TAC or sham surgeries for the control group, and the resultant pressure overload was allowed to progress over an 8-week time course (Figure 3.3A). Here, we hypothesized that *Zdhhc3* fKO mice would exhibit improvements in cardiac functional metrics, in addition to reductions in hypertrophy and fibrosis in the heart.

Following eight weeks of TAC, no differences in body weight were observed between mice in the sham and TAC groups or either genotype (Figure 3.3B). Heart weight-to-body-weight ratios were comparably increased in both Ctrl and *Zdhhc3* fKO animals in response to TAC (Figure 3.3C). Prior to animal sacrifice, animals were subject to echocardiography to assess cardiac function (Figure 3.3D-H). Further assessing hypertrophy, cardiac mass as estimated by echocardiography, and posterior wall thickness, measures were significantly increased in response to TAC in both genotypes compared to sham animals, with no differences seen between genotypes (Figure 3.3D/E). Left ventricular pump function as measured by ejection fraction was comparably reduced in response to TAC in both Ctrl and *Zdhhc3* fKO groups, though no

statistically significant differences were observed between genotypes (Figure 3.3F). No changes to ventricular dilation were observed between any group in measures of left ventricular end diameter diastole (LVED diastole) (Bostan et al., 2014). Left ventricular end diameter systole (LVED systole) was increased in response to TAC in both genotypes, with no differences observed in dilation between genotypes. Ventricular fibrosis was assessed by quantifying Picrosirius Red Staining of collagen on histological cardiac sections in both brightfield and with polarized light (Figure 3.3I-K). In response to TAC, Ctrl mice did not exhibit a statistically significant increase in fibrosis (Figure 3.3I-K). *Zdhhc3* fKO exhibited comparable levels of fibrosis in response to TAC compared to Ctrl (Figure 3.3J/K). Analysis of mRNA levels of pro-fibrotic genes yielded consistent results, with no significant differences found between Ctrl and *Zdhhc3* fKO animals despite upward trends in both TAC groups (Figure 3.3L-O).

Discussion

The reversible PTM palmitoylation plays a vital role in regulating the function and localization of signaling proteins in different cell types (Chamberlain & Shipston, 2015; Jiang et al., 2018; Tabaczar et al., 2017). This PTM is mediated by a family of enzymes called S-acyltransferases that reside in a number of intracellular membrane domains, including the plasma membrane, endoplasmic reticulum, and Golgi apparatus (Chamberlain & Shipston, 2015; Jiang et al., 2018; Tabaczar et al., 2017). zDHHC3, a Golgi-localized S-acyltransferase, has been previously linked to the palmitoylation of several proteins involved in pro-fibrotic signaling pathways (Navarro-Lérida et al., 2012; Tsutsumi et al., 2009; Zhang et al., 2020). Combined with recent work demonstrating that zDHHC3 palmitoylates Rac1 (Baldwin et al., 2023), a protein known to play an important role in fibroblast activation and migration, these findings have raised questions about whether zDHHC3-mediated palmitoylation might similarly govern pro-fibrotic

processes in CFs. At present, though, the role of palmitoylation in the regulation of CF signaling is poorly understood. These studies aimed to address this knowledge gap by investigating the specific role of zDHHC3 in CF activation and fibrosis using both in vitro and in vivo models.

Upon the completion of these analyses, zDHHC3-mediated palmitoylation does not appear to be a crucial regulatory mechanism in the transition of quiescent CFs to myofibroblasts in response to TGFβ1. Despite its role in pro-fibrotic signaling pathways in other cell types, the *Zdhhc3* gene-deleted CFs had no obvious effect on the expression of activated fibroblast markers such as αSMA in response to TGFβ1, or mRNA levels of common activated fibroblast marker genes. Migration of ACFs in vitro was similarly unaffected by the deletion of *Zdhhc3*. Further, *Zdhhc3* fKO mice subjected to pressure overload did not exhibit the hypothesized reduction of hypertrophy or fibrotic remodeling compared to Ctrl.

Given the lack of a phenotypic shift in CF activation or fibrosis with loss of *Zdhhc3*, it appears that palmitoylation mediated by zDHHC3 may not be essential for TGFβ1-induced CF activation and pressure overload-induced fibrosis. In attempting to explain these results, our primary hypothesis is that zDHHC3 is likely not the sole S-acyltransferase involved in regulating pro-fibrotic protein signaling. It has been demonstrated previously that S-acyltransferases can maintain overlapping substrate profiles (Chamberlain & Shipston, 2015; Roth et al., 2006), thus, it is possible that other zDHHCs may be compensating for the loss of zDHHC3 in CFs, leading to a sustained level of palmitoylation of pro-fibrotic signaling proteins even in the absence of zDHHC3. zDHHC7 has been demonstrated by multiple groups to palmitoylate common substrates with zDHHC3 (Abrami et al., 2021; Baldwin et al., 2023; Lievens et al., 2016; Tsutsumi et al., 2009; Zhang et al., 2020), and thus it is possible that zDHHC7 may be

compensating for the loss of zDHHC3 and contributing to the fibrotic response observed, necessitating future investigation.

An alternative explanation is that the deletion of *Zdhhc3* is indeed resulting in alterations in signal transduction within these cells, but simply due to the complex interplay amongst the many pro-fibrotic pathways being carried out by a number of key cell types, the changes to the palmitoylation state of certain zDHHC3 substrates in CFs is insufficient to abrogate the fibrotic response. In the context of the development of cardiac remodeling and fibrosis, CFs are only one of many key cell types; CFs interact with cardiomyocytes, immune cells, endothelial cells, etc. (Hara & Tallquist, 2023; Kumar et al., 2019; Major & McKinsey, 2019; Yang et al., 2023; Zhao et al., 2021), and these interactions may involve distinct regulatory pathways that are less reliant on zDHHC3-mediated palmitoylation. Additionally, while TGFβ1-induced activation does not appear to be majorly dependent on palmitoylation, it remains a possibility that other agonists involved in fibroblast activation may be more reliant on signaling regulated by zDHHC3, necessitating further research.

Our study highlights the cell type-specific nature of zDHHC3 activity in regulating fibrotic signaling. While zDHHC3-mediated palmitoylation may be a key regulator of pro-fibrotic signaling proteins in certain cell types, it appears to be dispensable for CF activation and fibrosis in vivo. These findings broaden our understanding of the cell type-specific regulation of fibrosis, but also raise several questions for further work. Future research aims to investigate other S-acyltransferase enzymes that may prove to be more essential for pro-fibrotic CF signaling. Further, additional efforts are necessary to identify protein substrates whose palmitoylation state changes during the transition from quiescent to activated fibroblast. Identifying these key enzymes will offer insights into how palmitoylation influences distinct

regulatory networks in CFs. Further exploration in this area has the potential to pave the way for more targeted and effective future strategies for the treatment of cardiac fibrosis.

Chapter III Figures

Figure 3.1. zDHHC3 is expressed in cardiac fibroblasts and localized to the Golgi

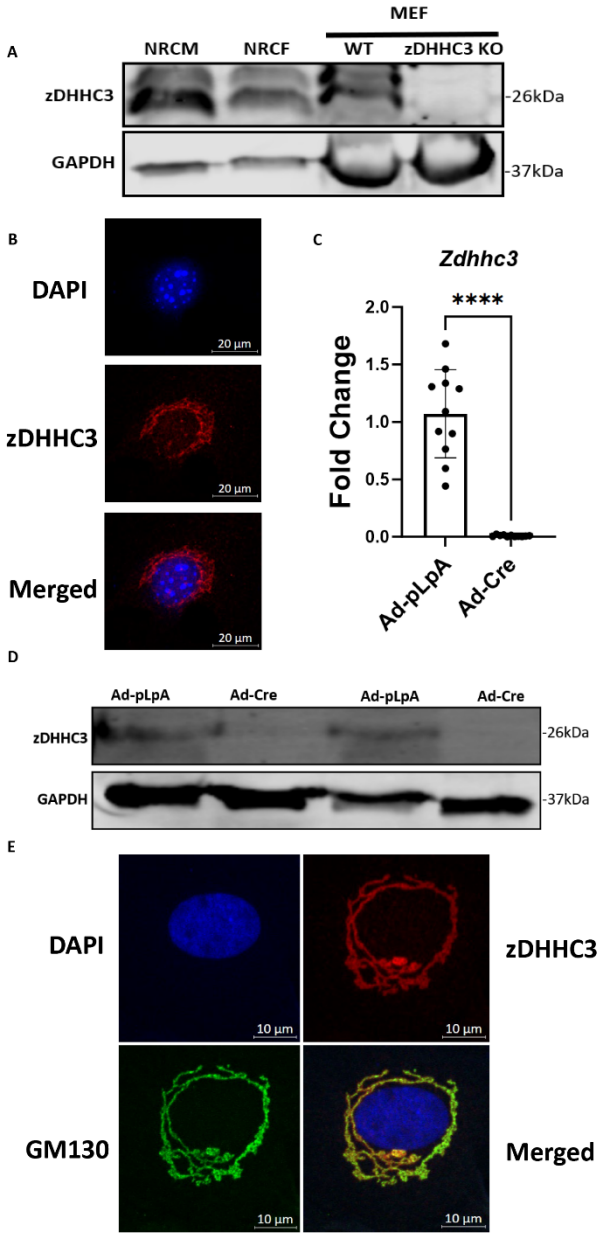

Figure 3.1: zDHHC3 is expressed in cardiac fibroblasts and localized to the Golgi. *(A) Confirmation of expression of zDHHC3 in cardiac fibroblasts (neonatal rat) via western blot. Protein samples from neonatal rat cardiomyocytes (NRCMs), neonatal rat cardiac fibroblasts (NRCFs), and immortalized WT and Zdhhc3 KO MEFs were assessed for levels of zDHHC3. (B) Immunocytochemical confirmation of zDHHC3 expression in adult mouse cardiac fibroblasts. Scale bar represents 20 µm. (C) Confirmation of Zdhhc3 KO in Zdhhc3 fl/fl ACFs treated with Ad-Cre measured by RTqPCR. mRNA levels normalized to housekeeping genes 18S,GAPDH. Primary ACFs from Zdhhc3 fl/fl mice were transduced with either Ad-pLpA or Ad-Cre to induce recombination, n=11. Students T-test (p<.0001), (D) confirmation of Zdhhc3 KO in ACF's via western blot. Zdhhc3 fl/fl ACFs transduced with either Ad-pLpA or Ad-Cre were assessed for protein levels of zDHHC3, (E) Immunocytochemical confirmation of DHHC3 localization to the Golgi apparatus in NRCFs. Scale bar represents 10 µm.*

Figure 3.2. zDHHC3 is not required for ACF migration or TGFβ1-induced activation

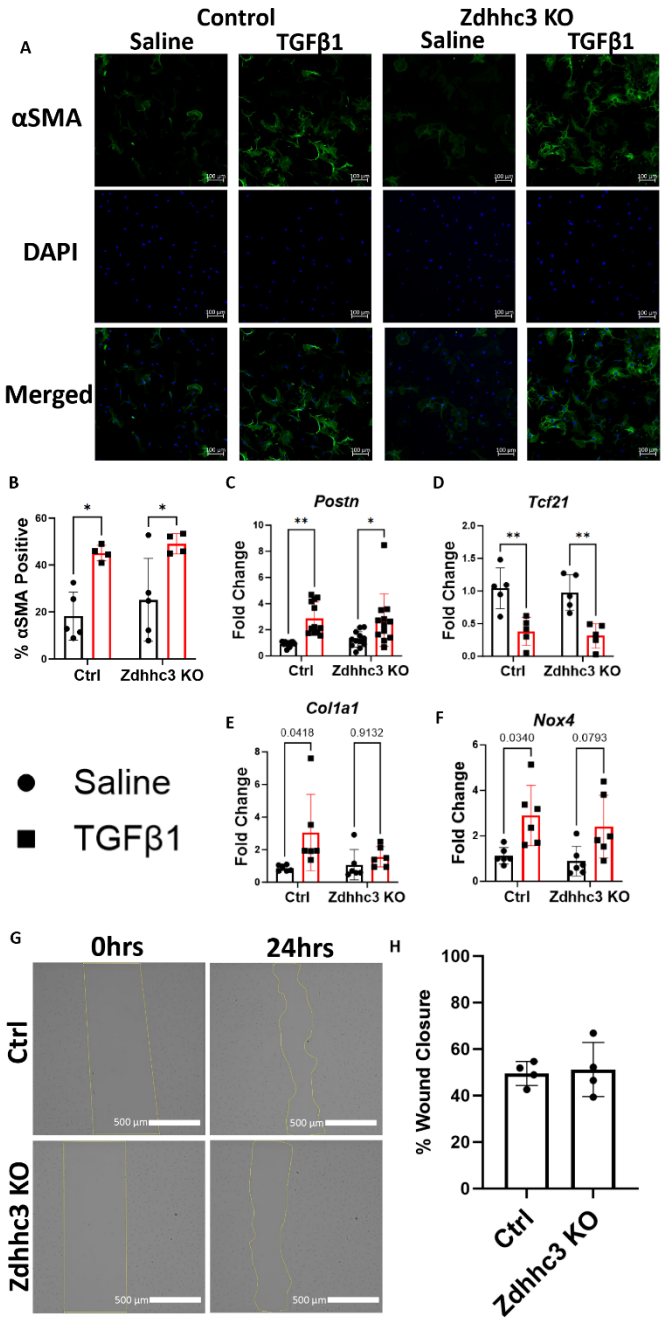

Figure 3.2: zDHHC3 is not required for ACF migration or TGFβ1-induced activation. *(A) Representative images of α-smooth muscle actin positivity (αSMA+) assay in Zdhhc3 fl/fl ACFs treated with Ad-pLpA (Ctrl) or Ad-Cre (Zdhhc3 KO) and saline or TGFβ1 (10 ng/ml, 72 hours). Scale bar represents 100 μm. (B) quantification of αSMA+ cells via ImageJ, n=4-5. Two-way ANOVA with Tukey's multiple comparisons test, Drug Treatment (p=.0003), Interaction (p=.79), (C-F) mRNA level quantification of various pro-fibrotic genes in Ctrl or Zdhhc3 KO ACFs treated with or without TGFβ (10 ng/ml, 72 hours), n=5-12. Two-way ANOVA with Tukey's multiple comparisons test; Postn Drug Treatment (p=<.0001), Interaction (p=.48), Tcf21 Drug Treatment (p=<.0001), Interaction (p=.98), Col1a1 Drug Treatment (p=.021), Interaction (p=.130), Nox4 Drug Treatment (p= .0008), Interaction (p=.77). (G) Representative images of scratch assay at 0 and 24 hours in primary Ctrl or Zdhhc3 KO ACFs, (H) Quantification of scratch area via ImageJ, n=5. Students T-test (p=.85). Scale bar represents 500 μm. Error bars indicate the mean +/- standard deviation, significance denoted as (p<0.05, *), (p<0.01, **), (p<.001, ***).*

Figure 3.3. *Zdhhc3* fKO mice exhibit normal responses to TAC-induced cardiac hypertrophy and fibrosis

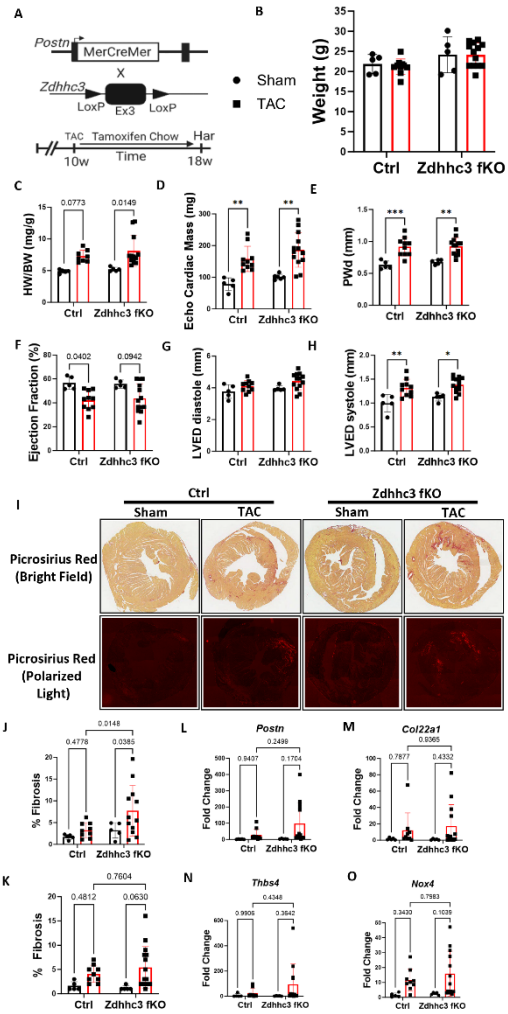

Figure 3.3: Zdhhc3 fKO mice exhibit normal responses to TAC-induced cardiac hypertrophy and fibrosis. *(A) Schematic of experimental design, (B) final weights at 8-weeks post-TAC. Two-way ANOVA with Tukey's multiple comparisons. Injury Model Condition (p=.765), Interaction (p=.78), (C) heart-weight to body-weight ratios (mg/g) of the indicated mice, n=5-13. Two-way ANOVA with Tukey's multiple comparisons test. Injury Model Condition (p=.0004), Interaction (p=.71). Echocardiography was performed on Ctrl Sham (n=5), Ctrl TAC (n=10), Zdhhc3 fKO Sham (n=5), and Zdhhc3 fKO TAC mice (n=13) to measure changes in cardiac function 8-weeks post-surgery. (D-H), echocardiographic measurement of (D) uncorrected cardiac mass (mg), Two-way ANOVA with Tukey's multiple comparisons test. Injury Model Condition (p=<.0001), Interaction (p=.87). (E) posterior wall thickness diastole (mm), Two-way ANOVA with Tukey's multiple comparisons test. Injury Model Condition (p=<.0001), Interaction (p=.69). (F) ejection fraction (%), Two-way ANOVA with Tukey's multiple comparisons test. Injury Model Condition (p=.0009), Interaction (p=.73). (G) left ventricular end diameter diastole (mm), Two-way ANOVA with Tukey's multiple comparisons test. Injury Model Condition (p=.023), Interaction (p=.76). (H) left ventricular end diameter systole (mm), Two-way ANOVA with Tukey's multiple comparisons test. Injury Model Condition (p<.0001), Interaction (p=.59). (I,top) Representative brightfield images of histological sections stained with Picrosirius red and to assess fibrosis.(I,bottom) Representative polarized light images of histological sections stained with Picrosirius Red to assess fibrosis (J) Quantification of fibrosis from brightfield images of Picrosirius red stained sections (%) via ImageJ. Two-way ANOVA with Tukey's multiple comparisons test. Injury Model Condition (p=.053), Interaction (p=.34). (K) Quantification of fibrosis from polarized light images of Picrosirius red stained sections (%) via Nikon NIS elements imaging software. Two-way ANOVA with Tukey's multiple comparisons test. Injury Model Condition (p=.008), Interaction (p=.48). (L-O), fibrotic gene expression measurements (fold change) via RTqPCR. Two-way ANOVA with Tukey's multiple comparisons test; Postn Injury Model Condition (p=.07), Interaction (p=.31), Col22a1 Injury Model Condition (p=.09), Interaction (.71), Thbs4 Injury Model Condition (p=.19), Interaction (p=.36), Nox4 Injury Model Condition (p=.008), Interaction (p=.69). Error bars indicate the mean +/- standard deviation, significance denoted as (p<0.05, *), (p<0.01, **), (p<.001, ***).*

References

Abrami, L., Audagnotto, M., Ho, S., Marcaida, M. J., Mesquita, F. S., Anwar, M. U., Sandoz, P. A., Fonti, G., Pojer, F., Dal Peraro, M., & van der Goot, F. G. (2021, Apr). Palmitoylated acyl protein thioesterase APT2 deforms membranes to extract substrate acyl chains. Nat Chem Biol, 17(4), 438-447. https://doi.org/10.1038/s41589-021-00753-2

Baldwin, T. A., Teuber, J. P., Kuwabara, Y., Subramani, A., Lin, S. J., Kanisicak, O., Vagnozzi, R. J., Zhang, W., Brody, M. J., & Molkentin, J. D. (2023, Nov 3). Palmitoylation-Dependent Regulation of Cardiomyocyte Rac1 Signaling Activity and Minor Effects on Cardiac Hypertrophy. J Biol Chem, 105426. https://doi.org/10.1016/j.jbc.2023.105426

Bertaud, A., Joshkon, A., Heim, X., Bachelier, R., Bardin, N., Leroyer, A. S., & Blot-Chabaud, M. (2023, Jan 16). Signaling Pathways and Potential Therapeutic Strategies in Cardiac Fibrosis. Int J Mol Sci, 24(2). https://doi.org/10.3390/ijms24021756

Bostan, C., Sinan, U. Y., Canbolat, P., Abaci, O., Munipoglu, S. K., & Kucukoglu, S. (2014, Oct). Factors predicting long-term mortality in patients with hypertrophic cardiomyopathy. Echocardiography, 31(9), 1056-1061. https://doi.org/10.1111/echo.12537

Bretherton, R., Bugg, D., Olszewski, E., & Davis, J. (2020, Sep). Regulators of cardiac fibroblast cell state. Matrix Biol, 91-92, 117-135. https://doi.org/10.1016/j.matbio.2020.04.002

Chamberlain, L. H., & Shipston, M. J. (2015, Apr). The physiology of protein S-acylation. Physiol Rev, 95(2), 341-376. https://doi.org/10.1152/physrev.00032.2014

Cho, E., & Park, M. (2016, Sep). Palmitoylation in Alzheimer's disease and other neurodegenerative diseases. Pharmacol Res, 111, 133-151. https://doi.org/10.1016/j.phrs.2016.06.008

De, I., & Sadhukhan, S. (2018, Jun). Emerging Roles of DHHC-mediated Protein S-palmitoylation in Physiological and Pathophysiological Context. Eur J Cell Biol, 97(5), 319-338. https://doi.org/10.1016/j.ejcb.2018.03.005

Essandoh, K., Philippe, J. M., Jenkins, P. M., & Brody, M. J. (2020). Palmitoylation: A Fatty Regulator of Myocardial Electrophysiology. Front Physiol, 11, 108. https://doi.org/10.3389/fphys.2020.00108

Essandoh, K., Subramani, A., Ferro, O. A., Teuber, J. P., Koripella, S., & Brody, M. J. (2023, May). zDHHC9 Regulates Cardiomyocyte Rab3a Activity and Atrial Natriuretic Peptide Secretion Through Palmitoylation of Rab3gap1. JACC Basic Transl Sci, 8(5), 518-542. https://doi.org/10.1016/j.jacbts.2022.11.003

Frangogiannis, N. G. (2021, May 25). Cardiac fibrosis. Cardiovasc Res, 117(6), 1450-1488. https://doi.org/10.1093/cvr/cvaa324

Fu, X., Khalil, H., Kanisicak, O., Boyer, J. G., Vagnozzi, R. J., Maliken, B. D., Sargent, M. A., Prasad, V., Valiente-Alandi, I., Blaxall, B. C., & Molkentin, J. D. (2018, May 1). Specialized fibroblast differentiated states underlie scar formation in the infarcted mouse heart. J Clin Invest, 128(5), 2127-2143. https://doi.org/10.1172/jci98215

Fu, X., Liu, Q., Li, C., Li, Y., & Wang, L. (2020). Cardiac Fibrosis and Cardiac Fibroblast Lineage-Tracing: Recent Advances. Front Physiol, 11, 416. https://doi.org/10.3389/fphys.2020.00416

Hara, A., & Tallquist, M. D. (2023, Jun). Fibroblast and Immune Cell Cross-Talk in Cardiac Fibrosis. Curr Cardiol Rep, 25(6), 485-493. https://doi.org/10.1007/s11886-023-01877-8

Ivey, M. J., & Tallquist, M. D. (2016, Oct 25). Defining the Cardiac Fibroblast. Circ J, 80(11), 2269-2276. https://doi.org/10.1253/circj.CJ-16-1003

Jiang, H., Zhang, X., Chen, X., Aramsangtienchai, P., Tong, Z., & Lin, H. (2018, Feb 14). Protein Lipidation: Occurrence, Mechanisms, Biological Functions, and Enabling Technologies. Chem Rev, 118(3), 919-988. https://doi.org/10.1021/acs.chemrev.6b00750

Kanisicak, O., Khalil, H., Ivey, M. J., Karch, J., Maliken, B. D., Correll, R. N., Brody, M. J., SC, J. L., Aronow, B. J., Tallquist, M. D., & Molkentin, J. D. (2016, Jul 22). Genetic lineage tracing defines myofibroblast origin and function in the injured heart. Nat Commun, 7, 12260. https://doi.org/10.1038/ncomms12260

Kumar, S., Wang, G., Zheng, N., Cheng, W., Ouyang, K., Lin, H., Liao, Y., & Liu, J. (2019, May). HIMF (Hypoxia-Induced Mitogenic Factor)-IL (Interleukin)-6 Signaling Mediates Cardiomyocyte-Fibroblast Crosstalk to Promote Cardiac Hypertrophy and Fibrosis. Hypertension, 73(5), 1058-1070. https://doi.org/10.1161/hypertensionaha.118.12267

Kunschmann, T., Puder, S., Fischer, T., Steffen, A., Rottner, K., & Mierke, C. T. (2019, May 22). The Small GTPase Rac1 Increases Cell Surface Stiffness and Enhances 3D Migration Into Extracellular Matrices. Sci Rep, 9(1), 7675. https://doi.org/10.1038/s41598-019-43975-0

Landry, N. M., & Dixon, I. M. C. (2020, Dec). Fibroblast mechanosensing, SKI and Hippo signaling and the cardiac fibroblast phenotype: Looking beyond TGF-β. Cell Signal, 76, 109802. https://doi.org/10.1016/j.cellsig.2020.109802

Lievens, P. M., Kuznetsova, T., Kochlamazashvili, G., Cesca, F., Gorinski, N., Galil, D. A., Cherkas, V., Ronkina, N., Lafera, J., Gaestel, M., Ponimaskin, E., & Dityatev, A. (2016, Sep 1). ZDHHC3 Tyrosine Phosphorylation Regulates Neural Cell Adhesion Molecule Palmitoylation. Mol Cell Biol, 36(17), 2208-2225. https://doi.org/10.1128/mcb.00144-16

Liu, S., Kapoor, M., & Leask, A. (2009, May). Rac1 expression by fibroblasts is required for tissue repair in vivo. Am J Pathol, 174(5), 1847-1856. https://doi.org/10.2353/ajpath.2009.080779

Lu, D., Sun, H. Q., Wang, H., Barylko, B., Fukata, Y., Fukata, M., Albanesi, J. P., & Yin, H. L. (2012, Jun 22). Phosphatidylinositol 4-kinase IIα is palmitoylated by Golgi-localized palmitoyltransferases in cholesterol-dependent manner. J Biol Chem, 287(26), 21856-21865. https://doi.org/10.1074/jbc.M112.348094

Main, A., & Fuller, W. (2022, Feb). Protein S-Palmitoylation: advances and challenges in studying a therapeutically important lipid modification. Febs j, 289(4), 861-882. https://doi.org/10.1111/febs.15781

Major, J. L., & McKinsey, T. A. (2019, Apr). Putting the Heat on Cardiac Fibrosis: Hsp20 Regulates Myocyte-To-Fibroblast Crosstalk. JACC Basic Transl Sci, 4(2), 200-203. https://doi.org/10.1016/j.jacbts.2019.03.007

Martínez-López, A., García-Casas, A., Bragado, P., Orimo, A., Castañeda-Saucedo, E., & Castillo-Lluva, S. (2021, Aug 19). Inhibition of RAC1 activity in cancer associated fibroblasts favours breast tumour development through IL-1β upregulation. Cancer Lett, 521, 14-28. https://doi.org/10.1016/j.canlet.2021.08.014

Navarro-Lérida, I., Sánchez-Perales, S., Calvo, M., Rentero, C., Zheng, Y., Enrich, C., & Del Pozo, M. A. (2012, Feb 1). A palmitoylation switch mechanism regulates Rac1 function and membrane organization. Embo j, 31(3), 534-551. https://doi.org/10.1038/emboj.2011.446

Reichardt, I. M., Robeson, K. Z., Regnier, M., & Davis, J. (2021, Mar). Controlling cardiac fibrosis through fibroblast state space modulation. Cell Signal, 79, 109888. https://doi.org/10.1016/j.cellsig.2020.109888

Roth, A. F., Wan, J., Bailey, A. O., Sun, B., Kuchar, J. A., Green, W. N., Phinney, B. S., Yates, J. R., 3rd, & Davis, N. G. (2006, Jun 2). Global analysis of protein palmitoylation in yeast. Cell, 125(5), 1003-1013. https://doi.org/10.1016/j.cell.2006.03.042

Solis, G. P., Kazemzadeh, A., Abrami, L., Valnohova, J., Alvarez, C., van der Goot, F. G., & Katanaev, V. L. (2022, 2022/04/19). Local and substrate-specific S-palmitoylation determines subcellular localization of Gαo. Nature Communications, 13(1), 2072. https://doi.org/10.1038/s41467-022-29685-8

Souders, C. A., Bowers, S. L., & Baudino, T. A. (2009, Dec 4). Cardiac fibroblast: the renaissance cell. Circ Res, 105(12), 1164-1176. https://doi.org/10.1161/circresaha.109.209809

Tabaczar, S., Czogalla, A., Podkalicka, J., Biernatowska, A., & Sikorski, A. F. (2017, Jun). Protein palmitoylation: Palmitoyltransferases and their specificity. Exp Biol Med (Maywood), 242(11), 1150-1157. https://doi.org/10.1177/1535370217707732

Tallquist, M. D., & Molkentin, J. D. (2017, Aug). Redefining the identity of cardiac fibroblasts. Nat Rev Cardiol, 14(8), 484-491. https://doi.org/10.1038/nrcardio.2017.57

Tschumperlin, D. J. (2013, Nov). Fibroblasts and the ground they walk on. Physiology (Bethesda), 28(6), 380-390. https://doi.org/10.1152/physiol.00024.2013

Tsutsumi, R., Fukata, Y., Noritake, J., Iwanaga, T., Perez, F., & Fukata, M. (2009, Jan). Identification of G protein alpha subunit-palmitoylating enzyme. Mol Cell Biol, 29(2), 435-447. https://doi.org/10.1128/mcb.01144-08

Umbarkar, P., Ejantkar, S., Tousif, S., & Lal, H. (2021, Sep 14). Mechanisms of Fibroblast Activation and Myocardial Fibrosis: Lessons Learned from FB-Specific Conditional Mouse Models. Cells, 10(9). https://doi.org/10.3390/cells10092412

Xu, S. W., Liu, S., Eastwood, M., Sonnylal, S., Denton, C. P., Abraham, D. J., & Leask, A. (2009, Oct 13). Rac inhibition reverses the phenotype of fibrotic fibroblasts. PLoS One, 4(10), e7438. https://doi.org/10.1371/journal.pone.0007438

Yang, X., Cheng, K., Wang, L. Y., & Jiang, J. G. (2023, Jul). The role of endothelial cell in cardiac hypertrophy: Focusing on angiogenesis and intercellular crosstalk. Biomed Pharmacother, 163, 114799. https://doi.org/10.1016/j.biopha.2023.114799

Zhang, M., Zhou, L., Xu, Y., Yang, M., Xu, Y., Komaniecki, G. P., Kosciuk, T., Chen, X., Lu, X., Zou, X., Linder, M. E., & Lin, H. (2020, Oct). A STAT3 palmitoylation cycle promotes T(H)17 differentiation and colitis. Nature, 586(7829), 434-439. https://doi.org/10.1038/s41586-020-2799-2

Zhang, Y., Qin, Z., Sun, W., Chu, F., & Zhou, F. (2021). Function of Protein S-Palmitoylation in Immunity and Immune-Related Diseases. Front Immunol, 12, 661202. https://doi.org/10.3389/fimmu.2021.661202

Zhao, J., Chen, Y., Chen, Q., Hong, T., Zhong, Z., He, J., & Ni, C. (2021). Curcumin Ameliorates Cardiac Fibrosis by Regulating Macrophage-Fibroblast Crosstalk via IL18-P-SMAD2/3 Signaling Pathway Inhibition. Front Pharmacol, 12, 784041. https://doi.org/10.3389/fphar.2021.784041

Chapter IV: Enzyme and Substrate-level Analysis of the Role of Palmitoylation in Cardiac Fibroblasts and Fibrosis

Abstract

The dynamic regulation of signaling proteins involved in cardiac fibroblast (CF) activation remains a major area of investigation, though little is known of how palmitoylation, a reversible lipid modification, plays a role in this regulation. From previous investigations into the involvement of S-acyltransferases in pro-fibrotic signaling, we found that *Zdhhc3* KO CFs responded in line with controls to transforming growth factor β 1 (TGFβ1) stimulation in terms of α-smooth muscle actin (αSMA) positivity and fibrotic gene mRNA levels. Further, mice with in vivo *Zdhhc3* KO in activated CFs did not exhibit obvious differences in TAC-induced cardiac remodeling, prompting additional efforts to elucidate critical enzymes/substrates that might prove more essential for CF signaling. The S-acyltransferase zDHHC7 is known to have overlapping substrate profiles with zDHHC3 and is a key regulator of a number of proteins involved in known pro-fibrotic pathways, including G-alpha q ($G\alpha_q$) and STAT3. We hypothesized that zDHHC7 may be a more critical regulator of CF activation or, further, that given the potential for compensatory effects, the simultaneous deletion of both enzymes is required to disrupt signaling pathways critical for CF activation. Taking a substrate-level approach, we also analyzed the role of palmitoylation in the signaling of Ras-related C3 botulinum toxin substrate 1 (Rac1), a small Rho family GTPase with key involvement in fibroblast activity that has been shown to be regulated by palmitoylation in other cell types. To determine the direct impact of palmitoylation on cellular processes without the potential for

compensatory mechanisms, we generated a Cre-inducible palmitoylation-deficient mutant Rac1 knock-in mouse model (Rac1 ConKI). Here, we sought to investigate the role of palmitoylation in CF activation using both the *Zdhhc7* KO and *Zdhhc3/7* KO models, as well as the Rac1 KI model. *Zdhhc7* KO adult cardiac fibroblasts (ACFs) exhibited lower mRNA levels of the pro-fibrotic gene *Postn* in response to TGFβ1, as well as deficits in wound closure compared to controls. In vivo, *Zdhhc7* KO and *Zdhhc3/7* KO mice treated with chronic infusion of angiotensin II/phenylephrine (AngII/PE) responded similarly to controls in their development of fibrosis and changes to pro-fibrotic gene expression and exhibited little to no difference in heart function or hypertrophy. Rac1 KI ACFs displayed a heightened NFAT and SRF transcription factor activity in response to stimulation in vitro, though no changes were seen in terms of migration, or activation at the protein or transcript levels compared to controls.

Introduction

Cardiac fibroblasts (CFs), one of the most abundant cell types in the heart, have become increasingly of interest due to a growing understanding of their role in maintaining cardiac homeostasis (Fu et al., 2018; Kanisicak et al., 2016; Pesce et al., 2023; Tallquist, 2020; Tallquist & Molkentin, 2017). Canonically, CFs are most known for their ability to secrete and regulate collagen deposition/turnover, both in terms of homeostatic extracellular matrix maintenance to provide structure to the heart, as well as in response to cardiac injury towards the formation of protective scarring (Fan et al., 2012; Maruyama & Imanaka-Yoshida, 2022; Souders et al., 2009). Recently, though, advances in genetic lineage tracing have provided strategies for more targeted investigations into CF biology, yielding a more sophisticated understanding of their additional roles in areas such as regulating cardiac inflammation, paracrine signaling, and cardiomyocyte crosstalk (Bretherton et al., 2020; Fu et al., 2020; Kanisicak et al., 2016). Despite these advances,

the signaling pathways that underlie these responses and how they are dynamically regulated to respond in both physiological and pathological contexts remain poorly understood. Thus, additional work is required to elucidate how CF signaling pathways are fine-tuned to produce the complex responses observed in these cells in the heart.

Given the comorbidity of fibrosis with a variety of diseases including hypertension (Díez, 2007; Kuwahara et al., 2004; Narayanan et al., 2023), diabetic cardiomyopathy (Cheng et al., 2023; Russo & Frangogiannis, 2016; Tuleta & Frangogiannis, 2021), and myocardial infarction (Hinderer & Schenke-Layland, 2019; Liang et al., 2019; van den Borne et al., 2010), one of the most central efforts towards investigating these pathways remains increasing our understanding of the signaling responsible for the transition of CF quiescence into their continuum of activation states (Bertaud et al., 2023; Bretherton et al., 2020; Hall et al., 2021; Mazarura et al., 2022). In response to both chemical and mechanical signals related to cardiac injury, CFs transition into the myofibroblast state and upregulate their proliferation, migration, ECM secretion and deposition, and cytokine release (Tallquist, 2020). Most notable of these activation pathways is the signaling mediated by transforming growth factor β 1 (TGFβ1), which binds to transforming growth factor β receptor II (TGFβRII) and initiates the canonical SMAD2/3 signaling cascade directly linked with fibroblast activation and fibrosis (Khalil et al., 2017; Saadat et al., 2020). The well-characterized renin-angiotensin-aldosterone system (RAAS) also plays a major role in CF activation, primarily through angiotensin II (AngII) binding to angiotensin II receptor type 1 (AT1R) (Bertaud et al., 2023; Forrester et al., 2018). AngII binding stimulates the activation, GTP-loading, and release of $G\alpha_q$, resulting in downstream intracellular calcium increases, PKC activation, and pro-fibrotic transcription factor activation (Forrester et al., 2018). Inflammatory signaling also contributes to CF activation, as IL6 binding to the interleukin-6 receptor (IL6R)

activates STAT3, a transcription factor that mediates a pro-fibrotic transcriptional response upon nuclear localization (Meléndez et al., 2010; Mir et al., 2012; Patel et al., 2019). Pathways relying on mechanosensation have also been identified, such as the previously described Hippo/YAP/TAZ axis, as well as stretch-induced activation of AT1R that induces fibroblast activation in response to mechanical stress (Garoffolo et al., 2022; Herum, Choppe, et al., 2017; Herum, Lunde, et al., 2017; Mia et al., 2022; Yatabe et al., 2009). These responses can be critical in cases of myocardial infarction/wound healing; however, chronic activation of CFs can lead to maladaptive accumulation of ECM components and the development of cardiac fibrosis (Frangogiannis, 2021; Kong et al., 2014), stressing the need for additional investigations to better our understanding of the underlying signaling.

One promising area in relation to the cellular regulation of CF signaling proteins is the role of post-translational modifications (PTMs). Palmitoylation, a reversible PTM mediated by a family of enzymes called S-acyltransferases, involves the attachment of a fatty acid chain to a cysteine residue of a substrate protein (Jiang et al., 2018; Tabaczar et al., 2017). Consequently, the attachment of this lipophilic group can influence protein stability, protein-protein interactions, and most commonly, targeted localization to different membrane domains within the cell (Jiang et al., 2018; Tabaczar et al., 2017). Notably, palmitoylation-mediated signaling has been demonstrated to play critical roles in a number of diseases (De & Sadhukhan, 2018; Main & Fuller, 2022), including cancer (Li et al., 2023; Zhou et al., 2023), neurological disorders (Cho & Park, 2016), and immunological disorders (Zhang et al., 2020; Zhang et al., 2021). Additionally, novel roles for palmitoylation in the heart have emerged in the regulation of cardiomyocyte ion channel physiology, hypertrophy, as well as Rab3a-mediated ANP release (Baldwin et al., 2023; Essandoh et al., 2020; Essandoh et al., 2023). Though, the role of

palmitoylation in regulating CF pro-fibrotic signaling remains unexplored, stressing the need for additional work in this area.

As part of efforts to explore the contribution of palmitoylation in CF signaling, previous work in our lab investigated the role of the Golgi-localized S-acyltransferase zDHHC3 in CF activation and fibrosis. Despite evidence for zDHHC3 regulating pro-fibrotic signaling pathways in other cell types, *Zdhhc3* deletion had no obvious effect on murine adult CF activation in response to TGFβ1, unstimulated migration, or the development of pressure overload-induced fibrosis in vivo. These results indicate that zDHHC3 may be dispensable in the regulation of CF activation and migration or, alternatively, that the compensatory activity of other S-acyltransferases may be enough to maintain the palmitoylation-mediated activity of affected substrates in the absence of zDHHC3. Though, further work is required to analyze more thoroughly the role of S-acyltransferases in CFs, and how palmitoylation may be regulating substrates critical for the fibrotic process.

zDHHC7 represents a promising candidate for additional investigation, given its demonstrated importance in modifying fibrotic-related signaling in other cell types, as well as its overlapping substrate profile with zDHHC3. Notably, zDHHC7-mediated palmitoylation cycling was recently shown to play an essential role in regulating the transcription factor signal transducer and activator of transcription 3 (STAT3) (Zhang et al., 2020). zDHHC3-mediated palmitoylation of STAT3 directs its phosphorylation through targeted plasma membrane localization in HEK293T cells, a second PTM critical for its activity in the nucleus (Zhang et al., 2020). STAT3 is well documented in the integration of a number of pro-fibrotic pathways in multiple cell types (Chakraborty et al., 2017; Kasembeli et al., 2018), though it is unknown how zDHHC7 may play a role in regulating STAT3 activity in CFs. Further, $G\alpha_q$ has also been shown

to be palmitoylated by zDHHC7 (Tsutsumi et al., 2009), and knockdown of *Zdhhc3* or *Zdhhc7* results in decreased plasma membrane localization of $G\alpha_q$. $G\alpha_q$ is known to mediate signaling cascades downstream of multiple receptors, including AT1R (Ohtsu et al., 2008), the adenosine A2B receptor (Alter et al., 2023), and α1 adrenergic receptors (Wang et al., 2016), many of which have been implicated in maladaptive cardiac remodeling, though how palmitoylation may be modulating these pathways underlying CF activation remains unknown.

Finally, we assessed the effects of individual pro-fibrotic substrate palmitoylation deficiency on cardiac fibroblast activation, as compensatory effects present in enzyme deletion strategies are eliminated. To this end, previous literature has demonstrated palmitoylation at cysteine 178 (C178) to be essential for the activation and localization of the small-GTPase Ras-related C3 botulinum toxin substrate 1 (Rac1) (Navarro-Lérida et al., 2012). Given the established role of Rac1 in fibroblast activation and migration (Kunschmann et al., 2019; Lavall et al., 2017; Liu et al., 2009; Lyu et al., 2021; Ma et al., 2023; Martínez-López et al., 2021), we have developed an inducible Rac1 conditional knock-in C178S palmitoylation-deficient mutant (Rac1 ConKI) mouse line, which provides an additional avenue to explore the role of palmitoylation in CFs.

Here, we sought to further characterize the role of palmitoylation in CF biology at both the enzyme and the substrate level in vitro and in vivo. Using a *Zdhhc7* KO mouse model, the dependence of zDHHC7 towards CF activation and migration was assessed in vitro. In vivo, *Zdhhc7* KO mice were also assessed for changes to cardiac remodeling in response to a chronic angiotensin II/phenylephrine (AngII/PE) infusion injury model. Concurrently, these experiments were performed with using our *Zdhhc3/7* double KO model, providing an avenue to investigate compensatory activity from either of the respective enzymes. In vitro activation, migration, and

transcription factor activity experiments were similarly conducted using ACFs from Rac1 ConKI mice to investigate the role of palmitoylation in CF biology at the substrate level. Together, these experiments aimed to provide a greater understanding of how palmitoylation may be involved in the signaling pathways underlying CF activation and fibrosis.

Methods

Animal models

C57B/6J (WT) mice were obtained from Jackson Laboratory (Strain #:000664). *Zdhhc3* fl/fl mice (C57B/6J background) (Baldwin et al., 2023) were crossed with *Postn-MCM +/-* mice (C57B/6J background) (Kanisicak et al., 2016) (Jacksons Labs, Strain #:029645) to generate tamoxifen-inducible activated CF-specific *Zdhhc3* KO animals. Whole body *Zdhhc7* -/- (C57B/6J background) (*Zdhhc7* KO) mice were also used (Hohoff et al., 2019) as previously described. *Zdhhc3* fl/fl mice were crossed with *Zdhhc7* KO mice to generate *Zdhhc3* fl/fl; *Zdhhc7* KO mice for use in in vitro experiments. *Zdhhc3* fl/fl; *Zdhhc7* KO were crossed with *Postn-MCM +/-* mice to generate a tamoxifen-inducible activated CF-specific *Zdhhc3* KO; *Zdhhc7* KO model (*Zdhhc3/7* KO). *Zdhhc17* fl/fl mice (FVB background) (Sanders et al., 2016) were obtained from Michael Hayden (Temple University). A Cre-inducible palmitoylation-deficient cysteine 178 to serine (C178S) Rac1 mutant knock-in mouse model was developed (C57B/6J background) by gene targeting using a mini gene strategy (Ozgene). Upon Cre-mediated excision, the wildtype Rac1 sequence is replaced with the C178S sequence, thus expressing Rac1 from the endogenous Rac1 locus. All animal procedures were approved by the Institutional Animal Care and Use Committee at the University of Michigan (IACUC protocol #PRO00009098) and were in accordance with the Guide for the Care and Use of Laboratory Animals (National Institutes of Health).

Cardiac fibroblast isolation

Adult CF isolation protocol was adapted from (Kanisicak et al., 2016). In brief, hearts were removed and minced into 8-10 pieces before being placed in a microfuge tube containing enzymatic digestion buffer made with 1.2 U/mL Dispase II (Sigma, #D4693) and 2 mg/mL Collagenase IV (Worthington, #LS004188) in Dulbecco's Modified Eagle Medium (DMEM) media (Corning, #10-013-CV), with 2% fetal bovine serum (FBS) (Corning, #35-010-CV) and 5% penicillin/streptomycin (P/S) (Corning, #30-002-CV). Tissue in the enzyme solution was then nutated in an incubator at 37°C for 20 min. Tissue solution/cell suspension were then triturated with a serological pipette, allowed to settle by sedimentation, and the supernatant was passed through a 40 μm filter into a fresh sterile collection tube. Collection tube was placed on ice, and fresh digestion buffer was added to heart pieces to repeat the process for two additional digestions. Following the third digestion, cooled samples were centrifuged at 4°C for 20 min at 350 x g to pellet cells. Supernatant was poured off from the tubes, and fibroblasts were resuspended in 37°C 10% FBS 1% P/S DMEM media. Cells were then plated and stored in 37°C 5% CO_2 incubator for 2 hours while fibroblasts attached to the dish. Media was then carefully aspirated and washed with warm serum-free DMEM media twice. Following the final wash step, cells were incubated in 1% FBS, 1% P/S DMEM media in the 37°C 5% CO_2 incubator.

PDMS coverslip creation

PDMS-coated coverslip generation was performed as previously described (Goldsmith et al., 2024). In brief, 10 g Sylgard 184 (Krayden Dow, #NC9285739) base was mixed with 1 g Sylgard 184 curing agent in a plastic cup, stirring vigorously for 5 minutes with a plastic scraper. Mixture was then placed in a vacuum desiccator for 10 minutes. Meanwhile, 6 g each of Sylgard 527 (Krayden Dow, #NC1208196) A and B were mixed in a separate plastic cup, again stirring

vigorously for 5 min with a plastic scraper. Sylgard 184 and 527 solutions were then mixed by adding 102 mg Sylgard 184 to a 50 mL conical, then adding 9.9 g Sylgard 527. The 50 mL conical containing both solutions was then thoroughly mixed by 5 sets of 10 sec vortexing followed by orbitally tilting the tube and rolling the Sylgard mixture around the interior of the tube for 10 sec. Solution was centrifuged for 3 min at 3200 x g, and vortexed again briefly, tilting the tube in different directions. 14 μL of the solution was then pipetted onto 12 mm glass coverslips (Electron Microscopy Sciences, #72230-01), degassed in vacuum desiccator for 30 min, then cured at 50°C overnight.

Cell culture/transductions

Primary ACFs were plated at ~30% confluency in 1% FBS DMEM media, and immediately transduced overnight with either pLpA empty vector control adenovirus (Ad-pLpA) (University of Michigan Vector Core) or Cre adenovirus (Ad-Cre) (University of Michigan Vector Core) overnight. Following transductions, P0 ACFs were washed three times with warm serum-free DMEM and cultured in 1% FBS DMEM media with 1% P/S for all other treatment conditions. For fibrotic gene expression and αSMA expression experiments, cells were incubated for an additional 24 hours following the wash-off of Ad-Cre before beginning a 72-hour treatment time course of either saline or 10 ng/mL TGFβ1 (Peprotech, #100-21). For luciferase assays, immediately following the overnight transduction with Cre adenovirus, cells were washed three times with warm serum-free DMEM media, and then transduced again overnight in 1% FBS DMEM media containing respective luciferase construct adenoviruses (Ad-Luc) (Ad-NFAT-Luc, Ad-NFκB-Luc, Ad-SRE-Luc) as described previously (Liu et al., 2012; Smith et al., 2017). Following both transduction steps, samples were stimulated with respective agonists (TGFβ1 or 20% FBS) in 1% FBS 1% P/S DMEM for 48 hours. After treatments, samples were

harvested according to the manufacturer's protocol using the Promega Luciferase Assay System (#E4550), and luminescence was measured with a Varioskan LUX Multimode Microplate Reader (#VL0000D0).

mRNA isolation and real-time PCR

For gene expression experiments, whole RNA samples were extracted from cardiac samples using the corresponding RNeasy kit (Qiagen), depending on the sample type. ACF samples intended for RNA extraction were aspirated to remove media, then washed twice with room temperature nuclease-free water. RNeasy Micro Kit (Qiagen, #74004) lysis buffer was added directly to experimental wells, and RNA was extracted according to manufacturer's protocol. For cardiac ventricle samples, heart tissue was placed in a nuclease-free tube before adding the appropriate volume of RNeasy Mini Kit (Qiagen, #74104) lysis buffer to the tube. Metal beads of equal volume to the sample were added to the tube, and samples were run at full power in a bead homogenizer for 5 min. RNA was then extracted from homogenized samples according to manufacturer's protocol. Samples were then quantified and assessed for quality with a Nanodrop. Prior to cDNA synthesis, samples were treated with DNase (Promega, #M6101) for 30 min to remove any remaining genomic DNA present in the sample. cDNA synthesis was performed using the High-Capacity cDNA Reverse Transcription Kit (Applied Biosystems, #4368814). mRNA levels were then quantified via RTqPCR using Power SYBR Green (Applied Biosystems, #4367659) reagent and gene specific primers (total reaction volume 15 µl). RTqPCR was performed using QuantStudio 7 Flex (Applied Biosystems). Primer sequences for all genes used in these experiments: *Postn* For 5'-CTGCTTCAGGGAGACACACC-3', Rev 5'-TCTGGCCTCTGGGTTTTCAC*TCF21; Col1a1* For 5'- CGATGGATTCCCGTTCGAGT-3', Rev 5'- GAGGCCTCGGTGGACATTAG-3'; *Col1a2* For 5'-GATACTTGAAGAATATGAAC-

3’, Rev 5’- AATGCTGAATCTAATGAA-3’; *Nox4* For 5’- CCAAATGTTGGGCGATTGTGT-3’, Rev 5’- CAGGACTGTCCGGCACATAG-3’; *Thbs4* For 5’- TGTGCGCTGTGTGAATTTGG-3’, Rev 5’-CAACATCAGTGCACACCTGC-3’; *Tcf21* For 5’-CCAACTGTACTTACCGATTCT-3’, Rev 5’- ACACATTGATAGGCTCTTCTTAT-3’.

Scratch assay

Primary ACFs were transduced as described previously, and cultured in 24-well dishes in 1% FBS 1% P/S DMEM media until confluent, changing media every 2 days. Upon confluency, a P20 pipette tip was used to manually scratch across the center of each well. Images of the scratch were taken on a Celigo Image Cytometer (Model 200-BFFL-5C) immediately after the scratch and then 24 hours post-scratch. The surface area of the scratch was quantified via ImageJ (NIH).

Immunocytochemistry and immunohistochemistry

Following experimental treatments, samples to be immunostained were washed twice with PBS, and fixed for 20 min with 100% ice-cold methanol in a 4°C ambient environment. Following fixation, samples were blocked with ICC buffer (blocking solution) (PBS, 5% goat serum, 1% BSA, 1% glycine, 0.2% triton X-100) for 1 hour at room temperature. Blocking solution was removed and anti-αSMA (Sigma-Aldrich, #A5228) primary antibody was applied to the samples diluted in blocking solution at a 1:1000 ratio, then incubated at 4°C overnight. Following primary incubation, samples were washed with PBS three times for 5 min. Alexa Flour secondary antibody solutions (Invitrogen) diluted in ICC buffer (1:1000) were then applied to the samples to incubate at room temperature for 1 hour. Samples were then washed again with PBS three times for 5 minutes. Stained coverslips were then mounted with ProLong Gold with

DAPI (Invitrogen, #P36931). Images were taken using a Zeiss LSM 880 confocal microscope with 10x objective. Quantification was performed with ImageJ (NIH).

Picrosirius Red staining of paraffin-embedded histological sections was performed at the University of Michigan School of Dentistry Histology Core. Images of stained sections were acquired at the University of Michigan Digital Pathology Core. The fibrotic area was quantified via ImageJ (NIH).

In vivo cardiac injury model

Adult male and female *Postn-MCM +/-* or WT (Ctrl), *Zdhhc7* KO*,* and *Postn-MCM +/-; Zdhhc3* fl/fl*; Zdhhc7* KO (*Zdhhc3/7* KO) mice aged 2-4 months were implanted with osmotic pumps (Alzet, #1002) containing AngII (1.5 mg/kg/day) (Sigma-Aldrich, #A9525)/PE (50 mg/kg/day) (Sigma-Aldrich, #P6126) to induce fibrosis over a two-week time course. Control mice received saline pumps. To induce loxP-targeted recombination, all mice received 75 mg/kg tamoxifen injection (ip) (Sigma-Aldrich, #T5648) the night prior to surgery, and two additional tamoxifen injections of equivalent doses on days 2 and 4 post-surgery, respectively, for a total of three injections. After a 2-week AngII/PE infusion time course, animals were subjected to echocardiography and immediately sacrificed for sample collection. All surgeries and echocardiography were performed at the University of Michigan Physiology Phenotyping Core.

Statistical analysis

All statistical analyses were performed using the statistical software package GraphPad Prism (Version 10.0.3). Independent samples t-tests were conducted to compare the means of two groups. One-way ANOVA was used to compare differences between groups three or more groups across one independent variable. A two-way ANOVA was conducted to test for significant differences between three or more groups across two dependent variables, as well as for

interaction effects. Tukey's multiple comparisons test was conducted to probe for differences between groups if ANOVA yielded significance. Results were considered statistically significant if $p < 0.05$.

Results

Effects of *Zdhhc7* KO and *Zdhhc3/7* KO on cardiac fibroblast fibrotic gene expression and migration

To determine the dependence of CF pro-fibrotic gene expression on *Zdhhc7* and *Zdhhc3/7,* ACFs were isolated side-by-side from WT mice and *Zdhhc3* fl/fl; *Zdhhc7* KO mice. Cells were cultured and transduced with either control Ad-pLpA or Ad-Cre to compare responses between WT ACFs treated with Ad-pLpA (Ctrl), *Zdhhc3* fl/fl; *Zdhhc7* KO ACFs treated with Ad-pLpA (*Zdhhc7* KO), and *Zdhhc3* fl/fl; *Zdhhc7* KO treated with Ad-Cre (*Zdhhc3/7* KO). Following the transduction period, all genotypes were subject to 72-hour saline or TGFβ1 (10 ng/mL) treatment to induce myofibroblast transition. RNA was isolated to perform RT-qPCR and analyze the expression levels of genes associated with myofibroblast differentiation (Figure 4.1 A-D).

Based upon the previous evidence for the role of zDHHC7 in the regulation of pro-fibrotic effector proteins like STAT3 and $G\alpha_q$, we hypothesized that the deletion of *Zdhhc7* in CFs would result in a blunting of their responses to pro-fibrotic stimuli. Additionally, should the lack of zDHHC7 result in compensation by zDHHC3, we hypothesized that *Zdhhc3/7* KO ACFs would exhibit reductions in activation in response to pro-fibrotic stimuli. In ACFs treated with TGFβ1, all three genotypes exhibited significantly increased expression of the myofibroblast marker *Postn* (Figure 4.1A). Both *Zdhhc7* KO and *Zdhhc3/7* KO ACFs had the same level of baseline *Postn* expression relative to Ctrl, and a significantly reduced *Postn* expression relative

to the increase seen in Ctrl ACFs when treated with TGFβ1. *Tcf21* expression trended downward in Ctrl cells treated with TGFβ1, and no statistically significant differences were observed between genotypes (Figure 4.1B). *Col1a1* displayed an upward trend in response to TGFβ1 (Figure 4.1C) in Ctrl ACFs, though no significant differences were observed between genotypes in either saline or in response to TGFβ1. *Col1a2* remained unchanged in response to TGFβ1 treatment in Ctrl ACFs (Figure 4.1D), but additionally showed a slight downward trend at baseline and with stimulation in *Zdhhc7* and *Zdhhc3/7* KO ACFs.

To further analyze the role of zDHHC3 and zDHHC7 in CF biology, we sought to investigate whether there would be reductions in pro-fibrotic transcription factor activity in *Zdhhc7* KO and *Zdhhc3/7* KO ACFs. Nuclear factor of activated T cells (NFAT) is a key transcription factor in CFs that activates pro-fibrotic transcription in a calcium/calcineurin-dependent manner (Davis et al., 2012; Herum et al., 2013). Similarly, nuclear factor κ B (NFκB) is well established in playing a role in cardiac inflammation and myofibroblast differentiation (Lu et al., 2021; Umbarkar et al., 2021). To this end, ACFs from each genotype were transduced with adenoviral NFAT and NFκB luciferase reporter genes to assess transcription factor activity in the absence of *Zdhhc3* and *Zdhhc7*. Following transduction, ACFs were treated with TGFβ1 for 48 hours, and transcription factor activity was assessed at the conclusion of the treatment period. TGFβ1 treatment induced upward trends in NFAT-Luc activity in all genotypes relative to saline, and no differences were observed between genotypes at baseline or in response to TGFβ1 (Figure 4.1E). No statistically significant differences in NFκB-Luc activity were observed irrespective of treatment or genotype (Figure 4.1F).

To investigate the dependence of migration on *Zdhhc7* and *Zdhhc3/7* in ACFs, we performed scratch assays to see how the deletion of these enzymes may influence migratory

ability in fibroblasts. Scratches were made in monolayers of Ctrl, *Zdhhc7* KO, and *Zdhhc3/7* KO ACFs, and images of the scratch were taken immediately, in addition to the 24-hour post-scratch time point to quantify wound closure. *Zdhhc7* KO ACFs exhibited a significantly reduced wound closure relative to Ctrls (Figure 4.1G/H). *Zdhhc3/7* KO ACFs, however, did not exhibit a statistically significant reduced wound closure compared to controls, though there was an appreciable trend towards reduced migration. To further corroborate that this was an effect specific to zDHHC7, we repeated these experiments with an additional S-acyltransferase KO model using *Zdhhc17* fl/fl ACFs treated with Ad-Cre. *Zdhhc17* KO ACF migration was consistent with Ctrl ACFs.

Effects of cardiac fibroblast *Zdhhc7* KO and *Zdhhc3/7* KO on AngII/PE-induced cardiac remodeling

Following the effects observed from *Zdhhc7* KO in vitro, we hypothesized that the reduction in migratory ability and minor changes to fibroblast gene expression in the absence of zDHHC7 may yield consequences for the development of fibrosis in vivo. To further explore the role of these enzymes in CF biology, we developed an in vivo model where *Zdhhc7* and *Zdhhc3* were both deleted in activated CFs. This was accomplished by crossing the previously described *Postn-MCM* +/-; *Zdhhc3* fl/fl line with our *Zdhhc7 KO* line, to generate *Postn-MCM* +/-; *Zdhhc3* fl/fl*; Zdhhc7 KO* (*Zdhhc3/7* KO) mice that exhibit a double deletion in CFs when treated with tamoxifen and in response to a cardiac injury that induces CF activation (*Postn* expression). Adult male and female *Postn-MCM +/-* or WT (Ctrl), *Zdhhc7* KO*,* and *Postn-MCM +/-; Zdhhc3* fl/fl*; Zdhhc7* KO (*Zdhhc3/7* KO) mice were then subject to a two-week time course of the common pro-fibrotic injury model, infusion of AngII (1.5 mg/kg/day)/PE (50 mg/kg/day) (Fu et al., 2018; Ock et al., 2021), delivered via surgically implanted osmotic pump. Ctrl mice received

osmotic pumps containing a saline solution. Following the treatment time course, mice were subjected to echocardiography to assess cardiac function before being sacrificed to measure cardiac hypertrophy, fibrosis, and pro-fibrotic gene expression.

In response to chronic AngII/PE, all genotypes exhibited significantly increased hypertrophy compared to saline controls as measured by heart weight/body weight ratios (Figure 4.2A). No difference was observed between genotypes in the development of hypertrophy. Consistent with the effects of AngII/PE infusion (Duangrat et al., 2022; Ock et al., 2021), no reductions in ejection fraction/fractional shortening were observed (Figure 4.2B/C) compared to saline Ctrls, nor were there any differences between genotypes under saline or AngII/PE conditions. Posterior wall thickness (PWd) was significantly increased across all three genotypes in response to AngII/PE (Figure 4.2D), with no differences among baseline readings. AngII/PE-treated *Zdhhc3/7* KO mice displayed a modest, statistically significant reduction in PWd compared to Ctrls (Figure 4.2D). Left ventricular end diameter systole (LVED systole) was significantly elevated in AngII/PE treated mice across all genotypes, with no differences observed between genotypes either at baseline or when treated with AngII/PE (Figure 4.2E). No differences in left ventricular end diameter diastole (LVED diastole) were observed between groups irrespective of treatment or genotype (Figure 4.2F).

To assess fibroblast activation in *Zdhhc7* KO and *Zdhhc3/7* KO mice, RTqPCR was performed from RNA extracted from whole heart tissue to measure mRNA levels of pro-fibrotic genes. *Postn* levels exhibited an upward trend in Ctrl and *Zdhhc7* KO mice treated with AngII/PE compared to saline controls (Figure 4.2G), and a significant elevation was observed in *Zdhhc3/7* KO mice treated with AngII/PE relative to saline controls. mRNA levels of *Thbs4* were significantly upregulated in response to AngII/PE relative to saline controls in all three genotypes

(Figure 4.2H), with no significant differences seen between genotypes either at baseline or between drug treatments. Ctrl mice showed an upward trend in *Nox4* expression in response to AngII/PE (Figure 4.2I), while *Zdhhc7* KO and *Zdhhc3/7* KO mice showed significantly increased *Nox4* expression with AngII/PE treatment compared to saline controls. *Zdhhc3/7* KO mice treated with AngII/PE exhibited a significantly elevated *Nox4* expression compared to AngII/PE-treated Ctrl mice (Figure 4.2I). *Col1a1* levels were significantly increased in response to AngII/PE in both Ctrl and *Zdhhc3/7* KO animals (Figure 4.2J), with a comparable upward trend in *Zdhhc7* KO mice. No significant differences were observed between genotypes at baseline or with drug treatment for *Col1a1* expression levels (Figure 4.2J).

Further assessing fibroblast activation at the tissue level, ventricular fibrosis was measured via quantification of Picrosirius Red Staining in histological cardiac sections. Ctrl mice treated with AngII/PE displayed a significant increase in fibrosis relative to saline controls (Figure 4.2K/L). *Zdhhc7* KO mice exhibited a trend toward elevated fibrosis in saline conditions. Conversely, *Zdhhc7* KO mice fibrosis trended lower in response to AngII/PE treatment, although the *Zdhhc7* KO fibrotic response to AngII/PE was not significantly higher compared to saline mice within genotype. *Zdhhc3/7* KO mice exhibited comparable responses to Ctrl mice both at baseline and in response to AngII/PE, though they also did not exhibit a statistically significant increase in fibrosis compared to saline controls.

Rac1 palmitoylation is not required for ACF migration or TGFβ1-induced activation

Given that palmitoylation of Rac1 at C178 has already been demonstrated to play a role in its signaling ability (Navarro-Lérida et al., 2012), we hypothesized that ACFs with a C178S palmitoylation-deficient mutation would exhibit reduced activation in response to pro-fibrotic stimuli. To test this, we utilized our newly developed mouse model with a Cre-inducible knock-

in of a C178S mutation, allowing us to test ACF activation in vitro with a Rac1 palmitoylation mutant expressed at endogenous expression levels. ACFs were isolated from Rac1 ConKI fl/fl mice and immediately transduced with either Ad-pLpA (Ctrl) or Ad-Cre (Rac1 KI) to induce recombination. 48 hours following recombination of the gene-targeted *Rac1* locus with Ad-Cre, cells were subject to 72 hours of 10 ng/mL TGFβ1, and immunostained for αSMA to calculate the percentage of myofibroblasts (Figure 4.3A, B). Immunostaining for α-smooth muscle actin (αSMA) is a commonly used metric of myofibroblast formation as αSMA only begins to be expressed upon the transition of ACFs into their activated state (Shinde et al., 2017). TGFβ1 treatment induced an increase in the percent of myofibroblasts at 72 hours in Ctrl ACFs, and Rac1 KI ACFs displayed comparable levels of activation both at baseline and with TGFβ1 after the 72-hour treatment time course (Figure 4.3A, B).

To analyze activation at the transcriptional level, we performed the same recombination of the gene-targeted *Rac1* locus with adenoviral Cre and TGFβ1 treatment time-course as described in the αSMA experiments. Here, RNA was isolated to perform RT-qPCR on genes related to fibroblast activation (Figure 4.3C-G). Consistent with αSMA data, TGFβ1 induced an increase in mRNA levels of *Postn*, *Col1a1*, and *Nox4* in Ctrl ACFs. Rac1 KI ACFs similarly exhibited significantly higher expression of *Postn*, and *Col1a1*, as well as a trend towards an increase in *Nox4* levels (Figures 4.3C, E, and G). No differences were observed between Ctrl and Rac1 KI ACFs in these genes. An upward trend in *Col1a2* and downward trend of *Tcf21* expression were elicited in response to TGFβ1, though no significant differences in *Tcf21* or *Col1a2* expression were seen between Ctrl and Rac1 KI ACFs at baseline or with agonist (Figures 4.3D, F).

Notably, despite the lack of changes seen to these commonly used metrics of fibroblast activation, Rac1 KI ACFs exhibited significant differences in terms of pro-fibrotic transcription factor activity. Both Ctrl and Rac1 KI ACFs exhibited significantly increased NFAT activity in response to TGFβ1 as assessed by luciferase reporter gene assays, and no changes relative to saline controls when treated with angiotensin II (Figure 4.3H). Further, Rac1 KI ACFs exhibited higher NFAT-Luc activity in response to TGFβ1 compared to TGFβ1-treated Ctrl ACFs. No changes were observed in NFκB-Luc activity between drug treatment or genotype conditions (n=2, data not shown). Serum response factor is a transcription factor that binds to serum response element (SRE) DNA sequences, and transcriptional changes downstream of SRF activation have been shown to upregulate the transition of quiescent fibroblasts into their activated state (Small, 2012). We also tested for changes in serum response factor (SRF) activity following higher serum concentration treatments using Ad-SRE-Luc. In response to 20% FBS culture conditions used to induce SRF activity, both Ctrl and Rac1 ConKI ACFs displayed elevated SRE-Luc responses (Figure 4.3I) compared to 1% FBS control conditions. Rac1 ConKI ACFs yielded a significantly higher increase in SRE-Luc in response to 20% FBS treatment compared to control ACFs with the same treatment (Figure 4.3I).

In addition to activation, Rac1 activity has been shown to play a role in the migratory ability of various cell types, including fibroblasts (Ma et al., 2023; Navarro-Lérida et al., 2012), and we hypothesized that Rac1 palmitoylation may play more of a role in their migratory ability. Using a scratch assay, we tested wound closure ability in Ctrl ACFs or those with the Rac1 KI mutation (Figure 4.3J/K). No differences were seen in the Rac1 KI ACFs in terms of migration, with both groups closing the scratch at comparable levels at the 24-hour time point (Figure 4.3J/K).

Discussion

The regulation of CF signaling proteins by palmitoylation remains an unexplored avenue of investigation, though one of great interest due to the increasingly established importance of this PTM in fine-tuning substrate activity (Cho & Park, 2016; Essandoh et al., 2020; Zhang et al., 2021). At present, little is known at either the enzyme or substrate level whether palmitoylation plays a critical role in fibroblast activation and migration, prompting previous investigations from our lab that focused on exploring how the Golgi-localized S-acyltransferase, zDHHC3, may be playing such a role. However, these initial analyses indicated that zDHHC3 may not be essential for CF activation and fibrosis, necessitating additional work to determine if other enzymes or substrates may be more relevant in the context of CF biology.

Following the evidence that *Zdhhc3* KO on its own did not result in obvious changes to CF activation and migration, we hypothesized that activity from other S-acyltransferases could be compensating for the loss of zDHHC3, and that enzymes with overlapping substrate profiles could be maintaining palmitoylation levels of substrates in the absence of zDHHC3. Alternatively, the removal of zDHHC3-mediated palmitoylation may simply not be enough to significantly alter the complex signaling initiated as part of CF activation. This possibility led us to hypothesize that other enzymes may prove to be more essential in CF activation and signaling. Previous work has demonstrated that zDHHC7 maintains a similar substrate profile to zDHHC3 (Baldwin et al., 2023; Chen et al., 2016; Hernandez et al., 2023; Zhang et al., 2020), as well as that zDHHC7 can act as the dominant enzyme for a shared substrate such as STAT3 (Zhang et al., 2020). Thus, we sought to determine whether zDHHC7 deletion on its own would lead to deficits in CF activation, in addition to whether the simultaneous deletion of zDHHC3 and zDHHC7 would be required in order to abrogate CF activation.

Collectively, the results of our in vitro and in vivo singular deletion of *Zdhhc7* or the combined knockout of both *Zdhhc3* and *Zdhhc7* exhibited only minor differences in terms of changes to fibroblast activation and fibrosis. Consistent with our hypothesis, a slight reduction of *Postn* expression was elicited upon the deletion of *Zdhhc7* alone in vitro, as well as with the double *Zdhhc3/7* KO, though it was not a dramatic effect. This result may not prove to be physiologically relevant and could, in part, be due to the increased variability present in the assay due to our model, which necessitates making comparisons between populations of cells isolated from separate mouse hearts. Further, given that *Postn* levels from in vivo *Zdhhc7* and *Zdhhc3/7* KO hearts were consistent with control mice in response to AngII/PE, there is not a clear case for the dependence of these enzymes when assessed in a more physiologically relevant model. Increases in other common fibrotic marker genes such as *Thbs4* and *Nox4* were not blunted as predicted, with *Nox4* levels even being significantly higher in *Zdhhc3/7* KO mice in response to AngII/PE compared to Ctrl mice. The results of our luciferase assays yielded no obvious differences in NFAT or NFκB activity either, and given the modest changes to fibrotic gene mRNA levels both in vitro and in vivo, it appears that despite the absence of these enzymes, ACF signaling pathways are sufficiently able to promote the myofibroblast transition.

In our assessment of the consequences of the loss of these enzymes on fibroblast migratory ability, a potentially unique role for *Zdhhc7* appeared. In previous work, we found evidence that *Zdhhc3* KO had no effect on unstimulated ACF migration, and here, that *Zdhhc17* KO ACFs also maintained migratory ability. Notably, *Zdhhc7* KO ACFs exhibited significant migratory deficits, suggesting that zDHHC7 may possess a unique role in ACF migration. While *Zdhhc3/7* KO ACFs did not exhibit a statistically significant reduction in migration as did *Zdhhc7* KO ACFs, additional replicates would likely yield a significant reduction as well. While

the mechanism of these effects remains unexplored, previous literature in this area demonstrated that zDHHC7 palmitoylates the cell polarity regulator SCRIB (Chen et al., 2016), a Rac1 interactor (Boczonadi et al., 2014) protein that has been implicated in various migratory signaling pathways in other cell types (Michaelis et al., 2013; Nola et al., 2008). It is possible zDHHC7 activity is regulating critical migratory signaling proteins such as SCRIB, though it is currently unknown whether these processes are operating in a similar fashion in CFs, and further work is required to elucidate the regulation of ACF migration by zDHHC7 and zDHHC3.

At the tissue level of the heart, we hypothesized that the slight in vitro effects in fibrotic gene expression in combination with migration deficits may elicit changes to remodeling in the injured heart. These results were not observed, though, with heart weight-to-body weight ratios being increased in all three genotypes in response to AngII/PE. In terms of fibrosis, responses of *Zdhhc3/7* KO mice were consistent with Ctrl mice, but our results display a paradoxical response in *Zdhhc7* KO mice, with a trend towards increased fibrosis at baseline, and a decreased response under AngII/PE conditions. While this could be a real effect, it is most likely attributed to high degrees of variability in this type of histological analysis. Not surprisingly, given the lack of changes in hypertrophy and fibrotic remodeling in the heart between control mice and *Zdhhc7* or *Zdhhc3/7* KO mice, cardiac function remained consistent between the genotypes.

Overall, these results collectively point to *Zdhhc3* and *Zdhhc7* having relatively minor roles in CF activation and fibrosis. Despite evidence for the importance of these enzymes in regulating key signaling pathways related to fibrosis in other cell types, the simultaneous deletion of *Zdhhc3* and *Zdhhc7* had only minor or negligible consequences on measures of fibroblast activation in vitro and in vivo. These results are in line with recently published work analyzing the role of these enzymes in another cardiac cell type, where the simultaneous deletion

of *Zdhhc3 and Zdhhc7* in cardiomyocytes elicited minimal changes to the development of cardiac remodeling (Baldwin et al., 2023). It remains a possibility that other S-acyltransferase enzymes expressed in CFs are maintaining levels of palmitoylation required for the pro-fibrotic pathways involved in TGFβ1 and AngII-induced signaling. Alternatively, these enzymes may prove to be essential for signaling pathways not explicitly analyzed in these studies, or for metrics of cardiac biology and remodeling not explicitly measured in these experiments such as inflammation or arrhythmia. Further work in necessary to continue to determine the role of these enzymes in CF signaling and biology.

In addition to our analyses of the consequences of manipulating palmitoylation through the modification of enzymatic activity, we similarly wanted to explore this area of fibroblast biology at the substrate level. When choosing a substrate, we decided upon Rac1 given its established role in CF biology (Lavall et al., 2017; Lyu et al., 2021), in addition to previous work demonstrating that Rac1 signaling ability is dependent on palmitoylation in other cell types (Navarro-Lérida et al., 2012). Rac1, a Rho-family GTPase (Bosco et al., 2009), has been demonstrated to play key roles in fibroblast activation and migration in multiple fibroblast cell types, including CFs (Lavall et al., 2017; Verma et al., 2011; Xu et al., 2009). Additionally, multiple groups have demonstrated that inhibiting Rac1 signaling can protect against AngII-induced cardiac fibrosis (Lyu et al., 2021; Pan et al., 2023). Furthermore, it has been shown that the signaling activity of Rac1 is dependent on the palmitoylation of C178 and that this modification influences its ability to localize the plasma membrane, as well as its GTP-loaded state (Navarro-Lérida et al., 2012). For these reasons, we hypothesized that C178S palmitoylation-deficient fibroblasts may exhibit reduced ACF activation due to changes in Rac1 activity, allowing us to assess the role of palmitoylation in a way that avoids the limitations

involved in our previous work where other S-acyltransferases could be compensating for the enzymes deleted in our models.

Using the Rac1 ConKI model, CFs transduced with Ad-Cre express a Rac1 palmitoylation mutant protein at endogenous levels, allowing us to explore how depalmitoylated Rac1 influences CF activation and migration in vitro. In measures of activation, Rac1 KI ACFs responded consistently with Ctrls both at baseline and in response to TGFβ1, with no reduced αSMA expression, or *Postn* or *Col1a1* expression observed, contrary to our predictions. These results by themselves indicate that the cardiac fibroblast activation signaling pathways induced by TGFβ1 do not appear to be dependent on Rac1 palmitoylation. However, Rac1 KI ACFs exhibited significantly elevated activity of two pro-fibrotic transcription factors, NFAT and SRF, in response to TGFβ1 and high levels of serum (20% FBS), respectively. Based on these data, it appears that Rac1 palmitoylation in ACFs is important for the proper activation of NFAT and SRF downstream of TGFβ1, and that a heightened pro-fibrotic signaling outcome through NFAT and SRF is being elicited through the inability of Rac1 palmitoylation. At present, it is uncertain as to how this may function mechanistically, though palmitoylated Rac1 may be downregulating NFAT and SRF, or potentially, depalmitoylated Rac1 has an enhanced ability to induce NFAT and SRF signaling. Further, the loss of Rac1 pro-fibrotic signaling when Rac1 cannot be palmitoylated may lead to the compensatory upregulation of adjacent signaling pathways that lead to NFAT and SRF induction. However, the increase in NFAT activation in response to TGFβ1 was not sufficient in inducing elevated αSMA, *Postn*, or *Col1a1* expression. These results collectively indicate that palmitoylation of Rac1 does appear to play a role in ACF signaling through at least the NFAT and SRF transcriptional pathways. Further work is necessary

to fully characterize how Rac1 palmitoylation influences ACF pro-fibrotic signaling and activation.

In the context of migration, Rac1 has been demonstrated by many groups to be a key regulator of fibroblast migration (Lavall et al., 2017; Liang et al., 2021; Ma et al., 2023). Thus, we also hypothesized that palmitoylation-deficient Rac1 would exhibit migratory deficits seen in KO models. Though, Rac1 KI ACFs displayed no changes in their ability to migrate in a scratch assay model. Experiments in COS7 cells assessing the consequences of this mutation using an overexpression model of endogenous Rac1 vs the Rac1 C178S palmitoylation mutant found that cells with the Rac1-palmitoylation mutation exhibited deficits in migration as assessed by the scratch assay (Navarro-Lérida et al., 2012). The differences in these results may be due to cell-specific differences in the requirement of Rac1 palmitoylation for migration, though the differences in the utilized models (overexpression vs endogenous Rac1 palmitoylation mutant) represent a confounding variable in the interpretation of these data. These data provide evidence that while Rac1 plays a role in migratory ability in fibroblasts, it appears that Rac1 palmitoylation is not required for cardiac fibroblast migration at this time point in unstimulated conditions. Though, additional testing is required to fully characterize the outcomes of manipulating Rac1 palmitoylation in the context of ACF migration.

Together, these results provide novel insights into the role of palmitoylation in CF activation and biology. Future studies are aimed at determining other S-acyltransferase enzymes that modify key signaling pathways involved in changes to fibroblast activation states and other responses like migration and contraction. Further, additional work will focus on a more comprehensive determination of substrates in ACFs that undergo palmitoylation to determine the

consequences of this PTM on their signaling ability and downstream changes to cellular responses.

Chapter IV Figures

Figure 4.1. Effects of *Zdhhc7* KO and *Zdhhc3/7* KO on cardiac fibroblast fibrotic gene expression and migration

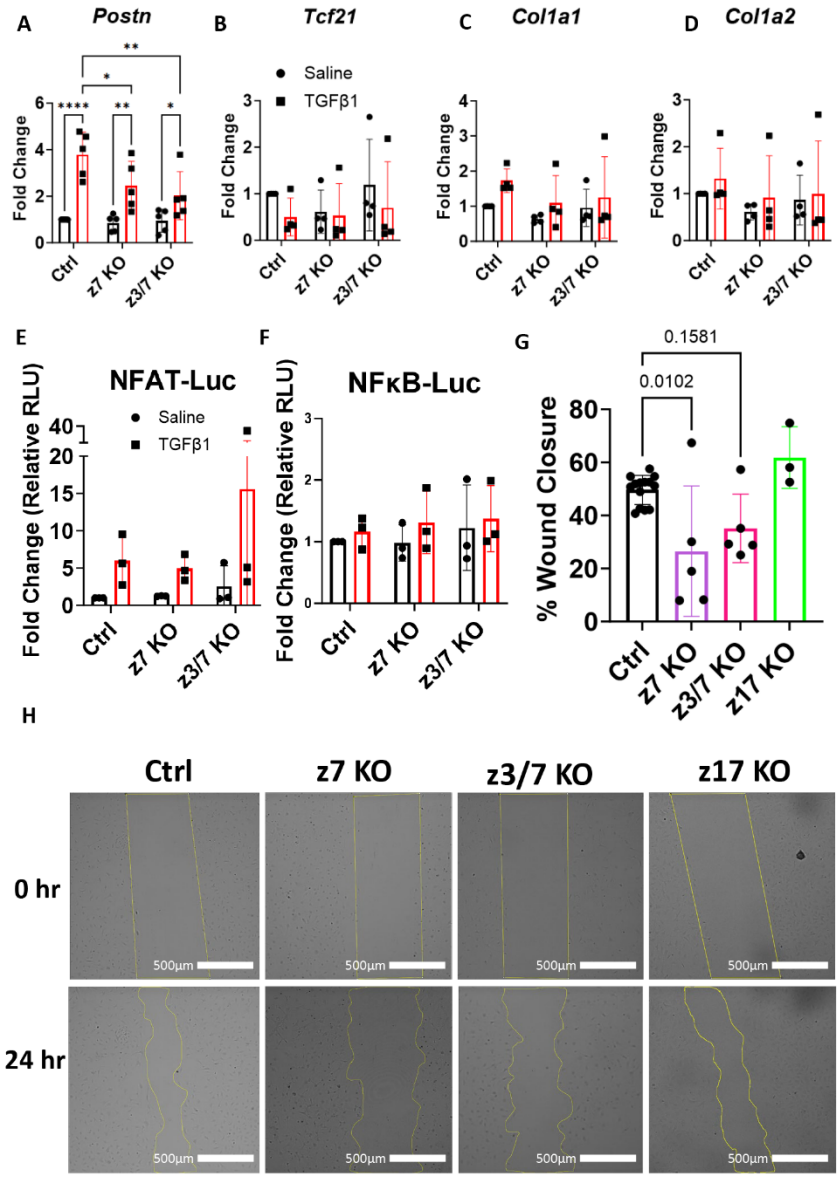

Figure 4.1: Effects of Zdhhc7 KO and Zdhhc3/7 KO on cardiac fibroblast fibrotic gene expression and migration. *(A-D) mRNA level quantification of various pro-fibrotic genes in Ctrl, Zdhhc7 KO (z7 KO), or Zdhhc3/7 KO (z3/7 KO) ACFs treated with or without TGFβ1 (10ng/ml, 72 hours), n=4-5. Two-way ANOVA with Tukey's multiple comparisons test; Postn Drug Treatment (p=<.0001), Interaction (p=.051), Tcf21 Drug Treatment (p=.22), Interaction (p=.79), Col1a1 Drug Treatment (p=.068), Interaction (p=.79), Col1a2 Drug Treatment (p=.39), Interaction (p=.95), (E/F) NFAT and NFκB-luciferase promoter activity quantification in Ctrl, z7 KO, or z3/7 KO treated with saline or TGFβ1 (10 ng/ml, 48 hours), n=3. Two-way ANOVA with Tukey's multiple comparisons test; (NFAT-Luc) Drug Treatment (p=<.091), Interaction (p=.59), (NFκB-Luc) Drug Treatment (p=.33), Interaction (p=.92), (G) Quantification of scratch area via ImageJ in primary Ctrl, z7 KO, z3/7 KO, and z17 KO ACFs, n=3-14. One-way ANOVA with Tukey's multiple comparisons test; (p=.0019), (H) Representative images of scratch assay at 0 and 24 hours in primary Ctrl, z7 KO, z3/7 KO, and z17 KO ACFs. Scale bar represents 500 μm. Error bars indicate the mean +/- standard deviation, significance denoted as (p<0.05, *), (p<0.01, **), (p<.001, ***), (p<.0001, ****).*

Figure 4.2. Effects of cardiac fibroblast *Zdhhc7* KO and *Zdhhc3/7* KO on AngII/PE-induced cardiac remodeling

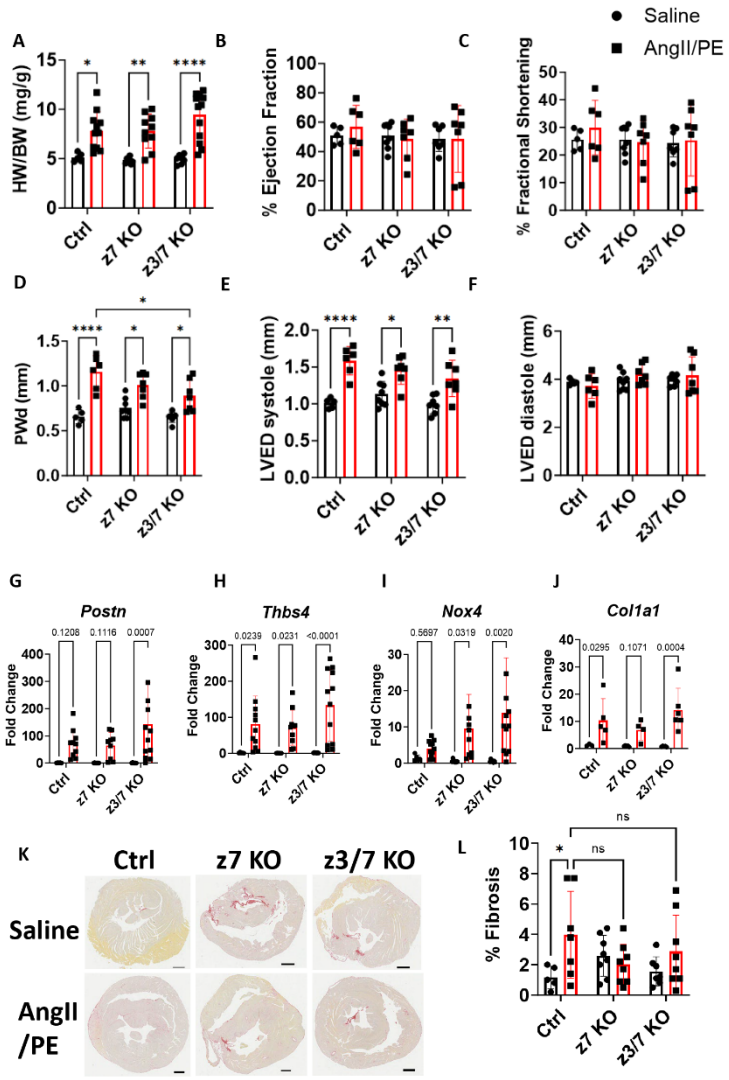

Figure 4.2: Effects of cardiac fibroblast Zdhhc7 KO and Zdhhc3/7 KO on AngII/PE-induced cardiac remodeling. *Echocardiography was performed on Ctrl saline (n=5), Ctrl AngII/PE (n=5), Zdhhc7 KO (z7 KO) saline (n=8), Zdhhc7 KO AngII/PE (n=7), Zdhhc3/7 KO (z Echocardiography was performed on Ctrl saline (n=5), Ctrl AngII/PE (n=5), Zdhhc7 KO (z7 KO) saline (n=8), Zdhhc7 KO AngII/PE (n=7), Zdhhc3/7 KO (z3/7) KO saline (n=7), and Zdhhc3/7 KO AngII/PE (n=7) to measure changes in cardiac function 2-weeks following implantation of osmotic pumps. (A) heart-weight to body-weight ratios, Two-way ANOVA with Tukey's multiple comparisons test. Injury Model Condition (p=<.0001), Interaction (p=.25). B-F, echocardiographic measurement of (B) ejection fraction (%), Two-way ANOVA with Tukey's multiple comparisons test. Injury Model Condition (p=.80), Interaction (p=.750), (C) fractional shortening (%), Two-way ANOVA with Tukey's multiple comparisons test. Injury Model Condition (p=.59), Interaction (p=.72), (D) posterior wall thickness diastole, Two-way ANOVA with Tukey's multiple comparisons test. Injury Model Condition (p=<.0001), Interaction (p=.0400). (E) left ventricular end diameter systole (mm), Two-way ANOVA with Tukey's multiple comparisons test. Injury Model Condition (p<.0001), Interaction (p=.18). (F) left ventricular end diameter diastole (mm), Two-way ANOVA with Tukey's multiple comparisons test. Injury Model Condition (p=.48), Interaction (p=.46), (G-J) fibrotic gene expression measurements via RTqPCR. Two-way ANOVA with Tukey's multiple comparisons test; Postn Injury Model Condition (p=.0003), Interaction (p=.32), Thbs4 Injury Model Condition (p=.0001), Interaction (p=.32), Nox4 Injury Model Condition (p=.0014), Interaction (p=.23), Col1a1 Injury Model Condition (p=.0001), Interaction (p=.31), (K) Representative images of histological sections stained with Picrosirius Red to assess fibrosis. (L) Quantification of fibrosis via ImageJ. Two-way ANOVA with Tukey's multiple comparisons test. Injury Model Condition (p=.040), Interaction (p=.064). Error bars indicate the mean +/- standard deviation, significance denoted as (p<0.05, *), (p<0.01, **), (p<.001, ***), (p<.0001, ****).*

Figure 4.3. Rac1 palmitoylation is not required for ACF migration or TGFβ1-induced activation

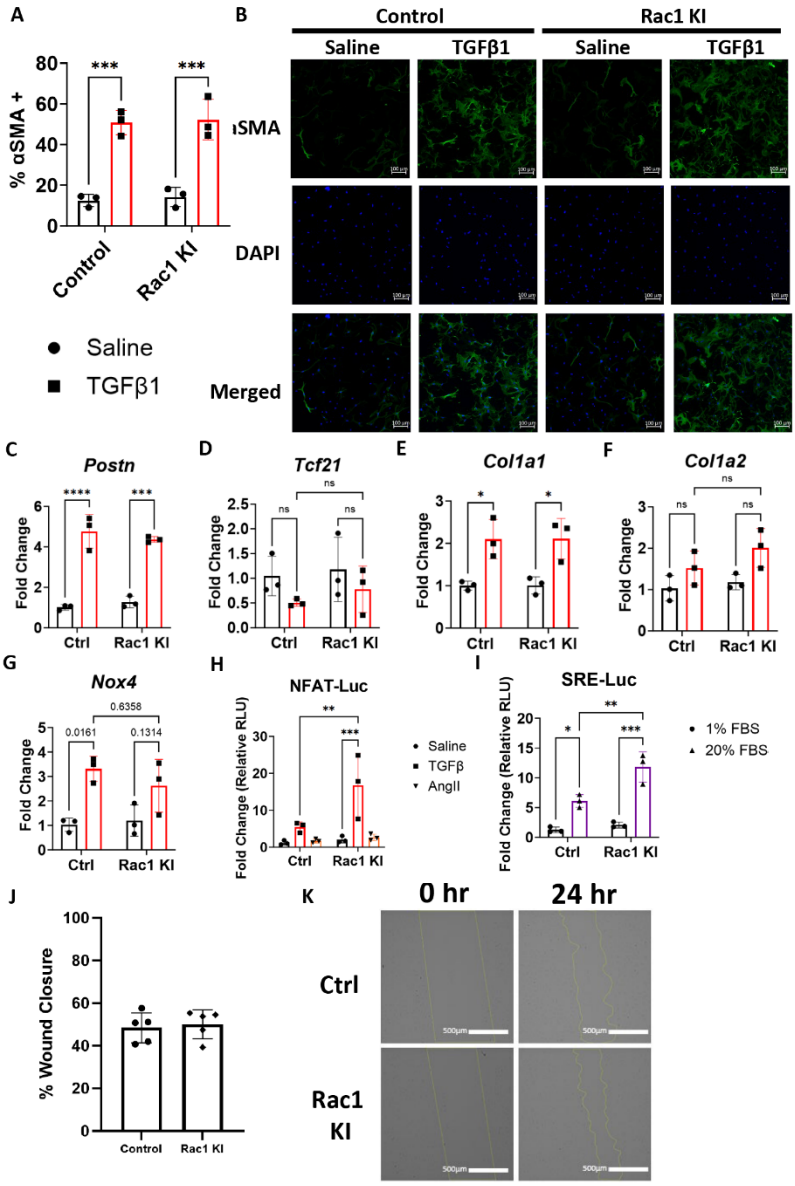

Figure 4.3: Rac1 palmitoylation is not required for ACF migration or TGFβ1-induced activation. *(A) Quantification of αSMA+ cells via ImageJ, n=3. Two-way ANOVA with Tukey's multiple comparisons test, Drug Treatment (p<.0001), Interaction (p=.970), (B) representative images of αSMA+ assay in Rac1 ConKI fl/fl ACFs treated with Ad-pLpA (Ctrl) or Ad-Cre (Rac1 KI) treated with saline or TGFβ1 (10 ng/ml, 72 hours). Scale bar represents 100 µm, (C-G) mRNA level quantification of various pro-fibrotic genes in Ctrl or Rac1 ConKI ACFs treated with or without TGFβ1 (10 ng/ml, 72 hours), n=3. Two-way ANOVA with Tukey's multiple comparisons test; Postn Drug Treatment (p=<.0001), Interaction (p=.24), Tcf21 Drug Treatment (p=.107), Interaction (p=.80), Col1a1 Drug Treatment (p=.0006), Interaction (p=.99), Col1a2 Drug Treatment (p=.013), Interaction (p=.44), Nox4 Drug Treatment (p= .0017), Interaction (p=.32), (H) NFAT luciferase promoter activity quantification in Ctrl or Rac1 KI ACFs treated with or without TGFβ1 (10 ng/ml, 48 hours), n=3. Two-way ANOVA with Tukey's multiple comparisons test; NFAT-Luc Drug Treatment (p=<.001), Interaction (p=.045), (I) SRE luciferase promoter activity quantification in Ctrl or Rac1 KI ACFs treated with 1% or 20% FBS for 48 hours, n=3. Two-way ANOVA with Tukey's multiple comparisons test, SRE-Luc Drug Treatment (p=<.0001), Interaction (p=.017), (J) Quantification of scratch area via ImageJ, n=5. Students T-test (p=.716), (K) Representative images of scratch assay at 0 and 24 hours in primary Ctrl or Rac1 KI ACFs Scale bar represents 500µm. Error bars indicate the mean +/- standard deviation, significance denoted as (p<0.05, *), (p<0.01, **), (p<.001, ***), (p<.0001, ****).*

References

Alter, C., Henseler, A. S., Owenier, C., Hesse, J., Ding, Z., Lautwein, T., Bahr, J., Hayat, S., Kramann, R., Kostenis, E., Scheller, J., & Schrader, J. (2023, Jun 1). IL-6 in the infarcted heart is preferentially formed by fibroblasts and modulated by purinergic signaling. J Clin Invest, 133(11). https://doi.org/10.1172/jci163799

Baldwin, T. A., Teuber, J. P., Kuwabara, Y., Subramani, A., Lin, S. J., Kanisicak, O., Vagnozzi, R. J., Zhang, W., Brody, M. J., & Molkentin, J. D. (2023, Nov 3). Palmitoylation-Dependent Regulation of Cardiomyocyte Rac1 Signaling Activity and Minor Effects on Cardiac Hypertrophy. J Biol Chem, 105426. https://doi.org/10.1016/j.jbc.2023.105426

Bertaud, A., Joshkon, A., Heim, X., Bachelier, R., Bardin, N., Leroyer, A. S., & Blot-Chabaud, M. (2023, Jan 16). Signaling Pathways and Potential Therapeutic Strategies in Cardiac Fibrosis. Int J Mol Sci, 24(2). https://doi.org/10.3390/ijms24021756

Boczonadi, V., Gillespie, R., Keenan, I., Ramsbottom, S. A., Donald-Wilson, C., Al Nazer, M., Humbert, P., Schwarz, R. J., Chaudhry, B., & Henderson, D. J. (2014, Oct 1). Scrib:Rac1 interactions are required for the morphogenesis of the ventricular myocardium. Cardiovasc Res, 104(1), 103-115. https://doi.org/10.1093/cvr/cvu193

Bosco, E. E., Mulloy, J. C., & Zheng, Y. (2009, Feb). Rac1 GTPase: a "Rac" of all trades. Cell Mol Life Sci, 66(3), 370-374. https://doi.org/10.1007/s00018-008-8552-x

Bretherton, R., Bugg, D., Olszewski, E., & Davis, J. (2020, Sep). Regulators of cardiac fibroblast cell state. Matrix Biol, 91-92, 117-135. https://doi.org/10.1016/j.matbio.2020.04.002

Chakraborty, D., Šumová, B., Mallano, T., Chen, C. W., Distler, A., Bergmann, C., Ludolph, I., Horch, R. E., Gelse, K., Ramming, A., Distler, O., Schett, G., Šenolt, L., & Distler, J. H. W. (2017, Oct 24). Activation of STAT3 integrates common profibrotic pathways to promote fibroblast activation and tissue fibrosis. Nat Commun, 8(1), 1130. https://doi.org/10.1038/s41467-017-01236-6

Chen, B., Zheng, B., DeRan, M., Jarugumilli, G. K., Fu, J., Brooks, Y. S., & Wu, X. (2016, Sep). ZDHHC7-mediated S-palmitoylation of Scribble regulates cell polarity. Nat Chem Biol, 12(9), 686-693. https://doi.org/10.1038/nchembio.2119

Cheng, Y., Wang, Y., Yin, R., Xu, Y., Zhang, L., Zhang, Y., Yang, L., & Zhao, D. (2023). Central role of cardiac fibroblasts in myocardial fibrosis of diabetic cardiomyopathy. Front Endocrinol (Lausanne), 14, 1162754. https://doi.org/10.3389/fendo.2023.1162754

Cho, E., & Park, M. (2016, Sep). Palmitoylation in Alzheimer's disease and other neurodegenerative diseases. Pharmacol Res, 111, 133-151. https://doi.org/10.1016/j.phrs.2016.06.008

Davis, J., Burr, A. R., Davis, G. F., Birnbaumer, L., & Molkentin, J. D. (2012, Oct 16). A TRPC6-dependent pathway for myofibroblast transdifferentiation and wound healing in vivo. Dev Cell, 23(4), 705-715. https://doi.org/10.1016/j.devcel.2012.08.017

De, I., & Sadhukhan, S. (2018, Jun). Emerging Roles of DHHC-mediated Protein S-palmitoylation in Physiological and Pathophysiological Context. Eur J Cell Biol, 97(5), 319-338. https://doi.org/10.1016/j.ejcb.2018.03.005

Díez, J. (2007, Jul). Mechanisms of cardiac fibrosis in hypertension. J Clin Hypertens (Greenwich), 9(7), 546-550. https://doi.org/10.1111/j.1524-6175.2007.06626.x

Duangrat, R., Parichatikanond, W., Morales, N. P., Pinthong, D., & Mangmool, S. (2022, Dec 15). Sustained AT(1)R stimulation induces upregulation of growth factors in human cardiac fibroblasts via G(αq)/TGF-β/ERK signaling that influences myocyte hypertrophy. Eur J Pharmacol, 937, 175384. https://doi.org/10.1016/j.ejphar.2022.175384

Essandoh, K., Philippe, J. M., Jenkins, P. M., & Brody, M. J. (2020). Palmitoylation: A Fatty Regulator of Myocardial Electrophysiology. Front Physiol, 11, 108. https://doi.org/10.3389/fphys.2020.00108

Essandoh, K., Subramani, A., Ferro, O. A., Teuber, J. P., Koripella, S., & Brody, M. J. (2023, May). zDHHC9 Regulates Cardiomyocyte Rab3a Activity and Atrial Natriuretic Peptide Secretion Through Palmitoylation of Rab3gap1. JACC Basic Transl Sci, 8(5), 518-542. https://doi.org/10.1016/j.jacbts.2022.11.003

Fan, D., Takawale, A., Lee, J., & Kassiri, Z. (2012, Sep 3). Cardiac fibroblasts, fibrosis and extracellular matrix remodeling in heart disease. Fibrogenesis Tissue Repair, 5(1), 15. https://doi.org/10.1186/1755-1536-5-15

Forrester, S. J., Booz, G. W., Sigmund, C. D., Coffman, T. M., Kawai, T., Rizzo, V., Scalia, R., & Eguchi, S. (2018, Jul 1). Angiotensin II Signal Transduction: An Update on Mechanisms of Physiology and Pathophysiology. Physiol Rev, 98(3), 1627-1738. https://doi.org/10.1152/physrev.00038.2017

Frangogiannis, N. G. (2021, May 25). Cardiac fibrosis. Cardiovasc Res, 117(6), 1450-1488. https://doi.org/10.1093/cvr/cvaa324

Fu, X., Khalil, H., Kanisicak, O., Boyer, J. G., Vagnozzi, R. J., Maliken, B. D., Sargent, M. A., Prasad, V., Valiente-Alandi, I., Blaxall, B. C., & Molkentin, J. D. (2018, May 1). Specialized fibroblast differentiated states underlie scar formation in the infarcted mouse heart. J Clin Invest, 128(5), 2127-2143. https://doi.org/10.1172/jci98215

Fu, X., Liu, Q., Li, C., Li, Y., & Wang, L. (2020). Cardiac Fibrosis and Cardiac Fibroblast Lineage-Tracing: Recent Advances. Front Physiol, 11, 416. https://doi.org/10.3389/fphys.2020.00416

Garoffolo, G., Casaburo, M., Amadeo, F., Salvi, M., Bernava, G., Piacentini, L., Chimenti, I., Zaccagnini, G., Milcovich, G., Zuccolo, E., Agrifoglio, M., Ragazzini, S., Baasansuren, O., Cozzolino, C., Chiesa, M., Ferrari, S., Carbonaro, D., Santoro, R., Manzoni, M., Casalis, L., Raucci, A., Molinari, F., Menicanti, L., Pagano, F., Ohashi, T., Martelli, F., Massai, D., Colombo, G. I., Messina, E., Morbiducci, U., & Pesce, M. (2022, Jul 22). Reduction of Cardiac Fibrosis by Interference With YAP-Dependent Transactivation. Circ Res, 131(3), 239-257. https://doi.org/10.1161/circresaha.121.319373

Hall, C., Gehmlich, K., Denning, C., & Pavlovic, D. (2021, Feb). Complex Relationship Between Cardiac Fibroblasts and Cardiomyocytes in Health and Disease. J Am Heart Assoc, 10(5), e019338. https://doi.org/10.1161/jaha.120.019338

Hernandez, L. M., Montersino, A., Niu, J., Guo, S., Faezov, B., Sanders, S. S., Dunbrack, R. L., & Thomas, G. M. (2023, 2023/08/01/). Palmitoylation-dependent control of JAK1 kinase signaling governs responses to neuropoietic cytokines and survival in DRG neurons. Journal of Biological Chemistry, 299(8), 104965. https://doi.org/https://doi.org/10.1016/j.jbc.2023.104965

Herum, K. M., Choppe, J., Kumar, A., Engler, A. J., & McCulloch, A. D. (2017, Jul 7). Mechanical regulation of cardiac fibroblast profibrotic phenotypes. Mol Biol Cell, 28(14), 1871-1882. https://doi.org/10.1091/mbc.E17-01-0014

Herum, K. M., Lunde, I. G., McCulloch, A. D., & Christensen, G. (2017, May 19). The Soft- and Hard-Heartedness of Cardiac Fibroblasts: Mechanotransduction Signaling Pathways in Fibrosis of the Heart. J Clin Med, 6(5). https://doi.org/10.3390/jcm6050053

Herum, K. M., Lunde, I. G., Skrbic, B., Florholmen, G., Behmen, D., Sjaastad, I., Carlson, C. R., Gomez, M. F., & Christensen, G. (2013, Jan). Syndecan-4 signaling via NFAT regulates extracellular matrix production and cardiac myofibroblast differentiation in response to mechanical stress. J Mol Cell Cardiol, 54, 73-81. https://doi.org/10.1016/j.yjmcc.2012.11.006

Hinderer, S., & Schenke-Layland, K. (2019, 2019/06/01/). Cardiac fibrosis – A short review of causes and therapeutic strategies. Advanced Drug Delivery Reviews, 146, 77-82. https://doi.org/https://doi.org/10.1016/j.addr.2019.05.011

Hohoff, C., Zhang, M., Ambrée, O., Kravchenko, M., Buschert, J., Kerkenberg, N., Gorinski, N., Abdel Galil, D., Schettler, C., Vom Werth, K. L., Wewer, M. F., Schneider, I., Grotegerd, D., Wachsmuth, L., Faber, C., Skryabin, B. V., Brosius, J., Ponimaskin, E., & Zhang, W. (2019, Jul). Deficiency of the palmitoyl acyltransferase ZDHHC7 impacts brain and behavior of mice in a sex-specific manner. Brain Struct Funct, 224(6), 2213-2230. https://doi.org/10.1007/s00429-019-01898-6

Jiang, H., Zhang, X., Chen, X., Aramsangtienchai, P., Tong, Z., & Lin, H. (2018, Feb 14). Protein Lipidation: Occurrence, Mechanisms, Biological Functions, and Enabling Technologies. Chem Rev, 118(3), 919-988. https://doi.org/10.1021/acs.chemrev.6b00750

Kanisicak, O., Khalil, H., Ivey, M. J., Karch, J., Maliken, B. D., Correll, R. N., Brody, M. J., SC, J. L., Aronow, B. J., Tallquist, M. D., & Molkentin, J. D. (2016, Jul 22). Genetic lineage tracing defines myofibroblast origin and function in the injured heart. Nat Commun, 7, 12260. https://doi.org/10.1038/ncomms12260

Kasembeli, M. M., Bharadwaj, U., Robinson, P., & Tweardy, D. J. (2018, Aug 5). Contribution of STAT3 to Inflammatory and Fibrotic Diseases and Prospects for its Targeting for Treatment. Int J Mol Sci, 19(8). https://doi.org/10.3390/ijms19082299

Khalil, H., Kanisicak, O., Prasad, V., Correll, R. N., Fu, X., Schips, T., Vagnozzi, R. J., Liu, R., Huynh, T., Lee, S. J., Karch, J., & Molkentin, J. D. (2017, Oct 2). Fibroblast-specific

TGF-β-Smad2/3 signaling underlies cardiac fibrosis. J Clin Invest, 127(10), 3770-3783. https://doi.org/10.1172/jci94753

Kong, P., Christia, P., & Frangogiannis, N. G. (2014, Feb). The pathogenesis of cardiac fibrosis. Cell Mol Life Sci, 71(4), 549-574. https://doi.org/10.1007/s00018-013-1349-6

Kunschmann, T., Puder, S., Fischer, T., Steffen, A., Rottner, K., & Mierke, C. T. (2019, May 22). The Small GTPase Rac1 Increases Cell Surface Stiffness and Enhances 3D Migration Into Extracellular Matrices. Sci Rep, 9(1), 7675. https://doi.org/10.1038/s41598-019-43975-0

Kuwahara, F., Kai, H., Tokuda, K., Takeya, M., Takeshita, A., Egashira, K., & Imaizumi, T. (2004, Apr). Hypertensive myocardial fibrosis and diastolic dysfunction: another model of inflammation? Hypertension, 43(4), 739-745. https://doi.org/10.1161/01.HYP.0000118584.33350.7d

Lavall, D., Schuster, P., Jacobs, N., Kazakov, A., Böhm, M., & Laufs, U. (2017, May 5). Rac1 GTPase regulates 11β hydroxysteroid dehydrogenase type 2 and fibrotic remodeling. J Biol Chem, 292(18), 7542-7553. https://doi.org/10.1074/jbc.M116.764449

Li, M., Zhang, L., & Chen, C. W. (2023, Sep 5). Diverse Roles of Protein Palmitoylation in Cancer Progression, Immunity, Stemness, and Beyond. Cells, 12(18). https://doi.org/10.3390/cells12182209

Liang, C., Wang, K., Li, Q., Bai, J., & Zhang, H. (2019, Oct 2). Influence of the distribution of fibrosis within an area of myocardial infarction on wave propagation in ventricular tissue. Sci Rep, 9(1), 14151. https://doi.org/10.1038/s41598-019-50478-5

Liang, J., Oyang, L., Rao, S., Han, Y., Luo, X., Yi, P., Lin, J., Xia, L., Hu, J., Tan, S., Tang, L., Pan, Q., Tang, Y., Zhou, Y., & Liao, Q. (2021). Rac1, A Potential Target for Tumor Therapy. Front Oncol, 11, 674426. https://doi.org/10.3389/fonc.2021.674426

Liu, Q., Chen, Y., Auger-Messier, M., & Molkentin, J. D. (2012, Apr 13). Interaction between NFκB and NFAT coordinates cardiac hypertrophy and pathological remodeling. Circ Res, 110(8), 1077-1086. https://doi.org/10.1161/circresaha.111.260729

Liu, S., Kapoor, M., & Leask, A. (2009, May). Rac1 expression by fibroblasts is required for tissue repair in vivo. Am J Pathol, 174(5), 1847-1856. https://doi.org/10.2353/ajpath.2009.080779

Lu, W., Meng, Z., Hernandez, R., & Zhou, C. (2021, Sep 22). Fibroblast-specific IKK-β deficiency ameliorates angiotensin II-induced adverse cardiac remodeling in mice. JCI Insight, 6(18). https://doi.org/10.1172/jci.insight.150161

Lyu, L., Chen, J., Wang, W., Yan, T., Lin, J., Gao, H., Li, H., Lv, R., Xu, F., Fang, L., & Chen, Y. (2021, Mar). Scoparone alleviates Ang II-induced pathological myocardial hypertrophy in mice by inhibiting oxidative stress. J Cell Mol Med, 25(6), 3136-3148. https://doi.org/10.1111/jcmm.16304

Ma, N., Xu, E., Luo, Q., & Song, G. (2023, Mar 27). Rac1: A Regulator of Cell Migration and a Potential Target for Cancer Therapy. Molecules, 28(7). https://doi.org/10.3390/molecules28072976

Main, A., & Fuller, W. (2022, Feb). Protein S-Palmitoylation: advances and challenges in studying a therapeutically important lipid modification. Febs j, 289(4), 861-882. https://doi.org/10.1111/febs.15781

Martínez-López, A., García-Casas, A., Bragado, P., Orimo, A., Castañeda-Saucedo, E., & Castillo-Lluva, S. (2021, Aug 19). Inhibition of RAC1 activity in cancer associated fibroblasts favours breast tumour development through IL-1β upregulation. Cancer Lett, 521, 14-28. https://doi.org/10.1016/j.canlet.2021.08.014

Maruyama, K., & Imanaka-Yoshida, K. (2022, Feb 27). The Pathogenesis of Cardiac Fibrosis: A Review of Recent Progress. Int J Mol Sci, 23(5). https://doi.org/10.3390/ijms23052617

Mazarura, G. R., Dallagnol, J. C. C., Chatenet, D., Allen, B. G., & Hébert, T. E. (2022, Sep 1). The complicated lives of GPCRs in cardiac fibroblasts. Am J Physiol Cell Physiol, 323(3), C813-c822. https://doi.org/10.1152/ajpcell.00120.2022

Meléndez, G. C., McLarty, J. L., Levick, S. P., Du, Y., Janicki, J. S., & Brower, G. L. (2010, Aug). Interleukin 6 mediates myocardial fibrosis, concentric hypertrophy, and diastolic dysfunction in rats. Hypertension, 56(2), 225-231. https://doi.org/10.1161/hypertensionaha.109.148635

Mia, M. M., Cibi, D. M., Ghani, S., Singh, A., Tee, N., Sivakumar, V., Bogireddi, H., Cook, S. A., Mao, J., & Singh, M. K. (2022, Jun 22). Loss of Yap/Taz in cardiac fibroblasts attenuates adverse remodelling and improves cardiac function. Cardiovasc Res, 118(7), 1785-1804. https://doi.org/10.1093/cvr/cvab205

Michaelis, U. R., Chavakis, E., Kruse, C., Jungblut, B., Kaluza, D., Wandzioch, K., Manavski, Y., Heide, H., Santoni, M. J., Potente, M., Eble, J. A., Borg, J. P., & Brandes, R. P. (2013, Mar 15). The polarity protein Scrib is essential for directed endothelial cell migration. Circ Res, 112(6), 924-934. https://doi.org/10.1161/circresaha.112.300592

Mir, S. A., Chatterjee, A., Mitra, A., Pathak, K., Mahata, S. K., & Sarkar, S. (2012, Jan 20). Inhibition of signal transducer and activator of transcription 3 (STAT3) attenuates interleukin-6 (IL-6)-induced collagen synthesis and resultant hypertrophy in rat heart. J Biol Chem, 287(4), 2666-2677. https://doi.org/10.1074/jbc.M111.246173

Narayanan, G., Halim, A., Hu, A., Avin, K. G., Lu, T., Zehnder, D., Hato, T., Chen, N. X., Moe, S. M., & Lim, K. (2023, Nov 1). Molecular Phenotyping and Mechanisms of Myocardial Fibrosis in Advanced Chronic Kidney Disease. Kidney360, 4(11), 1562-1579. https://doi.org/10.34067/kid.0000000000000276

Navarro-Lérida, I., Sánchez-Perales, S., Calvo, M., Rentero, C., Zheng, Y., Enrich, C., & Del Pozo, M. A. (2012, Feb 1). A palmitoylation switch mechanism regulates Rac1 function and membrane organization. Embo j, 31(3), 534-551. https://doi.org/10.1038/emboj.2011.446

Nola, S., Sebbagh, M., Marchetto, S., Osmani, N., Nourry, C., Audebert, S., Navarro, C., Rachel, R., Montcouquiol, M., Sans, N., Etienne-Manneville, S., Borg, J. P., & Santoni, M. J. (2008, Nov 15). Scrib regulates PAK activity during the cell migration process. Hum Mol Genet, 17(22), 3552-3565. https://doi.org/10.1093/hmg/ddn248

Ock, S., Ham, W., Kang, C. W., Kang, H., Lee, W. S., & Kim, J. (2021, Jul 9). IGF-1 protects against angiotensin II-induced cardiac fibrosis by targeting αSMA. Cell Death Dis, 12(7), 688. https://doi.org/10.1038/s41419-021-03965-5

Ohtsu, H., Higuchi, S., Shirai, H., Eguchi, K., Suzuki, H., Hinoki, A., Brailoiu, E., Eckhart, A. D., Frank, G. D., & Eguchi, S. (2008, Jul). Central role of Gq in the hypertrophic signal

transduction of angiotensin II in vascular smooth muscle cells. Endocrinology, 149(7), 3569-3575. https://doi.org/10.1210/en.2007-1694

Pan, J., Liu, M., Su, H., Hu, H., Chen, H., & Ma, L. (2023, Mar 9). Pharmacological Inhibition of P-Rex1/Rac1 Axis Blocked Angiotensin II-Induced Cardiac Fibrosis. Cardiovasc Drugs Ther. https://doi.org/10.1007/s10557-023-07442-3

Patel, N. J., Nassal, D. M., Greer-Short, A. D., Unudurthi, S. D., Scandling, B. W., Gratz, D., Xu, X., Kalyanasundaram, A., Fedorov, V. V., Accornero, F., Mohler, P. J., Gooch, K. J., & Hund, T. J. (2019, Oct 17). βIV-Spectrin/STAT3 complex regulates fibroblast phenotype, fibrosis, and cardiac function. JCI Insight, 4(20). https://doi.org/10.1172/jci.insight.131046

Pesce, M., Duda, G. N., Forte, G., Girao, H., Raya, A., Roca-Cusachs, P., Sluijter, J. P. G., Tschöpe, C., & Van Linthout, S. (2023, May). Cardiac fibroblasts and mechanosensation in heart development, health and disease. Nat Rev Cardiol, 20(5), 309-324. https://doi.org/10.1038/s41569-022-00799-2

Russo, I., & Frangogiannis, N. G. (2016, Jan). Diabetes-associated cardiac fibrosis: Cellular effectors, molecular mechanisms and therapeutic opportunities. J Mol Cell Cardiol, 90, 84-93. https://doi.org/10.1016/j.yjmcc.2015.12.011

Saadat, S., Noureddini, M., Mahjoubin-Tehran, M., Nazemi, S., Shojaie, L., Aschner, M., Maleki, B., Abbasi-Kolli, M., Rajabi Moghadam, H., Alani, B., & Mirzaei, H. (2020). Pivotal Role of TGF-β/Smad Signaling in Cardiac Fibrosis: Non-coding RNAs as Effectual Players. Front Cardiovasc Med, 7, 588347. https://doi.org/10.3389/fcvm.2020.588347

Sanders, S. S., Parsons, M. P., Mui, K. K., Southwell, A. L., Franciosi, S., Cheung, D., Waltl, S., Raymond, L. A., & Hayden, M. R. (2016, Dec 7). Sudden death due to paralysis and synaptic and behavioral deficits when Hip14/Zdhhc17 is deleted in adult mice. BMC Biol, 14(1), 108. https://doi.org/10.1186/s12915-016-0333-7

Shinde, A. V., Humeres, C., & Frangogiannis, N. G. (2017, Jan). The role of α-smooth muscle actin in fibroblast-mediated matrix contraction and remodeling. Biochim Biophys Acta Mol Basis Dis, 1863(1), 298-309. https://doi.org/10.1016/j.bbadis.2016.11.006

Small, E. M. (2012, Dec). The actin-MRTF-SRF gene regulatory axis and myofibroblast differentiation. J Cardiovasc Transl Res, 5(6), 794-804. https://doi.org/10.1007/s12265-012-9397-0

Smith, M. C., Hudson, C. A., Kimura, T. E., White, S. J., Sala-Newby, G. B., Newby, A. C., & Bond, M. (2017, Jun 16). Divergent Regulation of Actin Dynamics and Megakaryoblastic Leukemia-1 and -2 (Mkl1/2) by cAMP in Endothelial and Smooth Muscle Cells. Sci Rep, 7(1), 3681. https://doi.org/10.1038/s41598-017-03337-0

Souders, C. A., Bowers, S. L., & Baudino, T. A. (2009, Dec 4). Cardiac fibroblast: the renaissance cell. Circ Res, 105(12), 1164-1176. https://doi.org/10.1161/circresaha.109.209809

Tabaczar, S., Czogalla, A., Podkalicka, J., Biernatowska, A., & Sikorski, A. F. (2017, Jun). Protein palmitoylation: Palmitoyltransferases and their specificity. Exp Biol Med (Maywood), 242(11), 1150-1157. https://doi.org/10.1177/1535370217707732

Tallquist, M. D. (2020, Feb 10). Cardiac Fibroblast Diversity. Annu Rev Physiol, 82, 63-78. https://doi.org/10.1146/annurev-physiol-021119-034527

Tallquist, M. D., & Molkentin, J. D. (2017, Aug). Redefining the identity of cardiac fibroblasts. Nat Rev Cardiol, 14(8), 484-491. https://doi.org/10.1038/nrcardio.2017.57

Tsutsumi, R., Fukata, Y., Noritake, J., Iwanaga, T., Perez, F., & Fukata, M. (2009, Jan). Identification of G protein alpha subunit-palmitoylating enzyme. Mol Cell Biol, 29(2), 435-447. https://doi.org/10.1128/mcb.01144-08

Tuleta, I., & Frangogiannis, N. G. (2021, Sep). Fibrosis of the diabetic heart: Clinical significance, molecular mechanisms, and therapeutic opportunities. Adv Drug Deliv Rev, 176, 113904. https://doi.org/10.1016/j.addr.2021.113904

Umbarkar, P., Ejantkar, S., Tousif, S., & Lal, H. (2021, Sep 14). Mechanisms of Fibroblast Activation and Myocardial Fibrosis: Lessons Learned from FB-Specific Conditional Mouse Models. Cells, 10(9). https://doi.org/10.3390/cells10092412

van den Borne, S. W., Diez, J., Blankesteijn, W. M., Verjans, J., Hofstra, L., & Narula, J. (2010, Jan). Myocardial remodeling after infarction: the role of myofibroblasts. Nat Rev Cardiol, 7(1), 30-37. https://doi.org/10.1038/nrcardio.2009.199

Verma, S. K., Lal, H., Golden, H. B., Gerilechaogetu, F., Smith, M., Guleria, R. S., Foster, D. M., Lu, G., & Dostal, D. E. (2011, Apr 1). Rac1 and RhoA differentially regulate angiotensinogen gene expression in stretched cardiac fibroblasts. Cardiovasc Res, 90(1), 88-96. https://doi.org/10.1093/cvr/cvq385

Wang, J., Wang, Y., Zhang, W., Zhao, X., Chen, X., Xiao, W., Zhang, L., Chen, Y., & Zhu, W. (2016, Jan 1). Phenylephrine promotes cardiac fibroblast proliferation through calcineurin-NFAT pathway. Front Biosci (Landmark Ed), 21(3), 502-513. https://doi.org/10.2741/4405

Xu, S. W., Liu, S., Eastwood, M., Sonnylal, S., Denton, C. P., Abraham, D. J., & Leask, A. (2009, Oct 13). Rac inhibition reverses the phenotype of fibrotic fibroblasts. PLoS One, 4(10), e7438. https://doi.org/10.1371/journal.pone.0007438

Yatabe, J., Sanada, H., Yatabe, M. S., Hashimoto, S., Yoneda, M., Felder, R. A., Jose, P. A., & Watanabe, T. (2009, May). Angiotensin II type 1 receptor blocker attenuates the activation of ERK and NADPH oxidase by mechanical strain in mesangial cells in the absence of angiotensin II. Am J Physiol Renal Physiol, 296(5), F1052-1060. https://doi.org/10.1152/ajprenal.00580.2007

Zhang, M., Zhou, L., Xu, Y., Yang, M., Xu, Y., Komaniecki, G. P., Kosciuk, T., Chen, X., Lu, X., Zou, X., Linder, M. E., & Lin, H. (2020, Oct). A STAT3 palmitoylation cycle promotes T(H)17 differentiation and colitis. Nature, 586(7829), 434-439. https://doi.org/10.1038/s41586-020-2799-2

Zhang, Y., Qin, Z., Sun, W., Chu, F., & Zhou, F. (2021). Function of Protein S-Palmitoylation in Immunity and Immune-Related Diseases. Front Immunol, 12, 661202. https://doi.org/10.3389/fimmu.2021.661202

Zhou, B., Hao, Q., Liang, Y., & Kong, E. (2023, Jan). Protein palmitoylation in cancer: molecular functions and therapeutic potential. Mol Oncol, 17(1), 3-26. https://doi.org/10.1002/1878-0261.13308

Chapter V: General Discussion

Conclusions

Extracellular matrix (ECM) dysregulation can accompany a wide variety of cardiovascular diseases (CVDs), leading to maladaptive collagen accumulation, scar formation, and the development of cardiac fibrosis (Bretherton et al., 2020; Frangogiannis, 2021; Jiang et al., 2021; Kong et al., 2014). Cardiac fibrosis can impair contractility, induce diastolic dysfunction, potentiate arrhythmias, and ultimately contribute to heart failure (Frangogiannis, 2021; Kazbanov et al., 2016; Liu et al., 2022; Reed et al., 2011). Cardiac fibroblasts are the principal cellular mediators of this process, playing key roles in the generation and maintenance of the cardiac ECM at baseline, as well as scar formation in the injured heart (Fan et al., 2012; Tallquist, 2020; Tallquist & Molkentin, 2017). In response to injury, these cells are sensitive to a host of chemical and mechanical stimuli that originate in the diseased heart that regulate their activation and contribution to scar formation (Bretherton et al., 2020; Kanisicak et al., 2016; Tallquist & Molkentin, 2017). Given the increased understanding of the importance of these cells in heart physiology, substantial attention has been placed on elucidating the signaling pathways that mediate the cardiac fibroblast activation response (Bertaud et al., 2023; Bretherton et al., 2020; Herum, Lunde, et al., 2017). While advances have been made toward understanding the signaling pathways critical to regulating cardiac fibroblast activation, there is still uncertainty in how these signaling pathways coordinate the disease-dependent responses seen in the fibrotic developments accompanying CVD (Kong et al., 2014; Zeigler et al., 2016). The post-translational lipid modification palmitoylation has been increasingly implicated in the signaling

of cancer, immune disorders, neurological disorders, and recently, cardiomyocyte hypertrophy and exocytosis (Baldwin et al., 2023; Cai et al., 2023; Cho & Park, 2016; De & Sadhukhan, 2018; Essandoh et al., 2020; Essandoh et al., 2023; Main & Fuller, 2022). While novel roles for palmitoylation in cardiac signaling regulation have emerged, as well as ways in which palmitoylation regulates fibrotic signaling in other cell types (Baldwin et al., 2023; Navarro-Lérida et al., 2012; Tsutsumi et al., 2009; Xu et al., 2023; Zhang et al., 2020), there is an absence of existing literature detailing how cardiac fibroblast signaling pathways may be influenced by the PTM. To this end, we performed the foremost investigations into this area through the works presented in the previous chapters.

Cardiac fibroblast researchers rely upon in vitro model systems to investigate signaling pathways that contribute to fibroblast activation (Landry et al., 2019). As a result of their role in sensing the cardiac microenvironment and modulating the ECM, cardiac fibroblasts are acutely sensitive to mechanical forces and the stiffness of the surrounding heart tissue (Gilles et al., 2020; Landry & Dixon, 2020; Meagher et al., 2021). Mechanosensitive signaling mechanisms in these cells induce their activation in order to respond to injury, resulting in the myofibroblast phenotype and associated increases in proliferation, collagen synthesis and deposition, and cytokine secretion (Herum, Lunde, et al., 2017; Landry & Dixon, 2020; Landry et al., 2019; Meagher et al., 2021). Cardiac fibroblasts have gained notoriety for how their mechanosensitivity yields major difficulty in their study in vitro, as a quiescent population of primary cardiac fibroblasts quickly becomes highly activated in culture (Landry et al., 2019). High-baseline activation present in traditional cell culture plastic and glass dishes majorly reduces the dynamic range necessary for effective study of activation in these cells, as even treating with TGFβ1 cannot provide a meaningful induction relative to the control group even in

the absence of stimulation (Herum, Choppe, et al., 2017; Landry et al., 2019, 2021). As such, cardiac fibroblast researchers have developed ways to overcome this issue by conducting cell culture experiments in a more physiologic in vitro environment. To do this, researchers have turned to the use of "soft" substrate-coated dishes that can replicate the endogenous 5-10 kPa stiffness rating of the heart and allow for a longer fibroblast quiescence in culture (Cheng et al., 2021; Landry et al., 2019, 2021; Morningstar et al., 2021; Shiraishi et al., 2023; Wang et al., 2021). In the recent past, commercially available options have arisen that provide a way for researchers to maintain inactivated cells. However, they can be prohibitively expensive, reducing their accessibility.

Our attempts at investigating cardiac fibroblast activation involved TGFβ1-induction on traditional glass coverslips prior to the development of this protocol. Using conventional methods, baseline activation of primary ACFs was consistently ~90-100% positive for αSMA, irrespective of saline or TGFβ1 treatment. Thus, the attempts at answering our experimental questions were largely in vain as the baseline activation was too high to effectively induce an activation difference with pro-fibrotic agonists. To this end, we developed the protocol described here for the in-house generation of 8 kPa polydimethylsiloxane (PDMS)-based soft substrates for use in cardiac fibroblast cell culture. This protocol controls for a number of variables that influence cardiac fibroblast activation in vitro, including stiffness, total plated time, media, serum conditions, transduction efficiency, confluency, and TGFβ1 treatment time course. Attaining quiescent fibroblasts from the development of these assay conditions was instrumental in beginning to answer our experimental questions surrounding the involvement of S-acyltransferases and palmitoylation-mediated signaling in the heart. Additionally, the accessibility of lab-generated coverslips coated with 8kPa PDMS will likely be useful for other

cardiac fibroblast researchers who are similarly struggling with high baseline activation in their assays.

Following the development and optimization of the in vitro assay conditions, we conducted the first probes into the role of S-acyltransferases in the realm of cardiac fibroblast biology. Outside of cardiac signaling, zDHHC3 is known to regulate a number of pro-fibrotic signaling pathways, including STAT3, Rac1, and $G\alpha_q$ (Baldwin et al., 2023; Navarro-Lérida et al., 2012; Tsutsumi et al., 2009; Zhang et al., 2020). Thus, we originally hypothesized that zDHHC3-mediated palmitoylation would be critically involved in pro-fibrotic signaling pathways in cardiac fibroblasts, and that the deletion of *Zdhhc3* in vitro and in vivo would yield reductions in myofibroblast transformation and the development of fibrosis in response to injury, respectively. However, at the completion of our in vitro works investigating this hypothesis, it appears as though TGFβ1-induced signaling pathways were not reliant on zDHHC3 activity. αSMA positivity and pro-fibrotic gene expression in response to TGFβ1 were largely unaffected by the deletion of *Zdhhc3* in vitro. Similarly, cardiac fibroblast migration was consistent with controls in *Zdhhc3* KO cells.

Following the lack of a cardiac fibroblast activity phenotype in response to TGFβ1, an in vivo myofibroblast *Zdhhc3* KO model was generated in order to test for the dependence of cardiac fibroblast activation on this enzyme in contexts not adequately assessed as part of the in vitro experiments detailed here. Of course, it could be hypothesized that there would not be a reduction to in vivo fibrosis according to the *Zdhhc3* KO αSMA data response and lack of changes to activated fibroblast marker genes. Alternatively, we considered that it is also possible that zDHHC3 is not required for TGFβ1-induced activation, but plays a more essential role in other pathways not specifically altered through the in vitro analyses. While TGFβ1-induced

signaling is at the forefront of key pathways involved in activation, we hypothesized that an in vivo system that contains the full physiologic complexity of coordinated activation pathways may be more sensitive to the absence of *Zdhhc3*. Additionally, in vitro assays involve only one cell type, and given the possibility that *Zdhhc3* was required for a critical interaction between cardiac fibroblasts and other cells in the heart such as cardiomyocytes or immune cells, an in vivo system was necessary to explore these outcomes. However, in vivo myofibroblast-specific *Zdhhc3* KO did not yield a cardiac phenotype compared to control animals, suggesting that cardiac hypertrophy and fibrosis are not dependent on zDHHC3 in cardiac fibroblasts.

To investigate the role of these enzymes in cardiac fibroblast biology, our major strategy involved the targeted deletion of an individual enzyme and evaluating common metrics of fibroblast activation. While in many cases this is sufficient in inducing phenotypic changes, the potential for compensatory responses by other S-acyltransferases remained a major confounding factor in the interpretation of these results. The lack of an anti-fibrotic phenotype in vitro and in vivo in our *Zdhhc3* KO models led us to hypothesize that other enzymes may be compensating for the loss of zDHHC3. In consideration of which enzymes were most likely to provide this compensation, zDHHC7 has the greatest sequence homology with zDHHC3 of the S-acyltransferases, and is known to maintain an overlapping substrate profile with zDHHC3 (Baldwin et al., 2023; Tsutsumi et al., 2009; Zhang et al., 2020), and as such, the continuation of this line of research involved determining whether zDHHC7 was compensating for the loss of zDHHC3 in pro-fibrotic signaling through knocking out both enzymes simultaneously. Concurrently, we decided to investigate whether zDHHC7 signaling was required independently of zDHHC3 to further characterize the potential differences between the involvement of these enzymes in pro-fibrotic signaling. Surprisingly, besides a slightly decreased induction of

expression of the myofibroblast marker gene *Postn*, *Zdhhc7,* and *Zdhhc3/7* KO cardiac fibroblasts responded similarly to controls in expression of pro-fibrotic genes in vitro and did not exhibit any differences in NFAT or NFκB transcription factor activity in response to TGFβ1. While *Zdhhc7* KO ACFs exhibited a reduction in migratory ability in vitro, this result may not ultimately be physiologically relevant, as our in vivo studies indicate that mice with *Zdhhc7* KO and *Zdhhc3/7* KO in fibroblasts respond similarly to controls in response to AngII/PE-mediated cardiac injury.

At the conclusion of these investigations, it appears that zDHHC3 and zDHHC7 in cardiac fibroblasts are not essential for TAC and AngII/PE-induced hypertrophy and cardiac fibrosis. Considering the previously reported involvement of palmitoylation in the regulation of pro-fibrotic signaling proteins by these enzymes (Baldwin et al., 2023; Navarro-Lérida et al., 2012; Tsutsumi et al., 2009; Zhang et al., 2020), the lack of a phenotype was somewhat surprising. However, these results are consistent with the adjacent findings that deletion of *Zdhhc3 and Zdhhc7* in cardiomyocytes did not result in major changes to injury-induced cardiac remodeling (Baldwin et al., 2023). While there was substantial evidence for zDHHC3 involvement in Rac1 palmitoylation and activation of Rho family GTPases, as well as cardiomyocyte zDHHC3 activity majorly contributing to the development of cardiac remodeling, deletion of both *Zdhhc3* and *Zdhhc7* in cardiomyocytes did not result in protection from chronic hypertrophy in response to an 8-week TAC time-course and AngII infusion (Baldwin et al., 2023). The combination of these results indicate that these enzymes are not explicitly required for the hypertrophic and fibrotic remodeling processes in the heart in either cardiomyocytes or cardiac fibroblasts.

Though, there are a number of important limitations to consider in the interpretation of these results. These experiments largely relied upon genetic strategies where either S-acyltransferase whole-body knockout or LoxP-targeted mice were used to explore the dependence of fibroblast activation on individual zDHHCs. This is in large part due to the lack of individual zDHHC inhibitors, precluding us from using small molecule strategies to inhibit S-acyltransferase activity and determine the consequences on cardiac fibroblast activation (Lan et al., 2021). While pan-zDHHC inhibitors such as 2-bromopalmitate (2-BP) and cyanomethyl-N-myracrylamide (CMA) are capable of inhibiting palmitoylation at a global scale within the cell, it is difficult to draw meaningful conclusions from these results given how many signaling pathways rely upon palmitoylation to regulate their activity (Azizi et al., 2021; Davda et al., 2013). Furthermore, as 2-BP and CMA are not appropriate for use in vivo, experimental conclusions can be drawn using these compounds only from cellular applications. Thus, it remains a possibility that further enzymatic activity mediated by additional S-acyltransferases outside of zDHHC3 and zDHHC7 could be compensating for the loss of these enzymes; other enzymes may be more essential for regulating pro-fibrotic signaling in CFs, or that zDHHC enzymes simply do not play an appreciable role in CF activity. The individual knockout strategies detailed here only included 2 of the 23- known S-acyltransferases expressed in mammals. Aside from *Zdhhc3* and *Zdhhc7*, recent single-cell RNA sequencing data has determined that roughly half of the S-acyltransferases are expressed in cardiac fibroblasts, including *Zdhhc1*, *Zdhhc2*, *Zdhhc5*, *Zdhhc6*, *Zdhhc13*, *Zdhhc14*, *Zdhhc15*, *Zdhhc17*, *Zdhhc20*, and *Zdhhc21* (Chaffin et al., 2022).

Aside from the notion of enzymatic compensation, it is also relevant that these experiments only included murine models of heart disease and a limited assessment of the stress-

inducible pathways at play in cardiac fibroblasts. Of course, mouse models of cardiac disease are well established (Jia et al., 2020), though one additional possibility is that due to differences in the physiology in the mouse heart, the loss of zDHHC3 and zDHHC7 is not eliciting a phenotype that would otherwise be present in the human heart. Repeating these experiments with an alternative animal model, such as rabbits, would likely be more indicative of the true importance of these enzymes in cardiac fibroblast biology, given that their hearts more closely approximate human cardiac physiology compared to mice (Hornyik et al., 2022). However, our reliance on genetic strategies is a major impetus for using mice in order to generate a technically feasible and cost-effective model. Furthermore, these analyses were not an exhaustive characterization of the role of these enzymes in every aspect of cardiac biology. Additional metrics of cardiac biology that were not measured, such as intercellular communication, arrythmias, and fibroblast-mediated inflammation, could prove to be more reliant on zDHHC3 and zDHHC7 signaling. Our focus specifically on ventricular fibrosis is informed by commonly established cardiac injury models such as TAC and AngII/PE infusion, which show a direct link between pressure overload and ventricular remodeling, as well as AngII/PE-induced ventricular hypertrophy (Mazzolai et al., 2000; Platt et al., 2018; Yasunari et al., 2005). However, changes to atrial fibroblast activation when zDHHC3 and zDHHC7 are absent are also a possibility. Atrial fibrosis is a major contributor to the generation of atrial fibrillation (Ma et al., 2021), and thus, changes to atrial fibrosis in *Zdhhc3* and *Zdhhc7* KO conditions could be contributing to the generation of arrhythmias in the heart that would be unnoticed given our focus specifically on ventricular remodeling and function. Even within the ventricles, our analyses did not include assessments of cardiac arrhythmias, which could potentially present due to changes in ECM remodeling. With that being said, due to the significant differences in heart rate and electrophysiology between

mouse and human hearts (Kaese & Verheule, 2012), experiments in mice would not necessarily elucidate phenotypes present in human physiology.

An additional limitation is that the in vitro component of these analyses solely focused on myofibroblast transformation induced with TGFβ1 due to its major involvement in eliciting this phenotype (Frangogiannis, 2020). As discussed previously, a variety of pathways stimulated by other agonists such as AngII, IL6, and even mechanical stress are involved in cardiac fibroblast activation, and it is possible that S-acyltransferase activity may be more essential downstream of non-TGFβ1-induced pathways (Bertaud et al., 2023; Bretherton et al., 2020; Herum, Lunde, et al., 2017). In practice, the induction of murine cardiac fibroblast activation with agonists aside from TGFβ1 can be difficult to achieve, in part due to the technical limitations associated with mechanical stiffness of in vitro cell culture. Nonetheless, as a result of the sole use of TGFβ1 in our in vitro analyses, it cannot be concluded that zDHHC3 and zDHHC7 are not required for activation downstream of other pro-fibrotic ligands.

Given the importance of collagen in cardiac scar formation, staining for collagen with picrosirius red (PSR) is a common strategy for quantifying ECM remodeling (Fu et al., 2018; Khalil et al., 2019; Vogel et al., 2015). However, the assessment of fibrosis using PSR staining of collagen in histologic sections of the heart can present technical challenges. The lack of sensitivity in this method in being able to detect subtle or even substantial changes to collagen accumulation is a significant limitation of the assessment of fibrosis with PSR, as highlighted by previous works assessing cardiac ECM remodeling via PSR as well as mass spectrometry (Travers et al., 2021). In these data, they found no observable differences in fibrosis as measured by PSR in response to their cardiac injury model, however, assessment of cardiac ECM-fraction proteins with mass spectrometry indicated that over 100 proteins were upregulated in the injured

mouse hearts relative to controls (Travers et al., 2021). Thus, the sensitivity of picrosirius red staining can be inadequate in detecting changes to collagen levels and ECM changes in cardiac sections, even when significant changes to ECM composition are present as assessed by more sensitive testing such as mass spectrometry (Travers et al., 2021). The interpretations of our data in terms of determining the reliance of fibrotic responses on S-acyltransferases in CFs are similarly limited due to the lack of sensitivity present in this assay. It is thus possible that utilizing alternative measurements of cardiac ECM composition may have resulted in the elucidation of more subtle differences between control and *Zdhhc3/7* KO mice that were not obvious in PSR quantification. Further, collagen is only one of hundreds of proteins involved in the ECM, and thus, the conclusions drawn from our PSR staining data only represent potential changes to a single ECM protein, and any other changes to ECM remodeling in response to the loss of these enzymes would not be detected. Finally, the level of variability present between samples, even within the same injury model condition, can result in statistical variability and necessitate the use of increased sample sizes to achieve enough statistical power to properly compare groups.

In recognition of the possibility of enzymatic compensation, modulating palmitoylation involvement via the Rac1 C178S mutation provided an alternative analysis into how this PTM may be influencing a specific signaling protein involved in cardiac fibroblast activation. Due to the involvement of Rac1 in fibroblast activation and migration (Kunschmann et al., 2019; Lavall et al., 2017; Liu et al., 2009; Lyu et al., 2021; Ma et al., 2023; Martínez-López et al., 2021), as well as its known regulation by palmitoylation (Baldwin et al., 2023; Navarro-Lérida et al., 2012), we originally hypothesized that ACFs with a Rac1 C178S mutation would exhibit blunted myofibroblast transformation when stimulated. Our in vitro analyses using the Rac1 KI ACFs

indicate that TGFβ1-mediated activation in terms of elevated αSMA expression and pro-fibrotic gene mRNA levels can occur in the absence of Rac1 palmitoylation. This result could, in part, be due to the fact that Rac1 is not directly downstream of TGFβ1-mediated signaling, and it may be more likely that induction from other agonists, including those signaling through Gαq, would be blunted by the Rac1 palmitoylation mutant. However, these results are further complicated by the result that Rac1 palmitoylation mutant cardiac fibroblasts contrastingly exhibited heightened NFAT and SRF transcription factor activity in response to TGFβ1. This result indicates that Rac1 palmitoylation is required for the proper activation response of NFAT and SRF downstream of TGFβ1 in CFs and that the loss of Rac1 palmitoylation alters the proper signaling in such a way that increases NFAT/SRF activation. Changes to Rac1 localization and interaction with effector proteins could contribute to this effect, as depalmitoylated Rac1 could have an increased ability to promote signaling that increases NFAT and SRF activity. Compensatory pathways at play could induce NFAT and SRF activation in response to the loss of pro-fibrotic stimulation from Rac1 when its palmitoylation is prevented. Further investigations are required to determine how palmitoylation of Rac1 regulates NFAT and SRF activity in ACFs. While previous reports investigating Rac1 regulation by palmitoylation showed that overexpression of a Rac1 palmitoylation deficient mutant induced migration deficits in COS7 cells (Navarro-Lérida et al., 2012), in our model, primary ACFs with Rac1 palmitoylation deficiency at endogenous levels did not produce obvious defects in migratory ability at 24 hours. This result could be attributed to cell-specific differences, or potentially that the supraphysiological levels of palmitoylation deficient Rac1 in their overexpression system elicited a dominant negative effect (Navarro-Lérida et al., 2012). Further, Rac1 palmitoylation may be more required for signaling in response to stress, and thus, stimulation may be required to elicit a migratory phenotype not seen at

baseline in the absence of treatments. Finally, Rac1-mediated regulation of cytoskeletal organization, such as lamellipodia formation, cell spreading, and adhesion not measured here, could be more dependent on Rac1 palmitoylation and represent potential areas of future research.

Future Directions

Explorations into the role of palmitoylation in cardiac fibroblast signaling are in their infancy, and many exciting avenues of study remain to discover how the signaling pathways underlying fibroblast activation are modulated by this PTM in cardiac fibroblasts. Our major strategy involved the targeted deletion of individual enzymes and evaluating common metrics of fibroblast activation. While, in many cases, this is sufficient in inducing phenotypic changes, the potential for compensatory responses by other S-acyltransferases remains a possibility. As mentioned previously, there are a number of other S-acyltransferases that are expressed in ACFs, which may prove essential for the activation process and the development of fibrosis (Chaffin et al., 2022).

Further phenotyping could be considered to look into how other S-acyltransferases expressed in ACFs participate in the activation process. In future efforts to establish the importance of these enzymes in fibroblast biology, the utilization of individually deleted enzymes using KO mouse models may not be the optimal route. Alternatively, one strategy that could be undertaken would be to conduct a screen for S-acyltransferases expressed in cardiac fibroblasts using a quiescent population of human cardiac fibroblasts treated in the control condition and in response to a panel of pro-fibrotic ligands. To test for the dependence of these enzymes in αSMA expression, populations of quiescent fibroblasts could be treated with agonists such as TGFβ1, AngII, and IL6 following treatment with siRNAs targeting individual S-acyltransferases known to be expressed in cardiac fibroblasts. Combinatorial treatments could

additionally be conducted by grouping siRNAs for related enzymes in terms of sequence homology or cellular location. While this strategy would not be able to provide in vivo results, they could inform the generation of future animal models with genetic deletion of an enzyme or enzymes that exhibits a phenotype using the in vitro screen.

An additional area of future investigation is the global assessment of changes in palmitoylation levels of the cardiac fibroblast proteome between quiescent and activated cells. One of the foundational hypotheses for these works is that the signaling underlying myofibroblast transformation involves changes in the palmitoylation of proteins involved in these activation pathways. While single enzyme deletion approaches can be undertaken to investigate this, the literature on fibrotic signaling influencing palmitoylation remains quite limited at present, resulting in a limited data set from which to draw promising candidate proteins. One alternative strategy to navigate this is by performing a proteome-wide assessment of how protein palmitoylation levels of cardiac fibroblasts change in response to pro-fibrotic agonists. To test this, a quiescent population of cardiac fibroblasts could be activated with a pro-fibrotic stimulus such as TGFβ1 or AngII, presumably resulting in changes to the palmitoylation levels of substrates involved in the activation process. Techniques such as acyl resin-assisted capture and acyl-biotin exchange yield the capability to affinity-purify palmitoylated proteins (Baldwin et al., 2023; Buffa et al., 2023; Essandoh et al., 2023), allowing for analysis via mass spectrometry to quantify differences in substrate palmitoylation at the proteome level between the activated fibroblasts and a quiescent control. These data can provide insights into which proteins exhibit the largest differences in palmitoylation levels as part of the myofibroblast induction process, and upon determining a selection of promising candidate proteins, follow-up experiments to verify changes in their palmitoylation levels could be performed. A sufficiently

powered and controlled study could provide a highly novel and informative dataset of changes to cardiac fibroblast protein palmitoylation in response to TGFβ1, providing direction for a subsequent in-depth characterization of candidate proteins that had significant up or down-regulation of their palmitoylation levels. The opportunity for a comparison between other agonists is present as well, allowing for the uncovering of agonist-specific differences in directing the signaling responses underlying cardiac fibroblast activation. Overall, the generation of a data set of this type represents a favorable direction in terms of future inquiries in how substrate palmitoylation levels change in the ACF activation process. Future works that establish the importance of a particular pro-fibrotic substrate could potentially explore therapeutic strategies for inhibiting palmitoylation signaling, such as through APT inhibitors, compounds that inhibit enzyme/substrate interactions, or compounds that prevent substrate palmitoylation through cysteine alkylation (Chen et al., 2023; Hansen et al., 2018; Hansen et al., 2019; Moors et al., 2023; Zhang et al., 2020).

The result that Rac1 palmitoylation appears to be required for the proper induction of NFAT and SRF in response to TGFβ1 is intriguing, and further experiments could be conducted to characterize the consequences of this mutation in cardiac fibroblast signaling. A GTP-loading assay could provide evidence for how the loss of Rac1 palmitoylation influences its activation in CFs. Western blots for a panel of pro-fibrotic signaling proteins may also be illuminating as to whether there are changes to signaling protein activation levels in response to TGFβ1 in control ACFs and Rac1 palmitoylation mutant ACFs. To further explore the role of Rac1 palmitoylation in cardiac fibroblast activation, Rac1 ConKI mice could be crossed with a fibroblast specific Cre line such as PostnMCM, Tcf21MCM, or Pdgfra-CreERT2 to generate myofibroblast or cardiac fibroblast-specific knock-in mice (Chung et al., 2018; Kanisicak et al., 2016), which could be

used to assess in vivo the dependence of cardiac remodeling on Rac1 palmitoylation. Given the increased NFAT and SRF activity seen in vitro, this mutation may yield an in vivo phenotype due to alterations in transcription factor activity.

Aside from these general areas of inquiry intended to generate new leads for further enzyme or substrate characterization, one interesting area of future work in the context of cardiac fibroblast signaling involves directly evaluating how $G\alpha_q$ regulates cardiac fibroblast signaling and how palmitoylation contributes to its signaling ability. As discussed in previous sections, $G\alpha_q$ signaling is initiated downstream of many GPCRs known to be involved in fibroblast activation and the development of fibrosis, including angiotensin II type I receptor (AT1R), the adenosine A2B receptor, the α1 adrenergic receptor, and endothelin 1 (ET1) receptors A and B (Alter et al., 2023; Bai et al., 2013; Duangrat et al., 2023; Duangrat et al., 2022; Wang et al., 2016). Recent in vitro studies highlight the importance of $G\alpha_q$ in cardiac fibroblast signaling, and showed that the inhibition of $G\alpha_q$ using the small molecule inhibitor FR900359 (Schlegel et al., 2021) significantly reduced AngII-mediated, as well as ET1-mediated human cardiac fibroblast activation (Duangrat et al., 2023; Parichatikanond et al., 2023). Despite this, direct investigations into the relative contribution of $G\alpha_q$ in mediating ACF activation are lacking, and little is known about how $G\alpha_q$ palmitoylation may be regulating the downstream signaling of the many pro-fibrotic agonists that activate CFs. Preliminary investigations into this area from our lab provide evidence that $G\alpha_q$ inhibition with FR900359 significantly reduces TGFβ1-induced increases in NFAT and NFκB activity (Figure 5.1A, B). Further, induction of SRF activity with high serum concentrations was also significantly reduced with FR900359 treatment (Figure 5.1C). Future experiments aimed at determining the signaling protein changes that are contributing to these effects, as well as those involved downstream of $G\alpha_q$-coupled receptors, would provide key

information toward unraveling the importance of $G\alpha_q$ in cardiac fibroblast signaling. While previous reports have determined that $G\alpha_q$ is palmitoylated by zDHHC3 and zDHHC7 (Tsutsumi et al., 2009), the consequences of this modification on $G\alpha_q$ signaling similarly remain quite limited. We hypothesize that regulation of $G\alpha_q$ by palmitoylation contributes to its plasma membrane localization, and that disrupting the palmitoylation of $G\alpha_q$ may abrogate the fibrogenic signaling pathways it is involved in and reduce myofibroblast formation in vitro and fibrosis in the heart in vivo. Potentially promising areas of future research include determining whether $G\alpha_q$ palmitoylation influences its localization, ability to associate with GPCRs, and whether activation of $G\alpha_q$-coupled GPCRs can initiate PLC activation and intracellular calcium increases in the absence of $G\alpha_q$ palmitoylation. Further, if disruptions in signaling are observed, additional studies could focus on characterizing the influence of these changes on cardiac fibroblast activation in vitro and remodeling in the heart in vivo. These studies would provide crucial evidence for how palmitoylation modifies the activity of this crucial fibroblast regulatory protein and advance our understanding of GPCR-related signaling in general.

In conclusion, the field of cardiac fibroblast biology continues to expand, and there is an abundance of ongoing explorations into the intricacies of ACF signaling processes that facilitate cardiac fibroblast activation. The contributions of S-acyltransferases to cardiac fibroblast biology remain incompletely understood, prompting the need for continued research in exploring critical enzymes that may be regulating cardiac fibroblast activation pathways. Future investigations into this area may uncover additional roles for these enzymes in the facilitation of substrate signal transduction and determine the consequences of these modifications on downstream remodeling in the heart. Further characterization of these signaling pathways will likely contribute to the

identification of novel and clinically relevant targets and potentially lead to unique future strategies for the treatment of cardiac fibrosis.

Chapter V Figures

Figure 5.1. $G\alpha_q$ Inhibition with FR900359 Reduces Pro-fibrotic Transcription Factor Activity in Adult Cardiac Fibroblasts

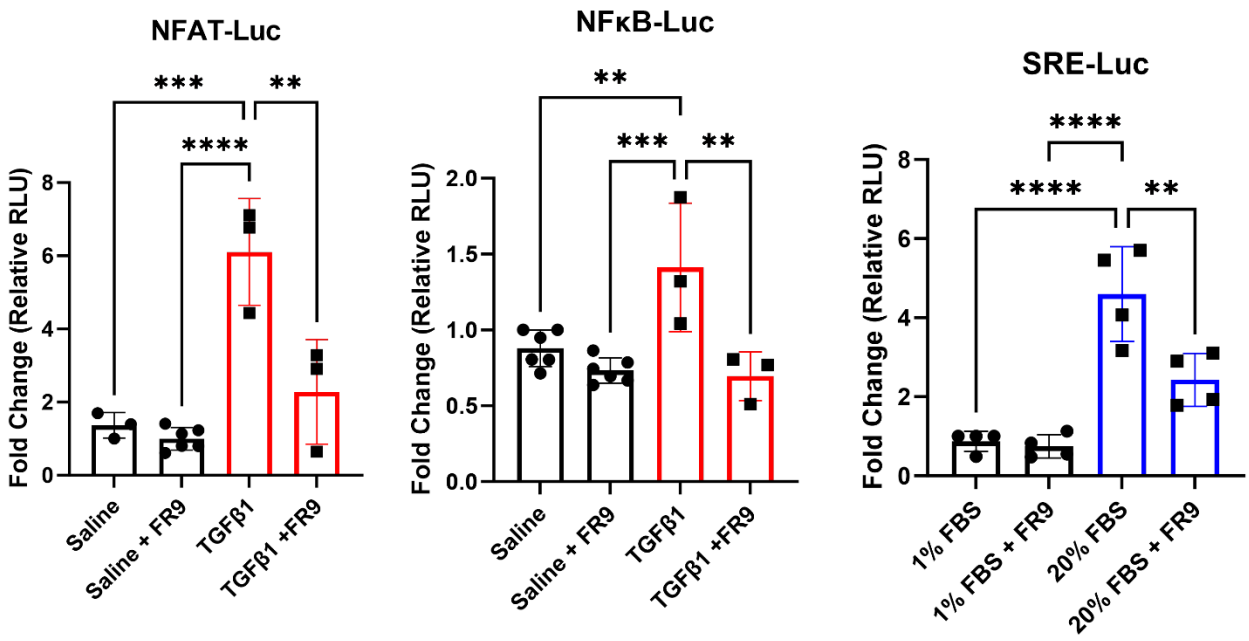

Figure 5.1: Gαq Inhibition with FR900359 Reduces Pro-fibrotic Transcription Factor Activity in Adult Cardiac Fibroblasts*. (A) NFAT luciferase promoter activity quantification in WT ACFs treated with either saline or TGFβ1 (10 ng/mL) +/- the Gαq inhibitor FR900359 (1 μM) (Cayman, #33666) for 48 hours, n=3-6. All FR900359-treated samples were pre-treated with FR900359 for 1 hour prior to experimental time course. One way ANOVA with Tukey's multiple comparisons test, (p=.0001), (B) NFκB luciferase promoter activity quantification in WT ACFs treated with either saline or TGFβ1 (10 ng/mL) +/- FR900359 (1 μM) for 48 hours, n=3-6. All FR900359-treated samples were pre-treated with FR900359 for 1 hour prior to experimental time course. One way ANOVA with Tukey's multiple comparisons test, (p=.0010), (C) SRE luciferase promoter activity quantification in WT ACFs treated with either 1% FBS or 20% FBS +/- FR900359 (1 μM) for 48 hours, n=4. All FR900359-treated samples were pre-treated with FR900359 for 1 hour prior to experimental time course. One way ANOVA with Tukey's multiple comparisons test, (p<.0001). Error bars indicate the mean +/- standard deviation, significance denoted as (p<0.05, *), (p<0.01, **), (p<.001, ***), (p<.0001, ****).*

References

Alter, C., Henseler, A. S., Owenier, C., Hesse, J., Ding, Z., Lautwein, T., Bahr, J., Hayat, S., Kramann, R., Kostenis, E., Scheller, J., & Schrader, J. (2023, Jun 1). IL-6 in the infarcted heart is preferentially formed by fibroblasts and modulated by purinergic signaling. J Clin Invest, 133(11). https://doi.org/10.1172/jci163799

Azizi, S. A., Lan, T., Delalande, C., Kathayat, R. S., Banales Mejia, F., Qin, A., Brookes, N., Sandoval, P. J., & Dickinson, B. C. (2021, Aug 20). Development of an Acrylamide-Based Inhibitor of Protein S-Acylation. ACS Chem Biol, 16(8), 1546-1556. https://doi.org/10.1021/acschembio.1c00405

Bai, J., Zhang, N., Hua, Y., Wang, B., Ling, L., Ferro, A., & Xu, B. (2013). Metformin inhibits angiotensin II-induced differentiation of cardiac fibroblasts into myofibroblasts. PLoS One, 8(9), e72120. https://doi.org/10.1371/journal.pone.0072120

Baldwin, T. A., Teuber, J. P., Kuwabara, Y., Subramani, A., Lin, S. J., Kanisicak, O., Vagnozzi, R. J., Zhang, W., Brody, M. J., & Molkentin, J. D. (2023, Nov 3). Palmitoylation-Dependent Regulation of Cardiomyocyte Rac1 Signaling Activity and Minor Effects on Cardiac Hypertrophy. J Biol Chem, 105426. https://doi.org/10.1016/j.jbc.2023.105426

Bertaud, A., Joshkon, A., Heim, X., Bachelier, R., Bardin, N., Leroyer, A. S., & Blot-Chabaud, M. (2023, Jan 16). Signaling Pathways and Potential Therapeutic Strategies in Cardiac Fibrosis. Int J Mol Sci, 24(2). https://doi.org/10.3390/ijms24021756

Bretherton, R., Bugg, D., Olszewski, E., & Davis, J. (2020, Sep). Regulators of cardiac fibroblast cell state. Matrix Biol, 91-92, 117-135. https://doi.org/10.1016/j.matbio.2020.04.002

Buffa, V., Adamo, G., Picciotto, S., Bongiovanni, A., & Romancino, D. P. (2023, Mar 21). A Simple, Semi-Quantitative Acyl Biotin Exchange-Based Method to Detect Protein S-Palmitoylation Levels. Membranes (Basel), 13(3). https://doi.org/10.3390/membranes13030361

Cai, J., Cui, J., & Wang, L. (2023, Oct). S-palmitoylation regulates innate immune signaling pathways: molecular mechanisms and targeted therapies. Eur J Immunol, 53(10), e2350476. https://doi.org/10.1002/eji.202350476

Chaffin, M., Papangeli, I., Simonson, B., Akkad, A.-D., Hill, M. C., Arduini, A., Fleming, S. J., Melanson, M., Hayat, S., Kost-Alimova, M., Atwa, O., Ye, J., Bedi, K. C., Nahrendorf, M., Kaushik, V. K., Stegmann, C. M., Margulies, K. B., Tucker, N. R., & Ellinor, P. T. (2022, 2022/08/01). Single-nucleus profiling of human dilated and hypertrophic cardiomyopathy. Nature, 608(7921), 174-180. https://doi.org/10.1038/s41586-022-04817-8

Chen, X., Niu, W., Fan, X., Yang, H., Zhao, C., Fan, J., Yao, X., & Fang, Z. (2023, Jan 5). Oct4A palmitoylation modulates tumorigenicity and stemness in human glioblastoma cells. Neuro Oncol, 25(1), 82-96. https://doi.org/10.1093/neuonc/noac157

Cheng, X., Wang, L., Wen, X., Gao, L., Li, G., Chang, G., Qin, S., & Zhang, D. (2021, May). TNAP is a novel regulator of cardiac fibrosis after myocardial infarction by mediating TGF-β/Smads and ERK1/2 signaling pathways. EBioMedicine, 67, 103370. https://doi.org/10.1016/j.ebiom.2021.103370

Cho, E., & Park, M. (2016, Sep). Palmitoylation in Alzheimer's disease and other neurodegenerative diseases. Pharmacol Res, 111, 133-151. https://doi.org/10.1016/j.phrs.2016.06.008

Chung, M. I., Bujnis, M., Barkauskas, C. E., Kobayashi, Y., & Hogan, B. L. M. (2018, May 11). Niche-mediated BMP/SMAD signaling regulates lung alveolar stem cell proliferation and differentiation. Development, 145(9). https://doi.org/10.1242/dev.163014

Davda, D., El Azzouny, M. A., Tom, C. T., Hernandez, J. L., Majmudar, J. D., Kennedy, R. T., & Martin, B. R. (2013, Sep 20). Profiling targets of the irreversible palmitoylation inhibitor 2-bromopalmitate. ACS Chem Biol, 8(9), 1912-1917. https://doi.org/10.1021/cb400380s

De, I., & Sadhukhan, S. (2018, Jun). Emerging Roles of DHHC-mediated Protein S-palmitoylation in Physiological and Pathophysiological Context. Eur J Cell Biol, 97(5), 319-338. https://doi.org/10.1016/j.ejcb.2018.03.005

Duangrat, R., Parichatikanond, W., Likitnukul, S., & Mangmool, S. (2023, Feb 24). Endothelin-1 Induces Cell Proliferation and Myofibroblast Differentiation through the ET(A)R/G(αq)/ERK Signaling Pathway in Human Cardiac Fibroblasts. Int J Mol Sci, 24(5). https://doi.org/10.3390/ijms24054475

Duangrat, R., Parichatikanond, W., Morales, N. P., Pinthong, D., & Mangmool, S. (2022, Dec 15). Sustained AT(1)R stimulation induces upregulation of growth factors in human cardiac fibroblasts via G(αq)/TGF-β/ERK signaling that influences myocyte hypertrophy. Eur J Pharmacol, 937, 175384. https://doi.org/10.1016/j.ejphar.2022.175384

Essandoh, K., Philippe, J. M., Jenkins, P. M., & Brody, M. J. (2020). Palmitoylation: A Fatty Regulator of Myocardial Electrophysiology. Front Physiol, 11, 108. https://doi.org/10.3389/fphys.2020.00108

Essandoh, K., Subramani, A., Ferro, O. A., Teuber, J. P., Koripella, S., & Brody, M. J. (2023, May). zDHHC9 Regulates Cardiomyocyte Rab3a Activity and Atrial Natriuretic Peptide Secretion Through Palmitoylation of Rab3gap1. JACC Basic Transl Sci, 8(5), 518-542. https://doi.org/10.1016/j.jacbts.2022.11.003

Fan, D., Takawale, A., Lee, J., & Kassiri, Z. (2012, Sep 3). Cardiac fibroblasts, fibrosis and extracellular matrix remodeling in heart disease. Fibrogenesis Tissue Repair, 5(1), 15. https://doi.org/10.1186/1755-1536-5-15

Frangogiannis, N. (2020, Mar 2). Transforming growth factor-β in tissue fibrosis. J Exp Med, 217(3), e20190103. https://doi.org/10.1084/jem.20190103

Frangogiannis, N. G. (2021, May 25). Cardiac fibrosis. Cardiovasc Res, 117(6), 1450-1488. https://doi.org/10.1093/cvr/cvaa324

Fu, X., Khalil, H., Kanisicak, O., Boyer, J. G., Vagnozzi, R. J., Maliken, B. D., Sargent, M. A., Prasad, V., Valiente-Alandi, I., Blaxall, B. C., & Molkentin, J. D. (2018, May 1). Specialized fibroblast differentiated states underlie scar formation in the infarcted mouse heart. J Clin Invest, 128(5), 2127-2143. https://doi.org/10.1172/jci98215

Gilles, G., McCulloch, A. D., Brakebusch, C. H., & Herum, K. M. (2020). Maintaining resting cardiac fibroblasts in vitro by disrupting mechanotransduction. PLoS One, 15(10), e0241390. https://doi.org/10.1371/journal.pone.0241390

Hansen, A. L., Buchan, G. J., Rühl, M., Mukai, K., Salvatore, S. R., Ogawa, E., Andersen, S. D., Iversen, M. B., Thielke, A. L., Gunderstofte, C., Motwani, M., Møller, C. T., Jakobsen, A. S., Fitzgerald, K. A., Roos, J., Lin, R., Maier, T. J., Goldbach-Mansky, R., Miner, C. A., Qian, W., Miner, J. J., Rigby, R. E., Rehwinkel, J., Jakobsen, M. R., Arai, H.,

Taguchi, T., Schopfer, F. J., Olagnier, D., & Holm, C. K. (2018, Aug 14). Nitro-fatty acids are formed in response to virus infection and are potent inhibitors of STING palmitoylation and signaling. Proc Natl Acad Sci U S A, 115(33), E7768-e7775. https://doi.org/10.1073/pnas.1806239115

Hansen, A. L., Mukai, K., Schopfer, F. J., Taguchi, T., & Holm, C. K. (2019, 2019/03/01). STING palmitoylation as a therapeutic target. Cellular & Molecular Immunology, 16(3), 236-241. https://doi.org/10.1038/s41423-019-0205-5

Herum, K. M., Choppe, J., Kumar, A., Engler, A. J., & McCulloch, A. D. (2017, Jul 7). Mechanical regulation of cardiac fibroblast profibrotic phenotypes. Mol Biol Cell, 28(14), 1871-1882. https://doi.org/10.1091/mbc.E17-01-0014

Herum, K. M., Lunde, I. G., McCulloch, A. D., & Christensen, G. (2017, May 19). The Soft- and Hard-Heartedness of Cardiac Fibroblasts: Mechanotransduction Signaling Pathways in Fibrosis of the Heart. J Clin Med, 6(5). https://doi.org/10.3390/jcm6050053

Hornyik, T., Rieder, M., Castiglione, A., Major, P., Baczko, I., Brunner, M., Koren, G., & Odening, K. E. (2022, Mar). Transgenic rabbit models for cardiac disease research. Br J Pharmacol, 179(5), 938-957. https://doi.org/10.1111/bph.15484

Jia, T., Wang, C., Han, Z., Wang, X., Ding, M., & Wang, Q. (2020). Experimental Rodent Models of Cardiovascular Diseases. Front Cardiovasc Med, 7, 588075. https://doi.org/10.3389/fcvm.2020.588075

Jiang, W., Xiong, Y., Li, X., & Yang, Y. (2021). Cardiac Fibrosis: Cellular Effectors, Molecular Pathways, and Exosomal Roles. Front Cardiovasc Med, 8, 715258. https://doi.org/10.3389/fcvm.2021.715258

Kaese, S., & Verheule, S. (2012). Cardiac electrophysiology in mice: a matter of size. Front Physiol, 3, 345. https://doi.org/10.3389/fphys.2012.00345

Kanisicak, O., Khalil, H., Ivey, M. J., Karch, J., Maliken, B. D., Correll, R. N., Brody, M. J., SC, J. L., Aronow, B. J., Tallquist, M. D., & Molkentin, J. D. (2016, Jul 22). Genetic lineage tracing defines myofibroblast origin and function in the injured heart. Nat Commun, 7, 12260. https://doi.org/10.1038/ncomms12260

Kazbanov, I. V., ten Tusscher, K. H. W. J., & Panfilov, A. V. (2016, 2016/02/10). Effects of Heterogeneous Diffuse Fibrosis on Arrhythmia Dynamics and Mechanism. Scientific Reports, 6(1), 20835. https://doi.org/10.1038/srep20835

Khalil, H., Kanisicak, O., Vagnozzi, R. J., Johansen, A. K., Maliken, B. D., Prasad, V., Boyer, J. G., Brody, M. J., Schips, T., Kilian, K. K., Correll, R. N., Kawasaki, K., Nagata, K., & Molkentin, J. D. (2019, Aug 8). Cell-specific ablation of Hsp47 defines the collagen-producing cells in the injured heart. JCI Insight, 4(15), e128722. https://doi.org/10.1172/jci.insight.128722

Kong, P., Christia, P., & Frangogiannis, N. G. (2014, Feb). The pathogenesis of cardiac fibrosis. Cell Mol Life Sci, 71(4), 549-574. https://doi.org/10.1007/s00018-013-1349-6

Kunschmann, T., Puder, S., Fischer, T., Steffen, A., Rottner, K., & Mierke, C. T. (2019, May 22). The Small GTPase Rac1 Increases Cell Surface Stiffness and Enhances 3D Migration Into Extracellular Matrices. Sci Rep, 9(1), 7675. https://doi.org/10.1038/s41598-019-43975-0

Lan, T., Delalande, C., & Dickinson, B. C. (2021, Dec). Inhibitors of DHHC family proteins. Curr Opin Chem Biol, 65, 118-125. https://doi.org/10.1016/j.cbpa.2021.07.002

Landry, N. M., & Dixon, I. M. C. (2020, Dec). Fibroblast mechanosensing, SKI and Hippo signaling and the cardiac fibroblast phenotype: Looking beyond TGF-β. Cell Signal, 76, 109802. https://doi.org/10.1016/j.cellsig.2020.109802

Landry, N. M., Rattan, S. G., & Dixon, I. M. C. (2019, Sep 9). An Improved Method of Maintaining Primary Murine Cardiac Fibroblasts in Two-Dimensional Cell Culture. Sci Rep, 9(1), 12889. https://doi.org/10.1038/s41598-019-49285-9

Landry, N. M., Rattan, S. G., & Dixon, I. M. C. (2021). Soft Substrate Culture to Mechanically Control Cardiac Myofibroblast Activation. Methods Mol Biol, 2299, 171-179. https://doi.org/10.1007/978-1-0716-1382-5_13

Lavall, D., Schuster, P., Jacobs, N., Kazakov, A., Böhm, M., & Laufs, U. (2017, May 5). Rac1 GTPase regulates 11β hydroxysteroid dehydrogenase type 2 and fibrotic remodeling. J Biol Chem, 292(18), 7542-7553. https://doi.org/10.1074/jbc.M116.764449

Liu, H., Fan, P., Jin, F., Huang, G., Guo, X., & Xu, F. (2022). Dynamic and static biomechanical traits of cardiac fibrosis. Front Bioeng Biotechnol, 10, 1042030. https://doi.org/10.3389/fbioe.2022.1042030

Liu, S., Kapoor, M., & Leask, A. (2009, May). Rac1 expression by fibroblasts is required for tissue repair in vivo. Am J Pathol, 174(5), 1847-1856. https://doi.org/10.2353/ajpath.2009.080779

Lyu, L., Chen, J., Wang, W., Yan, T., Lin, J., Gao, H., Li, H., Lv, R., Xu, F., Fang, L., & Chen, Y. (2021, Mar). Scoparone alleviates Ang II-induced pathological myocardial hypertrophy in mice by inhibiting oxidative stress. J Cell Mol Med, 25(6), 3136-3148. https://doi.org/10.1111/jcmm.16304

Ma, J., Chen, Q., & Ma, S. (2021, Mar). Left atrial fibrosis in atrial fibrillation: Mechanisms, clinical evaluation and management. J Cell Mol Med, 25(6), 2764-2775. https://doi.org/10.1111/jcmm.16350

Ma, N., Xu, E., Luo, Q., & Song, G. (2023, Mar 27). Rac1: A Regulator of Cell Migration and a Potential Target for Cancer Therapy. Molecules, 28(7). https://doi.org/10.3390/molecules28072976

Main, A., & Fuller, W. (2022, Feb). Protein S-Palmitoylation: advances and challenges in studying a therapeutically important lipid modification. Febs j, 289(4), 861-882. https://doi.org/10.1111/febs.15781

Martínez-López, A., García-Casas, A., Bragado, P., Orimo, A., Castañeda-Saucedo, E., & Castillo-Lluva, S. (2021, Aug 19). Inhibition of RAC1 activity in cancer associated fibroblasts favours breast tumour development through IL-1β upregulation. Cancer Lett, 521, 14-28. https://doi.org/10.1016/j.canlet.2021.08.014

Mazzolai, L., Pedrazzini, T., Nicoud, F., Gabbiani, G., Brunner, H. R., & Nussberger, J. (2000, Apr). Increased cardiac angiotensin II levels induce right and left ventricular hypertrophy in normotensive mice. Hypertension, 35(4), 985-991. https://doi.org/10.1161/01.hyp.35.4.985

Meagher, P. B., Lee, X. A., Lee, J., Visram, A., Friedberg, M. K., & Connelly, K. A. (2021, Mar 31). Cardiac Fibrosis: Key Role of Integrins in Cardiac Homeostasis and Remodeling. Cells, 10(4). https://doi.org/10.3390/cells10040770

Moors, T. E., Li, S., McCaffery, T. D., Ho, G. P. H., Bechade, P. A., Pham, L. N., Ericsson, M., & Nuber, S. (2023, Nov 15). Increased palmitoylation improves estrogen receptor alpha-dependent hippocampal synaptic deficits in a mouse model of synucleinopathy. Sci Adv, 9(46), eadj1454. https://doi.org/10.1126/sciadv.adj1454

Morningstar, J. E., Gensemer, C., Moore, R., Fulmer, D., Beck, T. C., Wang, C., Moore, K., Guo, L., Sieg, F., Nagata, Y., Bertrand, P., Spampinato, R. A., Glover, J., Poelzing, S., Gourdie, R. G., Watts, K., Richardson, W. J., Levine, R. A., Borger, M. A., & Norris, R. A. (2021, Dec 21). Mitral Valve Prolapse Induces Regionalized Myocardial Fibrosis. J Am Heart Assoc, 10(24), e022332. https://doi.org/10.1161/jaha.121.022332

Navarro-Lérida, I., Sánchez-Perales, S., Calvo, M., Rentero, C., Zheng, Y., Enrich, C., & Del Pozo, M. A. (2012, Feb 1). A palmitoylation switch mechanism regulates Rac1 function and membrane organization. Embo j, 31(3), 534-551. https://doi.org/10.1038/emboj.2011.446

Parichatikanond, W., Duangrat, R., & Mangmool, S. (2023, Jul 15). G(αq) protein-biased ligand of angiotensin II type 1 receptor mediates myofibroblast differentiation through TGF-β1/ERK axis in human cardiac fibroblasts. Eur J Pharmacol, 951, 175780. https://doi.org/10.1016/j.ejphar.2023.175780

Platt, M. J., Huber, J. S., Romanova, N., Brunt, K. R., & Simpson, J. A. (2018). Pathophysiological Mapping of Experimental Heart Failure: Left and Right Ventricular Remodeling in Transverse Aortic Constriction Is Temporally, Kinetically and Structurally Distinct. Front Physiol, 9, 472. https://doi.org/10.3389/fphys.2018.00472

Reed, A. L., Tanaka, A., Sorescu, D., Liu, H., Jeong, E. M., Sturdy, M., Walp, E. R., Dudley, S. C., Jr., & Sutliff, R. L. (2011, Sep). Diastolic dysfunction is associated with cardiac fibrosis in the senescence-accelerated mouse. Am J Physiol Heart Circ Physiol, 301(3), H824-831. https://doi.org/10.1152/ajpheart.00407.2010

Schlegel, J. G., Tahoun, M., Seidinger, A., Voss, J. H., Kuschak, M., Kehraus, S., Schneider, M., Matthey, M., Fleischmann, B. K., König, G. M., Wenzel, D., & Müller, C. E. (2021, Apr

9). Macrocyclic Gq Protein Inhibitors FR900359 and/or YM-254890-Fit for Translation? ACS Pharmacol Transl Sci, 4(2), 888-897. https://doi.org/10.1021/acsptsci.1c00021

Shiraishi, M., Suzuki, K., & Yamaguchi, A. (2023, Apr). Effect of mechanical tension on fibroblast transcriptome profile and regulatory mechanisms of myocardial collagen turnover. Faseb j, 37(4), e22841. https://doi.org/10.1096/fj.202201899R

Tallquist, M. D. (2020, Feb 10). Cardiac Fibroblast Diversity. Annu Rev Physiol, 82, 63-78. https://doi.org/10.1146/annurev-physiol-021119-034527

Tallquist, M. D., & Molkentin, J. D. (2017, Aug). Redefining the identity of cardiac fibroblasts. Nat Rev Cardiol, 14(8), 484-491. https://doi.org/10.1038/nrcardio.2017.57

Travers, J. G., Wennersten, S. A., Peña, B., Bagchi, R. A., Smith, H. E., Hirsch, R. A., Vanderlinden, L. A., Lin, Y. H., Dobrinskikh, E., Demos-Davies, K. M., Cavasin, M. A., Mestroni, L., Steinkühler, C., Lin, C. Y., Houser, S. R., Woulfe, K. C., Lam, M. P. Y., & McKinsey, T. A. (2021, May 11). HDAC Inhibition Reverses Preexisting Diastolic Dysfunction and Blocks Covert Extracellular Matrix Remodeling. Circulation, 143(19), 1874-1890. https://doi.org/10.1161/circulationaha.120.046462

Tsutsumi, R., Fukata, Y., Noritake, J., Iwanaga, T., Perez, F., & Fukata, M. (2009, Jan). Identification of G protein alpha subunit-palmitoylating enzyme. Mol Cell Biol, 29(2), 435-447. https://doi.org/10.1128/mcb.01144-08

Vogel, B., Siebert, H., Hofmann, U., & Frantz, S. (2015, 2015/01/01/). Determination of collagen content within picrosirius red stained paraffin-embedded tissue sections using fluorescence microscopy. MethodsX, 2, 124-134. https://doi.org/https://doi.org/10.1016/j.mex.2015.02.007

Wang, A., Cao, S., Stowe, J. C., & Valdez-Jasso, D. (2021, Apr 23). Substrate Stiffness and Stretch Regulate Profibrotic Mechanosignaling in Pulmonary Arterial Adventitial Fibroblasts. Cells, 10(5). https://doi.org/10.3390/cells10051000

Wang, J., Wang, Y., Zhang, W., Zhao, X., Chen, X., Xiao, W., Zhang, L., Chen, Y., & Zhu, W. (2016, Jan 1). Phenylephrine promotes cardiac fibroblast proliferation through calcineurin-NFAT pathway. Front Biosci (Landmark Ed), 21(3), 502-513. https://doi.org/10.2741/4405

Xu, M., Tan, J., Zhu, L., Ge, C., Zhang, Y., Gao, F., Dai, X., Kuang, Q., Chai, J., Zou, B., & Wang, B. (2023, Oct). Palmitoyltransferase ZDHHC3 Aggravates Nonalcoholic Steatohepatitis by Targeting S-Palmitoylated IRHOM2. Adv Sci (Weinh), 10(28), e2302130. https://doi.org/10.1002/advs.202302130

Yasunari, K., Maeda, K., Nakamura, M., Watanabe, T., Yoshikawa, J., & Hirohashi, K. (2005, Jan). Left ventricular hypertrophy and angiotensin II receptor blocking agents. Curr Med Chem Cardiovasc Hematol Agents, 3(1), 61-67. https://doi.org/10.2174/1568016052773342

Zeigler, A. C., Richardson, W. J., Holmes, J. W., & Saucerman, J. J. (2016, May). A computational model of cardiac fibroblast signaling predicts context-dependent drivers of myofibroblast differentiation. J Mol Cell Cardiol, 94, 72-81. https://doi.org/10.1016/j.yjmcc.2016.03.008

Zhang, M., Zhou, L., Xu, Y., Yang, M., Xu, Y., Komaniecki, G. P., Kosciuk, T., Chen, X., Lu, X., Zou, X., Linder, M. E., & Lin, H. (2020, Oct). A STAT3 palmitoylation cycle promotes T(H)17 differentiation and colitis. Nature, 586(7829), 434-439. https://doi.org/10.1038/s41586-020-2799-2